

Exploring sugar metabolism in bread wheat for improving drought tolerance

Presented by

Nusrat Khan

MSc in Genetics and Plant Breeding
(Bangladesh Agricultural University)

The thesis is presented in fulfilment of the requirements for the degree of

Doctor of Philosophy

School of Veterinary and Life Sciences, Murdoch University, Western Australia

March 2019

This thesis was supported by Murdoch University (Western Australia), via infrastructure at the State Agricultural Biotechnology Centre, and funding from an Australian Post Graduate Award. A co-contribution was provided by a Grains Industry Research and Development Corporation grant (GRS10796).

Declaration

Except where otherwise indicated, all work in this thesis is based on work carried out by me at the State Agricultural Biotechnology Centre (SABC) and the Co-operative Research Centre for Molecular Plant Breeding, Murdoch University, Australia. I declare the content of this thesis is my own account of my research and has not been previously submitted for a degree at any tertiary education centre. To the best of my knowledge, all work performed by others, published or unpublished, has been duly acknowledged.

Nusrat Khan

12 March 2019

Abstract

Remobilization of stem WSC is well known to contribute to grain yield in wheat. There is, however, extensive genetic variation in the contribution of stem WSC to grain yield under post-anthesis water-deficit. Fructan 1-exohydrolase (1-FEH) is one of the major enzymes contributing to WSC remobilisation and the maintenance of grain yield under water-deficit. 1-FEH has three isoforms (*1-FEH w1*, *w2* and *w3*) that degrade β -(2-1) fructan linkages thus contributing to fructan remobilization to grain. This thesis investigated the functional role of the three isoforms of the *1-FEH* gene in WSC remobilisation under post anthesis water-deficit. Individual performance of the three isoforms was investigated using the corresponding isoform mutation lines derived from the Australian wheat variety Chara. Results from glasshouse experiments showed that the mutation of isoform *1-FEH w3* slowed down WSC remobilisation under post anthesis water-deficit and reduced grain filling and yield. In contrast, mutations of *1-FEH w1* and *w2* did not affect WSC remobilisation under water-deficit. This means that *1-FEH w3* plays the leading functional role in WSC remobilisation during grain filling under water-deficit.

This differences in remobilisation of WSC components between the mutation lines correlated with the expressional differences of the three isoforms of the *1-FEH* gene across the lines. In the *1-FEH w3* mutation line, the expression of the other two isoforms (*1-FEH w2* and *w1*) had the same level as the non-mutated parental cultivar Chara. However, in the *1-FEH w2* and *w1* mutation lines, *1-FEH w3* showed significantly higher expression compared to Chara. The results indicated that the functional loss of the isoforms *1-FEH w2* and *w1* was made up by the higher expression of the isoform *1-FEH w3* but the functional loss of the *1-FEH w3* isoform was not compensated by the other isoforms. This explains the ability of *1-FEH w2* and *w1* mutation lines to maintain the same pattern of WSC remobilisation as the non-mutated parental cultivar. It was also, revealed that the expressional differences of the isoforms of the *1-FEH* gene across different mutation lines significantly influenced the degradation of WSC and its components under post anthesis water-deficit.

Fructan, a fructose-based polymer synthesized from sucrose by fructosyltransferases (FTs), is the main component of wheat stem WSC and is a major source of sugar supply under post anthesis water-deficit when photosynthesis is reduced. Quick degradation of fructan is essential to

remobilise sugar to developing grain under water-deficit and this is facilitated by *FEHs*. The *1-FEH w3* mutation line showed slower degradation and remobilization of fructan compared to the *1-FEH w2* and *w1* mutation lines and Chara. This slow degradation made the *1-FEH w3* mutation line partially susceptible to post anthesis water-deficit. Noticeably, differences in WSC component degradation and gene expression of *1-FEH* isoforms only became evident under post anthesis water-deficit and not in well-watered plants.

This thesis also characterised the *1-FEH* gene mutation, by mapping and annotating the mutated region. The F1 seeds, developed by back crossing the *1-FEH w1*, *w2* and *w3* mutation lines with Chara, were genotyped using the Infinium 90K SNP iSelect platform. Putative deletions were identified in the *FEH* mutation lines encompassing the *FEH* genomic regions. A total of 15, 20 and 15 SNPs were identified within the mutation regions of *1-FEH w1*, *w2*, and *w3*, respectively. Mapping analysis demonstrated that the mutation affected significantly longer regions than the target gene regions of *1-FEH w1*, *w3* and *w2*. From the annotation of the mutation regions, 8 and 6 non-target genes were discovered on chromosomes 6A and 6B, respectively. The annotation of the *1-FEH w2* mutated region was complicated by the presence of an extra three copies of the gene on chromosome 6D. Functional roles of the non-target genes was carried out following computational biology approaches and confirmed that none of the affected non-target genes were expected to have a direct influence on *1-FEH* gene function.

This study also ratified the association of the distinct role of the *1-FEH w3* gene in sugar remobilisation to the developing wheat grain. Accumulation of oligosaccharides at two seed developmental stages were examined in the *1-FEH w3* mutation line in comparison to Chara under well-watered and water-deficit conditions. This study successfully overcome the challenge of preparing 25 µm seed sections by adopting cryosectioning using egg white which provided compatibility with the mass spectrometric equipment and enabled the production of ions from the oligosaccharides by the laser. Hexose and its polymers were detected separately by the mass spectrometry imaging (MSI) without any enzymatic digestion thus providing information regarding the localisation of sugar accumulation within the tissues of developing seeds. The abundance and localisation pattern of the identified oligosaccharides was influenced by the post anthesis water-deficit treatment. Under water-deficit, the mutation of the *1-FEH w3* reduced the abundance of oligosaccharide accumulation in two stages of seed development (17 DAA and 22

DAA) indicating its pivotal role under post anthesis water-deficit. This is the first study to use MSI to explore sugar accumulation directly within the tissue of developing seeds of wheat.

This thesis established the individual role of three isoforms of *1-FEH* in remobilising WSC under post anthesis water-deficit and provides unequivocal evidence that *1-FEH w3* is taking the most vital role. This new insight into the distinct role of the *1-FEH* gene isoforms under post anthesis water-deficit should assist in providing new gene targets for water-deficit tolerant wheat breeding in the future.

Acknowledgements

Work presented in this thesis was possible by collaboration and support made by numerous individuals. First and foremost, I would like to thank my supervisors, Prof. Bernard Dell, Dr. Jingjuan Zhang and Prof. Rudi Appels for their support, encouragement and guidance throughout this research. It is such precious blessings to have all of you as supervisors. I am truly grateful for the wealth of knowledge I have gained from them and for their faith in me as a student.

I am deeply grateful to my principal supervisor Prof. Bernard Dell for his constant guidance encouragement and valuable suggestions in the course of experiment and writing of the thesis. I am truly thankful to have conducted this research under such an expert and knowledgeable person.

Than I would like to take the opportunity to thank Dr. Jingjuan Zhang, my co-supervisor, for her valuable advice and motivation. Her excellent supervision and suggestions were helpful in setting experiments and writing the thesis. She always helped me in trouble shooting problems both in my glasshouse and molecular work. My heartfelt gratitude to Prof. Rudi Appels for his supervision and helping me to collaborate with different organizations.

To the many friends and colleagues that have helped me on this long and winding road, thank you for all your help and support. A special thanks to Dr. Angela Juhasz for helping me in analysing my bioinformatics data.

I must acknowledge collective support of key members of State Agricultural Biotechnology Centre (SABC), Murdoch University for providing excellent facilities to carry out my research. Individuals to thank in this regard include Professor Michael G. K. Jones (SABC Director), Dr. David Berryman (SABC Manager) and Ms Frances Brigg (SABC Technical officer).

I would also like to thank three technical experts, two from Murdoch University Department of Biological science namely Jose Minetto and Gordon Thompson and other one from Department of Veterinary Science is Mike, for their valuable contribution in my PhD. Jose for practical knowledge and advice on how to manage large glasshouse trail and Gordon for demonstrating to cryosectioning and Mike for giving access to the cryotome machine and assisting me to use it.

To my family, I am eternally grateful for your unwavering love and support. To my parents, thank you for everything, but especially for giving me the desire to learn and the opportunity to try and fulfil it. Last of all to my husband, Dr. Shahidul Islam, without his support and encouragement this PhD was impossible, my daughter Shemonti and son Shafwan, who have made this whole journey worthwhile, this is for you!

List of abbreviations

Abbreviation	Description
ABA	Abscisic acid
ABS	Australian Bureau of Statistics
ANOVA	Analysis of variance
AUD	Australian dollar
cDNA	complementary DNA
CHCA	Cyano-4-hydroxycinnamic acid
C-INV	Cytoplasmic invertase
CSIRO	Commonwealth Scientific and Industrial Research Organisation
CW-INV	Cell wall invertase
DAA	Days after anthesis
DAFWA	Department of Agriculture and Food Western Australia
DArT	Diversity array technology
DEPI	Department of Environment and Primary Industry (Victoria)
DESI	Desorption electrospray ionization
DHB	2,5-dihydroxybenzoic
DNA	Deoxyribonucleic acid
DNase	Deoxiribonuclease
DPIRD	Department of Primary Industries and Regional Development
dw	Dry weight
EDTA	Ethylenediamine tetraacetic acid
FAO	Food and Agriculture Organization of the United Nations
FEH	Fructan exohydrolase
FFT	Fructan fructan transferase
FT	Fructosyl transferases
GAPDH	Glyceraldehydes-3-phosphate dehydrogenase
HIB	Heavy ion bombardment
IWGSC	International Wheat Genome Sequencing Consortium
LAESI	Laser ablation electrospray imaging
<i>m/z</i>	mass to charge
MALDI-TOF MS	Matrix-assisted laser desorption/ionisation time-of-flight mass spectrophotometry
mRNA	Messenger RNA
MSI	Mass spectrometry imaging
NGS	Next-generation sequencing
PCR	Polymerase chain reaction
POPSEQ	Population sequencing
qRT-PCR	Quantitative reverse transcription PCR
RNA	Ribonucleic acid
RNase	Ribonuclease
ROS	Reactive oxygen species
RT	Reverse transcription
SA	Sinapinic acid
SABC	State Agricultural Biotechnology Centre

SFT	Sucrose fructan fructosyl transferase
SIMS	Secondary ion mass spectrometry
SMMD	Simultaneous multiple mutation detection
SNP	Single nucleotide polymorphism
SSR	Simple sequence repeat
SST	Sucrose sucrose transferase
SST	Sucrose sucrose fructosyle transferase
Suc	Sucrose
Sus	Sucrose synthase
SUT	Sucrose transporter
Taq	<i>Thermus aquaticus</i> DNA polymerase
TBE	Tris-Boric-EDTA Buffer
TE	Tris-EDTA
TILLING	Targeting induced local lesions in genome
<i>T_m</i>	Melting temperature
UGPase	Glucose-1-phosphate
USDA	United States Department of Agriculture
UV	Ultra violet
VIN	Vacuolar invertases
WGA	Whole genome assembly
WSC	Water soluble carbohydrate

Table of Contents

Declaration	v
Abstract	vii
Acknowledgements	xi
List of abbreviations	xiii
Chapter 1: Introduction	1
1.1 Background of thesis research	1
1.2 Thesis aims and objectives	3
Chapter 2: Review of literature	5
2.1 introduction to wheat and drought	5
2.2 Effect of drought on wheat production	8
2.2.1 Drought during vegetative growth	8
2.2.2 Drought during reproductive growth	10
2.2.3 Pre – anthesis drought	10
2.2.4. Post-anthesis drought	11
2.3 Sugar transport system in wheat	12
2.3.1 Sucrose synthase	14
2.3.2 Invertases	14
I. Cell wall invertases	15
II. Vacuolar invertases	15
III. Cytoplasmic invertases	16
IV. Invertases involved in wheat reproductive stages	16
a) Role of IVR1	17
b) Role of fructan exohyrolase	17
2.3.3 Sucrose transporters	20
2.4 Mass spectrometry imaging	21
2.4.1 Principle of MSI	23
2.4.2 Different types of Ionization	24
2.4.3 Laser Ablation Electrospray imaging (LAESI)	24
2.4.4 Secondary ion mass spectrometry	25
2.4.5 Desorption Electrospray Ionization (DESI)	25
2.4.5 Matrix assisted laser desorption ionization imaging (MALDI)	26
2.5 Conclusion	28
Chapter 3: 1-FEH w3 in wheat accelerates stem water-soluble carbohydrate remobilization to grain under post anthesis water-deficit condition	29
3.1 Introduction	29
3.2 Materials and methods	30
3.2.1. Plant material	30
3.2.2 Water-deficit experiment	31

I. Experimental design	31
II. Potting mix	31
III. Seed germination	32
IV. Glasshouse set up	32
V. Imposing water-deficit	32
VI. Sampling	32
VII. Carbohydrate analysis	33
VIII. Calculation of WSC remobilization	33
IX. Data analysis	33
3.3. Results	34
3.3.1 Confirmation of gene mutations	34
3.3.2 Observation of the water-deficit regime	35
3.3.3 Stem WSC remobilisation and grain development	36
I. Influence of water-deficit and 1-FEH isoforms	36
a) Water-deficit promoted early remobilisation of WSC	36
b) Timing of decline in WSC differed among mutation lines	37
c) Response in grain development and yield	37
II. Grain weight at maturity was influenced by 1-FEH isoforms under water-deficit condition	39
III. 1-FEH w3 mutation affected stem WSC remobilization rate	41
IV. Correlations analysis of grain weight with WSC level and remobilisation rate	41
3.4 Discussion	42
3.4.1 1-FEH showed functionality only under water-deficit condition not under well-watered condition	42
3.4.2 Under water-deficit condition WSC remobilisation rate and grain filling was slowed down by 1-FEH w3 mutation	43
3.4.3 Components of grain yield were reduced in 1-FEH w3 mutation line but not in 1-FEH w2 or 1-FEH w1 mutation lines	44
3.4.4 Comparison of findings in preliminary and main experiments	44
3.5 Conclusion	46
Chapter 4: Expressional behaviour of different isoforms of 1-FEH gene under post anthesis water-deficit and its influence on WSC components	47
4.1 Introduction	47
4.2 Materials and methods	49
4.2.1 Carbohydrate analysis by HPAEC	49
4.2.2 Expression analyses by quantitative real-time PCR	50
I. RNA isolation and cDNA synthesis	50
II. Primers used for qRT-PCR:	50
III. PCR Amplification condition	50
4.2.3. Statistical analysis	51
4.3 Results	51
4.3.1. Effect of mutation of 1-FEH isoforms on carbohydrate composition under post anthesis water-deficit condition	52

4.3.2. Comparison of gene expression in all mutation lines and Chara under well-watered and water-deficit condition	64
4.3.3 Under water-deficit, high expression of 1-FEH w3 gene exhibited in w1 and w2 mutation lines	64
4.4 Discussion	68
4.4.1 Absence of 1-FEH w3 hindered fructan degradation	68
4.4.2 Mutation of 1-FEH w2 and w1 gene was compensated by high expression of 1-FEH w3 gene	70
4.4.3 Absence of 1-FEH w3 gene was not compensated by the other two isoforms	70
4.4.4 Absence of 1-FEH w3 made the line susceptible to water-deficit	71
4.4.5 Mutation of 1-FEH isoforms did not upset the activity of 6-FEH	71
4.4.6 1-FEH expression in well-watered condition	72
4.5 Conclusion	72
Chapter 5: Characterization of 1-FEH mutation lines using a 90K SNP array	73
5.1 Introduction	73
5.2 Materials and methods	75
5.2.1 Plant materials	75
5.2.2. Genotypic DNA extraction	76
5.2.3 90K SNP chip analysis	76
5.2.4 Data analysis	78
5.3 Results	78
5.3.1. An overview of the 90K SNP array	78
5.3.2. Mapping of mutation region in chromosomes	82
5.3.3. Annotation of the deleted/mutated region	86
5.4. Discussion	93
5.4.1 Chromosomal mapping of mutation region and candidate gene	94
5.4.2 Annotation of the deleted region	94
5.4.3 Function prediction of non-target deleted genes	95
I. Hydrolase	96
II. Ligase	96
III. Transferase	97
IV. Oxidoreductase	97
5.5 Conclusion	97
Chapter 6: Characterising sugar deposition in the developing wheat grain using mass spectrometric imaging (MSI) and influence of 1-FEH w3	99
6.1 Introduction	99
6.2 Materials and methods	102
6.2.1 Plant materials	102
6.2.2 Sample collection and storage	102
6.2.3 Seed slide preparation	102
6.2.4 Mass Spectrometer Imaging (MSI)	102
6.3 Results	104
6.3.1 Establishment of the seed sectioning procedure and sample preparation	104

6.3.2	<i>Mass spectrometry imaging successfully detected oligosaccharides and their localisation in the seeds</i>	105
6.3.3	<i>Relative abundances and localisation pattern of polysaccharides in wheat grain</i>	107
	<i>I. Differentiation in relative abundance and localisation pattern of oligosaccharides between seed from droughted and well-watered plants</i>	108
	<i>II. Differentiation in oligosaccharide relative abundance and localisation pattern between seed from droughted and well-watered plants</i>	109
6.3.4	<i>Influence of 1-FEH w3 mutation on oligosaccharide accumulation</i>	110
	<i>I. In water-deficit plants 1-FEH w3 mutation reduced the accumulation of oligosaccharide</i>	110
	<i>II. In well-watered condition 1-FEH w3 mutation delayed storage</i>	112
6.4	Discussion	113
6.4.1	<i>Characterising sugar accumulation pattern in developing grain is important to deal with drought</i>	113
6.4.2	<i>MSI technology has the potential to be used for characterising sugar accumulation in developing grain</i>	113
6.4.3	<i>Sugar accumulation abundance and pattern are influenced by seed developing stage and drought</i>	115
6.4.4	<i>Mutation of 1-FEH w3 decreased sugar accumulation under water-deficit</i>	115
6.4.5	<i>Under well-watered condition deletion of 1-FEH w3 delayed sugar remobilisation to the grain</i>	116
6.5	Conclusion	116
Chapter 7:	General discussion	117
7.1	Major outcomes of the thesis	117
7.1.1	<i>1-FEH w3 is the most important isoform of 1-FEH for WSC remobilisation and grain filling under post anthesis water-deficit</i>	117
7.1.2	<i>Gene expressional difference of 1-FEH isoforms elucidates the degradation of WSC components in the mutation lines under water-deficit</i>	118
7.1.3	<i>Sugar metabolism was influenced by 1-FEH mutation</i>	120
7.1.4	<i>Characterization of 1-FEH mutation lines using 90K SNP array</i>	121
7.1.5	<i>Characterising sugar accumulation pattern in developing grain</i>	123
7.1.6	<i>1-FEH showed functionality only under water-deficit not under well-watered condition</i>	124
7.1.7	<i>Post anthesis water-deficit resulted in early remobilisation of WSC</i>	125
7.2	Limitations of the thesis and future work	125
7.2.1	<i>Using precise gene mutation technology like CRISPR-Cas9 for functional confirmation</i>	125
7.2.2	<i>Using recently published IWGSC data for characterising gene mutation</i>	126
7.2.3	<i>Further studying sugar accumulation patterns using mass spectrometry imaging</i>	126
7.2.4	<i>Future breeding research</i>	126
7.3	Conclusion	127
Appendix 1		129
Appendix 2		137
References		141

Chapter 1: Introduction

1.1 Background of thesis research

Wheat (*Triticum aestivum* L.) is grown on more land area than any other commercial crop. According to FAO data (FAO 2016), wheat was grown on more than 220 million hectares, compared to 188 million hectares for maize and 160 million hectares for rice. Wheat supplies globally 20% of all food calories and in developing countries it is the second most important protein source (20%) after rice (Faostat 2009). Moreover, wheat is considered nutritionally the most important of the three major cereals, supplying 15 g nutrition per person per day whereas maize supplies only 3.5 g and for rice less than 1.5 g (Wheat Initiative 2017). By the year 2050 an additional 2.3 billion people need to be fed since the world population is expected to have grown by 34% (FAO 2009). Thus, by 2050 the demand for cereal is projected to grow by 56% (1048 million metric tons) from the demand for the base year 2000, and wheat is expected to contribute 26% of this increase (Hubert et al. 2010). It is estimated that the increase in annual wheat yield must rise from the present level of below 1% to at least 1.7% (Wheat Initiative 2017) to meet the increasing global demand. Furthermore, this needs to occur during a period of uncertain global climate change when increased severity and frequency of extreme weather events are anticipated (CSIRO and BoM 2016).

Abiotic stress is a major challenge in our quest for sustainable food production, as it may reduce potential crop yields by up to 70% (Verslues et al. 2006). Drought is the most significant environmental stress in agriculture worldwide (Borlaug and Dowswellss 2005) and productivity of wheat is often limited by scarcity of water. In Mediterranean climate regions in particular, grain filling occurs when temperatures are increasing and moisture supply is decreasing. Terminal drought (from grain set to grain fill) stress has a negative effect on grain weight and grain size (Artlip et al. 1995; Jamieson et al. 1995; Ji et al. 2010; Yang and Zhang 2006). Western Australia (WA) experienced some of its lowest rainfall in 2010 resulting in a severe decrease in grain production to less than 70% of the long-time average yield resulting in many farmers facing difficulty covering farm operating costs for that year (DAFWA 2014). Thus, improved productivity under periodic drought stress and understanding of physiological traits related with drought tolerance are key challenges for global agriculture.

Drought is a complex phenomenon, and because of the polygenic nature and low heritability of drought tolerance traits, conventional breeding approaches have so far had limited success in generating drought-tolerant, high-yielding wheat genotypes. Molecular genetic techniques

have the potential to assist breeders through the rapid identification of key candidate genes and potential QTLs functional traits for marker assisted breeding (Cattivelli et al. 2008; Fleury et al. 2010; Tuberosa and Salvi 2006). However, to achieve the potential benefits of these technologies, it is most important to understand the physiological traits associated with drought tolerance (Aprile et al. 2009; Rampino et al. 2006).

Even though growth can be affected by drought at any phenological stage, the most sensitive phases are the early reproductive and grain filling stages (Pradhan *et al.*, 2012). During post anthesis drought, photosynthesis declines because of decreases in leaf stomatal conductance and net CO₂ assimilation which limit the contribution of the current assimilates to grain development (Gebbing and Schnyder 1999, Yang et al. 2001, Ruuska et al. 2006). Commonly, these physiological changes result in kernel shrivelling, reduced test weight and loss in yield (Blum, -???). Wheat plants do not immediately exploit all the carbon skeletons derived from photosynthesis, resulting in the storage of water soluble carbohydrate (WSC) for short or long-term use. At the later stages of plant development, reserved carbohydrates are remobilized to reproductive sink tissue for grain filling. During post anthesis water deficit remobilization of carbohydrate is critical for grain yield. Under terminal drought conditions, remobilisation of WSC contributed as much as 30-50% of grain yield and 10–20% under well-watered conditions (Pheloung and Siddique 1991; Schnyder 1993; Gebbing and Schnyder 1999).

Stem WSCs mainly consist of fructan, glucose, fructose, sucrose and various oligosaccharides (Virgona and Barlow 1991). It has been reported that fructan is the main storage form of stem WSC in wheat (Goggin and Setter 2004, Schnyder 1993, Wardlaw and Willenbrink 1994). Examination of WSC composition in selected genotypes revealed that variation in total WSC was attributed mainly by the variation in the fructan component unlike the other soluble carbohydrates, sucrose and hexose (Sari et. al. 2006).

High concentration of stem WSC has been considered as an important selection criterion in the screening of wheat genotypes for breeding drought tolerant lines. However, Zhang et al. (2009) indicated that the concentration of stem WSC alone is not a simple or reliable criterion to identify wheat having potential grain yield under water deficit. Rather, the remobilization activity (rate and timing) of the stem WSC is also critical (Zhang et al. 2009).

Fructan 1-exohydrolase (1-FEH) which has three isoforms (1-FEH w1, w2 and w3) is one of the major enzymes degrading β - (2-1) fructan linkages thus contributing to fructan remobilization to grain. It has been suggested previously that 1-FEH w3 (1-FEH-6B) is a key enzyme involved in stem WSC remobilization (Van Riet et al., 2008; Zhang et al., 2009). It

can be presumed that the combined activities of all three isoforms potentially contribute to increase the utilization of stem WSC during grain filling under terminal drought.

1.2 Thesis aims and objectives

The crucial role of the *1-FEH* gene for remobilization of stored WSC under terminal drought condition for maintaining grain weight has already been established (Zhang et al. 2009). Out of the three isoforms: *1-FEH w1* (*1-FEH-6A*), *1-FEH w2* (*1-FEH-6D*) and *1-FEH w3* (*1-FEH-6B*), the dominant expression of *1-FEH w3* has been speculated (Zhang et al. 2015a) for facilitating higher fructan remobilization under drought conditions. However, there is still limitation in understanding the individual role of these three isoforms and whether the role of *1-FEH w3* is influenced by other isoforms. Therefore, the overall aim of the thesis is to determine the individual role of the three isoforms of *1-FEH* gene for grain filling in wheat.

The working hypothesis is: under terminal drought remobilization of stem WSC in wheat is accelerated by the activity of *1-FEH w3* with the help of other two isoforms to compensate the yield loss.

The thesis objectives are as follows:

1. Identify the most important isoform of *1-FEH* for WSC remobilization under post-anthesis water-deficit,
2. Investigate differences in *1-FEH* isoforms in gene expression and their influence on WSC components under post-anthesis water-deficit,
3. Characterize the genetic lines used in this experiment to confirm gene mutations, and
4. Quantify differences in sugar accumulation patterns in well-watered and water-deficit gene mutation lines.

Mutation lines of *1-FEH w1*, *1-FEH w2* and *1-FEH w3* derived from the Australian variety Chara will be used in glasshouse drought experiments to investigate the most important isoform of *1-FEH*.

Overall contents and structure of the thesis are presented in Fig. 1.1, which also shows the flow of knowledge generated out of this thesis.

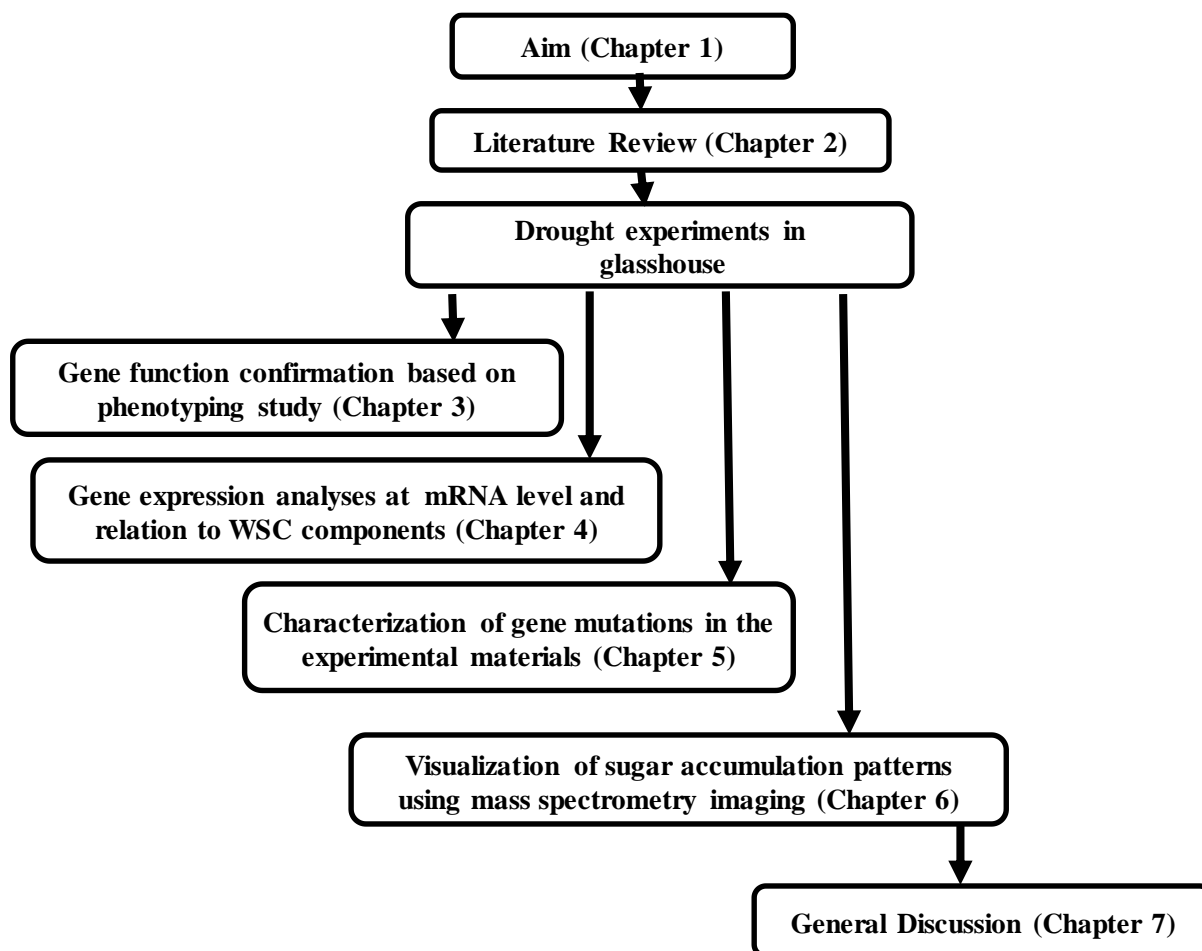


Fig. 1.1: Research components and the structure of the thesis.

Chapter 2: Review of literature

This thesis addresses the function of the three isoforms of the *1-FEH* gene regarding water soluble carbohydrate transportation to the grain in wheat under post-anthesis drought. This chapter reviews the knowledge in this field. It includes an introduction to wheat, highlighting impacts of drought on wheat production particularly when it occurs post-anthesis, describes sugar transportation systems in the plant, considers enzymes involved in regulating sugar transportation, and the contribution of 1-FEH in sugar transportation under drought. The review also covers the potential of mass spectrometric imaging (MSI), a cutting-edge technology, to localise sugar deposition in the developing grain.

2.1 Introduction to wheat and drought

Wheat is one of the first cereals to have been domesticated and its ability to self-pollinate greatly facilitated the selection of many distinct domesticated varieties. The archaeological record suggests that this occurred first in the region known as the Fertile Crescent. Recent findings narrow the first domestication of wheat down to a small region of south-eastern Turkey (Lev-Yadun et al. 2000) that has been dated to 9,000 BCE. Over time, wheat has become one of the most important food crops in terms of the harvested area, trade value and human nourishment. Its high nutritional value and comparatively easy harvesting and processing compared to other cereals made it a widely cultivated crop all over the world. More than half of the calories and nearly half of the protein for one third of the world's population is supplied from cereals (Henchion et al. 2017) and wheat is considered as the largest group of plant protein sources in the Western diet (Spiegel et al. 2013). Wheat accounts for about 21% of staple food and 200 million hectares of farmland worldwide (FAO 2009). In 2016, the world production of wheat was 749 million tons, making it the second most-produced cereal after maize (1060 million tons) (Faostat 2018).

By 2050, the global population is projected to increase by 34% and accordingly, agricultural production needs to be increased by 60–110% to meet these increasing demands (FAO 2009; Ray et al. 2013) as well as to provide food security to the current 870 million chronically undernourished (FAO WFP 2012) people. As a consequence, the production of important main crops like cereals is anticipated to be increased by 43% (Powell et al. 2012). However, this increase in production is a huge challenge as this growth will need to occur in a world with a changing climate, where more frequent weather extremes will impact on grain productivity

(Powell et al. 2012). The recent global increase in wheat yield is about 1% per annum which needs to increase to 2.4% to meet the 2050's demand (Ray et al. 2013). However, since the end of the 'Green Revolution' wheat and rice yields are not increasing as rapidly as expected (Fischer and Edmeades 2010; Rosegrant and Cline 2003; Tilman et al. 2002). The average annual yield increase (the total of wheat and rice) has steadily declined from 3.2% per annum to 1.5% per annum from the year 1960 to 2000 (Powell et al. 2012). Inadequate genetic biodiversity and environmental factors are significant factors that have influenced yield outcomes (Powell et al. 2012).

In Europe and the United States, climate change and lack of adaptation to stress are considered largely responsible for the decline in the rate of yield increase in wheat (Boyer 1982; Brisson et al. 2010). Stress is a complicated condition that limits crop productivity. Biotic stress is caused by insects, pathogens and other living agents, while abiotic stress is an environmental state (condition) that negatively influences the growth and yield which may include drought, flooding, salinity, metal toxicity, mineral deficiency, adverse pH, adverse temperature, air pollution, etc. For sustainable food production, abiotic stress is considered as the major challenge since this may reduce potential yields by as much as 70% in crop plants (Boyer 1982). Drought is a condition of moisture deficiency, having an adverse effect on vegetation, animals and humans over a sizeable area, and is considered as the most damaging abiotic stress (Borlaug and Dowswell 2005).

Australia is a relatively small producer of wheat, accounting for only 3% of annual world production. However, due to its small population, about 65% of the wheat produced is exported, ultimately contributing 15% of world trade (Gordon et al. 2016). Australia is the fourth largest exporter of wheat after the United States, Canada and the European Union (FAOSTAT 2011). However, Australian wheat production is highly sensitive to climatic factors. Various projections for temperature, rainfall, drought and storms suggest that maintaining current grain yields would be difficult for Australia. For example, rainfall has increased over the last 50 years over north-western Australia, but decreased in wheat-growing regions in the southwest of Western Australia, and in much of south-eastern Australia, especially in winter (Fig. 2.1).

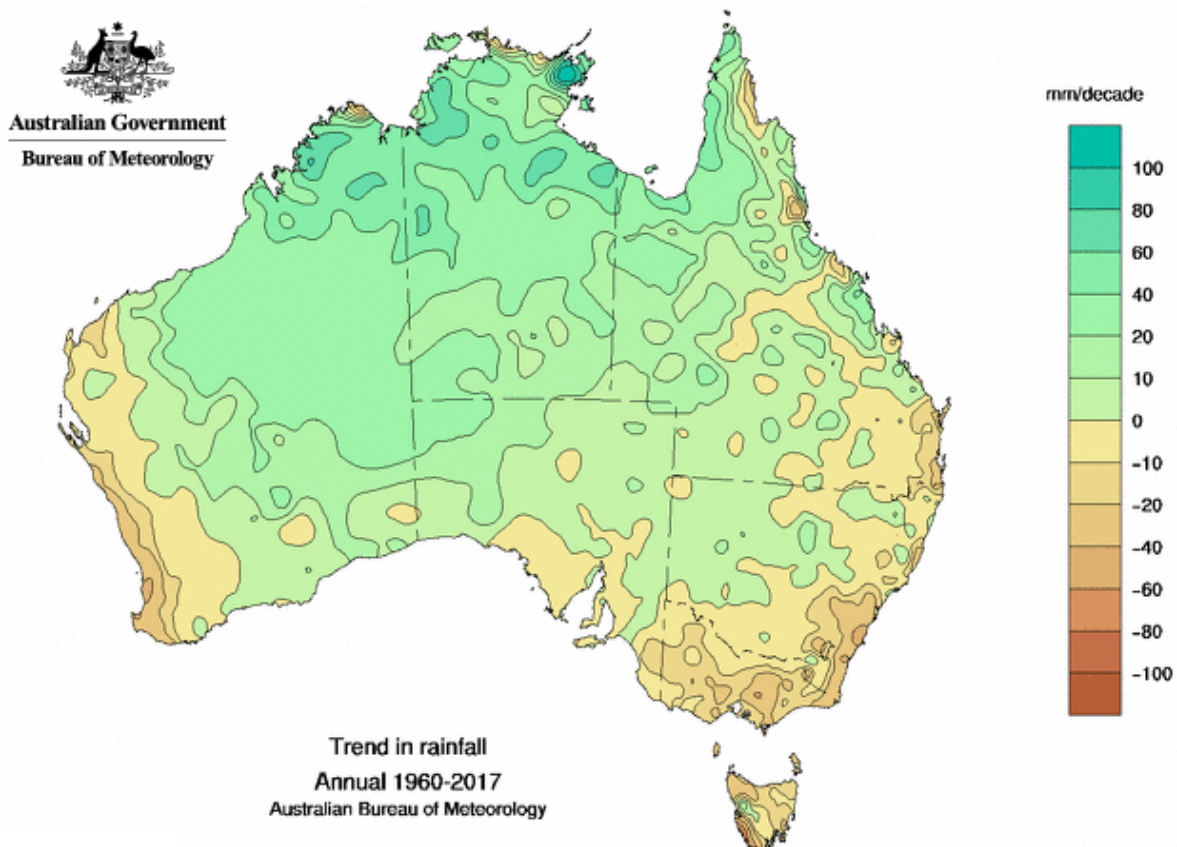


Fig. 2.1: Last 60 years annual rainfall trend in Australia. The brown areas are the parts that used to receive more rain in the 1960s. The dark green areas are now wetter than they used to be. The scale to the right column is mm/decade rainfall.

Western Australia (WA) is the largest wheat growing state in Australia, producing about 50% of the total production of Australia (DPIRD 2018). In south-west WA, more than 4 million ha is sown with wheat each year. The soil of the WA wheat belt is characterised by nutrient-poor sandy and duplex (sand over clay) soils with some clay soils in the eastern part of the region (Cima et al. 2004). The area tends to have an extreme Mediterranean-type climate with wet, cool winters and dry, hot summers with high solar radiation. In WA, wheat is mostly cultivated in areas with less than 550 mm annual rainfall and about half of the farms in the region receive on average less than 325 mm rain per year (Cima et al. 2004). The annual rainfall in south-west WA has declined by about 10% since the mid-1970s. In WA, more than 75% of the rainfall occurs between May and October, but since 1925, rainfall in early winter (which is very important for wheat reproductive development) has declined by 25%. By 2070 a significant change in winter rainfall has been predicted which will stand somewhere between 60% reduction and 10% increase (Pittock 2003). It is worth mentioning that most likely by 2030, a reduction of about 15% winter rainfall will be experienced which will rise to a level of 30%

reduction by 2070 (IOCI 2002). Since the last 30 years the region has experienced a significant drop in winter rain (Smith et al. 2000). Between May and July has rainfall declined by 19% since 1970 (CSIRO and BOM, 2016). This reduction in rainfall could be a major threat for the grain industry in south-west WA. The prospect of feeding an increasing global population in a world with increasingly erratic rain, temperature and drought patterns, presents a big challenge to plant scientists.

2.2 Effect of drought on wheat production

In crops, deviation from ideal growth environments often results in lower yields and a high economic impact on producers and consumers. Each yield component has an influence on the final grain yield as determined at different growth stages. During their life cycle, plants are often subjected to water deficits, which vary in duration and intensity. The complexity of plant stress adaptation makes breeding complicated for abiotic stress tolerance, particularly for drought. Knowledge of plant responses to drought, and other stresses, will help developing drought tolerant varieties (Muhammad Waseem 2011).

Drought affects all levels of plant performance, from morphological to molecular levels, and can impact all different phenological growth stages. Water deficit causes considerable yield loss and this depend on the severity and growth phases during which water deficit occurs. Water deficit in the early stage of development, i.e. before anthesis, reduces the number of spikes and kernel number per spike (Dolferus et al. 2011). By contrast, water deficit at post anthesis affects kernel weight (Plaut et al. 2004). An account of various drought stress effects and their extents are elaborated in the following sections.

2.2.1 Drought during vegetative growth

Crop yield is determined by germination time and rate, seedling vigour and time of maturity (Rauf et al. 2007). Germination of seed is the first and one of the most complex physiological process initiated by the imbibition of water. Even though a number of environmental factors influence wheat grain germination, the availability of soil moisture is considered the major one. For proper germination, the minimum water content required by the wheat grain is 35 - 45 % by weight (Bowden and Ferguson, 2008). Drought at this stage severely reduces germination success and in severe cases it causes total germination loss (Harris D et al. 2002; Kaya et al. 2006). Furthermore, even small-scale water stress during late emergence can adversely affect seedling vigour leading to reduced yield (Gul and Allan 1976). After germination, plant growth is promoted through cell division, cell elongation and differentiation which include complex

interactions of genetic, physiological, ecological and morphological events. All these events are sensitive to water availability. Turgor pressure, which is considered very important to cell growth, is reduced under drought (Farooq et al. 2009). Under severe water deficit, cell elongation can be inhibited by disruption of water flow from the xylem to the surrounding elongating cells (Nonami 1998).

Seedlings do not need large amounts of soil water because of their low leaf area index as well as low respiration rate. However, if drought occurs early in the life cycle, before the establishment of an extensive root system, limited access to deeper soil water may impair growth. Water deficit in the seedling stage reduces leaf water potential and relative water content, which reduces photosynthesis and yield potential. Also, water shortage reduces leaf size, stem extension and root proliferation which in turn interrupts plant water relations and reduces water-use efficiency (Anjum et al. 2011).

Water deficiency also leads to stomatal closure because of increased leaf and canopy temperature and this impairs gas exchange reducing the CO₂ supply for photosynthesis and also increases temperature (Siddique et.al 2001). It also reduces CO₂ assimilation by leaves, resulting in membrane damage and disturbed activity of various enzymes, especially those of CO₂ fixation and adenosine triphosphate synthesis (Farooq et al. 2009). In most plants, stomatal closure is the first reaction to drought stress. It is more closely related to soil moisture content than leaf water status. Hormonal stimulations within the plant body upon receipt of environmental signals regulate stomatal opening and closing. This stomatal programme is controlled by specialized "guard cells". The various different factors (light, water content of epidermal cells, temperature and mineral elements) stimulate guard cells activity, which control stomatal movements. During drought, the activation of different stress phytohormones triggers a signalling cascade in guard cells that results in stomatal closure and inhibits stomatal opening (Daszkowska-Golec and Szarejko 2013). Abscisic acid (ABA), is the main hormone that is involved in the process of stomatal closure. However, other phytohormones like jasmonic acid, brassinosteroids, cytokinins, or ethylene have also been reported to be involved in the stomatal response to stress (Casson and Hetherington 2010; Clauw et al. 2015; Nemeskéri et al. 2015; Torres-Ruiz et al. 2013). Furthermore, ABA that is transported in the xylem to the shoot, reduces leaf expansion, thereby preventing the dehydration of leaf tissues (Zhang et al. 2006). In addition, ABA may be involved in the mobilization of reserves under drought conditions (Barnabás et al. 2008).

Wheat tillering is highly sensitive to environmental variation, particularly to water availability. Wheat tillering is an important factor for yield that can be predicted by model simulation (Day 1985). The development of the coleoptile and first tiller are often restricted in a dry and crusty soil surface which results in a general reduction in tiller number per plant (Roy and Gallagher 1985). When plants were subjected to mild water deficit at their early stage of development, tillering ceased prematurely but, by producing a number of small-eared tillers upon recovery yield remained unchanged compared to the non-stressed plant (Blum et al. 1990). Thus, a short period of stress during early tillering may not reduce kernel number. By contrast, water deficit during main tillering causes a reduction in kernels per ear and total number of tillers per plant (Blum et al. 1990).

Water deficit at booting causes a greater reduction in plant height and number of tillers and delays heading (references). It also decreases ear length, stem length and number of spikelets per spike (Maqsood et al. 2012). However, tillers that initiate after drought are mostly unproductive and result in delayed maturity and non-uniform ripening of spikes (Gupta et al. 2001).

2.2.2 Drought during reproductive growth

The reproductive stage is the most sensitive part of a cereal's crop life-cycle to water deficit (O'Toole and Moya 1981; Saini and Westgate 1999; Salter and Goode 1967). During late spike development (pre-anthesis), drought can delay or completely inhibit flowering and post-anthesis drought causes the premature cessation of grain filling resulting in poor grain weight and size. In most parts of the wheat growing areas, during grain-filling, mean pan evaporation often exceeds average precipitation. Terminal drought is a characteristic of Mediterranean-type climates, rainfall decreases and evaporation and temperature increase in spring, when wheat reaches its reproductive stage (Rickert et al. 1987). The effects of terminal drought on wheat yields is predicted to increase in the near future due to projected climate change (Araus et al. 2002; de Oliveira et al. 2013)

2.2.3 Pre – anthesis drought

Compared to drought after anthesis which mainly affects grain size, drought before or at anthesis is more harmful as it causes a reduction in grain number (Ji et al. 2010). In cereal crops, the grain number is mainly determined at early developmental stage precisely prior to anthesis (Sreenivasulu and Schnurbusch 2012). Thus, drought stress at pre-anthesis potentially affects the development of the floral meristem and causes problems in spikelet initiation and

abortion of developing florets (Dolferus et al. 2011). Fewer spikes and a lower spikelet number reduces grain number. Reduction in grain number is being considered as the main contributor to yield loss under drought (Bingham 1966; Briggs et al. 1999; Fischer and Stockman 1980; Jamieson et al. 1995; Saini and Aspinall 1981; Westgate et al. 1996).

Pre-anthesis is mainly manifested as abortion of the developing pollen and reduction in the kernel number per spike. Pollen development in wheat is particularly sensitive to drought stress (Salter and Goode 1967). The young microspore (YM) stage (Salter and Goode 1967) is the most stress-sensitive period of reproduction in all cultivars of wheat that have been studied. Moreover, mild drought stress can irreversibly affect male gametophyte fertility, without affecting survival of the vegetative plant parts. The magnitude of reduction in grain number depends on the timing of drought stress in relation to plant development. However, spikelets and florets may also abort if drought occurs later during floral development (Dolferus et al. 2011).

As mentioned above, male sterility due to drought stress is a foremost problem in cereal crops. Pollen in well-watered wheat accumulate large quantities of starch during their final stages of development, which is used to support pollen germination and pollen tube growth. The most noticeable expression of water-stressed wheat pollen is their failure to accumulate starch (Lalonde et al. 1997; Saini et al. 1984). Even moderate water deficit at the YM stage induces male gametophyte sterility in wheat (Saini 1997; Saini and Westgate 1999). Pollen lose contact with the tapetum and they become unable to accumulate starch (Saini et al. 1984). Changes in carbohydrate availability and metabolism appear to be involved in the effects of stress during meiosis and anthesis. Similar disturbances in sugar metabolism have been seen in drought-stressed rice anthers (Sheoran and Saini 1996).

2.2.4. Post-anthesis drought

Post-anthesis drought is common in many wheat growing regions but specially those with Mediterranean climate as grain filling often occurs when temperatures are increasing and moisture supply is decreasing. This condition accelerates grain filling rate, but reduces the duration of filling and ultimately grain yield (Asseng et al. 2011; Wardlaw and Moncur 1995; Zahedi et al. 2003). Thus, terminal drought is considered as one of the most significant reasons for wheat yield loss. Furthermore, leaf senescence is increased and photosynthesis is reduced during post anthesis drought, which depresses final biomass, grain yield and harvest index (Kobata et al. 1992; Passioura 1983; Yang et al. 2001). Although grain number is not affected by post anthesis drought, depending on the time and intensity of the drought, grain yield and

harvest index both decline as a consequence of reduced grain size and grain weight (Passioura 1983; Plaut et al. 2004).

Grain development is the final stage of growth in cereals where fertilized ovaries develop into caryopses. Grain development starts between 1–5 days after anthesis (DAA), when cell proliferate in the endosperm, followed by the development of a multinucleated syncytial tissue (Olsen 2001). Then, between 6-24 DAA, cell division ends and cell enlargement begins with a sequential cellularization process that rapidly leads to grain filling with the accumulation of reserves (Altenbach et al. 2003). The grain water content also increases during this stage. As a whole, the transition from cell division to grain filling is a critical stage that occurs through different chronological and spatial steps, which includes a phase of cell division followed by differentiation and storage activity. Grain weight is the key component of the total yield which is determined by the length and duration of grain filling (Yang and Zhang 2006).

Starch biosynthesis and accumulation contribute the main process of grain filling. At the grain filling stage, photosynthates are transferred from leaves to the developing grain to be mainly stored in the endosperm. Drought at the early stage of grain filling causes a reduction in grain weight as a consequence of a reduction in the number of endosperm cells (Nicolas et al. 1985). In comparison, stress at later stages results in a reduction in the capacity to accumulate starch in the endosperm either because of the inadequate supply of assimilates for the grain (Blum 1998) or direct effects on the biosynthetic processes in the grain (Yang et al. 2002). The intensity and duration of water stress during grain development significantly influence the yield of cereals. When wheat plants were exposed to 20 days of water deficit during the endosperm cell division period, it reduced endosperm cell number by 30–40%, and the number of small starch granules per cells was also reduced by 45% (Nicolas et al. 1985). Thus, it is understandable that continuous sugar supply is essential in grain filling for maintaining grain size and weight, and this is dependent on the sugar transport system of the whole plant.

2.3 Sugar transport system in wheat

Increasing grain yield is associated with kernel number per unit area and kernel weight (Ma et al. 2012) which is closely related to sugar transport and sugar signalling. Carbohydrate metabolism is fundamental for plant growth and development. Besides starch, non-reducing disaccharides (sucrose and trehalose) are one of the most common class of reserves carbohydrate in plants (Sturm and Tang 1999). Among the sugars synthesized in a plant, only a few are transported in the phloem over a long-distance and sucrose is the main form (Lemoine et al. 2013). Sucrose and its components, glucose and fructose, play major roles in the transport,

storage, and metabolism of carbon in plants (Ji et al. 2005). Polysaccharides, like starch and fructans, are synthesised using sucrose as the substrate molecule. Sucrose also can work as energy source for respiration when it arrives from the source to the sink tissue (Le Roy et al. 2007).

Soluble sugars such as glucose and sucrose are essential to regulate plant's developmental and physiological processes, (Koch et al. 1996). Sugars play a vital role in plant metabolism and are involved in hormone signalling related to environmental stress (Finkelstein and Gibson 2002; Gazzarrini and McCourt 2001; Roitsch 1999; Sheen et al. 1999).

Sucrose is the main photoassimilate, usually produced in excess in mature leaves. Sucrose is the carbon energy source for sink organs of most plant species (Sturm and Tang 1999). Although sucrose is the main transporter of carbon it needs to be broken down to its components (glucose and fructose) for plant growth and development. Several isoforms of invertase and sucrose synthase are required for cleavage of sucrose. Glucose and fructose are linked via an α 1- β 2-glycosidic bond. Cleavage of this bond initiates sucrose utilization and the reaction is catalysed by two enzymes with entirely different properties: sucrose synthase and invertases (Fig. 2.2).

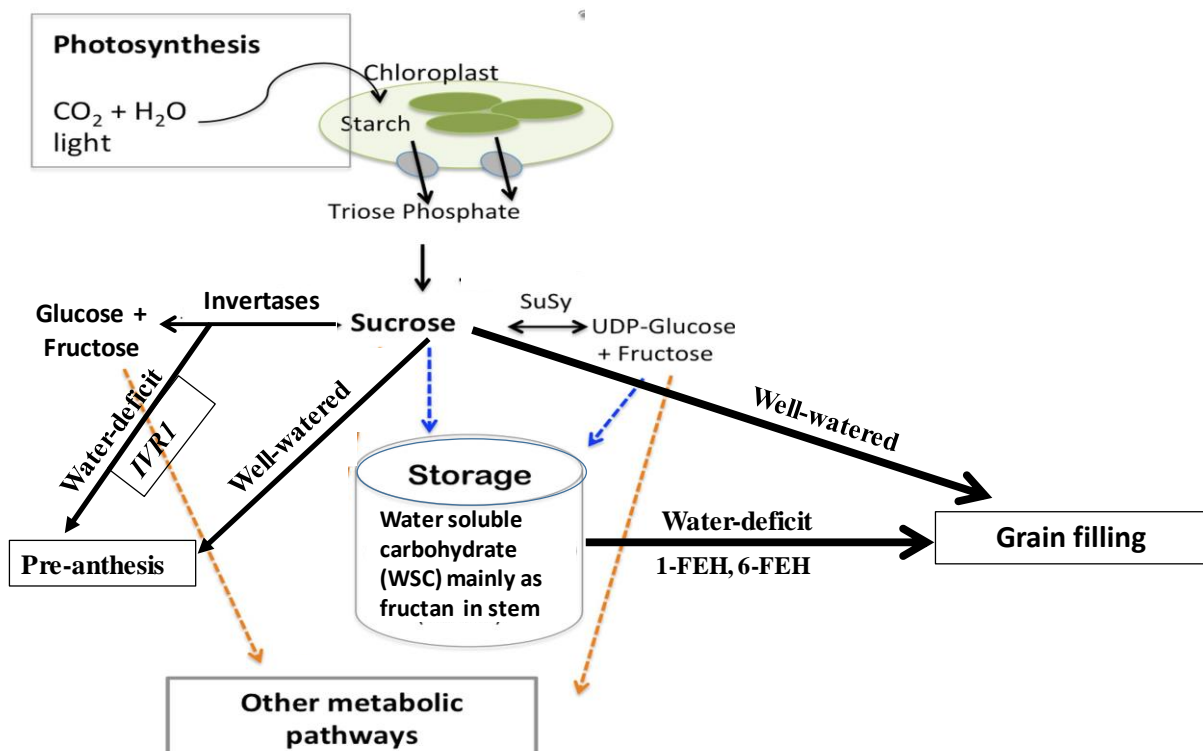


Fig. 2.2: Sugar transport system in wheat. Black arrows is show sucrose used in plant reproduction system, red arrows other metabolic pathways and blue arrows sucrose storage

2.3.1 *Sucrose synthase*

Sucrose synthase is a glycosyl transferase, which catalyzes the reversible conversion of sucrose, in the presence of UDP, into UDP-glucose and fructose. The remarkable attribute of sucrose synthase is its potential to mobilize sucrose into diverse pathways which are important for structural, storage and metabolic functions of plant cells (Chen and Chourey 1989; Heinlein and Starlinger 1989). Sucrose synthase provides substrates for starch synthesis in cereal endosperm, potato tubers and other storage organs of plants (Chourey and Nelson 1976; Claussen et al. 1985; Dale and Housley 1986). It is also involved in production of energy (ATP) for respiration (Chourey et al. 1998; Coleman et al. 2006; Ruan and Chourey 2006). The UDPG product of sucrose synthase is involved in the formation of starch (Asano et al. 2002), in the synthesis of cellulose (Salnikov et al. 2003; Subbaiah and Sachs 2001) and diverse cell wall polysaccharides (Albrecht and Mustroph 2003; Doblin et al. 2002). Sucrose synthase is also involved in supplying UDP-glucose for cell wall biosynthesis and carbon to meet the increased glycolytic demand during anaerobic and cold stress (C Maas et al. 1990; Hendrix 1990).

Another major function of sucrose synthase is its involvement in cell wall formation, which is supported by the inhibition of cell wall formation in maize when sucrose synthase was knocked-out (Koch et al. 1996). Immunolocalization has shown that sucrose synthase is localized in sieve-tube elements and companion cells in the phloem. This indicates the involvement of sucrose synthase in the catabolism of sucrose to generate ATP for phloem loading and unloading (Koch 2004). There are different isoforms of sucrose synthase, and most plant species have at least two isoforms, which usually have highly homologous amino acid sequences and similar biochemical properties. Sucrose synthase is mainly involved in biosynthesis of sugar polymers, including starch and cellulose and generation of energy (ATP) (Chourey et al. 1998; Coleman et al. 2009; Ruan and Chourey 2006).

2.3.2 *Invertases*

Invertases (INV) are important for metabolic signals that affect the expression of diverse classes of genes that are involved in the regulation of development (Chandra et al. 2012). Invertases respond to stress via controlling carbon allocation and sugar signalling (Barratt et al. 2009; Ruan et al. 2009). For example, invertase β -D-fructofuranosidase (EC 3.2.1.26), plays a significant role in carbon and energy consumption of prokaryotes and eukaryotes, as it catalyses the irreversible hydrolysis of sucrose to glucose and fructose. Produced hexoses are commonly used as metabolic fuel and signalling compounds.

Invertases exist in several isoforms with different biochemical properties and subcellular locations (Sturm 1996; Tymowska-Lalanne and Kreis 1998). They can be grouped on two properties: pH optima for activity, and cellular location. Considering pH optima, there are two groups. The first group, the acid invertases, cleaves sucrose most effectively at a pH between 4.5 - 5.0 and consists of an insoluble, extracellular, cell wall-bound form (cell wall invertases) and a soluble form located in the lumen of the vacuole (vacuolar invertases) (Haouazine-Takvorian et al. 1997; Sherson et al. 2003). The second group, the neutral/alkaline invertases, has a pH optimum of about 7.0 - 7.8. The neutral/alkaline invertases are entirely soluble and appear to be located in the cytosol (cytosol invertases) (Chen and Black 1992; Ende and Laere 1995). Alternatively, considering their sub-cellular locations, INVs are classified as vacuolar, apoplasmic (cell wall), and cytoplasmic isoforms (Sturm 1999), as VIN, CWIN, and CIN, respectively. Although VIN and CWIN are located in different compartments, they share some common biochemical properties like, the N-terminal domains of both have around 100 amino acid residues containing a signal peptide and an N-terminal propeptide that may be associated with protein folding, targeting, and the regulation of activity (Sturm 1999). Both VIN and CIN are soluble with an acidic isoelectric point (pI), whereas CWIN is insoluble and has a basic pI.

I. Cell wall invertases

Cell wall or apoplasmic invertases (CWIN) are hydrolytic enzymes that are tightly bound to the cell wall matrix and are believed to play a role in phloem unloading by ensuring a sharp concentration gradient from source to sink. In addition, CWIN is critical for plant reproductive development. Classically, it is expressed to hydrolyse extracellular sucrose for transport to the developing pollen and seed (Ruan et al. 2010). For example, the CWIN, Nin88, cloned from tobacco is specifically expressed in anthers, particularly the developing microspores and the surrounding tapetum layer (Goetz et al. 2001). The other major role is to re-direct photoassimilates to storage organs of plants and this has been validated in several species (Weschke et al. 2003). Besides, CWIN also plays a role in the regulation of sucrose partitioning, in wound responses and pathogen interactions.

II. Vacuolar invertases

Vacuolar invertases (VIN) hydrolyse sucrose into hexoses in the vacuole. The importance of VIN is to regulate the tissue sugar composition in both source and sink tissues. High VIN activity correlates to the accumulation of hexoses in many organs. For instance, in tomato (*Solanum lycopersicum*) VIN activity increases while hexose accumulates during fruit

ripening. Furthermore, suppression of acid invertase activity by antisense RNA has been shown to increase the sucrose content of tomato fruit (Klann et al. 1996; Ohyama et al. 1995). Post-harvest storage of potato tubers leads to the accumulation of hexose sugar which is proposed to result from sucrose hydrolysis by invertases (Zrenner et al. 1996). Reduction in hexose sugar accumulation in cold-stored potato tubers has been observed when vacuolar invertases are suppressed by antisense (Zrenner et al. 1996) indicating VIN's contributions in cold sweetening of storage potatoes. Another major function of VIN is to respond to stress. Reduction of VIN activities under water deficit correlate to male sterility in wheat and maize which indicates that vacuolar invertases help supply sugar to the reproductive organs (Roitsch and González 2004). The VINs also cleave sucrose in tissues undergoing cell expansion (Sturm and Tang 1999). Evidence indicates CWIN and VIN are involved in the earliest phases of flower development. Their activity supplies hexoses to developing anthers and ovaries before pollination occurs (Ruan et al. 2010).

III. Cytoplasmic invertases

In contrast to the significant progress that has been made in understanding the roles of CWIN and VIN, much less information is available on the function of cytoplasmic invertases (CIN). This is probably due to its instability and low activity (Roitsch and González 2004; Ruan et al. 2003). According to several recent studies, CINs may play a role in channelling sucrose in metabolism (Ruan et al. 2010). They are considered to be 'maintenance' enzymes involved in sucrose breakdown when the acid invertase and sucrose synthase activities are low (Winter and Huber 2000).

IV. Invertases involved in wheat reproductive stages

Sugar supply at the pre anthesis stage is particularly important in determining grain number. The invertase called "IVR1" plays a significant role at this stage (Koonjul et al. 2005). Furthermore, sugar supply to the developing grain at post anthesis is critical for confirming optimum grain size and weight (Van den Ende et al. 2004). A second invertase called "Fructan Exohydrolase or FEH" has a significant role in sugar supply at this stage. It has been reported that the both the enzymes IVR1 and FEH have the potential to supply sugar under drought stressed conditions when most of the normal sugar transportation system is disrupted. Thus, the role of these two invertases in the plant body appears to be crucial in managing sugar supplies during drought stress.

a) Role of IVRI

Stress during pre-anthesis is mainly manifested as abortion of developing pollen and reduction in kernel number per spike. The cause of reduction in grain number depends on the timing of drought stress in relation to plant development. Fewer spikes and a lower spikelet number during tillering and floral meristem differentiation can also reduce grain number, but spikelets and florets may also abort if drought occurs later during floral development as mentioned earlier. Wheat is particularly sensitive to drought stress during the YM stage (Salter and Goode 1967). Under moderate water deficit conditions, male gametophyte sterility can be induced in wheat (Saini 1997; Saini and Westgate 1999).

Expression of *IVRI*, the cell wall invertase (CW-INV) gene, is essential in maintaining pollen fertility. *IVRI* is expressed in tapetal tissues that surround the pollen during their development stage and supplies essential energy substrates through it to support pollen growth. Anther cell wall invertase activity and gene (*IVRI*) expression both are down regulated in drought-stressed wheat anthers, which leads to abnormal deposition, as well as changes in the profile of other sugars in anthers (Dorion et al. 1996; Koonjul et al. 2005)). Under water deficit condition, starch is accumulated in connective tissues of wheat anthers (Lalonde et al. 1997) which leads to starvation of the pollen's energy source, resulting in sterility, reduced grain number and ultimately reduced yield (Koonjul et al. 2005; Parish et al. 2012; Powell et al. 2012). A positive correlation between *IVRI* gene expression and pollen fertility has been observed (Ji et al. 2010) under drought which is consistent with similar studies (Koonjul et al. 2005).

In wheat, the *IVRI* gene family has eight isoforms. Among them five are recently identified by screening of IWGSC survey sequence annotation, which exist on multiple chromosome arms and on all three genomes (A, B and D): *IVRI-3A*, *IVRI-4A*, *IVRI-5B*, *IVRI.2-3B* and *IVRI-5D* (Webster et al. 2012). Whereas, three *IVRI* isoforms were previously characterised (*IVRI.1-1A*, *IVRI.2-1A* and *IVRI.1-3B*) (Koonjul et al. 2005). The sequence variation exists amongst the eight members of *IVRI* gene family. They are located on four separate chromosome arms of the wheat genome, *IVRI* provides wheat the flexibility to maintain carbohydrate supply to its developing reproductive structures, thus ensuring viable pollen development even though in drought conditions (Webster et al. 2012). The network involved in maintaining the sugars at an optimum level includes the interactions of a protein inhibitor with the invertase to moderate the breakdown of sucrose to glucose and fructose.

b) Role of fructan exohydrolase

Generally, plants do not immediately exploit all the carbon skeletons derived from photosynthesis. Rather plants stock them as short or long-term reserves. To store carbohydrates in vegetative tissues, plants mainly utilize two profoundly different approaches; either as starch, or as sucrose and its derivatives. Following flowering, the ability to accumulate carbohydrates in the stem and leaf sheaths and to remobilise these to the developing reproductive structures is important for grain weight and size. In the later stages of plant development, carbohydrate reserves are subsequently remobilized to reproductive sink tissue (for grain filling). Therefore, the contribution of stored carbohydrates may become the principal source of transported materials (Plaut et al. 2004) during post-anthesis growth. Under drought conditions when photosynthesis is arrested because of decreases in leaf stomatal conductance and net CO₂ assimilation (Gebbing and Schnyder 1999; Ruuska et al. 2006; Yang et al. 2001), the water-soluble carbohydrates play a significant role in maintaining grain size. In wheat, it has been reported that pre-anthesis reserves contribute between 8 and 27 % of the carbon in carbohydrates and from 30 to 47 % of the carbon in proteins of the grain (Gebbing and Schnyder 1999). This contribution further increases up to 40% under drought and heat stress (Davidson and Chevalier 1992).

Fructans, Fru-based oligo- and polysaccharides derived from sucrose (Valluru and Van den Ende 2008) are the main storage form of WSCs in wheat (Goggin and Setter 2004; Schnyder 1993; Wardlaw and Willenbrink 1994). Generally, fructans are stored for a short time in the proximal part of the internodes (Jeong and Housley 1990). Further can comprise 85% of the total WSC of wheat stem internodes (Donaghy et al. 2008). Only 15% of flowering species contain fructans as reserve carbohydrates, mainly within the families Asteraceae, Campanulaceae and Boraginaceae (dicots), and Poaceae and Liliaceae (monocots) (Hendry 1993).

Several types of fructan molecules can be distinguished depending on the linkage type between the fructosyl residues and the location of the glucose residue (Lewis 1993). Five major classes of structurally different fructans have been identified in higher plants, namely inulin, levan, mixed livan, inulin neoseris and levan neoseris. Fructans with a terminal glucose residue including the β (2,1), are called inulin type fructans, principally occurring in dicots, where inulin-type fructans accumulate as long-term reserve carbohydrates in underground storage organs such as roots and tubers (Le Roy et al. 2007). Fructans with the linear β (2,6) structures are called levan type or branched type fructans and these occur in some grasses. Mixed levan composed of both β (2,6) and β (2,1) linkages, is also known as “graminan” type fructan. Most

plant species belonging to the family Poaceae, such as wheat and barley (Bonnett et al. 1997; Carpita et al. 1989) contain “graminan” type fructan.

The inulin neoseries are linear (2-1)-linked β -D-fructosyl units linked to both C1 and C6 of the Glu moiety of the sucrose molecule which are found in the Liliaceae family (e.g. onion and asparagus; (Shiomi 1989). Lastly, levan neoseries are polymers of predominantly β (2-6)-linked fructosyl residues on either end of the Glu moiety of the Suc molecule. These fructans occur in a few grass species including oat (Livingston et al. 1993).

Fructan polymers are produced by the activity of fructosyltransferases (FT) enzymes. Three different fructosyltransferases (FTs) are putatively involved in wheat graminan biosynthesis: sucrose 1-fructosyltransferase (1-SST), fructan 6-fructosyltransferase (6-SFT) and fructan 1-fructosyltransferase (1-FFT) (Yoshida et al. 2007). 1-kestose and glucose are produced from sucrose molecules by the enzyme “sucrose 1-fructosyl transferase (1-SST)”. By using 1-kestose as the preferential donor, further elongation with β (2,1) fructosyl units is catalyzed by the enzyme fructan 1-fructosyl transferase (1-FFT) in dicot plants. By contrast, in cereals, 1-kestose is used as acceptor to produce branched fructan bifurcose (6-kestose) by the enzyme sucrose: fructan 6-fructosyl transferase (6-SFT). Linear levan is produced by further elongation of 6-kestose by the 6-SFT enzyme. Branched graminans can be obtained by the combined action of 6-SFT and 1-FFT (Van den Ende et al. 2003; Van den Ende et al. 2004).

1-SST is considered to play a key role for regulating the flow of carbon in plants (Nagaraj et al. 2004). The principal role for fructans is to bridge the temporal gaps between the reserve availability and demand for growth and metabolism. Mobilization of stored carbohydrates requires hydrolysis of fructans which is catalyzed by fructosylexohydrolases (FEHs). Wheat fructans are degraded by fructosylexohydrolases (FEHs) which only discharge terminal fructosyl units by using water as the acceptor. The degree of polymerization (DP) and total concentration of WSC is determined by the activities of both 1-SST and total FEH (Yukawa T 1991).

Fructan exohydrolases are enzymes which are responsible for fructan depolymerization (Barnabás et al. 2008). Till now, two different types of FEHs have been characterized and cloned: 1-FEHs preferentially degrading inulin type fructans with β - (2,1) linkage (Van den Ende et al. 2003; Van den Ende et al. 2001) and 6-FEHs preferentially degrading the β -(2,6) linkage which is called levan type fructans (Van den Ende et al. 2003; Van Riet et al. 2006). In addition, 6 & 1-FEHs is another type, which degrades both inulin and levan (De Coninck et al. 2005; Kawakami et al. 2005).

FEH activity has been localized in the vacuole although the cDNAs shows more similarity with cell wall than with vacuolar invertases (Wiemken et al. 1986). They also contain the conserved WECPD motif typical for cell-wall-like invertases (Tymowska-Lalanne and Kreis 1998). However, all FEHs have a low isoelectric point like the vacuolar invertases while most cell wall invertases have a high isoelectric point, which is probably due to stronger binding to the cell wall. However, it is proposed (Van den Ende et al. 2002) that FEHs are derived from cell-wall-like invertase ancestors, whereas fructan-synthesizing enzymes are likely to be derived from vacuolar invertases.

In plants, FEHs play many crucial roles through the hydrolysis of fructan reserves (Van den Ende et al. 2001). In cereal crops, during terminal drought condition, FEHs supplies sugar for grain filling from reserve source (Yang et al. 2004; Zhang et al. 2009). In some flowering plants, FEHs contribute to the osmotic pressure for petal expansion (e.g. *Campanula* flower, daylily opening) (Bielecki 1993; Vergauwen et al. 2000). It has been postulated that FEH contributes to frost tolerance by stabilizing membranes (inulin is broken down and stabilizes liposomes) (Hincha et al. 2000; Vereyken et al. 2003). Although, FEH is mainly involved in breakdown of fructan, it has been reported that 1-FEH might play a role in trimming of the linear β -(2,1)-linked fructofuranosyl unit during biosynthesis of fructan (Van den Ende et al. 2003).

Three isoforms of *1-FEH* have been found: *1-FEH w1* (1-FEH-6A), *1-FEH w2* (1-FEH-6D) and *1-FEH w3* (1-FEH-6B) (Zhang et al. 2008). It has been suggested that dominant expression of *1-FEH w3* might facilitate higher fructan remobilization under drought conditions (Zhang et al. 2009). However, recent studies indicate that not only 1-FEH but also 6-FEHs are playing a significant role in this regard (Joudi et al. 2012). Thus, it is likely that combined activities of more than one FEHs could potentially contribute to enhance the utilization of stem WSC under drought stress. Thus, further investigation is needed to characterise the expressional behaviour of all three isoforms under drought and the expression of 6-FEH as well. Moreover, the broken reserve carbohydrates released by FEH in the stem need to be transported to the developing grain. This long-distance transport is controlled by sucrose transporters.

2.3.3 Sucrose transporters

In higher plants, growth and development depends on efficient and controlled distribution of sucrose, from source to sink. The yield-determining factor in cereal crops is deposition of starch in seeds, which is mainly reliant on sugar supply from the source tissues through the phloem. Recent research findings have provided new understandings about the photo-assimilate

(sucrose) translocation mechanism, from sites of synthesis to the sites of utilisation or storage in sink organs. Briefly, sucrose produced in mesophyll cells is loaded into the sieve element-companion cell complex either apoplastically by sucrose transporters (Setou et al. 2010) for long distance transport or symplastically through plasmodesmata for short distance transport. For the apoplastic transport, sucrose enters into the cell wall space and is actively taken up by sucrose transporter, known as “SUTs” localized in companion cells that have no plasmodesmata connection and membrane projections (e.g. in spinach) (Lohaus et al. 1995; Truernit 2001). On the other hand, the symplastic transport comprises cell to cell movement through plasmodesmatal connections. Sucrose transporters play a central role, as they orchestrate sucrose allocation both intra-cellularly and at the whole plant level. Besides, they are also an essential components of signal transduction among sink and source metabolism (Kühn and Grof 2010).

Sucrose supply to terminal sink organs and apical meristems is crucial for the energy status and the control of flowering or tuber onset thereby affecting crop yield. In developing cereal seeds, phloem releases sucrose into maternal tissues such as the maize pedicel and the pericarp of wheat, barley and rice. As the endosperm and embryos are not simplistically connected, they are dependent on the apoplastic path way for supply (Lim et al. 2006). Sucrose transporters are tightly controlled at various levels, allowing adaptation to external stimuli such as temperature, light regime, photoperiod, pathogen attack or other stresses in the grains of barley, rice and wheat (Kühn and Grof 2010). A number of different plant species including rice, barley, wheat and maize, have genes encoding SUTs. On the basis of comparison of their deduced amino acid sequences, SUTs are categorized into three major groups: SUT1 (Type I), SUT2/SUC3 (Type II), and SUT4 (Type III) (Aoki et al. 2003; Kühn 2003).

SUT1 has been reported to play a major role at the maternal/filial interface where two essential transport steps, sucrose efflux and subsequently sucrose influx, take place. However, energy-independent effluxers have been identified in developing legume seeds (Kühn and Grof 2010).

2.4 Mass spectrometry imaging

Developmental changes in higher plants at the macro level can be identified by different phenotypic appearances. Furthermore, some heterogeneity at the cellular and subcellular level can be distinguished by microscopic examination. However, characterising the distribution of macromolecules (e.g. DNA, mRNA and protein) within tissues and organs is challenging which has been emphasized in last two decades (Amstalden van Hove et al. 2010). Knowledge of the complex biochemical process of plant development within cell, tissues, organs and whole

systems is limited by relating to only to the timing of developmental stage but also need to determine the distribution and localization of key molecular event. To localise metabolites, some techniques have been developed building on traditional histological methods that rely on an interaction between an external probe and an *in-situ* macromolecule. Immuno-localization of protein and *in situ* hybridization to mRNA and DNA are examples of this technique. In recent decades, Green Fluorescent Protein (Chalfie et al. 1994; Prasher 1995; Tsien 1998) and its variants with different fluorescence attributes have been used to visualize the location of protein gene products at cellular and subcellular levels. However, it is difficult to acquire data for metabolites which are relatively smaller in size and products of biological process catalyzed by enzymes. To overcome this limitation, over the last decade, emphasis has been placed on chemical imaging systems.

The proverb “A picture is worth a thousand words” states the idea that just a single image can describe a complex set of information. It also appropriately characterizes one of the main goals of visualization, namely making it possible to absorb large amounts of data quickly. Mass spectrometry imaging (MSI) is considered as one of the powerful techniques in this field. The principle of this imaging is combining molecular mass analysis with the localization and visualization of molecules on complex surfaces. Unlike other techniques, MSI is label-free and delivers instant information about the spatial distribution and quantity of metabolite within a thin tissue section or the surface of a sample (Alexandrov and Bartels 2013). MS imaging is considered as an efficient tool for identification and localization of elements, pharmaceuticals, metabolites, lipids, peptides and proteins in biological tissues (Alexandrov and Bartels 2013; Chaurand 2012; McDonnell and Heeren 2007).

Considerable developments in MSI has been achieved over the past decade with extensive applications within biology and medicine (Chaurand 2012; Jungmann and Heeren 2012; Watrous et al. 2011). At the beginning, MSI was mainly applied for clinical and (bio) pharmaceutical research such as biomarker discovery, drug development studies and food analyses (Caprioli et al. 1997; Chughtai and Heeren 2010; Prideaux and Stoeckli 2012; Schwamborn 2012; Shariatgorji et al. 2014). More recently, development in techniques and availability of the instrument commercially is leading to the application of MSI for assessing the spatial localisation of plant proteins (Bjarnholt et al. 2014). However, the use of MSI in plant science is quite limited and the number of biological results obtained with these methods is still small.

2.4.1 Principle of MSI

Mass spectrometry is an imaging technique, which has unique ability to provide an image in to identify structures and has the qualities to provide chemical information to unravel molecular changes in observed parts of the sample. Steps of MSI are tissue preparation, matrix application [for matrix-assisted laser desorption ionization (MALDI) applications], data acquisition, followed by data analysis and image construction. MS data are acquired by desorbing analyte molecules from the tissue followed by ionization to create positively or negatively charged ions. The technique is generally a combination of two features; the first is related to the mass spectrometry technique that permits the mass of the molecules to be determined, by measuring their m/z ratio and the second identification of the spatial distribution of the measured sample. Two different approaches of ion detection used in MSI instruments are, the microprobe (Chughtai and Heeren 2010) and the microscope (Luxembourg et al., 2004). Differences between two methods relate to how the spatial information is obtained. In the first approach, the sample is restored with appropriate ion sources (a laser beam or primary ion beam) and the analyte ions are detected separately from each point. Thus, the spectra obtained from different points provide both the m/z values and intensities of the signals. The distribution map of intensities is then plotted as a function of x and y localization. Finally, an image of the differential distribution of molecular substances (lipids, peptides, proteins, etc.) on the sample surface is produced.

In the microscope imaging mode, ion optical microscope elements are used to project the spatial distribution of the ions generated at the sample surface onto a position-sensitive detector such as a Micro Channel Plate (MCP). The spatial resolution is independent of the spot size of the ionizing beam. Ions are desorbed simultaneously from a relatively large sample area (typically 100 ± 300 mm in diameter) (McDonnell and Heeren 2007). The sample can be examined without moving the sample or the laser spot (Fig. 2.3). MCP and hybrid pixel detector are combined in this system. Where MCP is responsible for transformation of the single ion hit into the electron shower which is then detected by the hybrid pixel detector. So from the whole scanned area, a single m/z is acquired at once, while magnifying the image and retaining spatial information. As in this mode a large area is measured, hence a considerable reduction of time is required for a particular measurement.

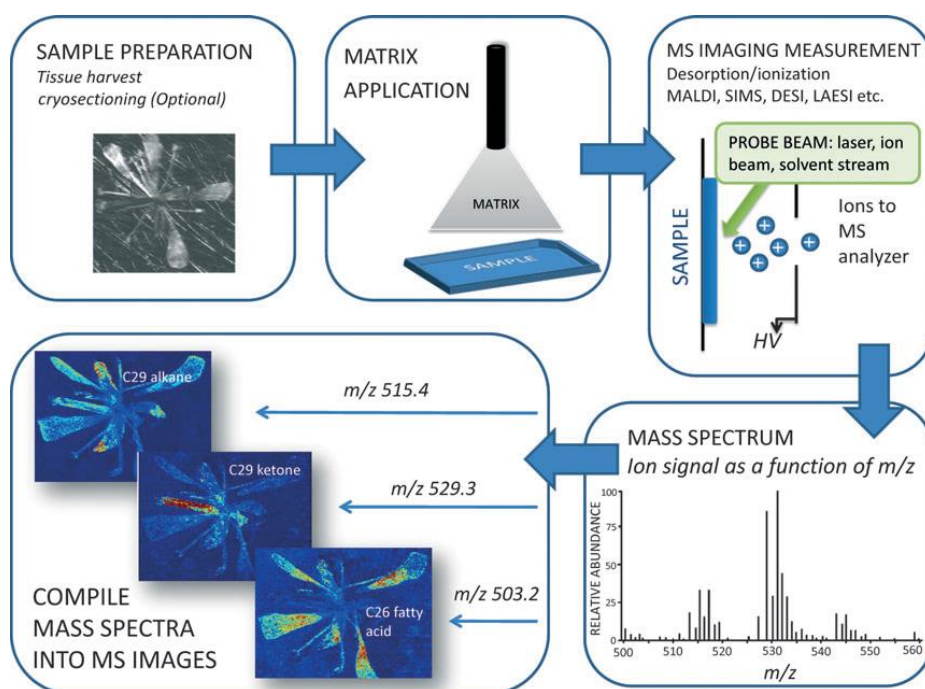


Fig. 2.2: Schematic representation of mass spectrometry imaging. Source (Lee et al. 2012).

2.4.2 Different types of Ionization

A variety of ionization sources are available depending on the probing beam that is used to interrogate tissue samples. Most commonly used ionization sources are laser ablation electrospray imaging (LAESI), Secondary Ion Mass Spectrometry (Bonnett et al.), Desorption Electrospray Ionization (DESI) and MALDI imaging (Matrix-assisted laser desorption imaging). Some of their features are described

2.4.3 Laser Ablation Electrospray imaging (LAESI)

This technique of mass spectrometry imaging offers analysis of biomolecules under ambient conditions and enables the action of explore diverse biochemical changes in organism at *in-vivo* condition with high specificity. Desorption and ionization processes are two separate steps for LAESI. In first step, mid infrared laser native water molecules absorb photons focused on the sample surface and an ablation event is created. Then, in the next step, the ablated molecules are post ionized by an electrospray solvent stream (Nemes and Vertes 2007). Laser application in this imaging not only for ablation of the sample to be ionized but also as a means to probe several layers in the sample which helps achieve depth profiling. The three-dimensional views of the distribution of analyte molecules are found to exhibit tissue specific metabolite

accumulation patterns which developed from the multiple acquirement of two dimensional MSI data (Nemes et al. 2009). LAESI has been successfully applied in imaging studies of plant material to acquire information of primary and secondary metabolites. LAESI is a direct analysis technique where pre-treatment of the sample and matrix application is not required and, furthermore, can be operate exclusively at atmospheric pressure (AP). However, it is significantly higher in price than other ion sources.

2.4.4 Secondary ion mass spectrometry

Secondary Ion Mass Spectrometry (SMS) was introduced for imaging in the 1980's (Briggs 1983) and considered as the first of the MS imaging techniques. At the very beginning, physicists and physical chemists were using this technique in research focused on the process desorption and ionization. SIMS operates under high vacuum and uses high energetic (5-40 kV) primary ions for ionization, which offers very high resolution over the other MS imaging techniques. As the energy is comparatively higher than the covalent bond energies, a higher degree of fragmentation occurs in the surface, which is considered to be the main disadvantage of this technique (Lee et al. 2012). Besides that, samples need to be freeze dried and then introduced into high vacuum pressure, which might cause a risk for volatile analytes to evaporate on vacuum before detection. SIMS instrument cost is significantly higher than other MSI instrument. Even though this was the first imaging technique still the availability of equipment in laboratories around the world is very limited. There is very little application of SIMS in plant material but has been used in some wood plants (Imai et al. 2005)

2.4.5 Desorption Electrospray Ionization (DESI)

To overcome the limitation of the analyte evaporation before detection a new ionization technique called as Desorption Electrospray Ionization (DESI) was introduced in 2004 (Takáts et al. 2004). DESI is carried out by directing electro sprayed charged droplets and solvent ions onto the surface to be analysed. The electrospray is generated by a low flow of solvent and the application of high voltage to the liquid. The droplets first produce a thin liquid film on the sample surface where compounds of interest are extracted. However, the basic principles of DESI ionization involve, similar to normal electrospray techniques that made it suitable for polar compounds in positive or negative ionization mode (Chaurand 2012; Lee et al. 2012). The limitation of DESI, compared with MALDI and SIMS is its spatial resolution. Typically, the ionization spot is around 200 μm and sometimes it might be 100 μm , although a resolution of 35 μm has been obtained (Campbell et al. 2012). But the advantages of the techniques are

that it can take place under ambient conditions and sample preparation is very easy since it doesn't require matrix application. Moreover, DESI can work both in positive and negative ion mode while MALDI only works at positive ion mode. Furthermore, DESI instruments are not very expensive and are widely available.

2.4.5 Matrix assisted laser desorption ionization imaging (MALDI)

MALDI is the most extensively used MS imaging technique for animal and plant tissues. This method is efficient for inspecting the distribution of molecules within biological systems through direct analysis of thin tissue sections.

Changes within tissues during plant development or from environmental factors can be obtained by MALDI-MSI, providing high resolution information about proteins, amino acids and other metabolites (Grassl et al. 2011). For this approach, tissue sections are coated with a thin layer of energy-absorbing matrix and then the samples are analysed to produce an ordered array of mass spectra. Molecules desorbed from the sample, typically are singly protonated, giving an ion at $(M+H)^+$, where M is the molecular mass. In mass spectrometry imaging, m/z (mass to charge) values provide the capability of mapping specific molecules into two-dimensional coordination of the original sample. For localizing specific compounds in the tissue or to obtain the total ion image in the sample, images are displayed as individual m/z values as a selected ion image. In MALDI imaging it is possible to get the metabolic status of the investigated tissue from a snapshot in one analysis and thus acquire information about known and unknown compounds based on functional characteristics (Sarsby et al. 2012).

Matrix application is considered as the unique part of MALDI-MSI because it is a critical factor of spatial resolution in addition to the number of ions detected (Cornett et al. 2007). The matrix contains small organic molecules which are designed to absorb energy of a pulsed laser beam. Matrix crystals are formed on the surface of the molecule during the matrix deposition. Co-crystallization of matrix with the analyte molecules is considered essential and depends on the solvent, time of incubation, and matrix concentration reference here. Energy absorbed from the laser beam causes explosive desorption of the matrix crystals, together with the analyte. The most common and least expensive devices available for applying matrix are hand-held aerosol sprayers or airbrushed but electric sprayers are also used for matrix application. The most commonly used matrices are *o*-cyano-4-hydroxycinnamic acid (CHCA), 2,5-dihydroxybenzoic (DHB) and sinapinic acid (SA) (Grassl et al. 2011).

Typically, tissue sample of 5-20 μm thick are spray-coated with the MALDI matrix. Then the samples are placed in the mass spectrometer. After that spectra are acquired at distinct places according to predefined rectangular x, y grid. Therefore, the resulting dataset contains an array of spectra where each spectrum is an independent molecular profile of the area which is irradiated by the laser. A spectrum consists of thousands of signals of measured mass and intensity. The intensity of any given signal, or combinations of signals, can then be plotted on the original coordinate system, generating an image of that signal over the sample surface. Thus, MALDI- MSI analysis is able give hundreds of such comparative distribution maps in a relatively short time, (Cornett et al. 2007). MALDI is considered as a “soft” ionization technique because molecules of ionized samples are not destroyed. It means spectra obtained from these images are less complicated and it is easy to measure higher molecular weight substances (Kaspar et al. 2011).

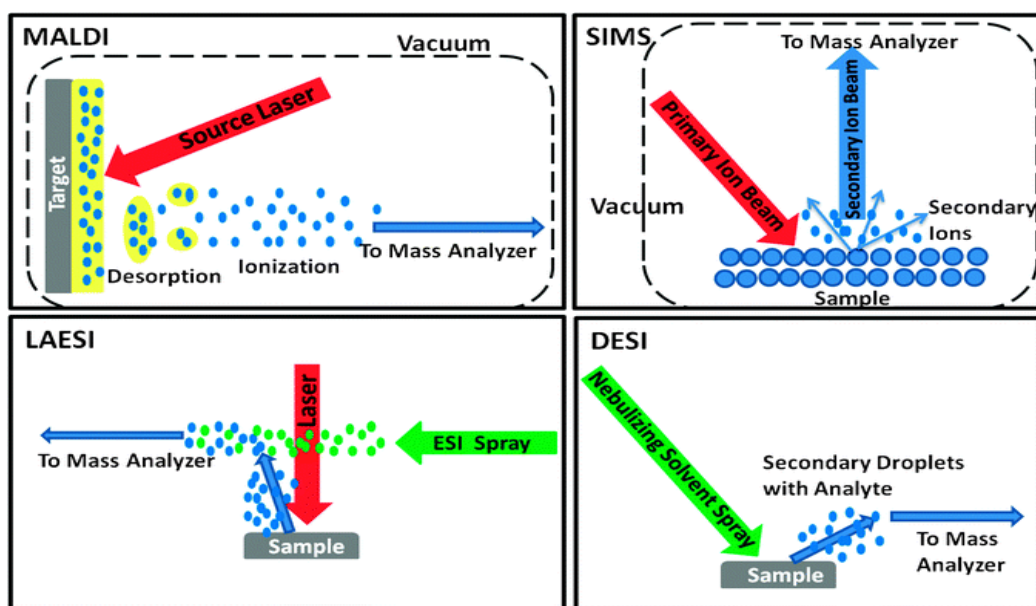


Fig. 2.3: Different types of ionization technique. Source (Siegel et al. 2018).

2.5 Conclusion

Abiotic stress, particularly drought is one of the most challenging obstacles in the push to increase wheat grain yield to meet the need of the future population. Drought during reproduction has devastating consequences for the transportation of sugars to the developing grain, resulting in lower grain weight. FEH have been reported to play a significant role in sugar transportation to the developing grain particularly under water deficit. However, the molecular basis of this enzyme family is complex, involving multiple genes. Thus, a better understanding of functional attributes of the enzymes involved in sugar transport in plants experiencing drought will build a stronger base for breeding programs towards drought tolerant varieties.

Chapter 3: *1-FEH w3* in wheat accelerates stem water-soluble carbohydrate remobilization to grain under post anthesis water-deficit condition

3.1 Introduction

As described in Chapter 2, water-deficit during grain filling is common in many parts of the world, reducing photosynthesis and increasing the dependency of wheat crops on water soluble carbohydrate stored in the stem for grain filling. Stem WSC is composed of glucose, fructose, sucrose and fructan. Wheat fructans are mainly of the ‘graminan-type’, containing both β -(2,1) and β -(2,6) linkages. Remobilization of stored carbohydrates requires depolymerisation (hydrolysis) of fructans which is regulated by the activity of a class of enzymes called fructan exohydrolases (FEHs) (Barnabás et al. 2008). So far, two different types of FEHs have been characterized and cloned: 1-FEHs that preferentially degrade inulin type fructans having β -(2,1) linkage (Van den Ende et al. 2003; Van den Ende et al. 2001); and 6-FEHs that degrade levan type fructans with β -(2,6) linkage (Doyle and Fischer 1979) (Van den Ende et al. 2003; Van Riet et al. 2006). However, there is another minor type of FEHs known as 6 & 1-FEHs which degrade both linkages (De Coninck et al. 2005; Kawakami et al. 2005).

1-FEH is the focus for the research in this chapter since it has been reported as catalysing fructan breakdown and is a putative β -(2,1)-trimmer during the period of active fructan biosynthesis (Van den Ende et al. 2003). Elevated 1-FEH activities lead to the breakdown of fructan thus releasing more sucrose and fructose when the demand for sucrose is high for grain filling (Kawakami and Yoshida 2005; Van den Ende et al. 2003; Van den Ende and Valluru 2008; Van Riet et al. 2008; Yang et al. 2004). Three isoforms of *1-FEH* gene have been reported: *1-FEH w1* (*1-FEH-6A*), *1-FEH w2* (*1-FEH-6D*) and *1-FEH w3* (*1-FEH-6B*). Zhang et al. (2009) suggested that dominant expression of *1-FEH w3* might facilitate higher fructan remobilization under terminal water-deficit (Zhang et al. 2009). However, the individual functions of the three isoforms are still unknown, probably due to the complex nature of the plant’s response to water-deficit stress.

Mutating particular gene/s of interest is a common genetic approach to study biological phenomena and defining gene function. Knocking out genes is a straightforward method of producing gene mutation lines, which has been used in many studies. While mutation lines are important for forward genetics studies of gene function, recent advancement in sequencing the

wheat genome (Appels et al. 2018) enables their applications in reverse genetics as well. For example, in *Arabidopsis*, the glucose *insensitive2* (gene2) mutant line helped to reveal the physiological function of specific hexokinase (HXK1) in the glucose-signalling network (Moore et al. 2003). However, in polyploidy plant species like wheat, which contain multiple copies of the same gene (homologous gene) encoded by each of the ancestral genomes, mutational gene inactivation/deletion is very important to determine whether different copies of the same or related genes are functionally active or redundant (Fitzgerald et al. 2010).

Knockout mutation lines of each of the three isoforms (*1-FEH w1*, *w2* and *w3*) were developed by heavy ion bombardment at CSIRO, Canberra, Australia. Since it has been reported that *1-FEH* plays a role in WSC remobilisation under water-deficit, the mutation lines of the three isoforms were developed on the background of Chara (Fitzgerald et al. 2010), which is moderately water-deficit tolerant, and a key commercial Australian wheat cultivar. According to publications and other reports, these were the only mutation lines available to investigate the function of *1-FEH w1*, *w2* and *w3*.

The purpose of this study was to characterise the response of each mutation line to WSC remobilisation and how that is influenced by terminal water stress. The null hypothesis of this study was: there is no variation in the roles of the three isoforms (*1-FEH w1*, *w2* and *w3*) of *1-FEH* on remobilisation of WSC under terminal water-deficit. The knowledge generated from this research project has the potential reveal the contribution of individual isoforms in stress management and will also contribute to the platform for more detailed investigation of their expressional behaviour.

3.2 Materials and methods

The experiment was carried out in a Murdoch University glasshouse to investigate the influence of individual isoforms of *1-FEH* on WSC remobilization under terminal water-deficit. A preliminary experiment was undertaken and is reported in Appendix 1.

3.2.1 Plant material

A set of mutation lines of the three isoforms of *1-FEH* (*1-FEH w1*, *w2* and *w3*), previously developed in Australian wheat cultivar Chara (described above in the Introduction), was bulked up by Dr. Jingjuan Zhang in Murdoch University glasshouse (2012) and used in this experiment. A total of six (Table 3.1.) germplasms were included in the study as follows: 1 line of *w1* mutant, 2 lines of *w2* mutant, 2 lines of *w3* mutant, and the parent Chara. The most efficient line has been selected in preliminary experiment (Appendix 1).

3.2.2 Water-deficit experiment

I. Experimental design

The experiment was set up as a Randomized Complete Block Design (RCBD) with 3-factors (Germplasm X Environment X Harvest) and 3 replications. Factor A: germplasm (6, as detailed Table 3.1); Factor B: treatments (2: water-deficit and control); Factor C: harvest (9, Table 3.1) resulting in a total of 324 pots. Pots were initially randomized following the DiGger design of R statistical software. To ensure equal solar radiation to all plants, pots were then rotated every alternate day.

Table 3.1: Experimental factors and levels in the main experiment.

Factor		Level	
A	Line	1	w1 mutant line -BW22-M3-22-w1
		2	w2 mutant line -BW18b-M3-646-w2
		3	w2 mutant line -BW21-M3-433-w2
		4	w3 mutant line -BW18b-M3-426-w3
		5	w3 mutant line -BW22-M3-571-w3
		6	Parent: Chara
B	Treatment	1	Terminal water-deficit (water-deficit imposed from anthesis (50% plants at flowering stage) until maturity)
		2	Well-watered
C	Growth stage	1	AR5 (Auricle distance 5 cm)
		2	Full emerged spikelet
		3	7 days after anthesis
		4	12 days after anthesis
		5	17 days after anthesis
		6	22 days after anthesis
		7	27 days after anthesis
		8	32 days after anthesis
		9	At maturity

II. Potting mix

The potting mix was the same as used previously to grow wheat in glasshouses at Murdoch University (Zhang et al. 2009). Briefly, basal fertilizer (mg /kg: 1220 N, 368 P, 819 K plus a standard micronutrient mix) were incorporated with a potting mix which consisted of 2 parts composted pine fine bark, 1-part coconut fibre peat and 2 parts coarse river sand. After homogenisation, 4 L free-draining polythene pots were filled with equal amounts (by weight) of the air-dried potting mix and steam pasteurized for 2 h before sowing.

III. Seed germination

Seed were germinated on wet filter paper in Petri dishes at 4°C for 14 days. Six seedlings were planted in each pot, and thinned to 4 plants per pot at the 3-leaf stage.

IV. Glasshouse set up

Temperature and relative humidity in the glasshouse were controlled within a threshold range. The average temperature thresholds for night and day were 15°C and 25°C, respectively, and for humidity were 80% and 50%, respectively. The day length was not controlled hence the photoperiod changed with season. The day lengths ranged from 12 hours in June to 14 hours in November. Plants were watered using an irrigation mat for 5 minutes each, 3 times per day.

V. Imposing water-deficit

The main stem was identified at the mid-tillering stage and the flowering date was recorded for every plant by tagging them on the first flowering date. When 50% of the plants were flowering, half of the plants were exposed to water-deficit until grain maturity by turning off the water supply from irrigation mat, and the other half were kept well-watered. In this stage, pots were arranged in four benches (two for water-deficit plants and two for well-watered plants). Weight of the unwatered pots was taken each second day to determine the extent of water loss and the well-watered plants were weighed once a week to confirm the well-watered condition (65% moisture). Water was turned off to the well-watered pots, when plants became yellow on maturity.

VI. Sampling

The first sample was collected at the AR5 stage followed by the second sample collected at spikelet initiation stage and the following six samplings for the preliminary and the main experiments were carried out with 4 days' interval after initiation of the water-deficit treatment (Table 3.1). The final sample was collected at the maturity. Sampling for WSC analysis was undertaken between 11.00 to 17.00 h to study the shoot carbohydrate reserve accumulation and remobilization pattern during grain filling. Three main stems were collected from each pot and Three replicates were collected for each samples.

Three organs (the stem, leaf sheath and blade) for each sample were collected from the main tiller of three plants of each pot and immediately put on dry ice. The remaining two plants were left for maturity and seed collection. Samples were than stored at -20°C. Frozen samples were

chopped manually using a tissue-lyser into less than 5 mm pieces in a cold room, mixed together and manually divided into two parts. One part was stored at -80°C for the RNA study and the other was kept at -20°C for WSC analysis.

Harvest data were collected at maturity from the main stem and the tillers of 9 plants from 3 pots per line per treatment. The following parameters were recorded: kernel number (KN) per main spike, KN per plant, and number of spikelets per plant. Grain was oven dried for 10 h at 60°C and grain weight per main spike, grain weight per plant, and thousand grain weight (TGW) of the main spike taken to determine the yield.

VII. Carbohydrate analysis

Samples (3 biological replicates and 3 technical replicates were used) for carbohydrate analysis were freeze dried (-50°C) for 72 h than oven dried (70°C) for 24 h. Samples were ground in a hammer mill (Glen Creston, England) to pass through a 0.5 mm sieve. Carbohydrate analysis was performed on 170 mg of each ground sample using boiling deionized water for carbohydrate extraction followed by colorimetry using anthrone reagent [0.2 g anthrone with 100 ml H₂SO₄ (98%)] (Fales 1951; Zhang et al. 2009).

VIII. Calculation of WSC remobilization

The WSC concentration was highest at 12 DAA in all mutation lines and Chara. The WSC started declining from 12 DAA and the rate of decline was high up to 22 DAA. Therefore, WSC remobilization was calculated from 12 DAA to 22 DAA.

WSC remobilization rate (%dw*day⁻¹) = (Stem WSC concentration (%dw) at 12 DAA - Stem WSC concentration (%dw) at 22 DAA)/10

IX. Data analysis

Analysis of variance (Stepanova and Alonso) on sugar components, and level of gene expression were performed using IBM SPSS Statistics V21.0. Post-hoc comparisons were conducted using Duncans new Multiple Range Test at $P < 0.05$. Graphs were generated using Sigmaplot 13.0.

Note that results for the Preliminary Experiment are given in Appendix mentioned in the discussion. Only the main Experiment is reported on in the results section of this chapter, due to the preliminary experiment being compromised by light.

3.3 Results

3.3.1 Confirmation of gene mutations

Mutations of the target isoforms of *1-FEH* gene in the lines used in this experiment were confirmed by polymeric chain reaction (PCR). A set of previously published primers: Forward: GACTCCATACAATCCCCAGGAC and Reverse: GACGCCAGCTCAAAACCTATCT were used to detect the mutations (Khoshro et al. 2014). The primer set has been designed on intron number 4 (Fig. 3.1). *1-FEH w1*, *w2* and *w3* have 7 exons and 6 introns. The exon sequences are highly conserved (over 97%) but there are variations within intron 1 and intron 4. Intron 4 harbours the largest sequence length variations between different isoforms. The primer amplifies isoform *w1* at 476bp; *w2* at 409bp and *w3* at 573 bp.

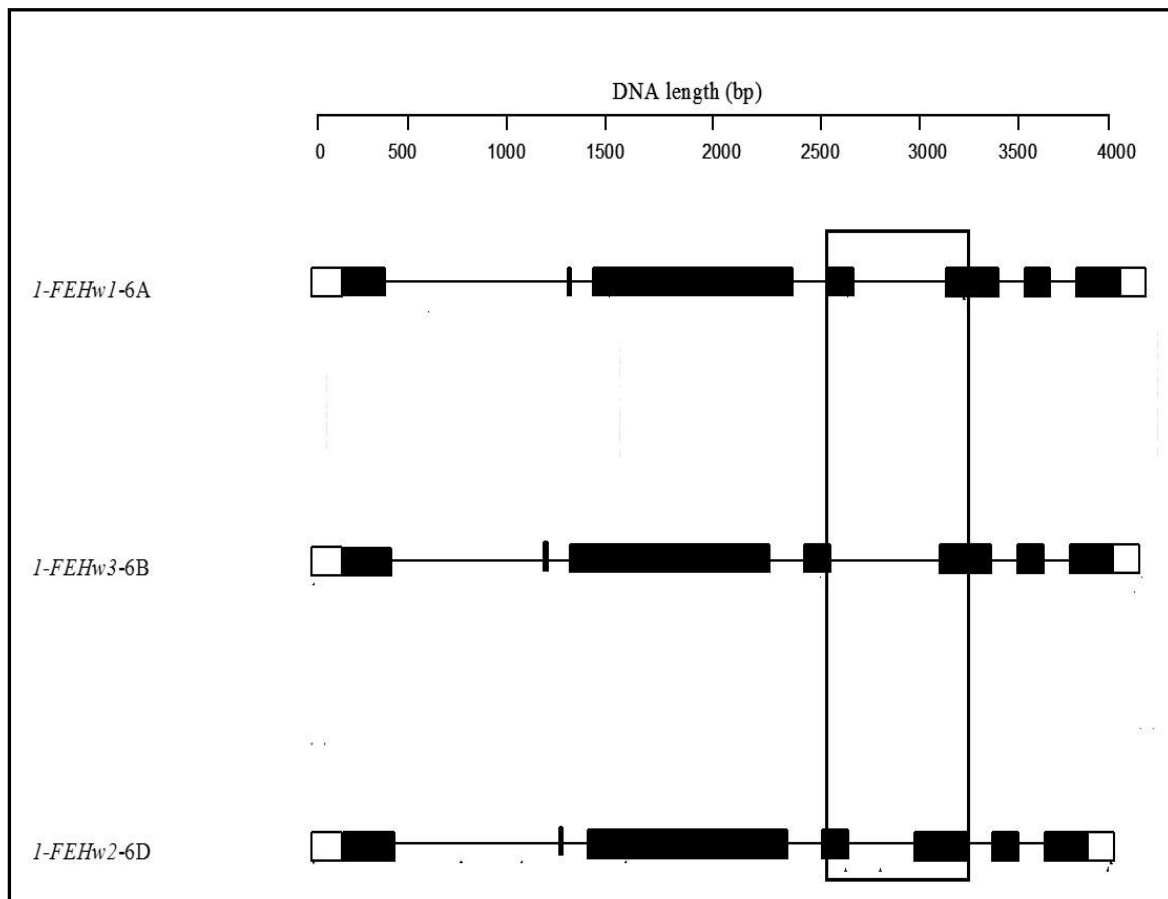


Fig. 3.1: Primer locations (the black box indicate the locations of primer in chromosomes 6A, 6B and 6D). Exons are indicated as thick black areas and introns are the narrow lines.

The parental cultivar Chara amplified at 476 bp (*1-FEH w1*), 409 bp (*1-FEH w2*) and 573 bp (*1-FEH w3*) indicating the presence of all of the three isoforms. In each mutation line, the corresponding isoform was absent while the other two isoforms were clearly detected (Fig.

3.2). For example, the *1-FEH w1* mutation line did not amplify at 476 bp but amplified at 409 and 573 bp indicating that the *w1* isoforms had been deleted in this line, but *w2* and *w3* remained as they are in the parental line.

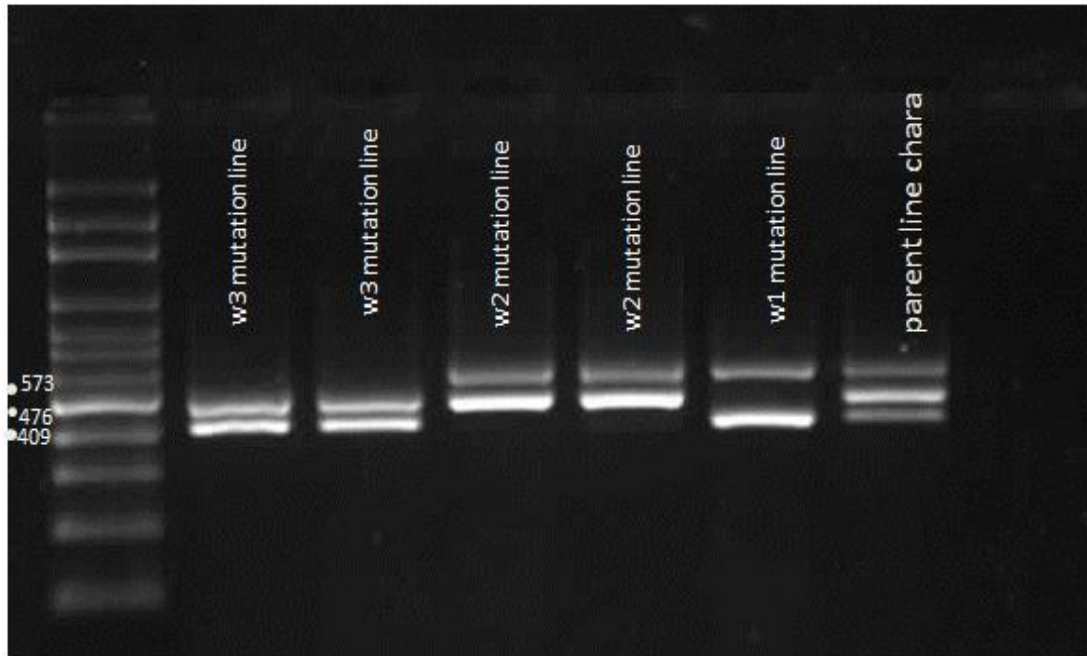


Fig. 3.2: Verification of deletion in different mutation lines: 573 bp band for *1-FEH w3* (present in 6B genome), 409 bp band for *1-FEH w2* (present in 6D genome) and 476 bp band for *1-FEH w1* (present in 6A genome).

3.3.2 Observation of the water-deficit regime

Plants were imposed to water-deficit when 50% of the plants started flowering by withdrawing the water supply beneath the pots. Passage of the water-deficit regime was measured by the soil water content, which gradually declined in the water-deficit affected pots (Fig. 3.3). Before the water-deficit treatment, soil was at field capacity (65% of soil moisture content). By 14 days after the water-deficit treatment was imposed, the soil moisture content had fallen to 22% and plants were showing signs of mild stress (first visible at 10 days) from leaf wilting. Plants reached permanent wilting point (13% soil moisture content) after 20 days of water being withheld. Water-deficit promoted early senescence compared to the well-watered plants (Fig. 3.3).

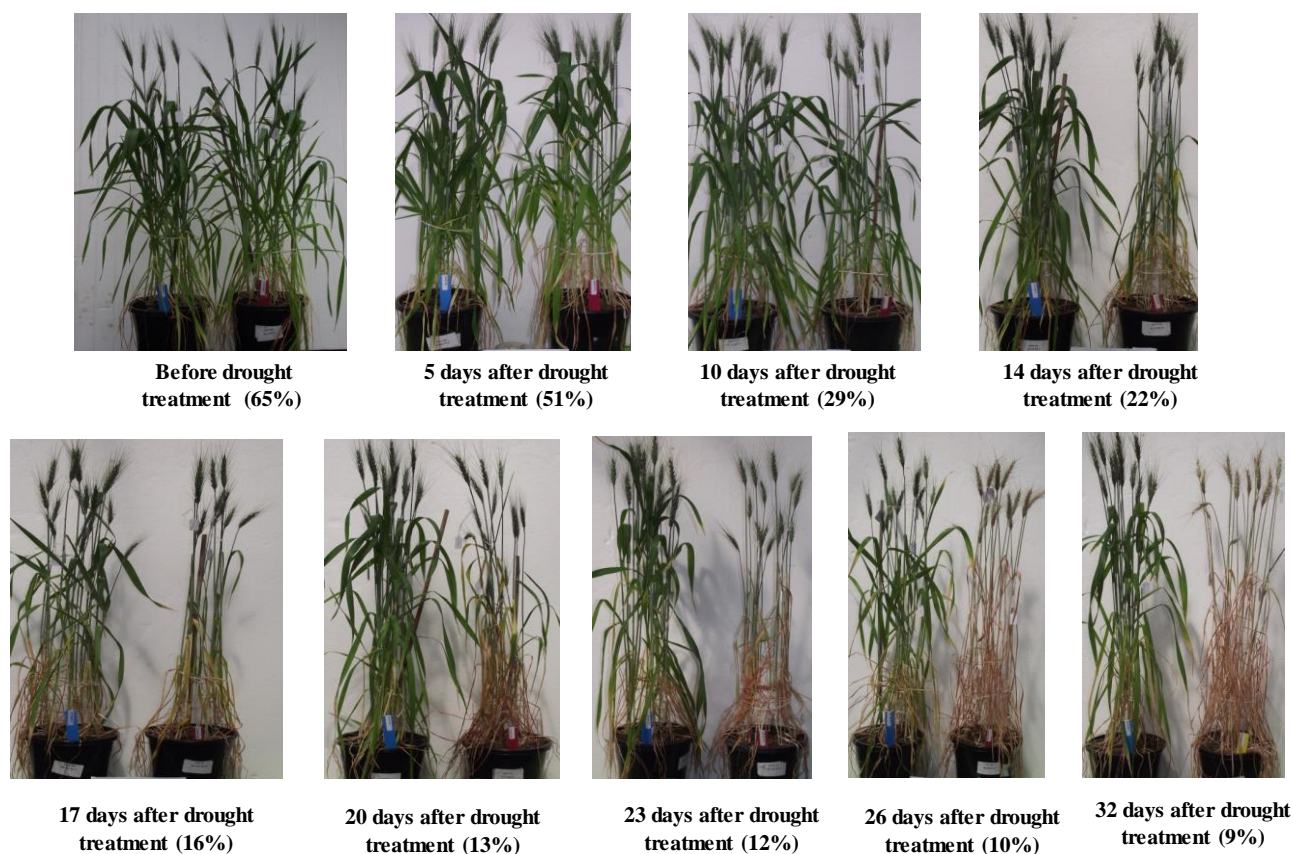


Fig. 3.3: Effect of the water-deficit treatment on physical appearance of wheat plants over time. In each panel, the pot on the left-hand side is well-watered and the pot on right hand side is the water-deficit treatment. The number as % under each panel is the soil moisture content of the water-deficit treated pot. Appearance of wilted leaves and early leaf senescence were noted in the water-deficit treated plants.

3.3.3 Stem WSC remobilisation and grain development

1. Influence of water-deficit and 1-FEH isoforms

a) Water-deficit promoted early remobilisation of WSC

In well-watered plants, stem WSC levels peaked at 27 days after anthesis (DAA). There were no significant differences among parent and mutation lines (*w1*, *w2* and *w3*) (Fig. 3.4). In well-watered plants the highest level of WSC was in Chara, with 34.98% WSC, followed by *w3*, *w2* and *w1* mutation lines with 33.9, 29.9 and 34.5%, respectively. By contrast, under water deficit, WSC peaked at 12 DAA, 15 days earlier than in the well-watered plants. The *w3* mutant line had significantly ($P < 0.05$) lower WSC concentration than the parent Chara, and the other two mutant lines were not different from the parent. The peak WSC concentrations were 31.0, 29.9, 28.5 and 26.3% dry weight in Chara, *1-FEH w1*, *1-FEH w2* and *1-FEH w3*, respectively.

b) Timing of decline in WSC differed among mutation lines

There was clear variation in the pattern of decline in WSC concentration in plants subjected to water deficit. The WSC remobilization rate was slower in the *1-FEH w3* mutant line compared to Chara and other two mutation lines. This was evident by the fact that the *1-FEH w3* mutation line maintained (at 22 DAA) a significantly higher (11.07%) level of stem WSC than Chara (5.72%, $p < 0.07$), *1-FEH w2* (6.68%) and *1-FEH w1* (9.45%) mutant lines (Fig. 3.5). However, there was no significant variation in the timing of decline in stem WSC concentration between Chara and the mutation lines *w3*, *w2* and *w1* in well-watered plants.

c) Response in grain development and yield

There was a negative correlation between WSC concentration and developing grain weight under water deficit (between 12 DAA to 32 DAA), but it was not the case in well-watered plants (Fig. 3.4). In water-deficit plants, the WSC concentration began to decrease from 12 DAA and developing grain weight started to increase, indicating WSC was being remobilised to the grain.

Even though at 12 DAA, there was no significant differences in the main spike seed weight, by 32 DAA (plants were nearly desiccated), the seed weight was significantly ($P < 0.05$) lower in the *1-FEH w3* mutation line (0.56 g/ear) compared to Chara (0.87g/ear) (Fig. 3.4). However, there were no significant differences in *1-FEH w2* and *1-FEH w1* mutation lines compared with Chara for these developmental stages. Whereas well watered plants grain filling was in middle condition.

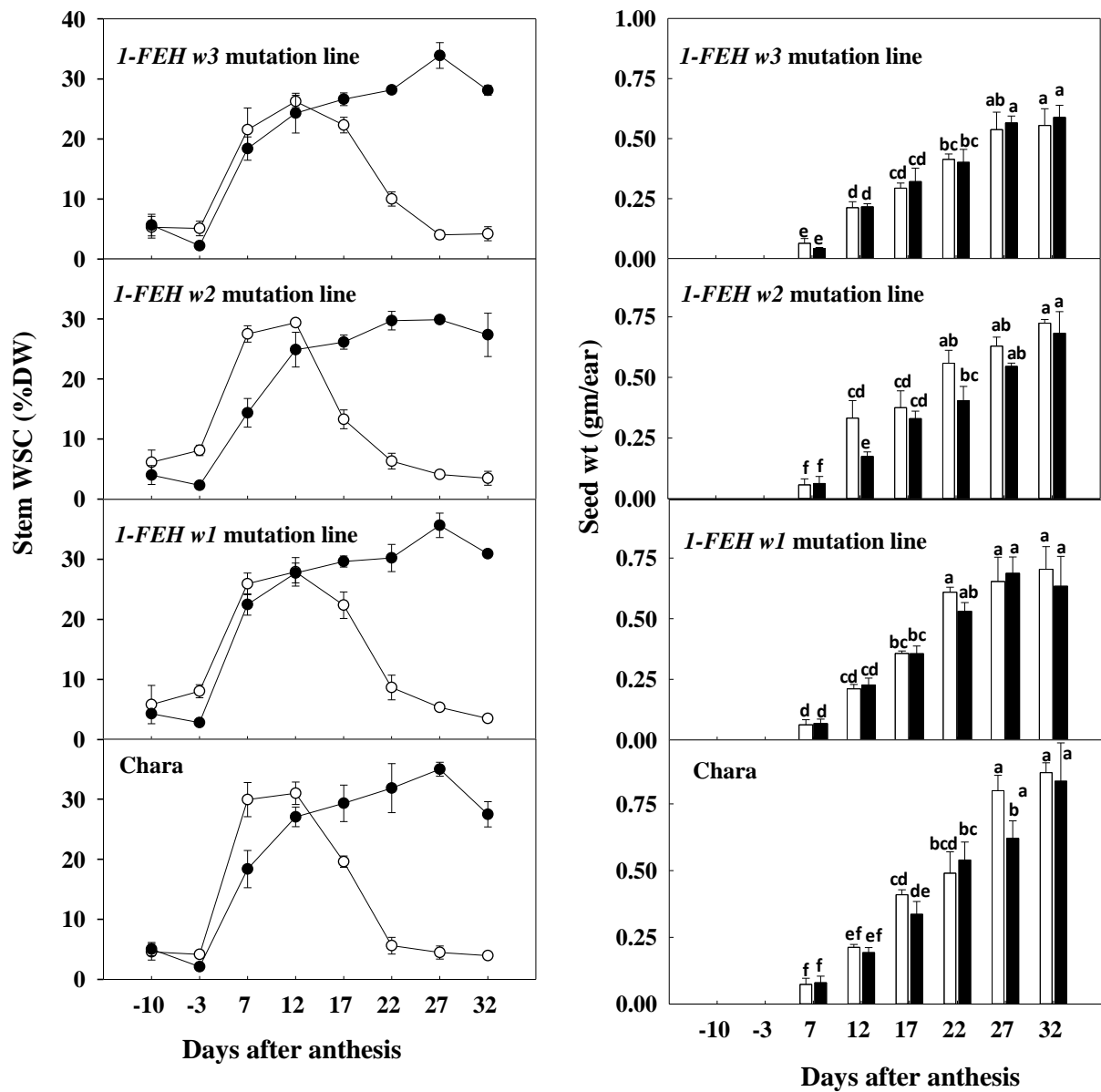


Fig. 3.4: Change in stem water soluble carbohydrate (WSC) concentration (a) and grain dry weight per ear with time after anthesis (b). Closed symbols and bars = well-watered and open symbols and bars = water-deficit; from 10 days before anthesis to 32 days after anthesis, error bars indicate the \pm SE of the mean of three replicates.

II. Grain weight at maturity was influenced by 1-FEH isoforms under water-deficit condition

Water-deficit reduced ($P < 0.05$) grain weight of the *w3* mutant line compared to Chara and the other two mutation lines (Fig. 3.5). Under water deficit, grain wt/main spike was the lowest in the *w3* mutation line ($0.41 \text{ g} \pm 0.03$) and the highest in Chara ($0.71 \text{ g} \pm 0.03 \text{ SE}$). The other two mutation lines *1-FEH w2* and *1-FEH w1* produced $0.63 \text{ g} \pm 0.05$ and $0.58 \text{ g} \pm 0.08$ grain/main spike, respectively. In contrast, in the well-watered treatment, the *w3* mutant line and Chara had similar seed wt/main spike ($1.43 \text{ g} \pm 0.09$ and $1.5 \text{ g} \pm 0.04$, respectively) followed by *w2* ($1.02 \text{ g} \pm 0.02$) and *w1* ($0.96 \text{ g} \pm 0.16$). The TGW (thousand grain wt) was significantly lower ($P < 0.05$) in the *w3* mutation line (17.47 g) compared to Chara (22.53 g) under water deficit, but the *w2* and *w1* mutation lines did not show any significant difference with Chara. Under the well-watered condition, there were no significant differences among the mutation lines and Chara.

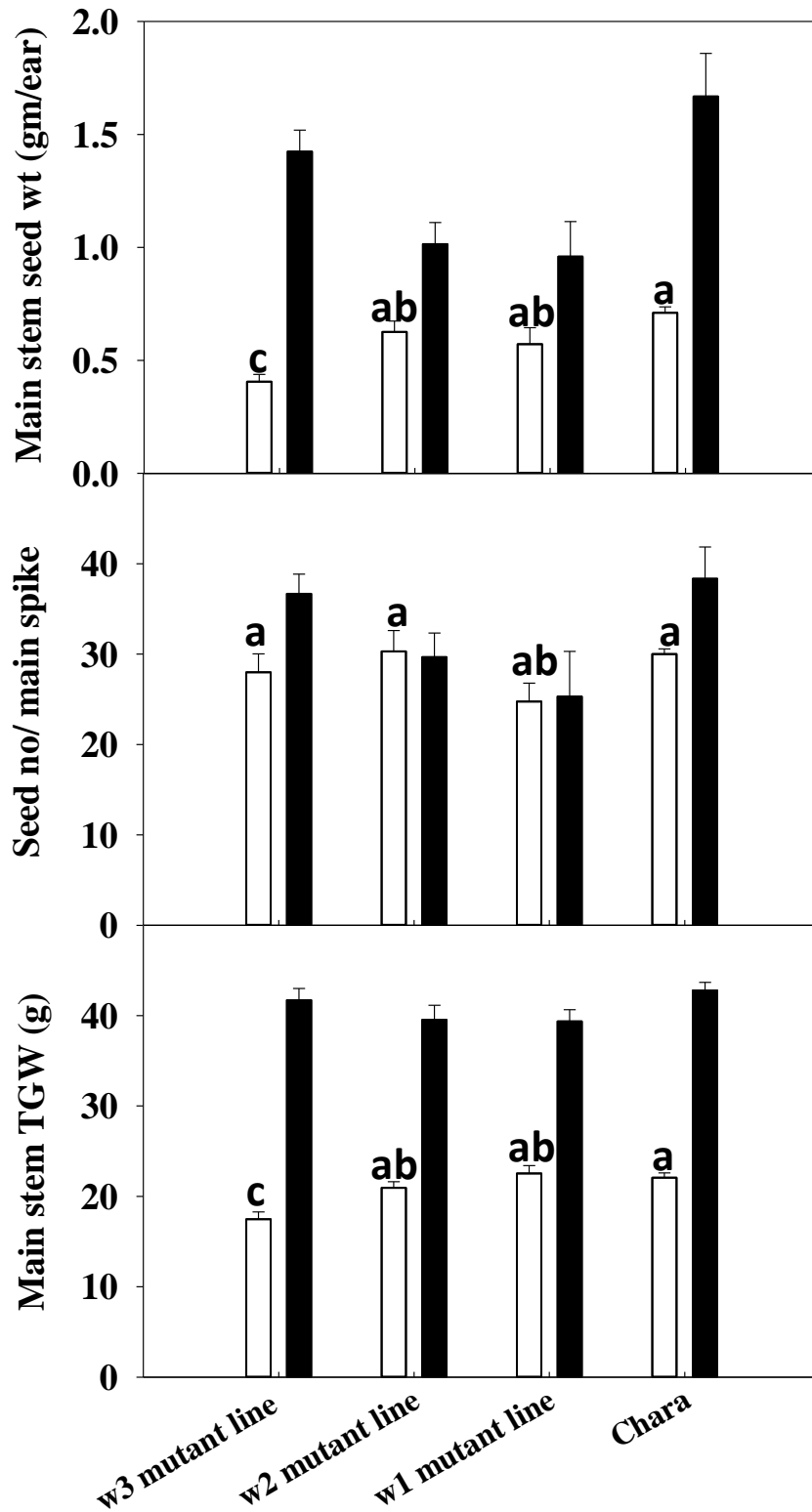


Fig. 3.5: Main stem seed wt(g), seed no/spike and TGW at maturity in well-watered and water-deficit plants in all mutation lines and parent line Chara. Closed symbols = well-watered and open symbols = water-deficit; vertical bars represent \pm SE of the mean of three replicates.

III. 1-FEH w3 mutation affected stem WSC remobilization rate

In 2014, under water deficit condition, remobilization of WSC was significantly ($P < 0.05$) lower in the w3 mutation line (15.18%) compared to Chara (25.24%), and was slightly slower (not significantly) than mutation lines w2 (21.80%) and w1 (20.46%) for the period 12 days after anthesis (peak value for WSC) to 22 days after anthesis (permanent wilting point) (Fig. 3.6).

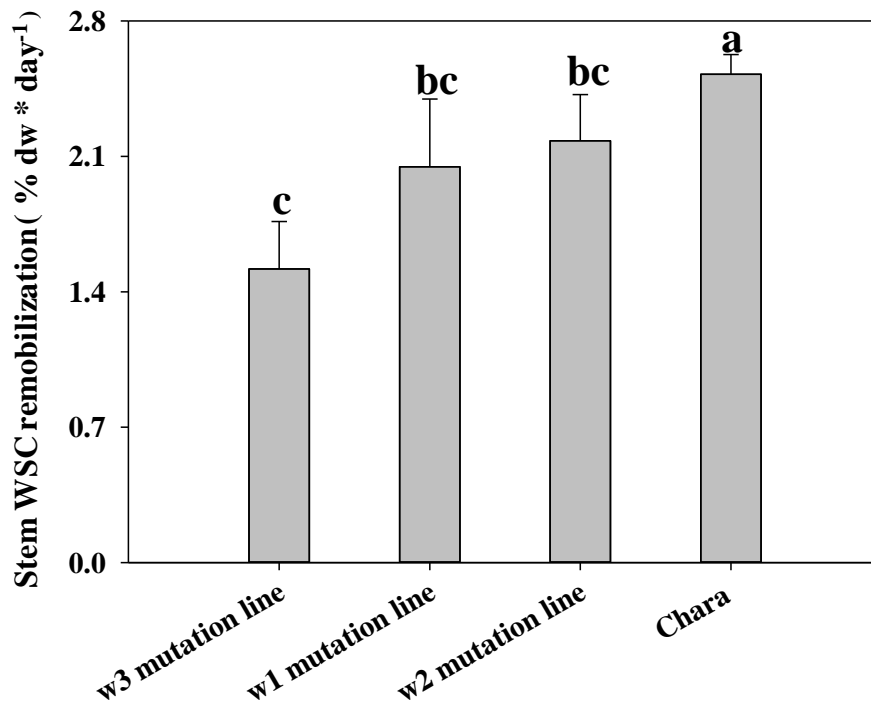


Fig. 3.6: Decline in stem WSC (%DW) in three mutation lines and Chara in the 2014 water-deficit experiment from 12 to 22 days after anthesis, values with the same letter are not statistically different at $P = 0.05$.

IV. Correlations analysis of grain weight with WSC level and remobilisation rate

To understand potential factors influencing grain weight under water-deficit, two correlation analyses were carried out: 1) main stem seed wt vs the highest level of WSC; and 2) grain wt/main stem vs WSC remobilisation rate (Fig. 3.7). The correlation co-efficient of grain wt/main stem with sugar remobilization rate was 0.78 ($r = 0.78$) ($P < 0.01$), and 0.66 ($r = 0.66$) ($P < 0.05$) in the case of the highest WSC level (Fig. 3.7). The results indicate grain wt/ main stem had stronger correlation with sugar remobilization rate than the highest WSC level.

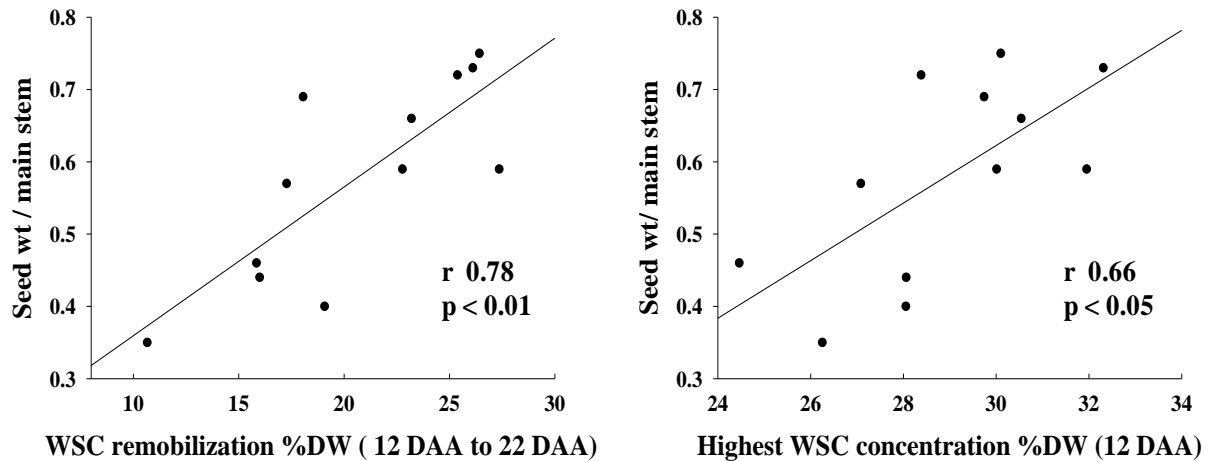


Fig. 3.7: Correlation with seed wt/main stem with WSC remobilization and WSC concentration.

3.4. Discussion

This chapter investigated the role of the three isoforms of *1-FEH* gene individually under terminal water-deficit. Mutation lines of the three isoforms demonstrated functional variation of the isoforms in WSC remobilization and grain filling. Measurement of WSC content in the stem during the grain-filling period was selected for evaluation because it is an easy and direct way to monitor differences in accumulation and mobilization of stem WSC.

3.4.1 *1-FEH* showed functionality only under water-deficit condition not under well-watered condition

The results of this study clearly demonstrated that the functional role of different isoforms of the *1-FEH* gene was influenced by water availability. In the case of WSC concentration, remobilisation rate, and grain weights there was no difference between the mutation lines compared to the parent Chara under well-watered conditions. However, under water-deficit, significant variations were observed in the WSC remobilization rate and grain weights. Thus, it is evident that the 1-FEH enzyme plays a significant role in stem WSC regulation in water-deficit plants leading to an effect on grain weight. In contrast, the equal performance of mutation lines and the parent in well-watered plants indicates that 1-FEH enzyme did not play a significant functional role in stem WSC accumulation or remobilisation at well-watered condition. Thus, a noticeable functionality of *1-FEH* in remobilization of stem WSC can be observed only when the plant undergoes terminal water-deficit. A previous study (Yang et al. 2000) indicated differences in these isoforms of *1-FEH* at the transcription level in water-deficit wheat. This study used the *1-FEH* mutation lines for the first time, which confirmed this

observation at the phenotype level. However, transcriptomic analysis of the three isoforms of the mutation lines under terminal water-deficit will add more information in characterising the *1-FEH* gene functions.

3.4.2 Under water-deficit condition WSC remobilisation rate and grain filling was slowed down by 1-FEH w3 mutation

Under water-deficit, WSC remobilization was slower in the *1-FEH w3* mutation line compared to *1-FEH w1* and *1-FEH w2* mutation lines and the parent Chara during the most vital period of WSC remobilization between 12 and 22 DAA (Fig. 3.6). As mentioned earlier, in water-deficit plants, the stem WSC peaked at 12 DAA indicating the starting point of WSC remobilisation. Generally, the stage when the concentration of WSC reaches the highest level is considered as the start of carbohydrate remobilization since the process leads to a decline in the WSC concentration (Cruz-Aguado et al. 2000). On the other hand, plants reached permanent wilting point at 22 DAA which would have reduced metabolic activity due to the scarcity of water. Thus, the period between 12 and 22 DAA in this trial was most crucial for WSC remobilisation under water-deficit. However, at 22 DAA stem WSC concentration still remained the highest in the *1-FEH w3* mutation line (10% DW) even though it had the lowest stem WSC content (26.25 %) at the peak at 12 DAA. This clearly indicates that the average remobilization rate of WSC was slowest in the *1-FEH w3* mutation line. Indeed, WSC remobilization was 39.8% slower in the *1-FEH w3* mutation line than in Chara. In contrast, mutation lines *1-FEH w1* (18.8% slower) and *1-FEH w2* (13.6% slower) maintained the statistically non-significant differences in remobilization as the parent Chara. So, it is clearly evident that *1-FEH w3* is playing an important role in remobilization of WSC under terminal water-deficit condition.

However, under water-deficit, the value of total WSC reached a peak at 12 DAA which was 15 days earlier than in the well-watered plants. Over all, the remobilisation of WSC started 2 weeks earlier in water-deficit plants. In the case of well-watered condition, the value of total WSC reached a peak at 27 DAA for all of the mutation lines and Chara.

Usually, seed development occurs over 6 weeks after anthesis and during the first two weeks only cell division takes place in the endosperm thus little dry weight is gained. But from 2 weeks after anthesis, starch and protein accumulation begin rapidly in the kernel and the dry weight increases almost in a linear manner. This is the crucial time for accumulation of most of the final kernel weight (Simmons et al. 1985). So, remobilization of WSC during the mid-grain filling stage is crucial to maintain grain weight (Zhang et al. 2014a).

3.4.3 Components of grain yield were reduced in *1-FEH w3* mutation line but not in *1-FEH w2* or *1-FEH w1* mutation lines

Absence of *1-FEH w3* slowdown the WSC remobilization and grain filling rates as well. (Fig. 3.4). Increase of grain wt/main spike (from 12 DAA to 32 DAA) was the highest in Chara 0.66 g ear⁻¹ followed by the *1-FEH w1* mutation line (0.50 g ear⁻¹) and *1-FEH w2* mutation line (0.40 g ear⁻¹) which were significantly higher ($p < 0.5$) than in the *1-FEH w3* mutation line (0.34 g ear⁻¹). This result suggests that the slow remobilization rate of WSC in the *1-FEH w3* mutation line directly affected seed development and ultimately resulted in a significant decrease in the final yield. Accordingly, the higher remobilization in the other two mutation lines (*1-FEH w1* and *1-FEH w2*) and the parent Chara, which carries the *1-FEH w3* wild type, helped to reduce the grain weight loss from water-deficit stress. This study that wheat without t *1-FEH w3* would be at a disadvantage when grown under post anthesis water deficit.

Thousand grain weight (TGW) was strongly affected by the *w3* mutation. For instance, the average reduction in TGW of water-deficit affected Chara in the 2014 experiment was 20.1 g while it was 24.9 g in *1-FEH w3* mutation line.

3.4.4 Comparison of findings in preliminary and main experiments

A preliminary experiment (Appendix 1) was conducted at 2013 where low light intensity during the early stage of development considerably reduced photosynthesis over the experimental units. This unavoidable circumstance resulted considerably low stem carbohydrate reserve (Gallagher et al. 2015) than the usual. This was caused by a problem in glasshouse design which was rectified in time for the main experiment. Regardless of the likely impact of shade non-uniformly across the experiment it is useful to compare the results with this chapter.

The major difference between the experiments was the WSC concentration which was lower in the preliminary experiment across all the lines including the parent line Chara in both well-watered (13.18% dw) and water-deficit (10.25% dw) condition (Fig. A.1). By contrast, in the main experiment (this chapter), it was 34.98% dw in well-watered plants and 30.98% dw in water-deficit plants (Fig. 3.4).

However, the major functional role of *1-FEH w3* was also confirmed in the preliminary experiment as outlined below. Although those phenotypes showed similar trends in both experiments, there was considerable variation between them.

- The *1-FEH w3* mutation line showed slower WSC remobilization compared to the parental cultivar Chara and other two mutation lines in both the experiments. The WSC remobilisation rate ($\text{dw} \cdot \text{day}^{-1}$) was 20% slower in the preliminary experiment (Fig. A.2), and 39% slower in the main experiment (Fig. 3.5).
- The highest TGW penalty due to water-deficit was recorded in the *1-FEH w3* mutation line in both experiments. In the preliminary experiment, the TGW penalty in the *1-FEH w3* mutation line (29.67%) was significantly higher than Chara (19%), *1-FEH w2* mutation line (16%) and *1-FEH w1* mutation line (12.45%) (Table A.1). Likewise, in the main experiment the *1-FEH w3* mutation line had showed the highest TGW penalty (58%) from the water-deficit treatment, the TGW was 48% in Chara (Fig. 3.5). The *1-FEH w2* and *1-FEH w1* mutation lines did not show any significant difference with Chara in main experiment.

The lower WSC concentration in the preliminary experiment from the shade ultimately resulted in reduced seed weight. In contrast, in the main experiment, seed weight was higher with higher WSC concentration, which clearly indicates that the higher WSC concentration was directly related with higher yield. In both experiments the *1-FEH w3* mutation line had the higher TGW loss under water deficit condition. These results correlated with the stem WSC remobilisation rate under water-deficit which was slower in the *1-FEH w3* mutation line compared to the other two mutation lines and the Chara. This indicates that the WSC remobilisation rate in the *1-FEH w3* mutation line was not fast enough to minimise the loss of grain unlike in the parent Chara and other two mutation lines.

From both the preliminary and main experiments it is evident that the three isoforms of *1-FEH* do not play equal roles in stem WSC remobilisation under water-deficit. As demonstrated by the results, the absence of *w1* and *w2* did not have any significant effect on WSC remobilization and seed wt development compared to the parent Chara. However, the absence of *1-FEH w3* disrupts sugar transportation to the developing grain in water-deficit plants resulting in lower seed weight. Chara and the mutation lines *1-FEH w1* and *1-FEH w2* had the *1-FEH w3* isoform which helped them to minimise the yield loss due to water-deficit. This study also confirms with the previous studies on *1-FEH* gene functionality under water-deficit (Khoshro et al. 2014; Zhang et al. 2015b). This study confirmed the potential of individual isoform *1-FEH w3* over the other isoforms in breeding to better manage yield under water-deficit.

3.5 Conclusion

The experimental results in this chapter define the individual functional potential of three isoforms of *1-FEH* in remobilizing WSC under terminal water-deficit. It was demonstrated that *1-FEH w3* plays the most crucial role in stem WSC remobilisation under post anthesis water-deficit. Thus, it could be a potential target for drought tolerant wheat breeding. To more completely define the role of these three isoforms in remobilizing different component of WSC and to investigate their difference at the transcription level, further investigation is needed. It is also important to know if wheat plants can increase the expression of any isoform to compensate for absence of one isoform. These will be investigated in the following chapters.

Chapter 4: Expressional behaviour of different isoforms of *1-FEH* gene under post anthesis water-deficit and its influence on WSC components

4.1 Introduction

In Chapter 3, it has been observed that there were no significant differences in water soluble carbohydrate level among the mutation lines and Chara in both well-watered and water-deficit conditions. However, thousand grain weight (TGW) was significantly lower in the *1-FEH w3* mutation line under post anthesis water-deficit condition. Moreover, the remobilization rate of WSC was slower in the *1-FEH w3* mutant line under water-deficit condition. That shows the loss of *1-FEH w3* functions in the stem WSC remobilization under post anthesis water-deficit condition. Therefore, conducting further investigation is required to understand the functional role of the three different isoforms of *1-FEH* in WSC remobilisation.

WSC, the main reserve source of carbohydrate for grain filling consists of different degree polymerizations (DP) of saccharides (Chapter 2), for example, glucose, fructose, sucrose and high DP fructans (Kobata et al. 1992; Pheloung and Siddique 1991; Schnyder 1993). Fructans, are the dominant component of WSC in wheat stems (Goggin and Setter 2004; Joudi et al. 2012; Xue et al. 2008). Fructans play a vital role in the recovery of biotic and abiotic stress in grain filling (Livingston et al. 2009; Valluru and Van den Ende 2008). In particular, fructans protect the cell membrane under water-deficit stress in the form of mixture of high and low degree of polymerization (DP) (Valluru and Van den Ende 2008; Zhang et al. 2015a). One of the two main roles of fructans under stress is acting as phloem-mobile signalling compounds which mostly carried out by the small fructans (Keunen et al. 2013; Van den Ende 2013). Another role is, fructans may contribute to overall cellular reactive oxygen species (ROS) homeostasis by a direct ROS scavenging mechanism (Peshev et al. 2013).

Wheat fructans are usually in the form of the graminan type. Bifurcose (or 1&6 kestotetraose) is a branched fructan which serves as a typical building block for graminan-type fructans. Biosynthesis of fructans have been shown in Fig. 4.1.

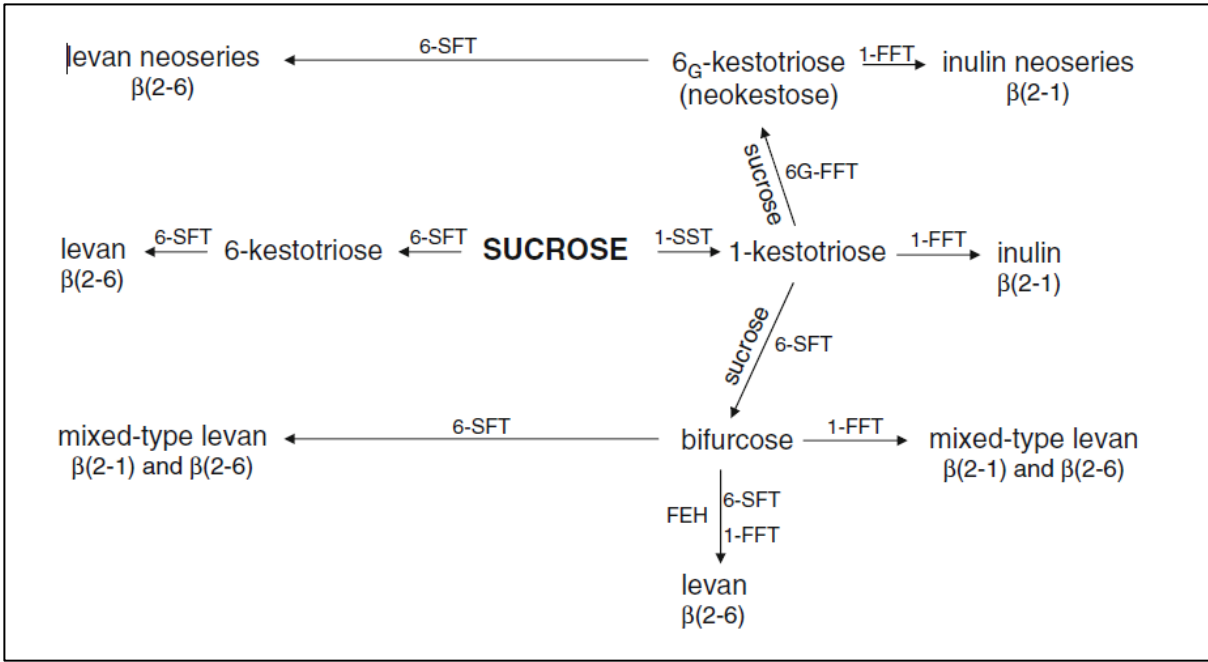


Fig. 4.1: Schematic presentation of fructan biosynthesis. Source (Livingston et al. 2009).

Sucrose 1-fructosyltransferase (1-SST), fructan 6fructosyltransferase (6-SFT), fructan1-fructosyltransferase (1-FFT).

It can be presumed that, the exploitation of stem WSC during grain filling period under water-deficit stress is boosted by the potential contribution of all stem FEHs enzyme (Fig. 4.2). Wheat FEH activities can be studied through the gene expression on transcription level (Van Laere and Van Den Ende 2002; Zhang et al. 2009). Although, it has been reported that 1-FEH might playing main role (Van den Ende et al. 2003). However, 6-FEHs are also expected to play an important role (Joudi et al. 2012)

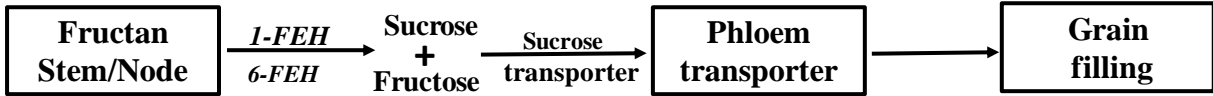


Fig. 4.2: Schematic presentation of fructan degradation.

A previous study showed that the *1-FEH w3* gene is one of the major contributors in stem fructan remobilization to grain based on the relatively higher expression of this isoform compared to the other two isoforms; *1-FEH w1* and *w2*, under terminal water-deficit (Zhang et al. 2015b). However, the individual functional role of these three isoforms of *1-FEH* on stem WSC remobilisation under water-deficit has not been reported. Distinct function of a particular gene can be characterised by inducing complete loss of gene function through mutagenesis.

This study used the mutation lines of all the isoforms of the gene to provide further confirmation of the distinct function of the *I-FEH* isoforms.

As discussed earlier that, biosynthesis and degradation of the components of stem WSC go through complex and interactive pathways leading to the remobilisation of carbohydrate to the grain. This WSC is particularly a major source of carbohydrate for grain filling under water-deficit condition. Thus, to characterise the influence of *I-FEH* isoforms on WSC remobilisation, a detailed investigation on the degradation and remobilisation pattern of the important components of WSC is crucial. More specifically, the comparative analysis of the WSC components between the *I-FEH* isoforms mutation lines will provide an understanding of the mechanisms involved in the contributions of the individual isoforms in WSC remobilisation under water-deficit.

In many cases, it has been observed that the isoforms of a particular gene are functionally linked and work in a network. Hence, there is a speculation that in a mutation line of a particular *I-FEH* isoform, expression of other isoforms could increase to make up the functional loss of the mutated isoform. Therefore, this study also investigated the relative gene expression of other isoforms in the mutation lines and related this to the phenotypic behaviours.

The hypothesis examined in this chapter is that the expressional differences of isoforms of *I-FEH* gene might explain the observed differences in remobilisation of WSC components across mutation lines.

4.2 Materials and methods

To investigate changes in stem WSC in detail, the levels of specific stem WSC components were quantified using the same extracted WSC (Chapter 3, materials and methods) from the 2014 samples.

4.2.1 Carbohydrate analysis by HPAEC

A 200 µl aliquot of the same sample was passed through a 0.3 ml bed volume of Dowex[®]-50 H+ and a 0.3 ml bed volume of Dowex[®]-1-acetate, followed by rinsing six times with 200 µl distilled water. The eluate was seven times diluted and then centrifuged at 13 000 g for 5 min. Twenty-five microlitres of the diluted samples were analysed by high-performance anion exchange chromatography with pulsed amperometric detection (HPAEC-PAD). CarboPacw PA100 anion exchange column with pulsed amperometric detection and equipped with a gold electrode (potentials: E1, + 0.05 V; E2, +0.6 V; E3, -0.8 V) was used. The flow rate was 0.25

ml per min. The column was equilibrated with 90 mM NaOH for 9 min before injection. The sugars were eluted with a Na-acetate gradient:

0–10 mM from 0 min to 6 min; 10–100 mM from 6 min to 16 min. Finally, the column was regenerated with 500 mM Na-acetate for 1 min. Quantification of WSC components were performed using the peak area with external standards (provided by Dr. Jingjuan Zhang) for glucose, fructose, sucrose, 1-kestose, 6-kestotriose, neokestose, nystose and bifurcose. The total fructan concentration was calculated as the amount of the WSC concentration (as determined by the anthrone method) minus the concentration of glucose, fructose and sucrose.

4.2.2 Expression analyses by quantitative real-time PCR

I. RNA isolation and cDNA synthesis

RNA was extracted from wheat stem (including sheath) from three replicates of same samples used for WSC analysis (Chapter 3). Using TRIzol® reagent (Invitrogen, Carlsbad, CA, USA), total RNA was isolated from approximately 120 mg dry-weight of frozen ground stem tissue. RNA was purified by chloroform extraction and was precipitated by isopropanol and then washed with Promega RNA extraction kit. The RNA concentration was quantified using NanoDrop (ND 1000 Spectrophotometer, Thermo Fisher Scientific). To make all RNA extracts the same concentration, RNA were diluted in to 20 ng/ µl. Total RNA (0.20 µg) was reverse transcribed in a 20 µl reaction with random primers using a High-Capacity cDNA Reverse Transcription Kit (Applied Biosystems). Then cDNA was checked for genomic DNA contamination. After that cDNA products were the diluted to make 50 times dilution for *1-FEH w1* and *w2* primers and 500 times dilution for the *1-FEH w3* primers and stored at -20°C.

II. Primers used for qRT-PCR

With regards to the gene expression analysis for each isoform of *1-FEH w1*, *w2* and *w3*, the primers should be part of the cDNA sequence. Since these three isoforms are very conserved, single nucleotide polymorphisms (SNPs) were used for the primer design of specific chromosomes in exon 3, as this exon is the largest in the *1-FEH* gene sequences. Three SNPs occurred in this exon (Zhang et al. 2008) (Table 4.1).

III. PCR Amplification condition

Quantitative Reverse Transcription-PCR (qRT-PCR) was carried out using Corbett Rotor-Gene RG-6000 (Corbett Research, Queensland, Australia). The qRT-PCR reactions were done in triplicates with the Power SYBR_ Green PCR Master Mix. The PCR condition was 95°C

for 10 min, followed by 45 cycles of 95°C for 15 secs and 58°C for *1-FEH w2/ 1-FEH w1* primers for 1 min that was 62°C for the *1-FEH w3* primers and at last step 14°C for ∞. To normalize the amounts of FEH gene, the GAPDH transcript level in the different samples was used as internal control. Gene expression was quantified using the relative standard curve method.

Table 4.1: Primers used for the qRT-PCR.

genes		Primers (5' to 3')
<i>1-FEH w1</i>	Forward	CCGCGTTAGTGCGGGATA
	Reverse	CACCAGTGTATATGATGAC
<i>1-FEH w2</i>	Forward	CCGCGTTAGTACGGGATA
	Reverse	GCCTGATGTTGATCTATGTCG
<i>1-FEH w3</i>	Forward	CCGCGTTAGTGCGGGACA
	Reverse	GCCTGATTTTGATCTATGTCAC
GAPDH	Forward	CGAAGCCAGCAACCTATGAT
	Reverse	CAAAGTGGTCGTTTCAGAGCA

4.2.3 Statistical analysis

Analysis of variance (Stepanova and Alonso) on sugar components, and level of gene expression were performed using IBM SPSS Statistics V21.0. *Post-hoc* comparisons were conducted using Duncan Multiple Range tests at $P < 0.05$. Graphs were generated using sigma plot 13.0.

4.3 Results

In Chapter 3, the results of total WSCs content revealed that there were no significant differences at the highest level of the stem WSC concentration among the mutation lines and Chara under terminal water-deficit condition. However, the remobilization of WSC was significantly slower in the *1-FEH w3* mutation line, which reduced on grain yield. To investigate the changes to stem WSC in details, the levels of specific stem WSC components were quantified using a HPAEC method. The main WSC components included glucose, fructose, sucrose, 1-kestose, 6-kestose, bifurcose and mixed fructan. The levels of sucrose, fructose and glucose were analysed along with total fructan levels.

4.3.1. Effect of mutation of *1-FEH* isoforms on carbohydrate composition under post anthesis water-deficit condition

Levels of stem WSC components were influenced by the *1-FEH* gene isoforms under post anthesis water-deficit condition. The degradation or remobilisation of mixed fructan and fructose were highly regulated by *1-FEH w3* under terminal water-deficit. However, remobilisation of glucose and sucrose were not influenced by the isoforms of *1-FEH*. The dynamic fluxes of the WSC components are described in the following sections.

Fructan:

In the wheat stem, fructan reached its highest level at 7 days after anthesis in Chara, *1-FEH w2* and *1-FEH w1* mutation lines, but delayed to 12 days after anthesis in the *1-FEH w3* mutation line (Fig. 4.3). Thus the remobilization of fructan started 5 days later in the *1-FEH w3* mutation line compared to Chara and the other mutation lines. The degradation rate was also different between these two groups. In the *1-FEH w3* mutation line, the degradation was slower between 12 and 17 DAA and then declined faster until 22 DAA. By contrast, there was a sharp degradation of fructan between 7 and 22 DAA in Chara and other two mutation lines (*1-FEH w1* and *1-FEH w2*).

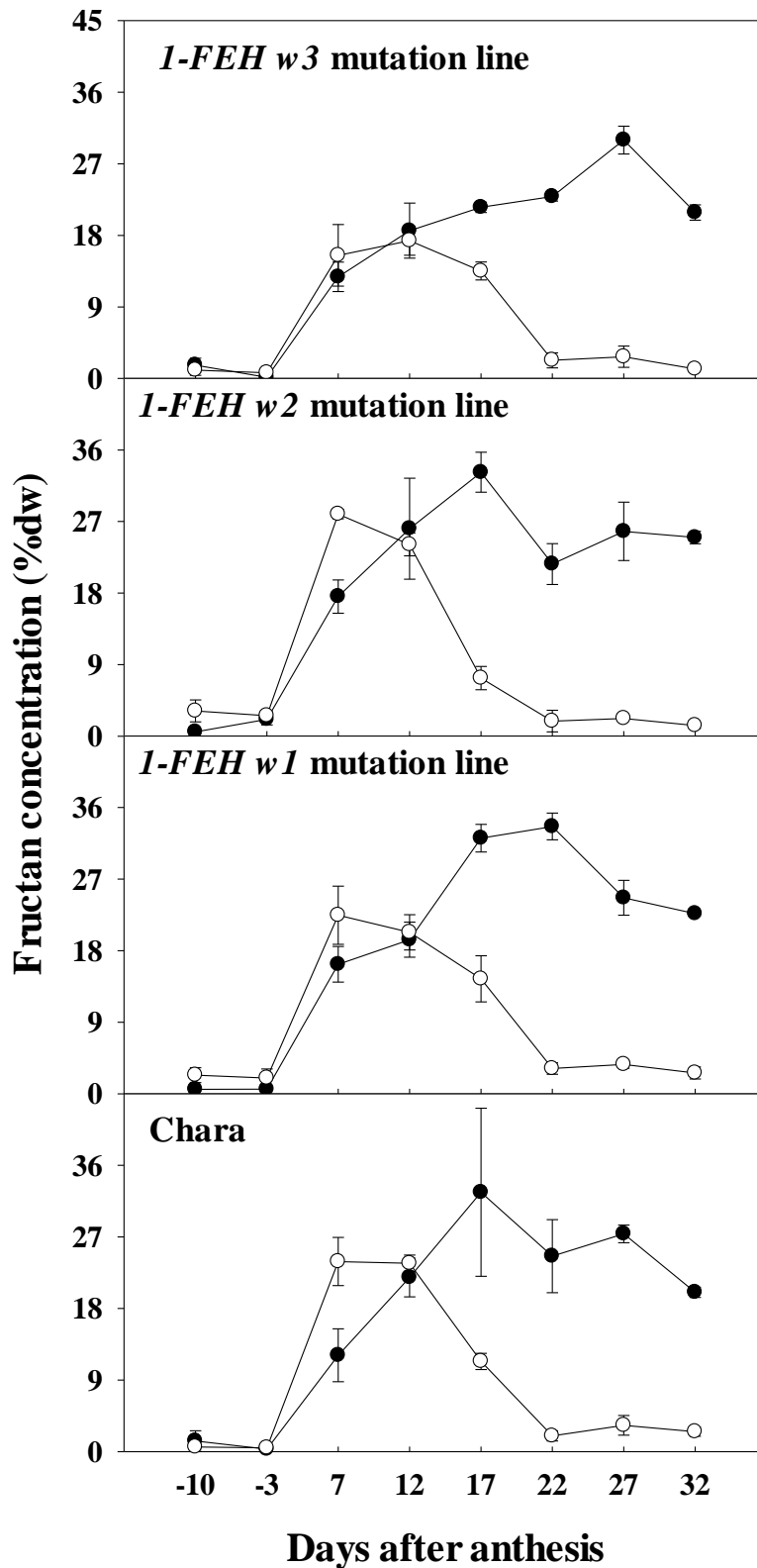


Fig. 4.3: Stem Fructan accumulation and degradation patterns under well-watered (closed symbol) and water-deficit (open symbol) conditions, from 10 days before anthesis to 32 days after anthesis; vertical bars represent \pm SE of the mean of three replicates.

Under water-deficit condition, in the period 7-22 DAA, the fructan degradation rate was slower in *1-FEH w3* mutation line compare to other lines (Fig. 4.4). The degradation rate was significantly reduced relative to the *1-FEH w2* mutation line whereas it was close to be significant ($p= 0.06$) as compared with Chara (Fig. 4.4)

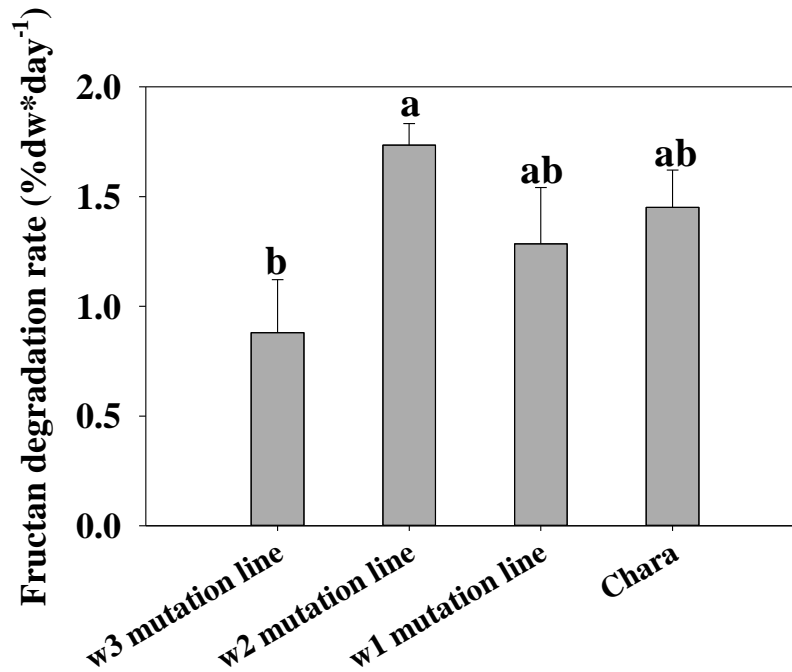


Fig. 4.4: Degradation rate of stem fructan (% dw*day⁻¹) in different mutation lines and Chara under water-deficit condition, from 7 to 22 days after anthesis. The vertical bars represent \pm SE of mean of three replicates. Values with the same letter are statistically not different at $P = 0.05$.

Bifurcose:

Bifurcose degradation pattern was similar to the fructan degradation pattern. In the *1-FEH w3* mutation line, bifurcose peaked at 7 DAA, which was 5 days earlier than other lines. The highest concentration of bifurcose was around 2% of dry weight (dw) in all the lines (Fig. 4.5). The bifurcose degradation was much slower in the well-watered condition than under water-deficit.

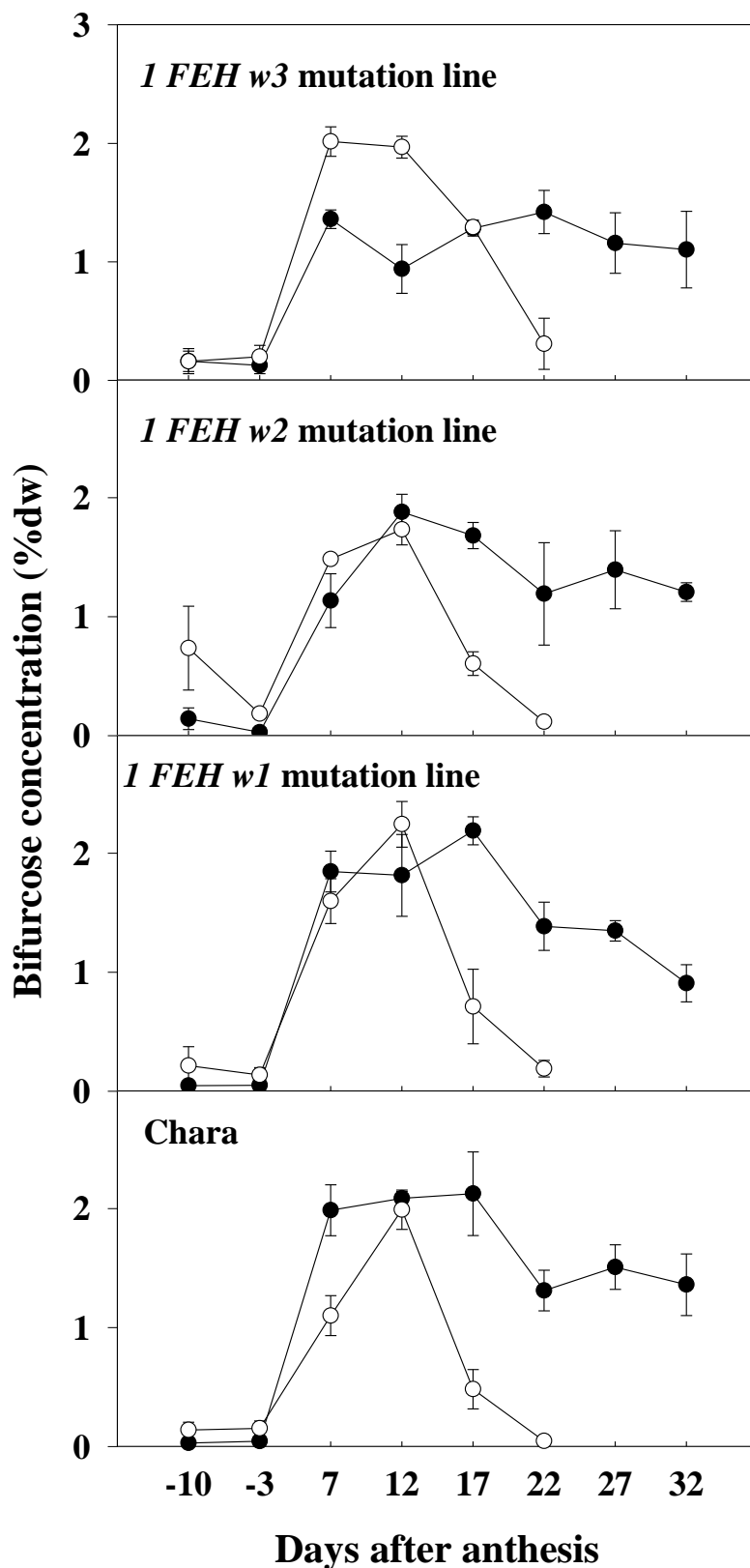


Fig. 4.5: Stem bifurcose accumulation and degradation patterns under well-watered (closed symbol) and water-deficit (open symbol) conditions, 10 days before anthesis to 32 days after anthesis; vertical bars represent \pm SE of the mean of three replicates.

The bifurcose degradation rate between 12 to 17 DAA, was significantly reduced in the *I-FEH w3* mutation line compared to other lines in the water-deficit condition (Fig. 4.6), which showed that bifurcose was weakly degraded in the mutation line *I-FEH w3*.

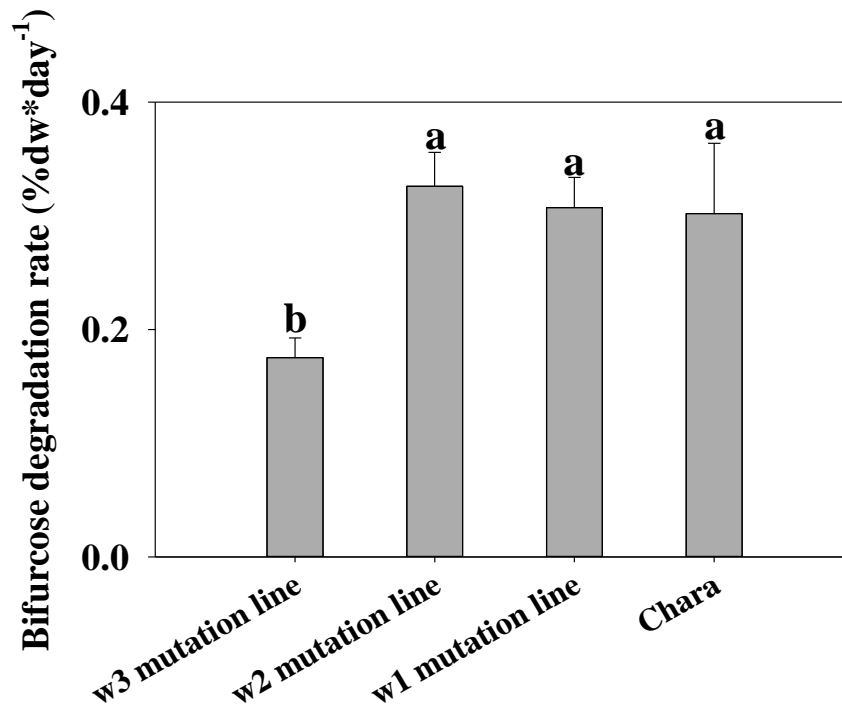


Fig. 4.6: Degradation rate of stem bifurcose (% dw*day⁻¹) in different mutation lines of *w1*, *w2*, *w3*, and Chara under water-deficit condition from 12 to 22 days after anthesis. The vertical bars represent \pm SE. Values with the same letter are statistically not different at $P = 0.05$.

6-kestose:

The patterns of accumulation and degradation of 6-kestose were very similar across all lines studied (Fig. 4.9). The highest concentration of 6-kestose was just above 3.5% dw in all the lines at 12 DAA in the water-deficit condition. Thereafter, the 6-kestose levels declined sharply to around zero from 12 to 22 DAA in all the lines. There were no significant differences among the lines in water-deficit conditions as well as in well-watered condition

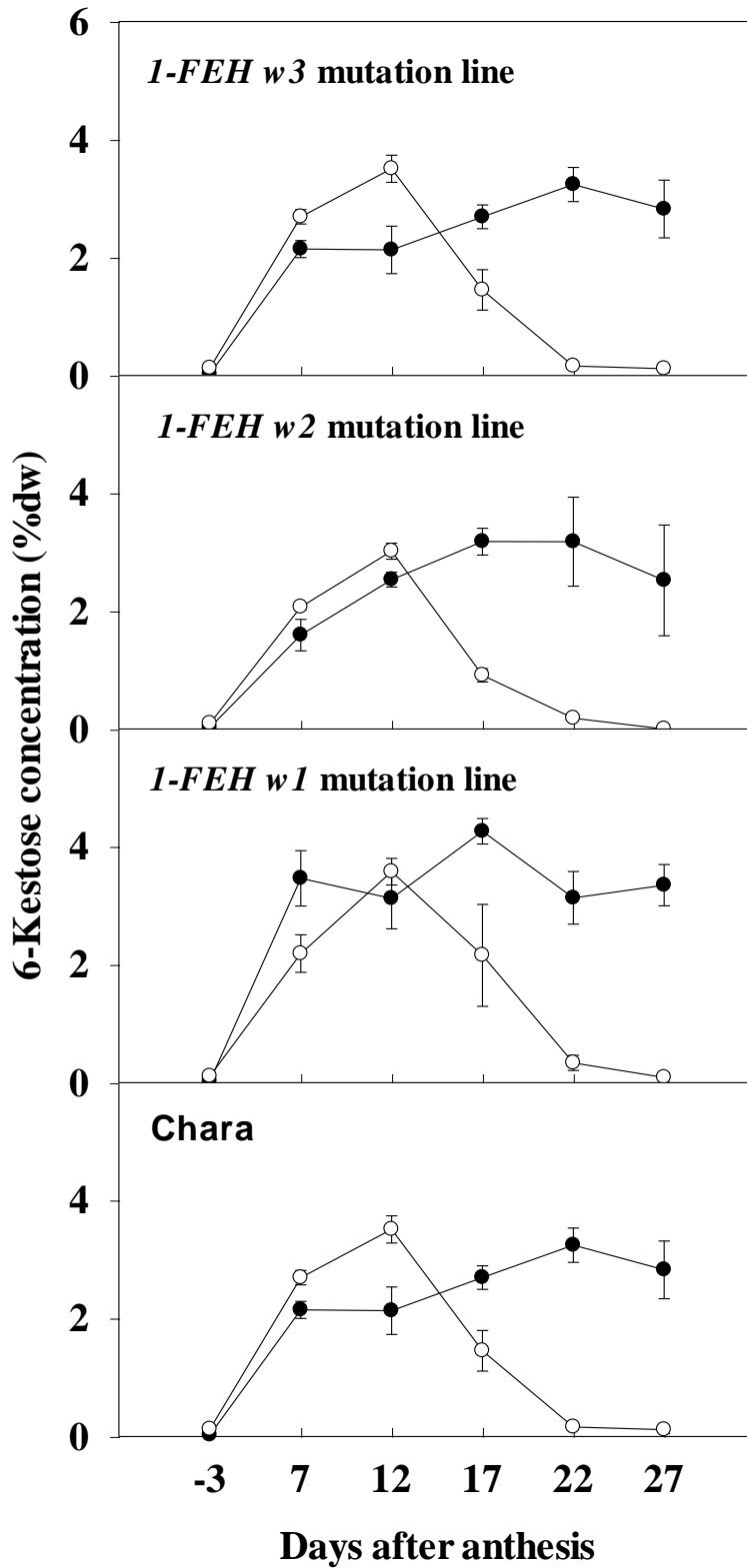


Fig. 4.7: Stem 6-kestose accumulation and degradation patterns under well-watered (closed symbol) and water-deficit (open symbol) conditions, 10 days before anthesis to 32 days after anthesis; vertical bars represent \pm SE of the mean of three replicates.

Sucrose:

The accumulation and reduction patterns of sucrose were very similar between the lines under water-deficit (Fig. 4.6). In all the lines, sucrose reached its highest level at 12 DAA and consistently decreased until 27 DAA. At the peak point, the sucrose level was higher in the water-deficit condition than in well-watered plants for the *1-FEH w3* and *1-FEH w2* mutation lines, whereas the sucrose peaks were similar in the *1-FEH w1* mutation line and Chara. The reduction rate of sucrose was much slower in well-watered plants compared to those with water-deficit condition. At 32 DAA, more than 50% of the peak level of sucrose remained in the stem in well-watered plants.

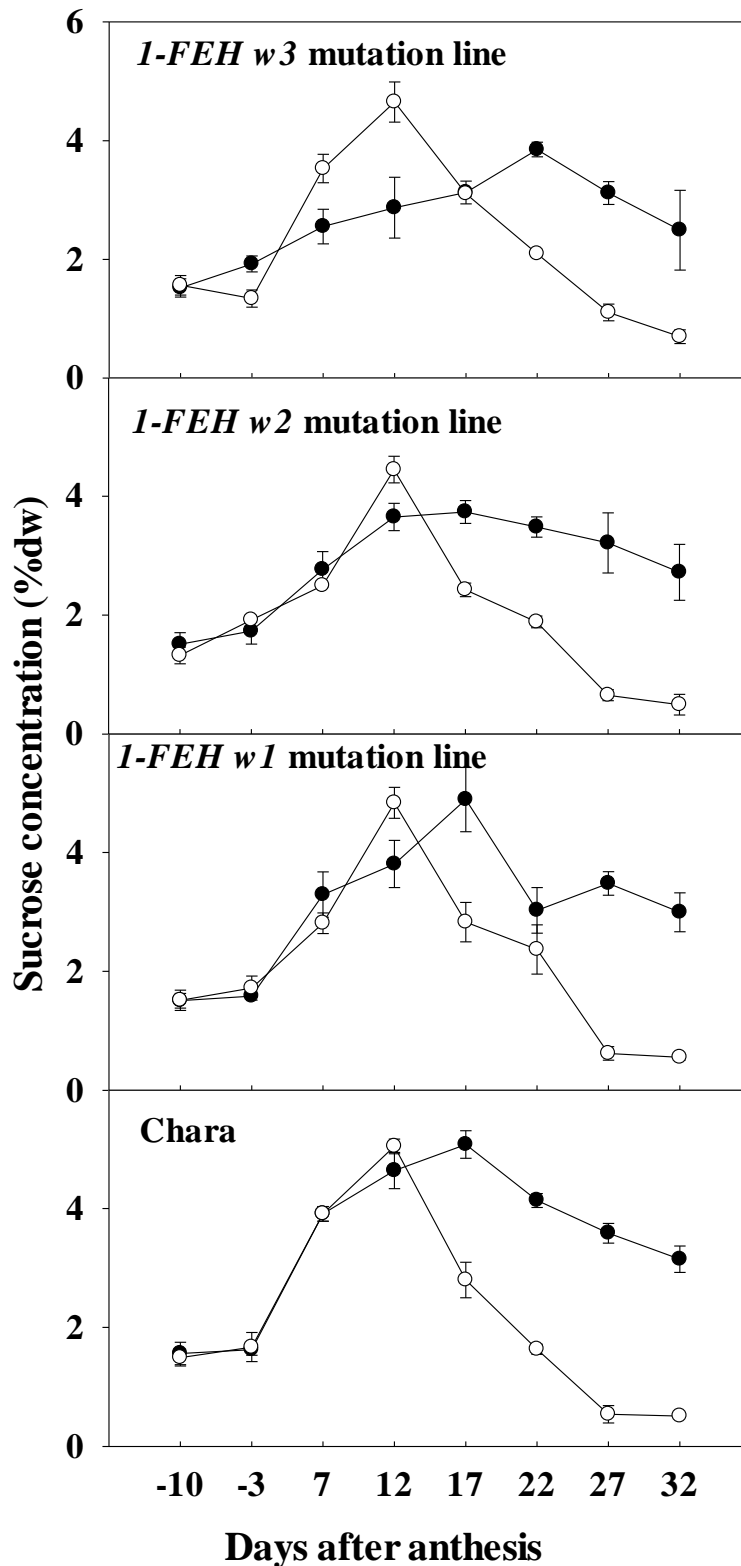


Fig. 4.8: Stem sucrose accumulation and degradation patterns under well-watered (closed symbol) and water-deficit (open symbol) conditions, from 10 days before anthesis to 32 days after anthesis; vertical bars represent \pm SE of the mean of three replicates.

Fructose

The levels of fructose increased markedly after 12 DAA and reached their highest level at 17 DAA in Chara and *1-FEH w1* and *1-FEH w2* mutation lines, compared to 22 DAA in the *1-FEH w3* mutation line (Fig. 4.9). The fructose levels dropped markedly between 17 and 22 DAA in Chara and the *1-FEH w1* and *1-FEH w2* mutation lines. The decline in fructose was delayed by 5 days behind in the *1-FEH w3* mutation line, between 22 and 27 DAA.

The patterns of fructose accumulation and degradation in well-watered condition remained similar. Compared with the water-deficit condition, the maximum level of fructose was lower in all the lines in well-watered plants.

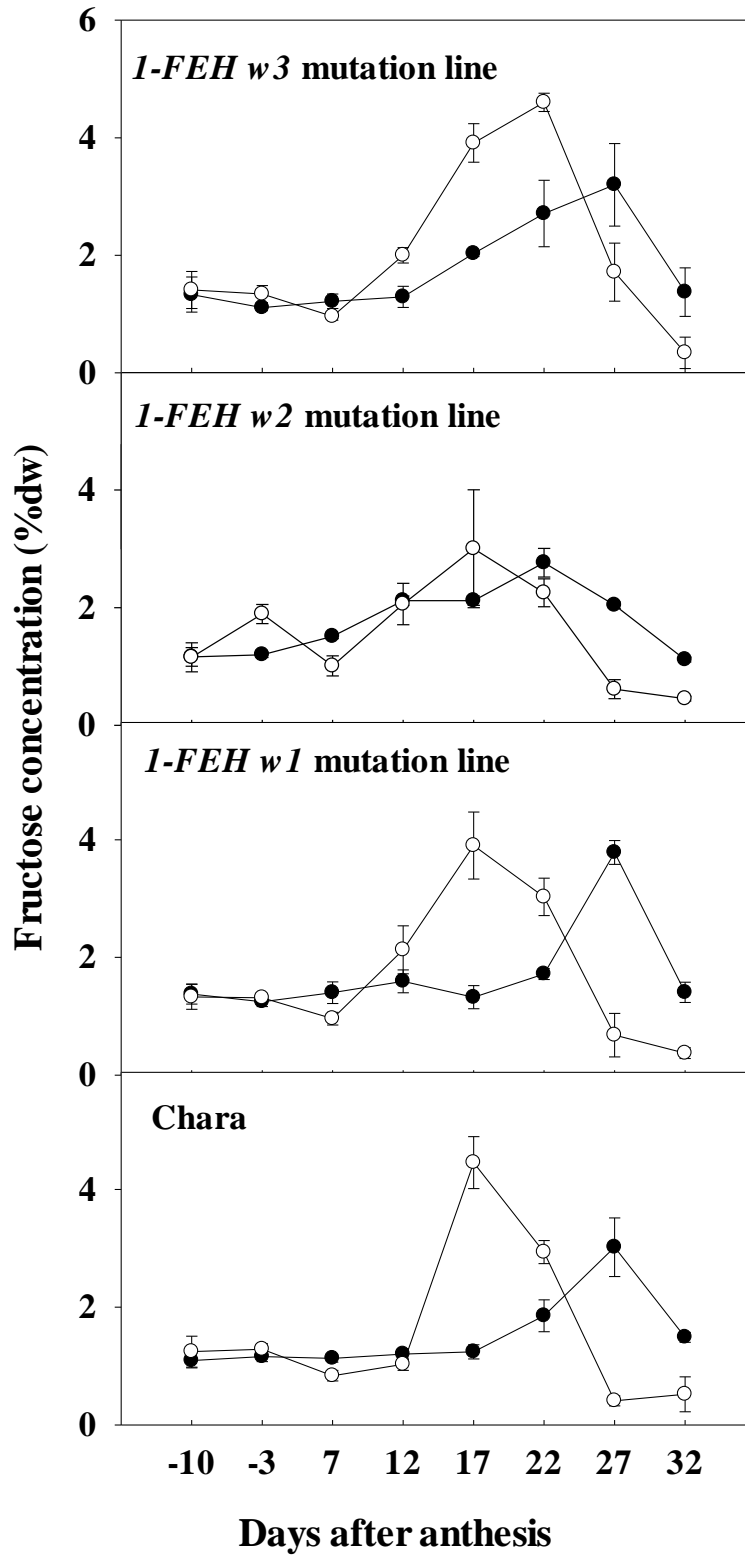


Fig. 4.9: Stem fructose accumulation and degradation patterns under well-watered (closed symbol) and water-deficit (open symbol) conditions, from 10 days before anthesis to 32 days after anthesis; vertical bars represent \pm SE of the mean of three replicates.

Glucose:

Glucose concentrations were much lower compared to the other components of WSC (Fig. 4.10). The glucose levels of the *1-FEH w3* and *1-FEH w1* mutation lines were higher in water-deficit plants compare to well-watered plants. There were no differences between Chara and the *1-FEH w2* mutation line between well-watered and water-deficit conditions in glucose accumulation and degradation.

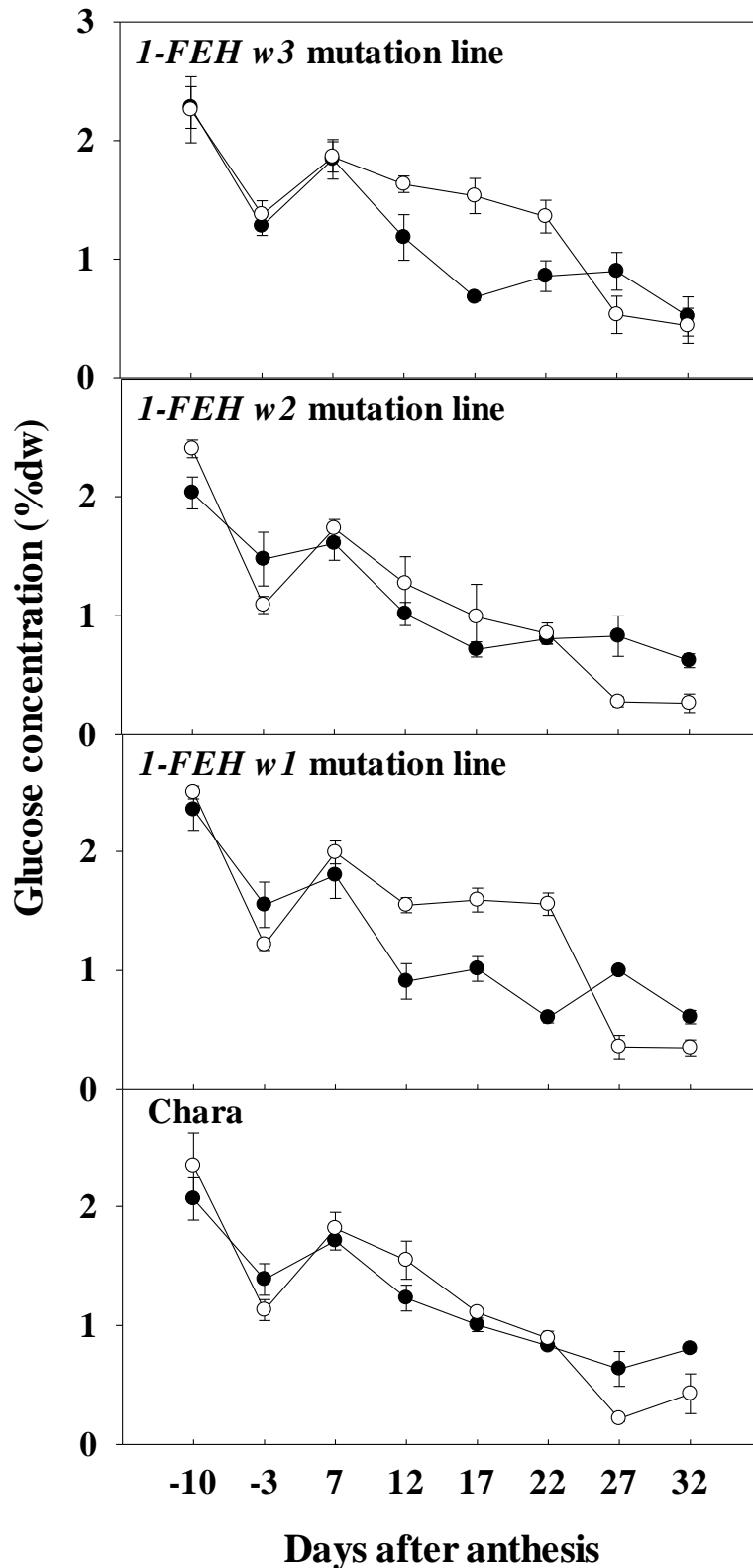


Fig. 4.10: Stem glucose accumulation and degradation patterns under well-watered (closed symbol) and water-deficit (open symbol) conditions, from 10 days before anthesis to 32 days after anthesis; vertical bars represent \pm SE of the mean of three replicates.

4.3.2 Comparison of gene expression in all mutation lines and Chara under well-watered and water-deficit condition

The determination of normalized gene expression was conducted from 7 DAA (5 days after water was withheld to 22 DAA (permanent wilting point of plants). After 22 DAA, the droughted plants were too dry to extract RNA. The gene expression data demonstrated that the *1-FEH w1*, *w2* and *w3* genes were not expressed in the corresponding gene mutation lines which confirmed the inactivation of the gene. The key findings of the transcriptomic analysis are presented below.

4.3.3 Under water-deficit, high expression of *1-FEH w3* gene exhibited in *w1* and *w2* mutation lines

Under water-deficit, significantly higher expression of the *1-FEH w3* gene was observed in the *1-FEH w1* and *w2* mutation lines at 17 DAA compared to Chara (Fig. 4.11). Meanwhile, in well-watered condition, the expression levels of *1-FEH w3* were gradually increased after anthesis in *1-FEH w1* and *w2* mutation lines, and parental line Chara.

The high expression levels of *1-FEH w2* appeared at 22 DAA in *1-FEH w1* and *1-FEH w3* mutation lines under both water deficit and well-watered conditions, while in Chara, *1-FEH w2* showed highest expression at 22 DAA in well-watered condition (Fig. 4.12). The highest level of *1-FEH w2* gene expression was under 120 units.

The levels of *1-FEH w1* gene expression were much lower than that of *1-FEH w2* and *w3* in all *1-FEH w2*, *w3* lines, and parental line Chara. The highest gene expression level was below 24 unit. Slightly different patterns were observed between different water regimes between lines (Fig. 4.13).

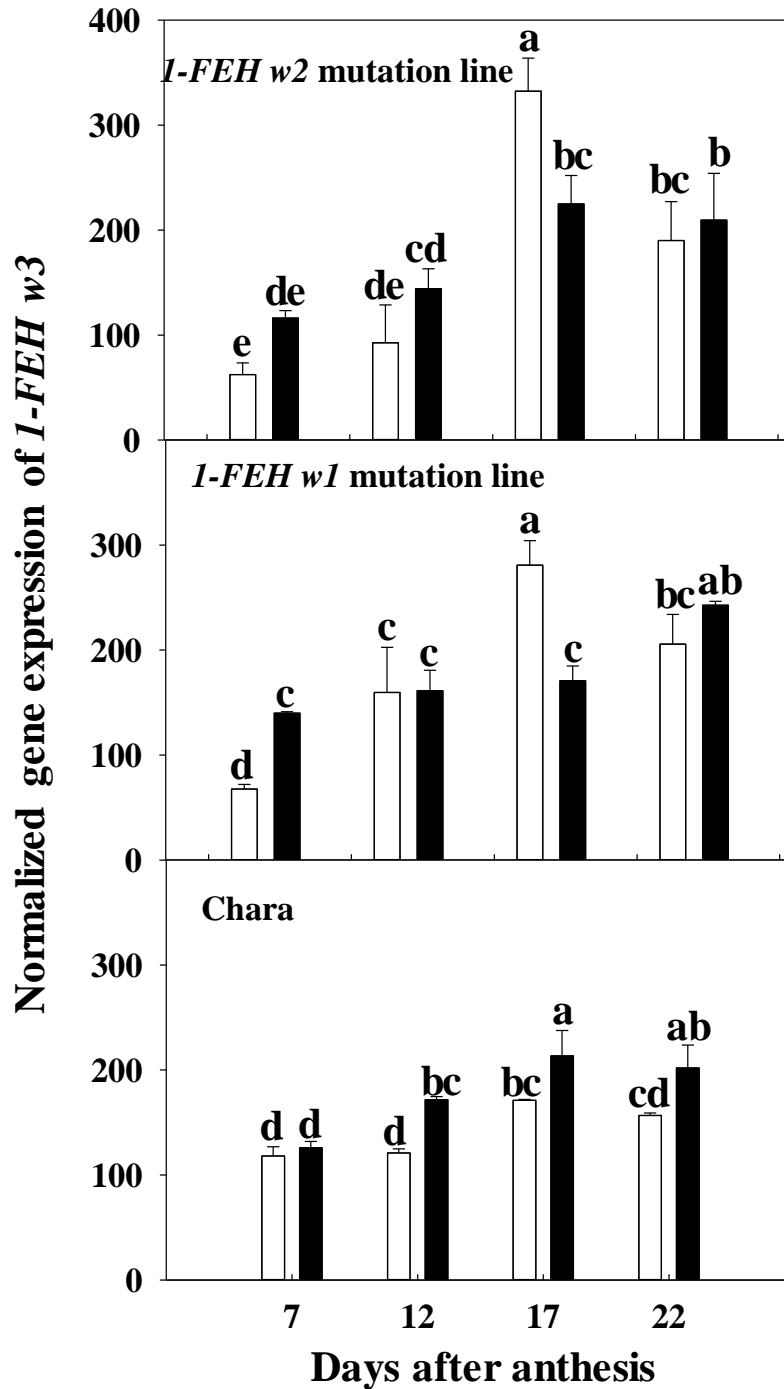


Fig. 4.11: Normalized *I-FEH w3* gene expression patterns in 1-FEH w1, w2 and Chara under well-watered condition (closed bars), and water-deficit condition (open bars), from 7 days after anthesis to 22 days after anthesis, using the same tissue sources that were used for stem water-soluble carbohydrate analysis; vertical bars represent \pm SE of the mean of three replicates. Values with the same letters are statistically not different at $P = 0.05$.

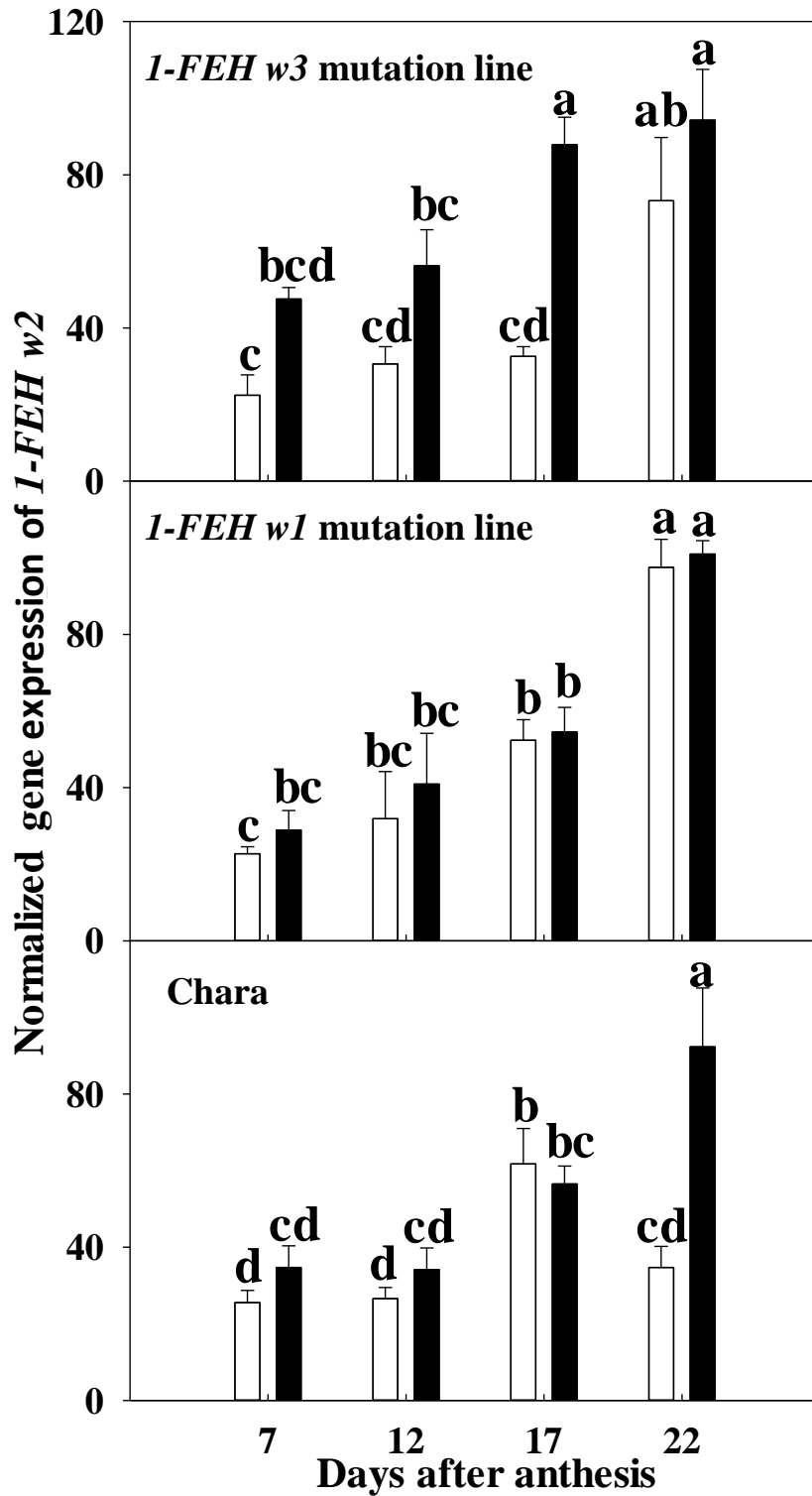


Fig. 4.12: Normalized *1-FEH w2* gene expression patterns in all mutation line and Chara under well-watered condition (closed symbol), and water-deficit condition (open symbol), from 7 days after anthesis to 22 days after anthesis, using the same tissue sources that were used for stem water-soluble carbohydrate analysis; vertical bars represent \pm SE of the mean of three replicates. Values with the same letters are statistically not different at $P = 0.05$.

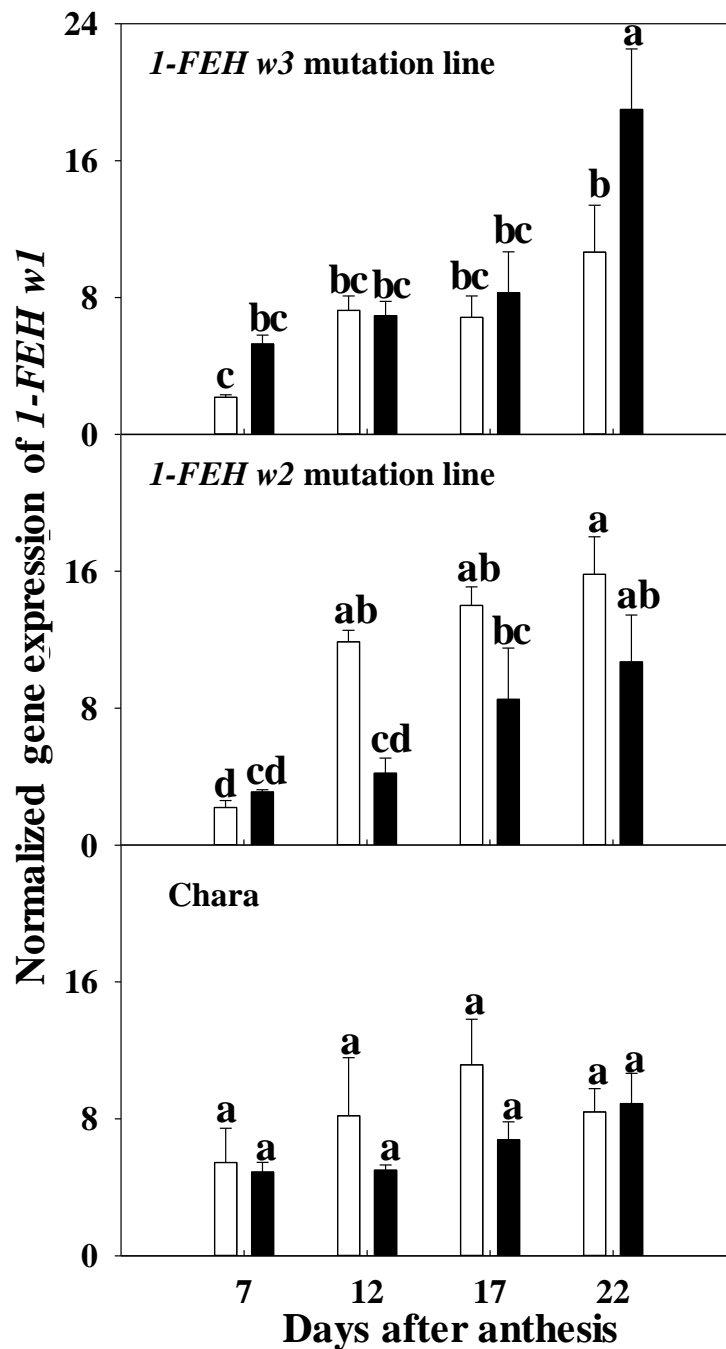


Fig. 4.13: Normalized *I-FEH w1* gene expression patterns in all mutation line and Chara under well-watered condition (closed symbol), and water-deficit condition (open symbol), from 7 days after anthesis to 22 days after anthesis, using the same tissue sources that were used for stem water-soluble carbohydrate analysis; vertical bars represent \pm SE of the mean of three replicates. Values with the same letters are statistically not different at $P = 0.05$.

Under water-deficit, the gene expression patterns of the *1-FEH* isoforms were different during the grain development. The expression of isoforms *1-FEH w1* and *1-FEH w2* increased gradually between 7 and 22 DAA (Fig. 4.12 and Fig. 4.13). Whereas, the expression of the *1-FEH w3* isoform increased steadily until 17 DAA and then started to decrease (Fig. 4.11).

Overall, there was higher expression of *1-FEH w3* compared to the other two isoforms in water-deficit plants. The highest expression of *1-FEH w3* genes reached up to 325 units, compare to 100 units for *1-FEH w2* gene expression. In contrast, *1-FEH w1* gene expression showed the lowest level, reaching a maximum of 22 units.

There was no significant difference in *1-FEH* gene expression among the lines in well-watered plants (Figs, 4.10, 4.11 and 4.12).

4.4 Discussion

In a previous study, it was shown that high levels of stem WSC combined with *1-FEH* mediated remobilization efficiency may contribute to high TGW, especially under post anthesis water-deficit (Zhang et al. 2015b). Among the three isoforms of *1-FEH*, *1-FEH w3* has been considered as the main contributor in WSC remobilization under post anthesis water-deficit based on comparing the relative expression of those genes. However, specific role of these three isoforms in WSC remobilization, have not been fully identified. Hence, this study used the mutation lines of the individual isoforms of *1-FEH* to investigate their role in WSC remobilisation. This chapter has provided more detailed information on possible mechanisms underlying remobilization efficiency of fructan and other component of WSC along with the gene expression data. This gives an insight into the efficiency of the isoforms of *1-FEH*. The main findings of this research are discussed below.

4.4.1 Absence of 1-FEH w3 hindered fructan degradation

Based on the investigation in this chapter, it was evident that fructan degradation was slower in the *1-FEH w3* mutation line compared to the other two mutation lines and Chara under post anthesis water-deficit condition, whereas there were no significant differences in well-watered plants. It is widely accepted that after anthesis, fructans are predominant in the stem WSC pool (approximately 70% of the total WSC) which deliver carbon skeletons during grain filling (Wardlaw and Willenbrink 2000; Zhang et al. 2014b). In post anthesis water-deficit, rapid remobilization of fructan from the stem to the grain is vital to achieve the optimum grain weight

because they can compensate for the negative effect of reduced sugar supply (Dreccer et al. 2009; Goggin and Setter 2004; Wardlaw and Willenbrink 1994; Zhang et al. 2015b). In Chara, *1-FEH w2*, and *1-FEH w1* lines, remobilization of fructan started 5 days earlier than in the *1-FEH w3* mutation line (Fig. 4.3) and fructan degradation was slower than the other line (Fig. 4.4) This is in agreement with the results of glasshouse trial (Chapter 3), where the *1-FEH w3* mutation line had significantly lower grain weight and TGW compared to the other two mutation lines and Chara. The concentration of the different carbohydrate components changed in different way during the grain growth.

This study demonstrated that the expressional difference of the different isoforms of *1-FEH* were related to the variations in fructan degradation under terminal water-deficit condition. In particular, loss of *1-FEH w3* gene expression in the *1-FEH w3* mutation line (Fig. 4.5) resulted in delayed and slower degradation of fructan. In contrast, higher expression of the *1-FEH w3* gene in the *1-FEH w2* and *1-FEH w1* mutation lines and in Chara resulted in quicker and faster degradation of fructan. Accordingly, the fructose level peaked 5 days earlier in these lines compared to the *1-FEH w3* mutation lines. Expression of the *1-FEH w3* gene started to increase from 12 DAA and reached peak at 17 DAA (Fig. 4.11). Whereas, fructan degradation was faster at 12 DAA and fructose concentration reached at the peak at 17 DAA in *1-FEH w2* and *1-FEH w1* mutation lines and in Chara (Fig. 4.11). Zhang et al. (2015), also showed that high expression of the *1-FEH w3* gene contributed to the high levels of fructan and stem WSC remobilization to the grains in bread-wheat under water-deficit conditions.

Bifurcose is a branched fructan and works as a main structural unit of graminan type fructan and accumulates in the stem of wheat and other cereals stem. In the *1-FEH w3* mutation line bifurcose peaked 5 days earlier (at 7 DAA) than the other lines (Fig. 4.5). However, all the lines started degrading fructan at the same time which was 12 DAA (Fig 4.6). Moreover, for the first 5 days (up to 17 DAA) degradation was very slow in *1-FEH w3* mutation line while it was faster in *1-FEH w1*, *1-FEH w2* and Chara (Fig. 4.6). However, after 17DAA the degradation rate was faster in *1-FEH w3* mutation line (Fig. 4.5). These results correlate with the data on fructan degradation. Faster degradation of bifurcose and an increase in fructose is an indication of the faster remobilization of fructan (Zhang et al. 2015b).

The delayed start of fructan degradation (at 17 DAA) in the *1-FEH w3* mutation line (Fig. 4.3) did not allow sufficient time to remobilise the fructose to the grain for its development. The fructose concentration peaked at 22 DAA (Fig. 4.9) when plant reached at permanent wilting point. It is assumed that at that stage the plants had slowed down normal metabolism to a level where it was not possible to transport enough sugar to the developing gain in the *1-FEH w3*

mutation line to gain the usual grain weight. These findings clearly indicate, that slowing down fructan degradation in the *1-FEH w3* mutation line had a negative effect on final grain weight due to the absence of the *1-FEH w3* gene.

4.4.2 Mutation of 1-FEH w2 and w1 gene was compensated by high expression of 1-FEH w3 gene

Among the three mutation lines of the *1-FEH* isoforms, only the *1-FEH w3* mutation line, had significantly lower seed weight under water-deficit condition compared to Chara and the other two mutation lines. Notably, the *1-FEH w2* and *w1* mutation lines didn't portray any significant phenotypic differences from parent Chara (Chapter 3, Fig. 3.6). When a mutant fail to show a targeted phenotypic difference, the first hypothesis to test is 'there are upregulation of related genes which is making up the loss of function of the target gene'.

According to the WSC remobilization study (chapter 3 Fig. 3.5) and fructan degradation result (Fig. 4.4), it appears that the period between 12 and 22 DAA is the critical stage for sugar remobilization in developing grain to compensate for grain wt. Also, it was evident that *1-FEH w3* gene was over expressed in *w2* and *w1* mutation lines in water-deficit plants at 17 DAA and also at 22 DAA (Fig. 4.11). The expression of *w1* and *w2* gene in the *1-FEH w2* and *1-FEH w1* mutation lines respectively was higher after 22 DAA (Figs, 4.12 and 4.13). Thus, it can be concluded that overexpression of the *1-FEH w3* gene helped in the rapid remobilization of sugar and playing the vital role in maintaining grain yield under water-deficit.

4.4.3 Absence of 1-FEH w3 gene was not compensated by the other two isoforms

Unlike the *1-FEH w2* and *1-FEH w3* mutation lines, the phenotypic effect of the *1-FEH w3* mutation line was not masked by overexpression of other two isoforms. In the *1-FEH w3* mutation line, expression of the *1-FEH w2* and *1-FEH w1* genes was significantly lower than Parent Chara up to 17 DAA (Figs, 4.12 and 4.13). However, at 22 DAA there was a rise in gene expression but it was not overexpressed compare to Chara (Figs, 4.10 and 4.11). This might be the reason for the slower remobilization of WSC (Chapter 3, Fig. .3.5) and fructan (Fig. 4.4) under water-deficit which ultimately resulted in significantly lower grain wt (Chapter 3, Fig. 3.6) compared to other mutation line and Chara. From this observation, it can be concluded that, *w3* is the most important isoform among the three of *1-FEH* in sugar remobilization under water-deficit and that the other two isoforms do not influence on the role of *1-FEH w3*.

4.4.4 Absence of *1-FEH w3* made the line susceptible to water-deficit

Sucrose is the major transport compound in plants in general and in wheat in particular (Joudi et al. 2012; Ruan 2014). Sucrose is the initial substrate of fructan biosynthesis and at later stages breaks down to fructan to provide additional sucrose supply. So, to understand the mechanism of fructan metabolism during grain filling, it is necessary to investigate the metabolism sucrose as well. This is crucial under water deficit after anthesis when fructan can be converted to sucrose, which can effectively compensate for the low photosynthetic supply and can help the plant to maintain its grain-filling rate (Yang et al. 2004).

Two distinct patterns have been observed across the lines used in this study in terms of time to reach at the highest levels of sucrose and fructan, and this subsequent degradation. In the first pattern, the highest levels of sucrose and fructan were observed at the same time which was at 12 DAA in the *1-FEH w3* mutation line (Figs, 4.8 and 4.3). In the second pattern, the highest level of fructan was observed 5 days earlier than the highest level of sucrose in the mutation lines *1-FEH w2* and *1-FEH w1* and Chara (Fig. 4.3 and 4.8). These two patterns could be associated with their ability to tolerate terminal water-deficit. In drought tolerant genotypes, the sucrose concentration under water-deficit occurs after the fructan peak but in susceptible genotypes it occurs simultaneously with the fructan peak (Yáñez et al. 2017; Yang et al. 2004). From the results, it is now clear that the absence of the *1-FEH w3* gene made the line more susceptible to water-deficit. From other studies, it has been proposed that drought tolerant varieties have higher concentrations of glucose compare to susceptible one (Joudi et al. 2012; Yáñez et al. 2017). Moreover, in the experiment there were no significant differences in glucose concentration both in well-watered and water-deficit condition during the time course among the lines (Fig. 4.10). Therefore, we can presume that, the *1-FEH w3* gene has a strong influence on water-deficit tolerance but it is not the only regulatory factor.

4.4.5 Mutation of *1-FEH* isoforms did not upset the activity of *6-FEH*

Graminan fructan is a mixture of β (2,1) and β (2,6) linkages. Thus, the activities of both *1-FEH* and *6-FEH* genes are required to breakdown the fructan. 6-Kestose is considered to have β (2,6) which is broken down by *6-FEH*. In all mutation lines and Chara, there were no significant differences among the concentration and accumulation and degradation patterns of 6 kestose in both well-watered and water-deficit plants (Fig. 4.7) which indicate that mutation of the *1-FEH* isoforms did not influence the activity of *6 FEH*. So, it can be concluded that the differences in fructan degradation pattern in the *1-FEH* mutation lines is due to the effect of the mutation of that specific *1-FEH* isoform and not influenced by other FEH.

4.4.6 *1-FEH* expression in well-watered condition

Even though, *1-FEH* showed differences in their expression level in mutation line under terminal water-deficit (Figs, 4.11, 4.12 and 4.13) there were no significant differences in the expression level of these isoforms in the mutation line in well-watered plants (Figs, 4.11, 4.12 and 4.13). Besides that, the WSC data and grain wt. (Chapter 3) they did not show any significant differences indicating that the isoforms of *1-FEH* only worked in stressed plants not under normal conditions. A similar phenomenon was observed by Zhang et al. (2016) on water-deficit tolerant wheat cultivars (Zhang et al. 2016). However, this study for the first time used the *1-FEH* isoforms mutation lines which provided improved confirmation of functional differences of the isoforms between water-deficit and well-watered conditions.

4.5 Conclusion

The results suggested that *1-FEH w3* plays the most vital role in sugar remobilization to developing grain under post anthesis water-deficit. Functional loss of *1-FEH w3* gene slowed down fructan degradation under water-deficit condition and resulted in lower TGW and grain wt. On the other hand, functional loss of the *1-FEH w1* or *1-FEH w2* was compensated by the other two respective isoforms as evident by the significant upregulation at the transcript level. However, further investigation is required to confirm that this phenotypic difference was only due to the gene function loss of the target gene. This can be achieved by investigating the mutation region; whether only the target gene was mutated or any other gene was affected which might have similar function to the target gene. The next chapter investigates all the three mutation lines and characterizes the mutation region using a 90K SNP array.

Chapter 5: Characterization of *1-FEH* mutation lines using a 90K SNP array

5.1 Introduction

Mutational inactivation of plant genes is an essential tool in gene function studies and has contributed substantially to our current knowledge in this area (Lloyd and Meinke 2012). Use of plants with inactivated or deleted genes encoding particular traits of interest is a common process in research for crop improvement (Knoll et al. 2011). Loss of *1-FEH* gene function in the mutation lines used in this thesis was evident from the phenotypic study (Chapter 3) and gene expression analysis (Chapter 4).

Use of mutational gene inactivation/deletion (Timothy et al. 2014) in polyploid plant species is complicated by the existence of multiple copies of the same gene (homoeologous genes) encoded by each genome. The bread wheat genome is hexaploid, possessing three 'subgenomes', designated 'A', 'B' and 'D', approximately 17 Gb in total size which is 40 times the size of the rice genome. In addition to its extremely large size, the wheat genome contains a high percentage of repetitive segments (80 – 90%) (Šafář et al. 2010; Wanjugi et al. 2009). Generally, most wheat genes have six homoeologous copies and two alleles from each of the sub-genomes, which potentially leads to a high functional redundancy (Fitzgerald et al. 2012; Lai et al. 2012). This gene redundancy causes complications in gene knockout strategies and wheat appears to be extremely tolerant of mutation due to its polyploid genome. Although generally such high tolerance to mutation is desirable to keep the gene functional through the generations, the genomic redundancy is challenging for the production of loss-of-function mutants for a gene of interest (Wang et al. 2012). Moreover, the mutation lines used in this thesis were produced by heavy ion bombardment that induces DNA damage in a random manner and is known to cause different types of mutation including base substitutions, deletions and chromosomal alteration (Cecchini et al. 1998; Morita et al. 2009). Therefore, it is important to investigate how gene inactivation is working; for example, whether it is by DNA sequence alterations or by complete deletion, and also if the mutation has caused any polymorphism in the coding sequence or modification in gene function. Most importantly, any closely linked genes, which might influence WSC remobilization, need to be identified.

Characterization of causal mutations typically begins with genetic mapping, gene sequencing, generating marker data, and resequencing the gene underlying the mutated phenotype (Lukowitz et al. 2000; Nordström et al. 2013). Simultaneous Multiple Mutation Detection

(SMMD), TILLING, Single Sequence Repeat (SSRs) or microsatellite markers, Cleaved Amplified Polymorphic Sequences (CAPS) and whole genome sequencing are commonly used approaches for genetic mapping. In particular, SMMD using an electrochemical array is a very powerful tool for gene mutation detection (Wakai et al. 2004). In this technique, an enzyme is used to simultaneously distinguish several genetic mutations such as SNP (single nucleotide polymorphism), insertion, deletion and translocation depending on the melting temperature (T_m) (Wakai et al. 2004). On the other hand, TILLING is a sensitive mutation detection strategy, which allows directed identification of mutations in a specific gene (McCallum et al. 2000). Mutations are detected by testing for mismatches between the wild type and mutant heteroduplexes. This technique is very effective for point mutations, re-arrangements and small deletions but not for whole-gene deletions. Moreover, TILLING requires independent amplification of homoeologous gene copies (Fitzgerald et al. 2010) to prevent heteroduplexes forming between closely related sequences, which is not possible for polyploid species like wheat.

All the processes mentioned above are now superseded by whole genome sequencing approaches (Nordström et al. 2013; Zuryn et al. 2010). Whole genome sequencing is a straightforward and powerful tool to directly identify mutagen-induced nucleotide changes that are linked to the causal mutation and to recognize specific genomic location of the mutated region (Nordström et al. 2013). High-density SNP arrays have been optimized and successfully used for genetic studies of a number of economically important crops (Akond et al. 2013; Ganai et al. 2011; Sim et al. 2012; Wiedmann et al. 2008; Zhao et al. 2011). For example, a 44K SNP genotyping chip successfully identified dozens of alleles controlling 34 morphological, developmental and agronomic traits of rice through the GWAS (Genome Wide Association Study) of 413 diverse rice accessions (Zhao et al. 2011). In the case of maize, a 50K SNP chip has been used to study the genetic control of maize kernel composition in a nested association-mapping panel (Cook et al. 2012) and successfully identified signatures of wild relative allele introgressions in the maize genome (Hufford et al. 2012). In wheat, construction of high-resolution genetic maps based on the microarray hybridization-based technique called Diversity Arrays Technology (DArT) was developed that enabled high-throughput genotyping without relying on sequence information (Akbari et al. 2006). Advancement in next-generation sequencing (NGS) technology have made it possible to screen for SNPs which have been used to develop high-throughput SNP-typing platforms such as BeadExpress (Trebbe et al. 2011), KASPar (Allen et al. 2011) and Infinium (Cavanagh et al. 2013). A 9K SNP wheat chip was used to detect genomic regions targeted by breeding and improvement selection (Akhunov et

al. 2009; Cavanagh et al. 2013). More recently, Wang et al. (2014) reported a 90K SNP iSelect array that comprises approximately 90,000 gene-associated SNPs with the potential of providing dense coverage of the wheat genome. This technology offers a resource for diversity studies and high-resolution dissection of complex traits in wheat. Due to the *International Wheat Genome Sequencing Consortium* (IWGSC) whole genome assembly (WGA), comprised of Illumina short sequence reads assembled with NRGene's DeNovoMAGIC™ software a reference sequence of wheat is available. It produced scaffolds totalling 14.5 Gb with a L50 of 7.1 Mb that have been assigned to chromosomal locations using POPSEQ data and scaffolds linked using HiC mapping. Over 99% of the chromosome survey contig maps have been completed in the IWGSC WGA v0.4 assembly (13 Jun 2016, IWGSC News).

In this study, a 90K iSelect array was used to survey SNPs across the mutation lines and the parent cultivar Chara. Data obtained from the 90K analysis were compared with the recently released wheat whole genome assembly. The IWGSC project team has been fine-tuning the data so that the genome assembly released to the scientific community at the time of this analysis was of the possible highest quality (R Appels, personal communication). It accurately represents more than 90 percent of the highly complex bread wheat genome, contains over 97 percent of known genes, and assigns the data to the 21 wheat chromosomes.

The objective of this study was to investigate the *1-FEH* gene mutations, map the mutation region in the chromosome and annotate the mutational region. The hypothesis is that in the mutation region, no other gene is mutated except the gene of interest.

5.2 Materials and methods

5.2.1 Plant materials

The *1-FEH w1*, *w2* and *w3* mutation lines derived from the Australian bread wheat cultivar Chara (Chapter 3) were back crossed (Table 5.1) in 2015 in a Murdoch University glasshouse to check the stability of mutation and also to reduce background genetic noise due to mutations elsewhere in the genome. The parent Chara was used as the female parent. The potting mix, plant nutrition and watering protocols have been described previously (Chapter 3). The F1 seeds were collected on maturation at 65 days after pollination and were used for developing the iSelect 90K SNP array.

Table 5.1: Crossing of Chara and mutation lines.

Female parent	Male parent mutation line	Mutation gene
Chara	BW22-M3-22-w1	<i>1-FEH w1</i>
Chara	BW21-M3-433-w2	<i>1-FEH w2</i>
Chara	BW18b-M3-426-w3	<i>1-FEH w3</i>

5.2.2 Genotypic DNA extraction

The F1 seeds (4 to 5 seeds) from all the backcrosses (Table 5.1) were placed in Petri dishes for germination and were kept at room temperature (27°C). All the seeds germinated in 3 days. Tissues were collected from the two youngest leaves of 10 days old seedlings and immediately stored at -20°C for genomic DNA extraction. DNA was extracted using Illustra DNA Extraction Kit Phytopure (illustra Nucleon Phytopure Genomic DNA Extraction Kits, GE Healthcare) following the standard protocol supplied by the manufacturer (Illustra Nucleon Phytopure for small sample, 0.1g RPN8510).

One microliter of extracted DNA was run on 1% agarose gel along with standard lambda DNA (Axyzen Life Sciences) to check the quality. The DNA concentration was quantified using NanoDrop (ND 1000 Spectrophotometer, Thermo Fisher Scientific). The DNA samples were then diluted to 20 ng μL^{-1} in 50 μL EB buffer (10 mM Tris-HCl pH 8.5) that stabilized the DNA. The extracted DNA samples were stored at -20 °C and shipped to AgriBio, Latrobe University, Melbourne for genotyping with the 90K SNP chip.

5.2.3 90K SNP chip analysis

The Infinium 90K SNP iSelect platform was used for genotyping using BeadStation and iScan according to the manufacturer's protocol from Illumina. Deletions in the HIB (Heavy Ion Bombardment) mutants were identified from output files using Illumina's GenomeStudio v2011.1 (Illumina Inc.) and custom MS Excel macros and/or perl scrip, where shifts away from the euploid SNP cluster position indicate a deleted locus.

Standard cluster files provided with infinium products identify expected intensity levels of genotype classes for each SNP. Raw intensity data for the 3 *FEH* HIBs and 3 *FEH* HIB x Chara backcrosses (as well as pre-existing data for Chara and other unrelated CSIRO HIBs) were loaded into Genomestudio and the NormTheta (x-axis coordinate) and NormR (y-axis coordinate) values from the SNP cluster plots were exported. Shifts in cluster position were

calculated between the euploid Chara and each of the mutant samples. The differences in Norm Theta and in NormR were calculated following the formula: $\text{Theta [Chara]} - \text{Theta [samples]}$. Shifts in cluster position were also calculated between the average HIB position (96 unrelated HIB mutants genotyped of Chara previously used in a different project and each of the *FEH* mutant samples). The 96 HIBs were used as an extra tool for helping to identify putative deletions due to the presence of Chara biotypes (i.e. different versions of 'Chara'). Differences in Norma Theta and in Norma R were calculated using the formula: $\text{Theta [Av. HIB]} - \text{Theta [sample]}$.

The 96 HIBs were used as an additional tool for helping to identify putative deletions due to the presence of Chara biotypes (i.e. different versions of "Chara"). SNP loci putatively tracking deleted segments were identified in each of the FEH HIB mutants. SNP with a minimum cluster shift between Chara and the HIB mutant of 0.1 along the Norm Theta axis, were considered to be putative markers for a deletion.

In order to help clarify the position of the *FEH* genes in chromosomes 6A, 6B and 6D, sequences similar to the *FEH* gene sequence (FJ184991) had been aligned in Gydle against the NR gene Chinese Spring genome assembly made available by R Appels through the IWGSC. Regions in the wheat NRgene scaffolds containing 1-*FEH*-like sequences were identified from the alignment. SNPs were retained if they showed evidence for deletion, and/or if they were mapped to 6A, 6B or 6D based on NRgene assembly or other mapping information. All other uninformative SNPs were removed from the report.

Markers were ordered by chromosome, then by their position in the NRgene assembly. Markers putatively flanking deleted segments were identified for each HIB line by looking at the shift in cluster Position. All SNPs were considered, even those with cluster shifts <0.2 Norm Theta and/or <0.5 Norm R. These markers were visually assessed in GenomeStudio to assess polymorphisms relative to Chara. In order to validate that the deletion detected was in fact located on the subgenome of interest (e.g. 6A) rather than a homoeologue (e.g. 6B or 6D), 90K SNPs with only one hybridization site in the NRgene assembly were identified. Those single-site SNPs located near either end of the deletion were visually assessed in GenomeStudio. A 'null' allele, where there is no fluorescence due to deletion of the hybridisation site, was considered to be indicative of the deletion occurring on the subgenome specified by the NRgene scaffold. In order to estimate the size of the deletion, information for the NRgene scaffolds (HiC Bin, PopSeq cM) and 90K mapping information (SNP consensus map) were reported.

5.2.4 Data analysis

For mapping and analysing the SNP data provided by AgriBio, Latrobe University, Melbourne, UGENE - Integrated Bioinformatics Tools (<http://ugene.net/>), UniprotKB (<http://www.uniprot.org/>), and CLC Main Workbench - QIAGEN Bioinformatics were used. CDS sequences and exons of *1-FEH-w1*, *w2* and *w3* were used for blast analysis against the IWGSC WGA v0.4 pseudo chromosomes 6A, 6B and 6D. For studying gene expression of these gene copies, public RNAseq data exVIP (<http://www.wheat-expression.com/#>) was used. Chromosome 6 group specific IWGSC MIPS gene models v2.2 (July 2014) were used to identify genes in the deleted chromosome regions. Sequence annotations, including GO terms and Pfam domain information along with structural predictions performed using the Phyre² Protein Homology/analogy Recognition Engine V 2.0 were used to determine the molecular function of these genes.

5.3 Results

5.3.1 An overview of the 90K SNP array

From iSelect illumine 90K SNP array analysis, putative deletions were identified in the *FEH* HIBs encompassing the *FEH* genomic regions (Table 5.2). According to deletion summary a map was constructed (Fig. 5.1) depending on pop seq position. This gave a clear idea about the deleted region of the *FEH* HIB mutant lines. The 6B mutants had smaller deletions compared to the 6A and 6D mutants (Fig. 5.1). For each HIB line, markers at each end of the deletion were identified to estimate the size of the deletion.

SNPs with minimum cluster shift between Chara and the HIB mutant of 0.1 along the Norm theta axis or 0.5 along the NormR axis, were considered to be putative markers for a deletion. Deletions were confirmed by the Chara X mutant backcross, which were located at a 'HET' position, i.e. halfway between the mutant and the euploid Chara. The Infinium assay probes bound to multiple sites in the genome due to the presence of homologues (e.g. 6A, 6B and 6D) and paralogues, and polymorphism on any one of these sites were detected based on cluster position. Deletion of a segment of DNA in a HIB mutant affected the number of loci to which the probe could hybridise. This resulted in a shift in the NormTheta and/or NormR axes relative to the euploid sample, i.e. Chara (. 5.2 as an example).

When the probe had only one hybridisation site in the genome (e.g. hybridises to 6A but not 6B or 6D), deletion of a hybridisation site resulted in a 'null' allele, i.e. a lack of fluorescent signal (Fig. 5.3 as an example). Those single-site SNPs, located near either end of the deletion, were visually assessed in Genome Studio. A 'null' allele was considered to be indicative of the

deletion occurring on the sub genome specified by the NRgene Scaffolds. Biotypes were observed between the Chara used to make HIBs and Chara used to backcross with the HIBs (Fig. 5.4).

Table 5.2: Summary of deletions observed in each *1-FEH* mutant (screenshot of 90K inifnum SNP deletion summary results). D (Red): deletion detected on target chromosome; d: deletion detected on homoeologous chromosome. H (Grey): deletion detected on target chromosome in heterozygous condition, h: deletion detected on homoeologous chromosome in heterozygous condition. Highlighted (yellow) area showing NRgene PopSeq position for targeted gene.

Chr	Region containing FEH-like sequence	6A	6A x C	6B	6B x C	6B	6B x C	6D	6D	6D x C	SNP index	Description of observed poly	HIC Bin	HIC scaffold orientation	NRgene PopSeq Chr Assignment	NRgene PopSeq Position	NRgene Total number of QueryHits across genome	Original 90K consensus map	New 90K consensus cM (Hayden et al, unpublished)
6AS	.	D	H	76092	Poly	12	1	6A	10.92	3	65.33	58.4
6AS	.	D	H	3722	Null	12	1	6A	10.92	1	.	62.77-67.48
6AS	FEH_6A	D	H	25	1	6A	30.69	.	.	.
6AS	.	D	H	71378	Null	25	1	6A	30.69	1	115.71	93.64-104.11
6AS	.	D	H	d	h	d	h	d	h	.	55811	Poly	25	1	6A	30.69	3	.	.
6AS	.	D	H	d	.	1675	Poly	26	1	6A	31.15	1	.	.
6AS	.	D	H	41259	Poly	27	1	6A	31.45	1	.	.
6AS	.	D	H	3378	Poly	27	1	6A	31.45	1	140.54	110.38-112.35
6AS	.	D	H	10826	Poly	27	1	6A	31.45	3	.	.
6BS	.	.	.	D	H	D	H	.	.	.	10716	Null	54	1	6B	41.19	1	160.39	88.3
6BS	FEH_6B	.	.	D	H	D	H	55	1	6B	41.08	.	.	.
6BS	.	d	h	D	H	D	H	d	d	h	55811	Poly	55	1	6B	41.08	3	.	81.79-103.52
6BS	.	.	.	D	H	D	H	.	.	.	75083	Poly	55	1	6B	41.08	1	160.39	84.04-89.1
6BS	D	H	.	.	.	76997	Poly	55	1	6B	41.08	1	160.39	89.1
6BS	D	H	.	.	.	47681	Null	55	1	6B	41.08	1	.	.
6BS	.	d	.	.	.	D	H	.	d	h	64837	Poly	55	1	6B	41.08	6	.	103.6
6DS	D	.	28097	Poly	25	1	6D	35.01	2	.	.
6DS	.	d	h	D	D	H	18485	Poly	26	1	6D	37.95	1	.	.
6DS	FEH_6D	26	1	6D	37.95	.	.	.
6DS	.	d	h	d	h	d	h	D	D	H	55811	Poly	26	1	6D	37.95	3	.	.
6DS	.	d	h	d	h	d	h	D	D	H	46499	Poly	26	1	6D	37.95	1	.	.
6DS	D	.	18413	Null	26	1	6D	37.95	1	.	.
6DS	D	.	44564	Poly	29	-1	6D	42.97	3	.	.
.
6DL	D	.	65035	Poly	82	1	6D	53.80	3	186.66	81.82
6DL	D	.	12893	Poly	82	1	6D	53.80	1	.	.
6DL	D	.	18347	Poly	99	1	6D	82.90	1	239.2	86.97-107.76
6DL	.	.	.	d	h	.	.	.	D	.	19348	Poly	107	NA	6D	94.60	2	256.38	86.97-107.76

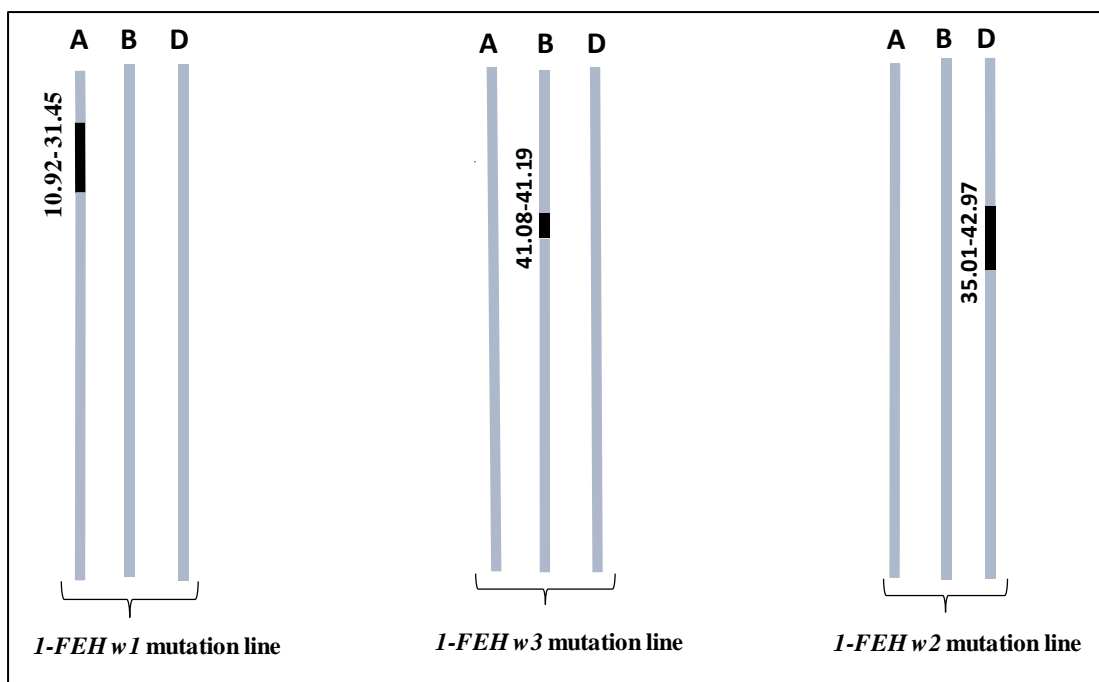


Fig. 5.1: Diagram of deletion in chromosome arm of mutant lines (pop seq position).

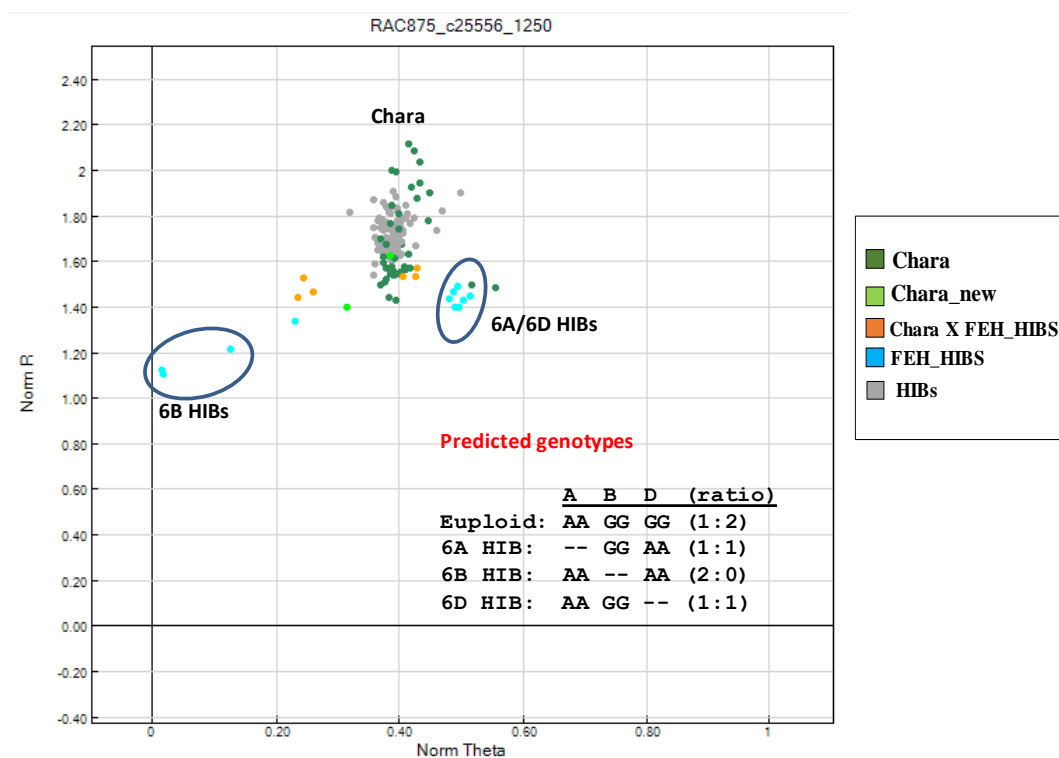


Fig. 5.2: Example of SNP detecting a deletion in all homeologues (SNP#55811). This SNP probe hybridised to a region within the *1-FEH* gene in all three homoeologues and detects a deletion in each HIB line. The genotypes are predicted based on shifts in NormTheta (x-axis), which reflect the ratio of A/T to C/G alleles. [Screenshot from GenomeStudio]. Chara (dark green), provided Chara (light green), provided HIB mutants (light blue) and other HIBs genotype previously (light grey).

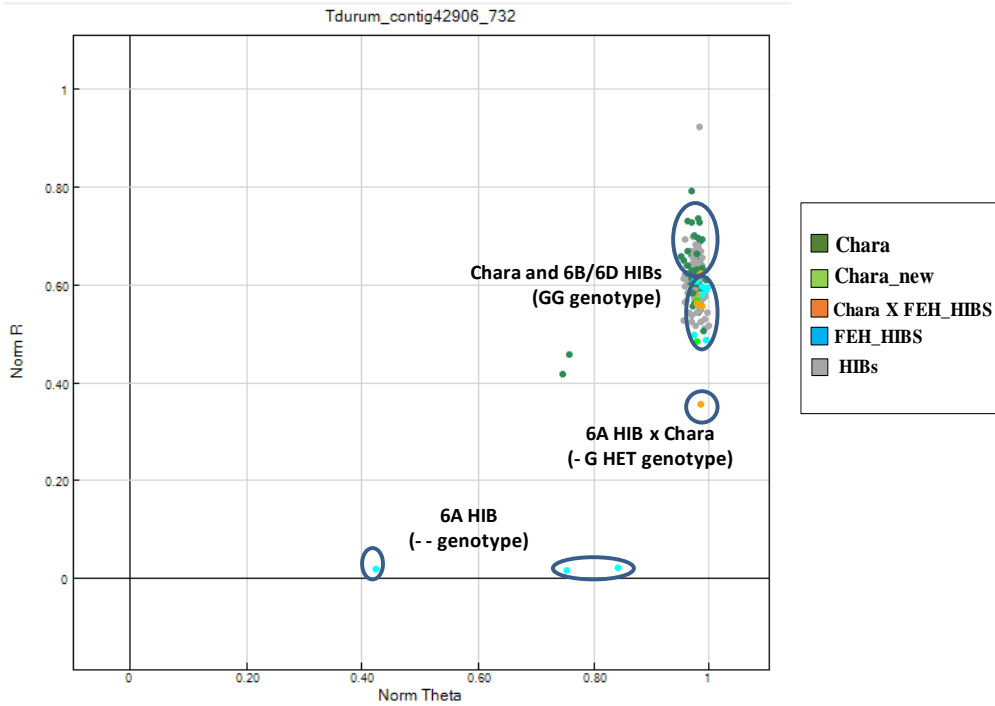


Fig. 5.3: Null allele for SNP#71378 in 6A HIB (Genome Studio Screen shot). Chara (dark green), provided Chara (light green), provided HIB mutants (light blue) and other HIBs genotyped previously (light grey).

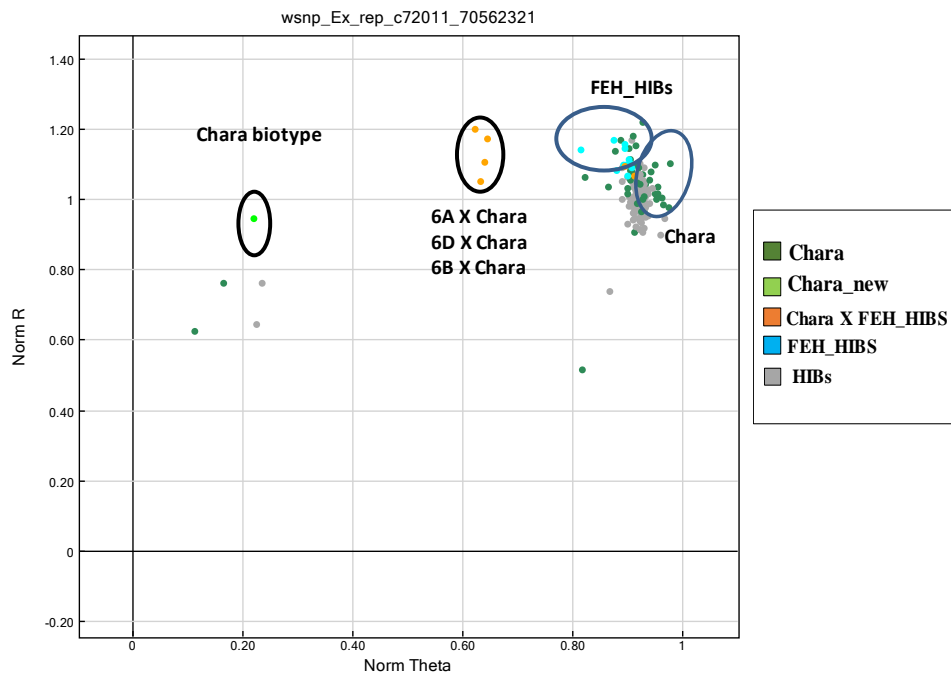


Fig. 5.4 Example of Chara biotype. The provided Chara (light green) is located in a different position compared to all provided HIB mutants (light blue) and other HIBs genotyped previously (light grey).

5.3.2 Mapping of mutation region in chromosomes

A high-density polymorphism cluster was identified from sequence data obtained from Illumina 90K SNP analysis, which is considered to be a mutated region of that chromosome. This high-density region was found in to NRgene scaffold 90107, scaffold 123806 and scaffold 33960 in chromosomes 6A, 6B and 6D, respectively. By detecting the approximate genomic location of the causal mutation, the affected gene was subsequently identified within this region and mapped. Deletion size in scaffold 90107 (chromosome 6A) was 1299655 bp; from 1551189 bp to 2850844 bp (Fig. 5.5). The deletion was 2748910 bp (from 296427 bp to 3045337 bp) (Fig. 5.6) and 1717718 bp (from 940630 bp to 2658348 bp) (Fig. 5.7) in scaffold 123806 (chromosome 6B) and scaffold 123806 (chromosome 6D), respectively.

A total of 15 SNPs were identified within the mutation region of *1-FEH w1* on scaffold 90107 on chromosome 6A (Table 5.3). Nine were within the target gene (*1-FEH w1*) and six were on non-target genes (Fig. 5.2). Similarly, a total of 15 SNPs were identified within the mutation region of *1-FEH w3* on scaffold 123806 at chromosome 6B (Table 5.4). Seven were within the target gene (*1-FEH w3*) and remainder of the eight SNPs were on non-target genes (Fig. 5.3). In the case of *1-FEH w2* mutation region on the scaffold 33960 at chromosome 6D, a total of 20 SNPs were identified (Table 5.5). Only six of them were within the target gene (*1-FEH w1*) and 14 were on non-target genes (Fig. 5.2).

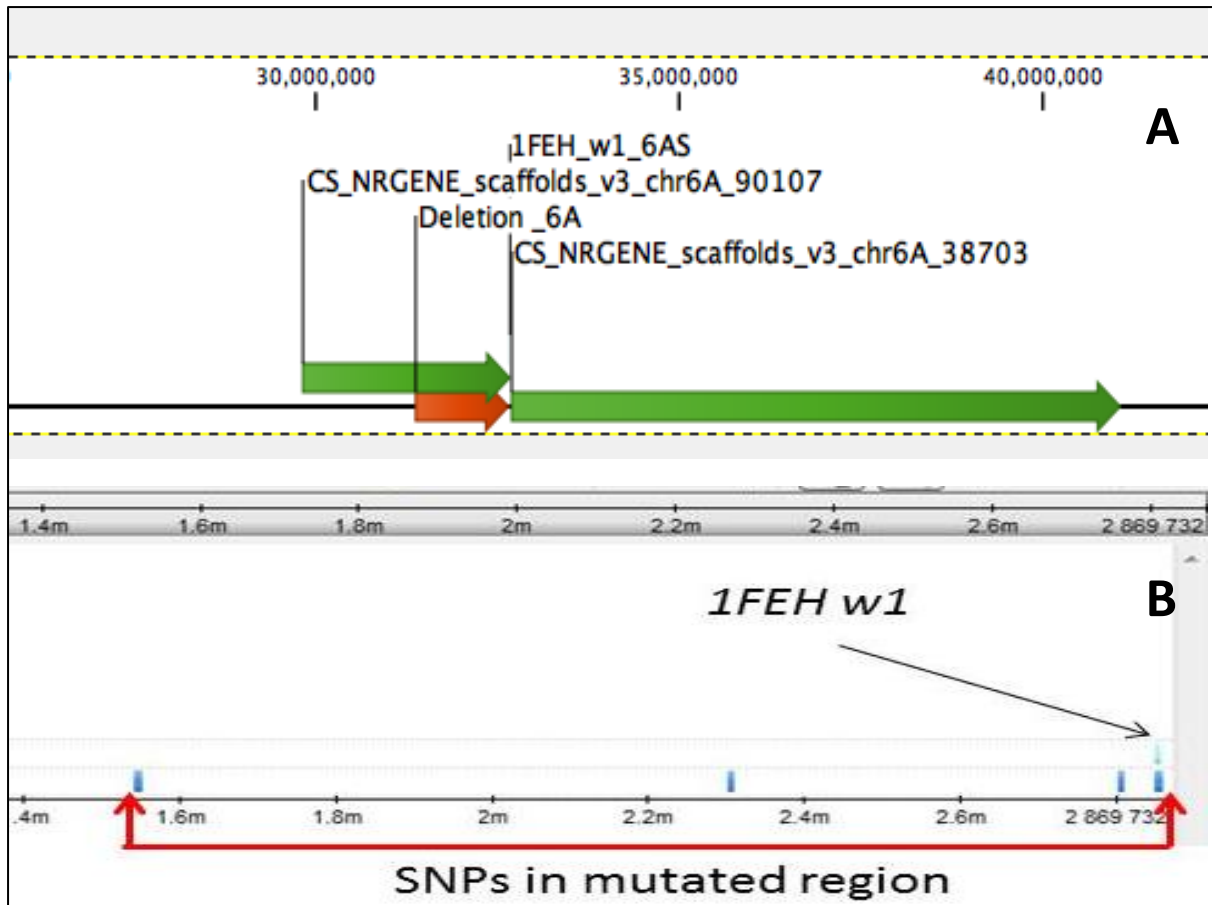


Fig. 5.5: Mutation region on the scaffold 90107 at chromosome 6A with the target gene *1-FEH w1*. **PanelA:** shows the mutation region in the context of position at the scaffold, **Panel B:** shows the position of SNPs and the target gene within the mutation region.

Table 5.3: List of SNPs in the mutated region of *1-FEH w1* on scaffold 90107 (chromosome 6A).

SI no	SNP ID	SNP name	Scaffold start	Scaffold stop	SNP location in gene
1	IWB74684	tp1b0040h19_458	1541626	1541673	Non targeted gene
2	IWB11722	BS00091666_51	1542944	1542993	
3	IWB6111	BS00009782_51	1543602	1543651	
4	IWB49620	Kukri_rep_c113626_110	1543854	1543903	
5	IWB40242	Kukri_c100884_175	1543929	1543978	
6	IWB72839	Tdurum_contig61934_60	1571518	1571567	
7	IWB71378	Tdurum_contig42906_732	2847465	2847514	
8	IWA5402	wsnp_Ex_rep_c67468_66069282	2849060	2849109	
9	IWB73939	Tdurum_contig9544_978	2849111	2849160	
10	IWB55811	RAC875_c25556_1250	2849279	2849328	
11	IWB5079	BobWhite_rep_c54320_201	2849977	2850026	
12	IWA5400	wsnp_Ex_rep_c67468_66068537	2850285	2850334	
13	IWA3319	wsnp_Ex_c31149_39975724	2850501	2850550	
14	IWA7443	wsnp_Ku_rep_c68790_67933679	2850549	2850598	
15	IWB3945	BobWhite_c56928_186	2850573	2850622	

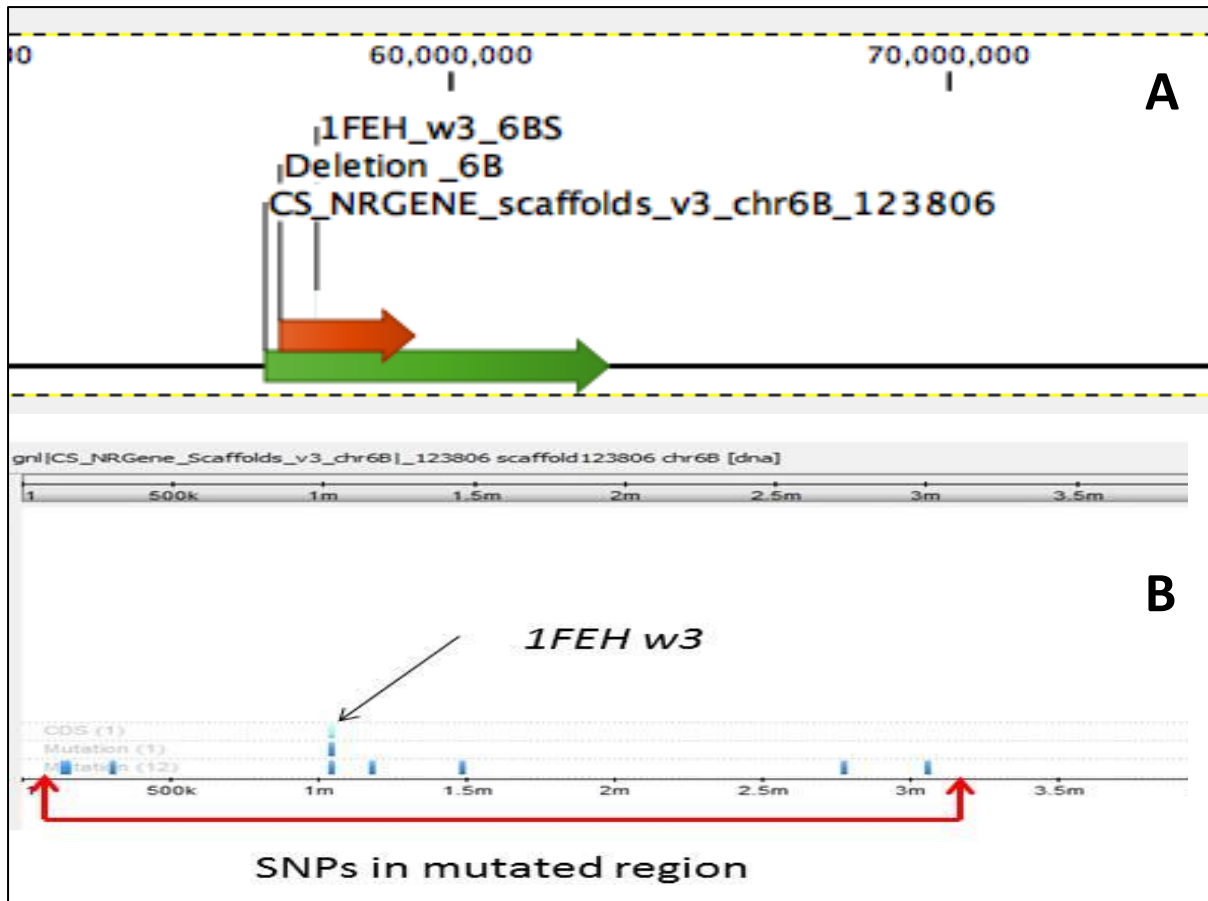


Fig. 5.6: Mutation region on the scaffold 123806 at chromosome 6B with the target gene *1-FEH w3*. **Panel A:** shows the mutation region in the context of position at the scaffold, **Panel B:** shows the position of SNPs and the target gene within the mutation region.

Table 5.4: List of SNPs in the mutated region of *1-FEH w3* on scaffold 123806 at chromosome 6B.

Sl No	SNP id	SNP name	Scaffold start	Scaffold stop	NR gene scaffold name
1	IWB68436	Tdurum_contig15643_316	127820	127869	Non targeted gene
2	IWB68436	Tdurum_contig15643_316	146074	146121	
3	IWB10716	BS00074183_51	296427	296476	
4	IWA5402	w SNP_ Ex_rep_c67468_66069282	1035881	1035930	Targeted gene (<i>1-FEH w3</i>)
5	IWB55811	RAC875_c25556_1250	1036100	1036149	
6	IWB39835	Ku_c68790_566	1036891	1036940	
7	IWB5079	BobWhite_rep_c54320_201	1036897	1036946	
8	IWA7443	w SNP_ Ku_rep_c68790_67933679	1037469	1037518	
9	IWB3945	BobWhite_c56928_186	1037493	1037542	
10	IWB50563	Kukri_rep_c97927_380	1037548	1037596	
11	IWB3945	BobWhite_c56928_186	1074811	1074857	
12	IWB65434	TA001668-0792	1169399	1169448	Non targeted gene
13	IWB70158	Tdurum_contig31061_225	1473605	1473654	
14	IWB13538	CAP12_c7629_189	2763034	2763083	
15	IWB75083	tp1b0055h14_483	3045288	3045337	

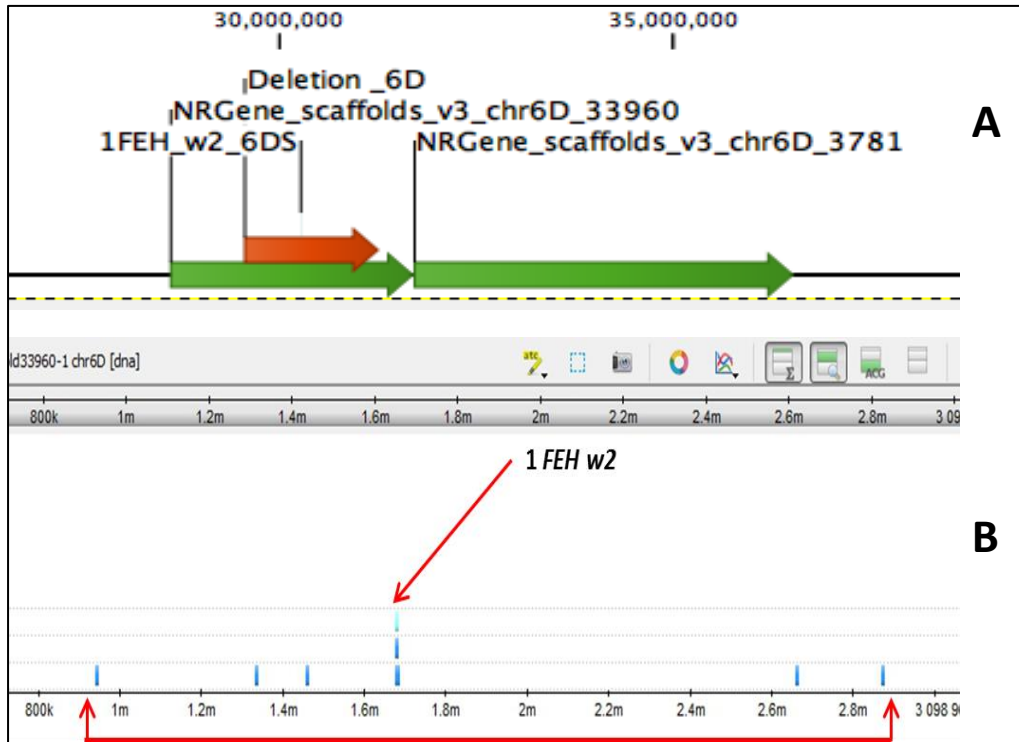


Fig. 5.7: Mutation region on the scaffold 33960 at chromosome 6D with the target gene *1-FEH w2*. **Panel A:** shows the mutation region in the context of position at the scaffold, **Panel B:** shows the position of SNPs and the target gene within the mutation region.

Table 5.5: List of SNPs in the mutated region of *1-FEH w2* on scaffold 33960 at chromosome 6D.

SL no	SNP id	SNP name	Scaffold start	Scaffold stop	NR gene scaffold name
1	IWB72866	Tdurum_contig62141_148	96,293	96,342	Non targeted gene
2	IWB10887	BS00074183_51	1330312	1330361	
3	IWB67654	Tdurum_contig12558_205	1456428	1456477	
4	IWB5079	BobWhite_rep_c54320_201	1620535	1620581	
5	IWB32525	GENE-1530_594	1632751	1632800	
6	IWB32524	GENE-1530_548	1632840	1632889	
7	IWA5402	wsnp_Ex_rep_c67468_66069282	1633553	1633602	
8	IWB50563	Kukri_rep_c97927_380	1640855	1640903	
9	IWA3320	wsnp_Ex_c31149_39975883	1640873	1640922	
10	IWB32525	GENE-1530_594	1641560	1641609	
11	IWB32524	GENE-1530_548	1641649	1641698	
12	IWB50563	Kukri_rep_c97927_380	1676927	1676976	
13	IWA3320	wsnp_Ex_c31149_39975883	1676946	1676995	
14	IWA3319	wsnp_Ex_c31149_39975724	1677054	1677103	
15	IWB5079	BobWhite_rep_c54320_201	1677578	1677627	
16	IWB55811	RAC875_c25556_1250	1678210	1678259	
17	IWA5402	wsnp_Ex_rep_c67468_66069282	1678429	1678478	
18	IWB46499	Kukri_c5531_358	1678711	1678760	Non targeted gene
19	IWB18413	D_GBF1XID01EJNX8_134	2658301	2658348	
20	IWB68436	Tdurum_contig15643_316	2868488	2868537	

5.3.3 Annotation of the deleted/mutated region

Identifying the gene structures of both the target and non-target genes within the mutation region is one of the most crucial parts in understanding the consequence of mutation. Mutated regions of chromosomes 6A, 6B and 6D of the *1-FEH* mutation lines were annotated with IWGSC WGA v0.4 assembly using CLC Genomic Workbench (www.qiagenbioinformatics.com/products/clc-main-workbench). The analysis provided the information to assess the putative effect of mutation by mapping the genes present in the mutated region. Annotation involves marking where the target gene starts and stops in the sequence and whether any other closely related genes of interest are positioned in the mutated segment.

From the annotation of mutation region of the *1-FEH w1* mutated line, 9 genes were identified on chromosome 6A including *1-FEH w1* (Table 5.6, Fig. 5.8). Accordingly, 7 genes were identified in the *1-FEH w3* mutation region on chromosome 6B including *1-FEH w3* gene (Table 5.7, Fig. 5.9). However, annotation of the *1-FEH w2* mutated region on chromosome 6D appeared to be more complicated. In IWGSC WGA v0.4 assemblies, chromosome 6D was not yet fully assembled (R Appels personal communication), so it became difficult to identify the position of the deletion region. Thus, for the *1-FEH w2* mutated region, analysis was carried out using unmapped CDs sequence. There, in addition to *1-FEH w2*, an extra three copies of *1-FEH* were identified and named as *1-FEH w2 1-FEH w2-2*, *1-FEH w2-3* and copy 4 (Fig. 5.10). Gene copy 4 contained a 15,831 bp insertion in the coding region and is most likely an inactive gene.

Identified genes were used for blast analysis to obtain translated protein sequences. Protein annotations and 3D model structuring were carried out using the software *Phyre²* to characterise the gene function (Tables 5.10 and 5.11). *Phyre²* based annotations were generally consistent with annotation gained from orthologue sequences. Tables 5.9 and 5.10 present translated protein sequences and basic protein structures (*Phyre²* annotation) to show the differences between the *1-FEH w3* gene and Beta-fructofuranosidase (Table 5.8) and *1-FEH w2* gene, *1-FEH w2-2* and *1-FEH w2-3* of *1-FEH w2* gene (Table 5.9).

Based on the protein annotation, all genes were categorised according to their broad functional attributes (Table 5.12). All the proteins fell within four major functional groups: Hydrolase, Ligase, Oxidoreductase and Transferase, respectively. One protein was identified as *de-novo*. Hydrolase appeared as the largest group with 12 genes within this functional group followed by the Ligase group with 6 genes.

This study identified an extra three copies of the *1-FEH w2* gene (*1-FEH-w2-2*, *1-FEHw2-3*, *1-FEHw2-4*) which were investigated further. Protein sequence of Gene *1-FEHw2-4* was not found since it contains a large insertion in the coding region, and can be considered an inactive gene. The other two copies represented complete CDS sequences. To find out whether the other two gene copies are active and are expressed in different growth stages or tissues or stress conditions, an expression analysis study was carried out using exVIP (<http://www.wheat-expression.com>) on publicly available RNAseq data (Figs, 5.11 and 5.12). The analysis result demonstrated that both copies of *1-FEH w2-2* and *1-FEH w2-3* were mainly expressed in the grain and *1-FEH w2-3* showed higher expression than *1-FEH w2-2*, while *1-FEH w2* was not expressed in the grain (Fig. 5.11). In stem and leaves, *1-FEH w2-1* had higher expression than *1-FEH w2-2* and *1-FEH w2-3* (Fig. 5.12). In the root, only *1-FEH w2* was expressed (Fig. 5.13).

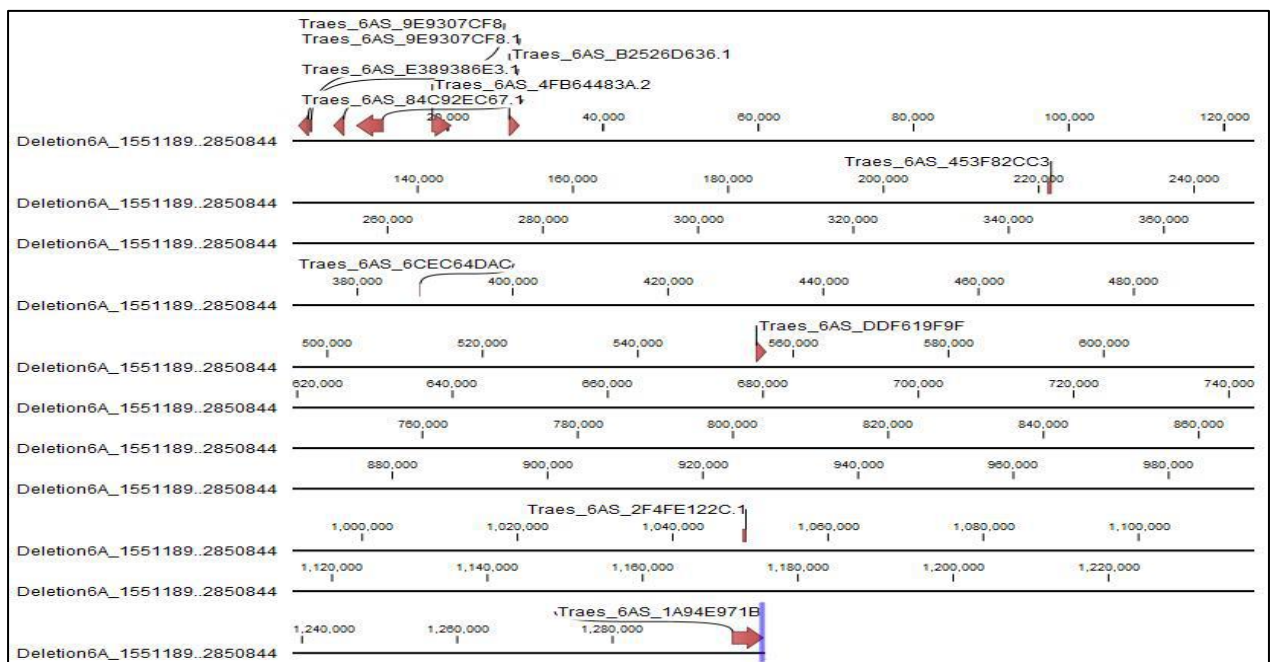


Fig. 5.8: Annotation of the mutated region of *1-FEH w1* on chromosome 6A (scaffold 90107, 1551189 bp – 2850844 bp).

Table 5.6: List of the genes positioned in the mutated region of *1-FEH w1* on chromosome 6A (scaffold 90107, 1551189 bp – 2850844 bp).

Transcription ID	Gene ID	Name	Uniprot ID	Function
Traes_6AS_9E9307CF8	TRIAE_CS42_6AS_TGACv1_486348_AA1560160	Uncharacterized protein	A0A1D6AH30	Transferase activity, transferring hexosyl groups
Traes_6AS_E389386E3	TRIAE_CS42_6AS_TGACv1_486348_AA1560160	Uncharacterized protein	A0A1D6AH30	Ligase, catalytic activity
Traes_6AS_84C92EC67	TRIAE_CS42_6AS_TGACv1_486348_AA1560161	Uncharacterized protein	W5GEM1	non translating CDS
Traes_6AS_4FB64483A	TRIAE_CS42_6AS_TGACv1_486348_AA1560130	Uncharacterized protein	A0A1D6AH27	Transferase (Glutathione-S-Trfase)
Traes_6AS_B2526D636	TRIAE_CS42_6AS_TGACv1_486348_AA1560120	Uncharacterized protein	A0A1D6AH26	transferase activity, transferring hexosyl groups
Traes_6AS_6CEC64DAC	TRIAE_CS42_6AS_TGACv1_486161_AA1557660	Uncharacterized protein	A0A1D6AGM4	Hydrolase (peptidase)
Traes_6AS_DDF619F9F	TRIAE_CS42_6AS_TGACv1_485766_AA1551710	Uncharacterized protein	A0A1D5V0P2	Ligase
Traes_6AS_2F4FE122C	TRIAE_CS42_6AS_TGACv1_496254_AA1578120	Uncharacterized protein	A0A1D6AK09	Oxidoreductase
Traes_6AS_1A94E971B	TRIAE_CS42_6AS_TGACv1_487805_AA1573030	Fructan 1-exohydrolase	Q84PN8/A0A096U TV0/	hydrolase activity, fructan beta-(2,1)-fructosidase activity

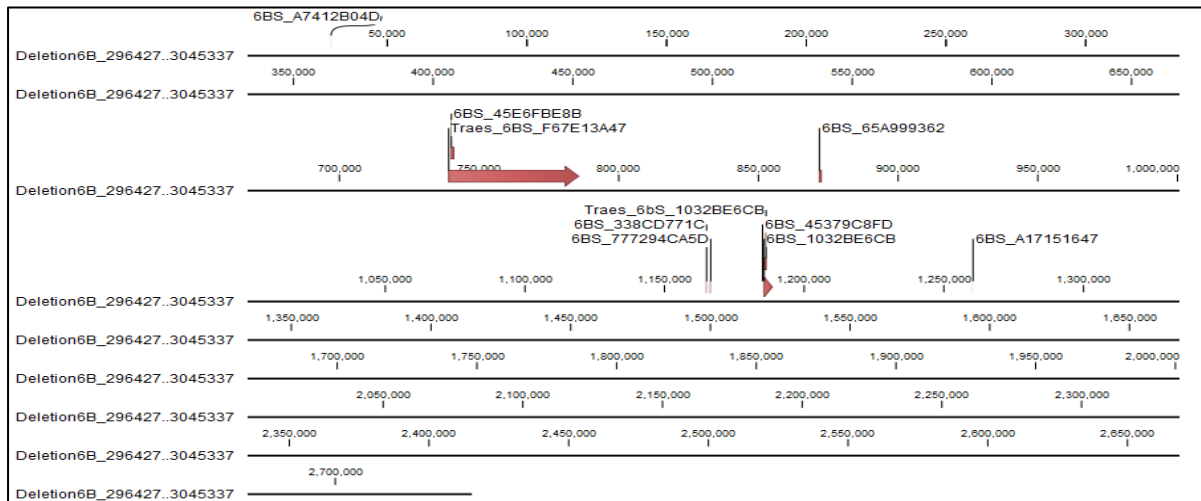


Fig. 5.9: Annotation of the mutated region of *1-FEH w3* on chromosome 6B (scaffold 123806, 296427 bp – 3045337 bp).

Table 5.7: List of the genes positioned in the mutated region of *1-FEH w3* on chromosome 6B (scaffold 123806, 296427 bp – 3045337 bp).

Transcription ID	Gene ID	NAME	Uniprot ID	Function
Traes_6BS_A7412B04D	TRIAE_CS42_6BS_TGACv1_515217_AA1668210	Uncharacterized protein	W5GS37	Non translating
Traes_6BS_45E6FBE8B	TRIAE_CS42_6BS_TGACv1_515484_AA1670340	<i>1-FEH</i>	B6DZC8	hydrolase activity, hydrolyzing O-glycosyl compounds
Traes_6BS_F67E13A47	TRIAE_CS42_6BS_TGACv1_514515_AA1660840	Beta-fructofuranosidase, insoluble isoenzyme 4	A0A1D6AZI1	hydrolase activity, hydrolyzing O-glycosyl compounds
Traes_6BS_65A999362	TRIAE_CS42_6BS_TGACv1_515390_AA1669820	Uncharacterized protein	A0A1D6B1A1	Hydrolase: ubiquitin iso-peptidase activity
Traes_6BS_338CD771C	TRIAE_CS42_6BS_TGACv1_514103_AA1655240	Uncharacterized protein	A0A1D6AYC2	cAMP/cGMP binding motif
Traes_6BS_45379C8FD	TRIAE_CS42_6BS_TGACv1_515928_AA1672940	Uncharacterized protein	A0A1D6B1V3	ubiquitin iso-peptidase activity
Traes_6BS_1032BE6CB	TRIAE_CS42_6BS_TGACv1_514103_AA1655220	Uncharacterized protein	A0A1D6AYB9	ubiquitin iso-peptidase activity

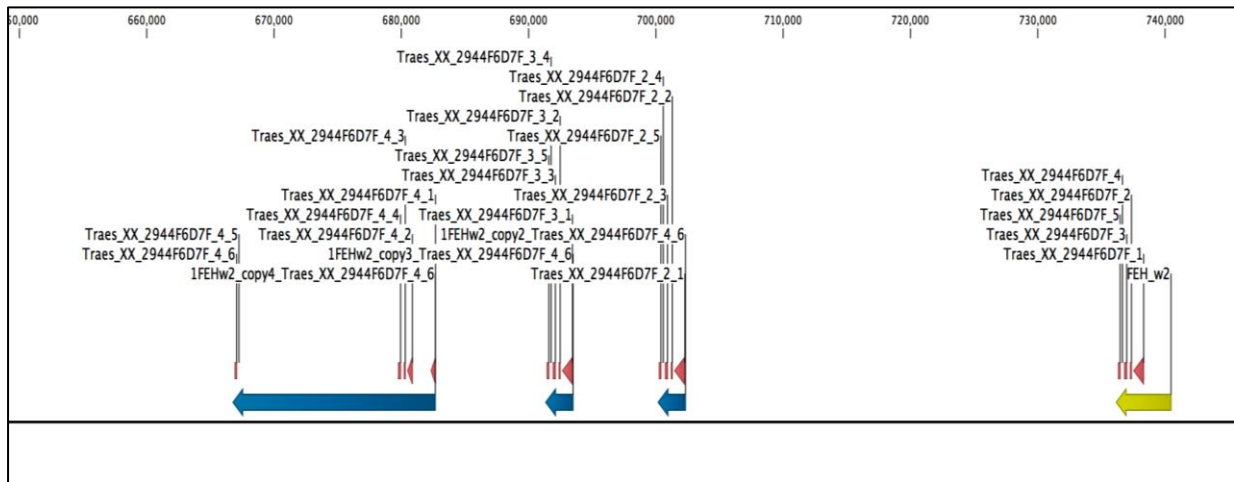
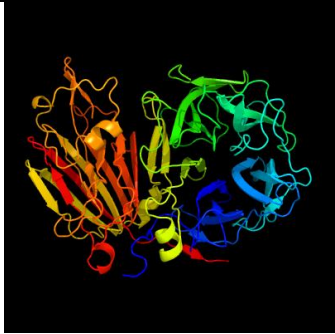
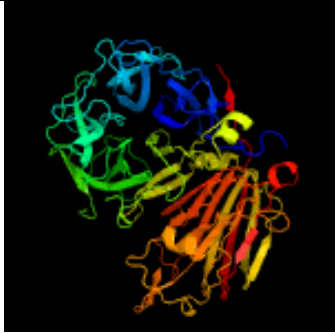



Fig. 5.10: Annotation of the mutated region of *1-FEH w2* on chromosome 6D (scaffold 33960, 940630 bp – 2658348 bp).

Table 5.8: Amino acid sequence and basic protein structure (Phyre² annotation) of *1-FEH w3* gene and Beta-fructofuranosidase.

Trace ID	Amino acid sequence	Phyre ² annotation	Basic protein structure via Phyre ² annotation (Kelley et al. 2015)
Traes_6BS_45E6 FBE8B GENE ID TRIAE_CS42_6 BS_TGACv1_51 5484_AA167034 0 Uniprot ID B6DZC8	MAQAWAFLLPVLVLSYVTSFLPTYIT GPLCGDGGGRSLFLCAQAPKDQDPSA STMYKTAHFHQPAKNWMNDPSGPMYFN GIYHEFYQYNLNGPIFGDIVWGHVSVDL ANWIGLEPALVRDTPSIDIDGCWTGSVTL PGGKPIIHYTGGDIDQNAQNIAPKNRSD PYLREWIKADNNPVLRPDEPGMNSIEFRD PTTGWIGPDGLWRMAVGGELNGYSAAL LYKSEDFLNWTKVDHPLYSHNGSNMWE CPDFFAVLPGNAGLDLSAIPQGAHHA LKMSVDSVDKYMIGVYDLHRDAFVDPN VVDDRRLWLRIDYGTIFYASKSFFDPNKN RRIIWGWSRETDSPSDDLAKGWAGLHTI PRTIWLADGDKQLLQWPVEEIESLRTNEI NHQGLELNKGLDFEIKEVDAFQADVEIG FELASIDDADFPDPSWLLDPEKHCGEAG ASVPGGIGPFGLVILASDNMDEHTEVYFR VYKSQEKYMLMCSDLRSSLRPDLEKP AYGGFPEFDEKERKISLRTLIDRSAVESF GGGGRVCITSRVYPAVLADVGSAGHIYAF NNGGATVRVPQLSAWTRMKAQVNVK GWSAI	PDB header: hydrolase PDB Molecule: fructan 1- exohydrolase iia; PDBTitle: crystal structure of fructan 1-exohydrolase iia (e201q) from cichorium2 intybus in complex with 1-kesto Name: Fructan 1-exohydrolase	
Traes_6BS_F67 E13A47 Gene ID TRIAE_CS42_6 BS_TGACv1_51 4515_AA166084 0 Uniprot ID A0A1D6AZII	MYCFAFQIIAGLPSSTIEDVHMGSSDPCG LMYYKGIYHNFYQYNPHCALWCWGDI WGHVSVDLNVWQLEPVIEPDNPSDIDG CWTGSAITLGGQPVILYTGRRDRKQV QNLVLPKNPSDPYLRWTKIGNNPVIQPV VPGLNRSQFRDPTTGWIGPDGLWRIA AELKGYTAALLYKSEDFLSWTVDHPLY SQNYSNMRKCNMWECLDFFAVLPGNN SGLDMSAAILRGTKHALKMSVDYFDKY LIGVYDLKRD AFLPDTIVDDCRLWLRIDY GHFASKSFFDSKGRRIIWGWSQEA SDDVAKGWAGIHTIPRTIWLDSNGKQLL QWPVDEIESLRTNEINHQGLELNKGMDF EINGVDTFQADVEIYFELTSINA AEPFNSS WLFDPPEHCCEAGASVHGGIGPGLVILA SNNMDEHTVVHFRVYKSQKYMILMCS DLRRSSIRPSPTYAYGGFFELDLAKERQI SLRTLIDRS AVESFGGGGRVCITSRVYPA VLAGVGAHMYAFNNGSATVRVPQLSA WTRMKAQVNVKGSWSAI	PDB header Glyco_hydro PDB Molecule Invertase PDBTitle: crystal structure of a cell-wall invertase from <i>Arabidopsis thaliana</i> Name: Uncharacterised protein	

Table 5.9: Amino acid sequence and basic protein structure (Phyre² annotation) of *1-FEH w2-1*, *1-FEH w2-2* and *c 1-FEH w2-3*.

Trace ID	Amino acid sequence	Phyre ² annotation	Basic protein structure via Phyre ² annotation(Kelley et al. 2015)
TRIAE_CS42_U_TGACv1_64353 1_AA2132820 Uni prot ID Q84LA1	MAQAWAFLLPVLVLGYSYVTSLFPPSYISNP LCGGDGGRLFLCAQAPKDDPSPAVSTM YKTAFFHQPAKNWMDPSGPMYFNIGIYH EFYQYNLNGPIFGDIVWGHSVSTDLVNW GLEPALVRDTPSIDIDGCWTGVTILPGGKP IIYTGGDIDQHQAQNIAPKNRSDPYLRE WIKAPNNPVLRPDEPGMNSIEFRDPTTGW GPDGLWRMAVGGELNGYSAALLYKSEDF LNWTKVDHPLYSHNGSNMWECPDFFAVL PGNAGLDLSAIPQGAHALKMSVDSV DKYMIGVYDLQRDAFVPDNVVDDRRLWL RIDYGTIFYASKSFFDSNKNRRIIWGWSRET DPSDDLKKGWAGLHTIPRTIWLADGDKQ LLQWPVEIESLRTNEISHQIELNKGDLFE KEVDQAFQADVEIDFELASIDDADPFPSW LLDPEKHCEAGASVPGGIGPFLVILASD NMDEHTEVYFRVYKSQEKYMVLMCSDLR RSSLRPDLEKPAYGGFFEDLEKERKISLRT LIDRS AVESFGGGGRVCITSRVYPAVLADV GRAHIYAFNNGSATVRVPQLSAWTMRKA QVNVEKGWSAI*	PDB header: hydrolase PDB Molecule: fructan 1-exohydrolase iia; PDBTitle: crystal structure of fructan 1-exohydrolase iia (e201q) from cichorium2 intybus in complex with 1-kestose Name Fructosyl 1 exhyrolase (<i>1-FEH w2</i>)	
TRIAE_CS42_U_TGACv1_64515 4_AA2143350 Uniprot A0A1D6B1A1	VSTRYRTAYHFQPPRNWINDPCGLMYK GIYHNFYQYNPHCALWCWGDITWGHSVS TDLVNWIQLEPVIEPDNPSIDIDGCWTGSAT ILSGGQPVILYTGGSRDKCCVQNLVHPKN PSDPYLREWTKTGNPNVQPVPGLNRSQ FRDPTTGWIGPDGLWRIA V G A E L K S Y T A A L L Y K S E D F L S W T R V D H P L Y S Q N L S N I V E C N M W E C L D F F A V L P G N T G L D M S A A I L R G T K H A L K M S V G Y F D K Y L I G V Y D L K R D A F V P D T I V D D C R L W L K I D Y G N F Y A S K S F F D S K K G R R I I W G S K E A D C R S D D V A K G W A G I H T I P R T I W L D S N G K Q L L Q W P V D E I E S L R T N E I N H Q G L E L N K G D M F E I N G V D T F Q A D V E I Y F E L T S I N A E A P F N P S W L L D P E K H C E A G A S V H G G I G P F L V I L A S N N M D E H T V V H F R V Y K S Q Q K Y M I L M C S D L R R S S I R P S R Y T P A Y G G F F E L D L A K E R K I S L R T L I D R S A V E S F G G G R V C I T S R V Y P A V L A D V G R A H M Y A F N N G S A T V R V P Q L S A W T M R K A Q V N V E K G W S A I	PDB header: hydrolase PDB Molecule: fructan 1-exohydrolase iia; PDBTitle: crystal structure of fructan 1-exohydrolase iia (e201q) from cichorium2 intybus in complex with 1-kestose Name Fructosyl 1 exhyrolase (<i>1-FEH w2-2</i>)	
TRIAE_CS42_U_TGACv1_64515 4_AA2143370 Uniprot ID A0A1D6B1V4	VSTTYRTAYHFQPPRNWINDPCGLMYK GIYHNFYQYNPHCALWCWGDIAWGHSVS TDLVNWIQLEPVIEPDNPSIDIDGCWTGSAT ILSGGQPVILYTGVS RDNCVQNL LFPKNP SDPYLREWTKAGNNPVIQPVVPLNRSQ RDPTTGWIGPDGLWRIA V G A Q L Y S Y N A A L L Y K S E D F L S W T R V D H P L Y S H N L S N M W E C P D F F A V L P G N S G L D M S V S I P R G A K H A L K M S V G Y F D K Y L I G V Y D L K R D A F V P D T I V D D C R L W L R I D Y G D F Y A S K S F F D S K K G R R I I W G W S Q E A D C R S D D V A K G W A G I H T I P R T I W L D S D G E Q L L Q W P V D E I E S L R T N E I N H Q G L E L N K G D M F E I N G V D T F Q A D V E I Y F E L T S I N A E P F N P S W L L D P E K H C E A G A S V H G G I G P F G L V I L A S N N M D E H T V V H F R V Y K S Q Q K Y M I L M C S D L R R S S I R P S R Y T P A Y G G F F E L D L A K E R K I S L R T L I D R S A V E S F G G G R V C I T S R V Y P A V L A D V G R A H M Y A F N N G S A T V R V P Q L S A W T M R N A H V N V E N G R S A I	PDB header: hydrolase PDB Molecule: fructan 1-exohydrolase iia; PDBTitle: crystal structure of fructan 1-exohydrolase iia (e201q) from cichorium2 intybus in complex with 1-kestose Name Fructosyl 1 exhyrolase (<i>1-FEH w2-3</i>)	

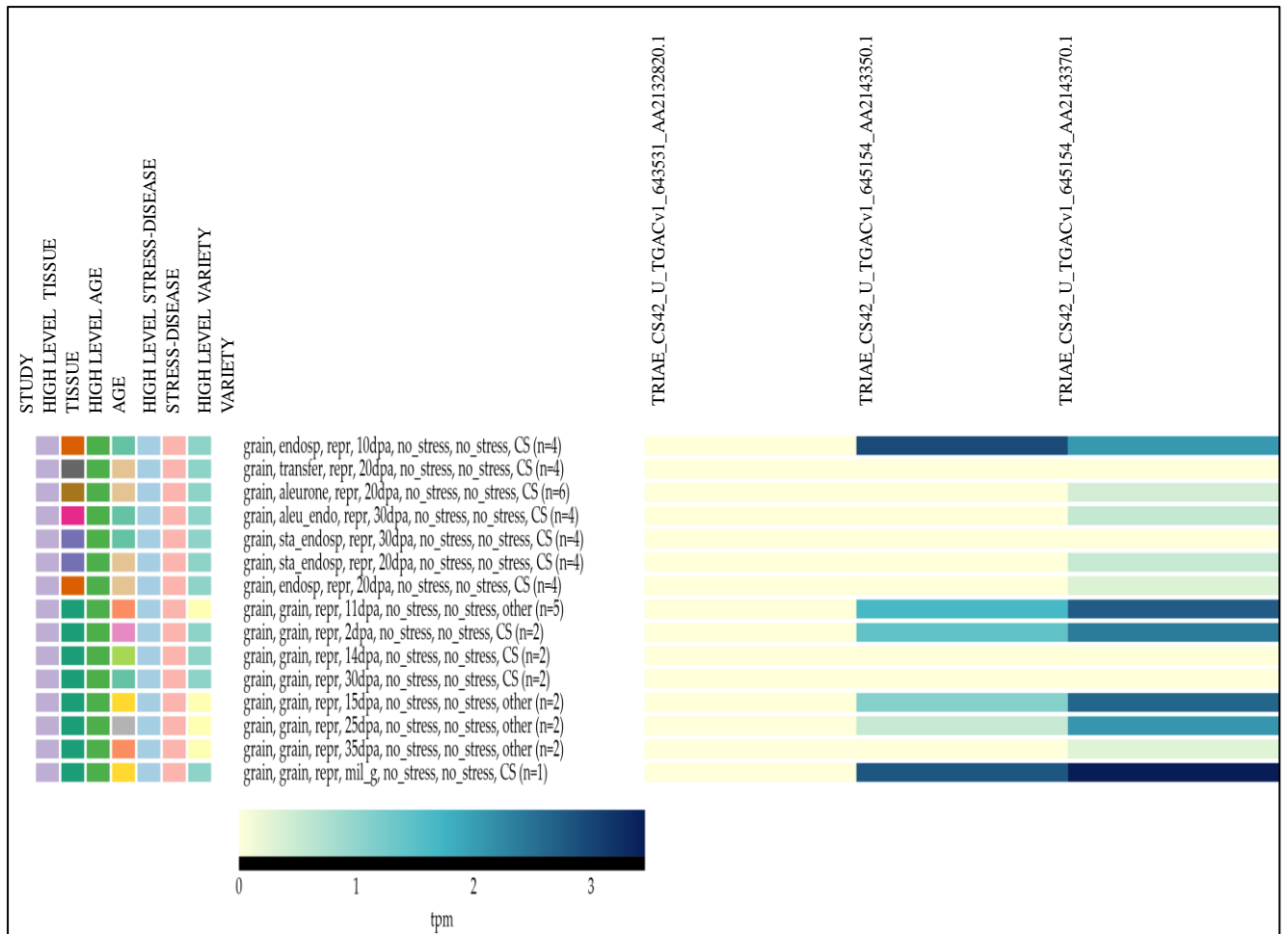


Fig. 5.11: Expression of *1-FEH w2-1*, *1-FEH w2-2* and *1-FEH w2-3* in grain at different developmental stages.

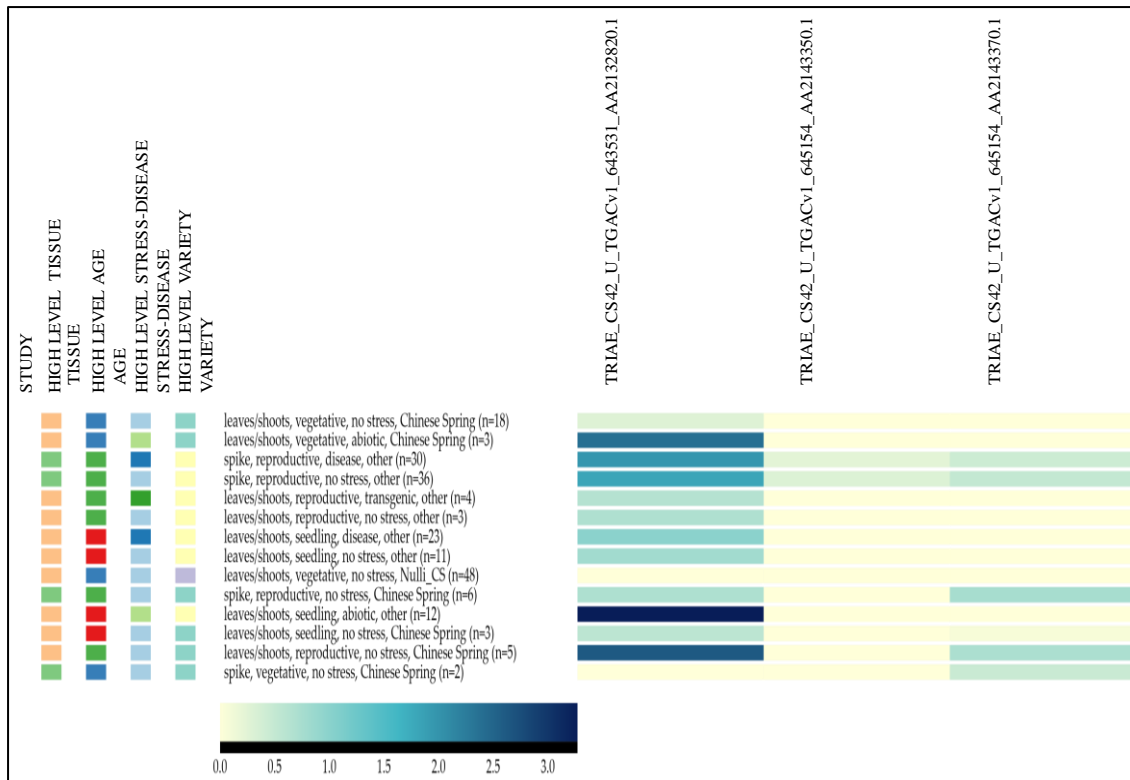


Fig. 5.12: Expression of *1-FEH w2*, *1-FEH w2-2* and *1-FEH w2-3* in stem and leaves at different developmental stages.

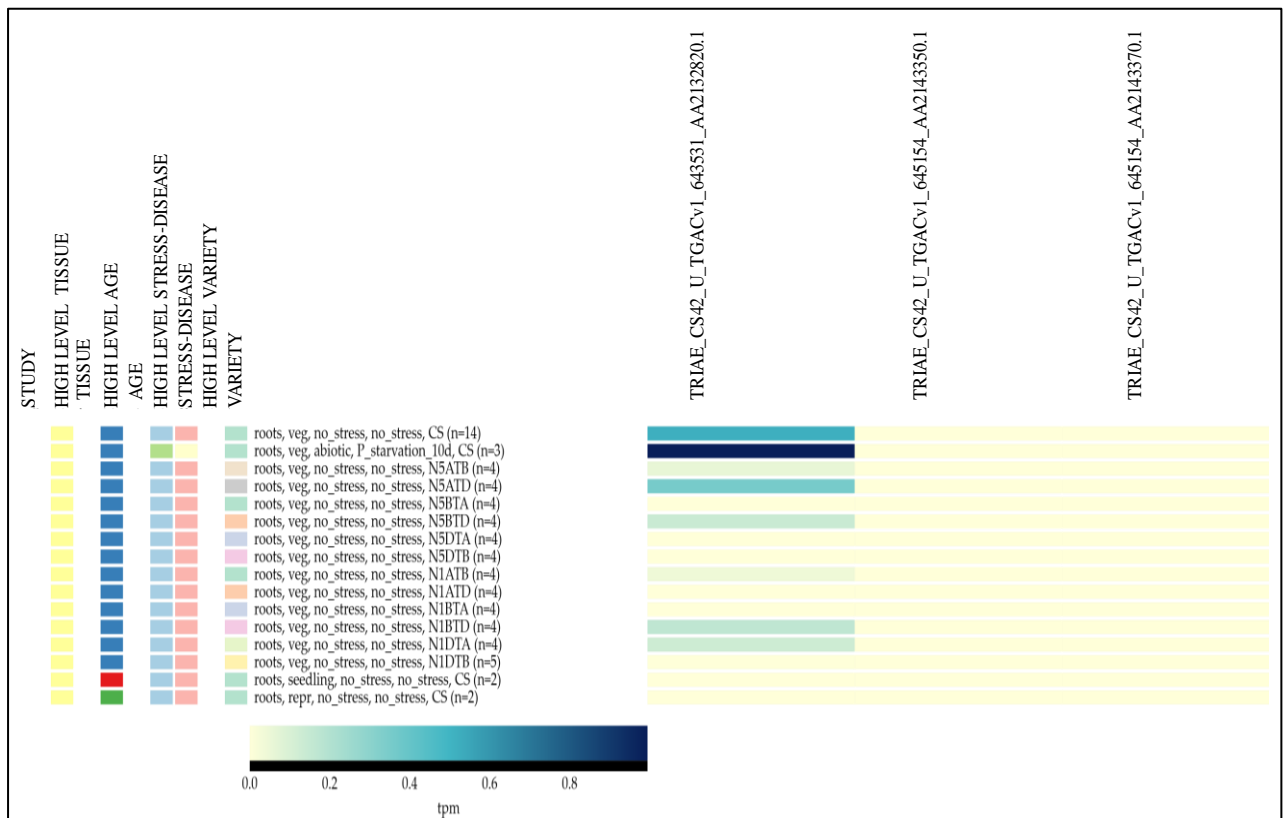


Fig. 5.13: Expression of *1-FEH w2*, *1-FEH w2-2* and *1-FEH w2-3* in roots at different developmental stages.

Table 5.10: Functional classification of the proteins positioned within the mutated segment.

Major classification of protein annotated	Chromosome 6A	Chromosome 6B	Chromosome 6D
Hydrolase	TRIAE_CS42_6AS_TGACv1_48616_1_AA1557660 TRIAE_CS42_6AS_TGACv1_48780_5_AA1573030 TRIAE_CS42_6AS_TGACv1_48616_1_AA1557660	TRIAE_CS42_6BS_TGACv1_515390_AA1669820 TRIAE_CS42_6BS_TGACv1_514515_AA1660840 TRIAE_CS42_6BS_TGACv1_515484_AA1670340 TRIAE_CS42_6BS_TGACv1_515390_AA1669820 TRIAE_CS42_6BS_TGACv1_514103_AA1655220 TGACv1_514103_AA1655220	TRIAE_CS42_U_TGACv1_64_3531_AA2132820 TRIAE_CS42_U_TGACv1_64_5154_AA2143350 TRIAE_CS42_U_TGACv1_64_5154_AA2143370
Ligase	<u>TRIAE_CS42_6AS_TGACv1_48634_8_AA1560160</u> TRIAE_CS42_6AS_TGACv1_48616_1_AA1557660 TRIAE_CS42_6AS_TGACv1_48576_6_AA1551710	TRIAE_CS42_6BS_TGACv1_515390_AA1669820 TRIAE_CS42_6BS_TGACv1_515390_AA1669820 TRIAE_CS42_6BS_TGACv1_514103_AA1655220	
Oxidoreductase	TRIAE_CS42_6AS_TGACv1_49625_4_AA1578120		
De Novo Protein	<u>TRIAE_CS42_6AS_TGACv1_48634_8_AA1560161</u>		
Transferase	<u>TRIAE_CS42_6AS_TGACv1_48634_8_AA1560160</u> TRIAE_CS42_6AS_TGACv1_48634_8_AA1560130	TRIAE_CS42_6BS_TGACv1_514103_AA1655240	

5.4 Discussion

Characterization of the *I-FEH* mutation lines was carried out using high-density SNP genotyping array and bioinformatics approaches that provided detailed information regarding the physical modification of mutated segments on the chromosomes and the nature of the mutation. This information is crucial to explain the functional loss of the *I-FEH* genes in the mutation lines.

It is important to note that the backcrossing step was necessary for the analysis of mutants obtained from all mutagenesis screens, irrespective of the type of mutant identification strategy used or type of mutagen used or organism used. Deletion mutations typically do not revert, so failure to revert is a hint that a mutation may be a deletion. To identify mutation regions, we focused on high-density variation on a single chromosome for each mutant which correspond to regions of high mutagen induced damage that were not removed during back crossing and therefore most likely genetically linked to the casual mutation (Zuryn et al. 2010). We therefore focused our attention on these physical regions to identify candidate mutations. This technique offers the opportunity to compile and compare between the parent line, mutation lines and backcrossed lines and to identify the mutation region.

5.4.1 Chromosomal mapping of mutation region and candidate gene

To validate the phenotypic expression of gene function loss due to mutation it is important to characterise the structural changes that happened in the genes and adjacent regions of the chromosomes. Mapping of the mutation-defined gene is the first step towards the localization of a mutation to a particular chromosome. The high-density SNPs clusters identified on NR gene scaffold_90107, 123806 and scaffold_33960 in chromosomes 6A, 6B and 6D, respectively, clearly demonstrated the physical location of the mutated regions of the *1-FEH* mutation lines. The advancement of wheat whole genome sequencing (R Appels personal communication, IWGSC outputs) has transformed our ability to identify the chromosomal region of mutation by comparing the mutated line with the parent line. Previously, mapping of mutation regions was a time consuming, laborious and painstaking process which involved mapping with genetic and/or single nucleotide polymorphism (SNP) markers (Sarin et al. 2008). Now, the completion of the wheat whole genome sequence gives us an opportunity to overcome those limitations. The sizes of the mutated/deleted regions were largely variable among the mutation lines. The largest deletion region was identified in the *1-FEH w3* mutation line, which was 2748910 bp in scaffold 123806 (chromosome 6B). Deletion sizes of mutation lines *1-FEH w2* and *1-FEH w1* were 1717718 bp at scaffold 33960 (chromosome 6D) and 1299655 bp at scaffold 90107 (chromosome 6A), respectively. Generally, mutation by heavy ion irradiation mutates a larger region compare to other ion radiation or chemical mutagenesis, and it can be highly variable. Thus, it was worth characterising the mutated region on the corresponding chromosome.

5.4.2 Annotation of the deleted region

Mapping analysis demonstrated that the mutation affected significantly longer regions than the target gene regions of *1-FEH w1*, *w3* and *w2* present on the NR gene scaffold of chromosomes 6A, 6B and 6D. Thus, it was crucial to annotate the whole mutated region to understand the effect of deletion on the measured phenotypes. This analysis provided us with the functional information both of target and non-target mutated genes. Investigation was also carried out to identify whether any non-target genes located within the mutated region are influencing the function of the target gene.

At the mutation region of *1-FEH w1* on chromosome 6A, eight non-target genes were identified and 7 non-target genes were identified in the *1-FEH w3* mutation region on chromosome 6B. These findings clearly indicated that the mutation targeting functional loss of *1-FEH w1* and *w3* affected a considerable number of genes at the adjacent chromosomal location. From the

annotation of the mutated region of *1-FEH w2* it appeared that 3 extra copies of the *1-FEH w2* gene were present in that region. Two of the three additional copies seem to be active based on the public RNAseq data. Possible presence of additional gene copies has been reported earlier (Zhang 2008). Among these three copies, protein sequence of copy 4 was not identified due to its large intron but *1-FEH w2-2* and *3* showed expressions. *1-FEH w2* showed higher expression in stem, leaf and roots whereas *1-FEH w2-2* and *1-FEH w2-3* showed very low expression in stems and leaves and no expression in roots. Furthermore, *1-FEH w2-2* and *3* have been reported to be highly expressed in the grain while the *1-FEH w2* did not have any expression in the grain. Thus, based on the high expression in the stem, leaf and root it has become evident that *1-FEH w2* mostly contributes to supplying sugar to the grain under drought from the water-soluble carbohydrate stored in the leaf sheath, stem (Xue et al. 2008) and root tissue (Zhang et al. 2016). It is most unlikely that the genes *1-FEH w2-2* and *1-FEH w2-3* are playing the same role since they did not have significant expression in leaf, stem and root tissues. Hence, the corresponding phenotypic results of decreased sugar supply to the grain in *1-FEH w2* mutation line might be due to the absence of *1-FEH w2-1* gene, and not because of *1-FEH w2-2* or *1-FEH w2-3*.

5.4.3 Function prediction of non-target deleted genes

Following the annotation of the mutation regions, further investigation on functional alteration of non-target genes became essential to validate whether the phenotypic change in the mutated plant is due to the deletion of the target genes (*1-FEH w1/ w2/ w3*). However, confirming the functional roles of the non-target genes has been challenging since most of the genes were identified as genes encoding uncharacterized protein based on sequence blasts in the available databases. Thus, function prediction of uncharacterized protein sequences was carried out following computational biology approaches. Assigning function to the uncharacterized proteins is imperative but challenging. The usual approach is based on similarity searches using annotation databases. A number of tools and databases have been used to predict information about gene function using orthologue genes with high sequence similarity and proteins with significant structural homology. Moreover, 3D structure models of predicted proteins were generated from the sequences using Phyre² to further confirm the function. The Phyre² based annotations were generally consistent with annotations obtained from other sources.

Phyre² annotations were treated with caution, since they were sometimes based on relatively small sections of the gene models. However, they were a useful source of possible functional analysis based on fundamental structure/function-features of the amino acid sequences.

Functional categorisation of the genes was carried out across all the mutated regions and are listed in Table 5.10. Genes annotated in the mutation region, mostly are hydrolases. Functional properties of the non-target genes positioned at the mutated regions of *1-FEH* genes are described below based on predicted protein functions.

I. Hydrolase

Hydrolase or hydrolytic enzyme catalyses the hydrolysis of chemical bonds. Isoforms of *1-FEH* are hydrolase enzymes, which break down the β -(2-1) linkage of fructan, a storage carbohydrate in cereals. From the annotation we identified *1-FEH w1*, *w2* and *w3* in the mutated regions of chromosome 6A, 6D and 6B respectively. In 6A only *1-FEH w1* has glycoside hydrolase activity which means it breaks the sugar bond. Similarly, *1-FEH w2-1*, *1-FEH w2-2* and *1-FEH w2-3* in chromosome 6D share the same function, whereas, besides *1-FEH w3*, another gene (Beta-fructofuranosidase, insoluble isoenzyme 4) in chromosome 6B has glycoside hydrolase activity. Besides, a very small part of that gene has been identified in the mutation region and that overlapped with *1-FEH w3*, so it very unlikely that this small part has any influence on the sugar transport system (Fig. 5.9). One other gene in 6A and three more genes in 6B have hydrolytic function but they were identified as peptidase which indicate they hydrolyse peptide bonds and do not have any relation with sugar hydrolysis.

II. Ligase

The second largest group of genes identified in the mutated region belong to the ligase group. Three of them are annotated in chromosome 6A and three in chromosome 6B. No genes with ligase function were annotated in chromosome 6D. Ligase is an enzyme that helps in binding substrates. Ligase is a highly diverse and important group of enzymes that act within the proteasome pathway. However, ligase does not affect sugar metabolism so these annotated genes might not influence the activity of the *1-FEH* gene.

III. Transferase

Three of the genes were annotated in the transferase group. Among them, two are on chromosome 6A and one on 6B. Transferase is a class of enzymes that transfer specific functional groups (e.g. a methyl or glycosyl group) from one molecule (called the donor) to another (called the acceptor). TRIAE_CS42_6AS_TGACv1_486348_AA1560130 belongs to glutathione S-transferases, which participates in the detoxification of reactive electrophilic compounds by catalysing their conjugation to glutathione. By contrast,

TRIAE_CS42_6AS_TGACv1_486348_AA1560120 is a gene with UDP glycosyl transferase (UGT) function, which catalyzes the addition of the glycosyl group from a UTP-sugar to a small hydrophobic molecule. There might be a possibility for this gene to have a combined effect on sugar metabolism. However, a very small fragment of this gene is present in the deleted region indicating there will not be major interference with gene function of *1-FEH*.

IV. Oxidoreductase

TRIAE_CS42_6AS_TGACv1_496254_AA1578120 on chromosome 6A was annotated in this group. Oxidoreductases are a class of enzymes that catalyse oxidation and reduction reactions by transferring electrons from one molecule (the oxidant) to another (the reductant). This one does not have any relation with sugar transportation.

5.5 Conclusion

From this analysis it is evident that in all of the mutation lines the deleted regions were larger than the targeted gene sizes. Although some other genes were also deleted in those regions, none of them has direct influence on *1-FEH w1*, *w2* and *w3* gene function. So, it can be concluded that the phenotypic results found in this mutated line is most likely due to the deletion of isoforms of *1-FEH*.

Chapter 6: Characterising sugar deposition in the developing wheat grain using mass spectrometric imaging (MSI) and influence of *1-FEH w3*

6.1 Introduction

Results presented in Chapters 3 and 4 showed that *1-FEH w3* plays a vital role in remobilization of sugar under terminal drought. In order to confirm direct relationship of the *1-FEH w3* gene function with the sugar deposition in the grain, further investigation focusing on the sugar deposition pattern at the tissue level are warranted. A previous study investigated the total FEH activity in developing wheat kernels by linking gene function with sugar metabolite activity following Quantitative Analysis and Microscopy (Verspreet et al. 2013a). However, no direct relationship between metabolites and genes has been established yet. Thus, a mass spectrometry imaging experiment was carried out to investigate gene function in relation to sugar deposition in the grain. Sugar deposition at different stages of grain development therefore were investigated in the *1-FEH w3* mutation line in comparison with its parent Chara under well-watered and drought conditions.

Generally, carbohydrate concentration is changed in different stages of grain development (Verspreet et al. 2013b). Three main phases in relation to assimilation of compounds in the grain have been identified during kernel development in previous studies (Bechtel et al. 2009; Shewry et al. 2012). The early development stage (0-14 DAA) includes fertilization, syncytium formation, cellularization, endosperm cell differentiation and endosperm cell expansion. Commonly at this stage sugar deposition does not occur. The next stage is grain filling (15-35 DAA) when most of the storage compounds accumulate in the grain. Thus, this is the most important stage for sugar deposition activities in the grain. The final phase is physiological maturity (36-60 DAA), when programmed cell death, dormancy and desiccation take place and sugar deposition is almost completed. Thus, the composition of the mature grain is determined over specific grain filling periods and depends on the unhindered supply of assimilates from the plant, mainly in the form of sucrose, through the vascular bundle into the endosperm.

During grain filling, maintenance of sink potency depends on the cleavage of sucrose by invertases and sucrose synthase. Invertases are important for the production of the hexose sugar signal which is controlled by the sucrose to hexose ratio, that regulates the cell cycle and cell division (Bihmidine et al. 2013; Koch 2004; Roessner-Tunali et al. 2003; Weber et al. 1997; Wind et al. 2010). The regulatory mechanism related to sugar deposition during the

development of the grain is far more than a simple system. For instance, under favourable conditions, sucrose is mainly supplied from current photosynthetic assimilate while in stress conditions the supplies come largely from stem reserves. These reserves consist mainly of water soluble, non-reducing, acid labile oligomers and polymers of fructose and sucrose. Fructans are remobilized as sucrose (Fisher and Gifford 1986) and transported via the phloem to the kernel where they can be resynthesized and temporarily stored. It has long been known that fructosyl oligosaccharides are enriched in the endosperm cavity of the wheat grain during late storage (20 to 27 DAA) (Schnyder et al. 1993; Ugalde and Jenner 1990). In the grain, the presence of fructans has been associated with both sucrose phloem unloading (De Gara et al. 2003; Pollock et al. 1999) and osmoregulation during cell expansion and growth (Schnyder et al. 1993). The *1-FEH* gene has been reported to be largely involved in regulating the network. From the results of Chapter 4 of this thesis, it is evident that one isoform of the *1-FEH* gene (*1-FEH w3*) was expressed the highest at 17 DAA in the water deficit condition and started declining at 22 DAA. These two stages have made significant differences in WSC remobilization and gene expression level under water-deficit condition in the *1-FEH w3* mutation line and parent Chara. These differences ultimately resulted in lower seed wt. in the *1-FEH w3* mutation line.

Details of metabolic activity in the developing grains are now achievable because methodology has been developed up to the cellular level. Quantitative study of different metabolites and identifying their distribution with electron microscopy have been reported in several studies (Bechtel et al. 2009; Shewry et al. 2012; Verspreet et al. 2013b). Visualization can also be obtained by fluorescence microscopy, confocal microscopy, *in situ* hybridization or immunohistochemistry, which provide further high spatial resolution (Haritatos et al. 2000, Wittich and Vreugdenhil 1998). However, chemical information is typically limited to very few compounds in these kind of experimentations despite the fact that an improved understanding of plant metabolism relies on analytical capabilities for the accurate identification of metabolites.

With the advance of sophisticated separation techniques, mass spectrometry approaches are now able to identify a large number of metabolites (Kueger et al. 2012). Mass spectrometry (MS) metabolomic studies are usually based on homogenized samples which can cause loss of detailed information about compound localizations and can also result in complex molecular patterns. On the other hand, Mass Spectrometry Imaging (MSI) has an unique ability to recognize structures and to identify molecular changes that occur in the precisely defined part of the sample (Bodzon-Kulakowska and Suder 2015). Thus, MSI provides a platform for the

detailed localization of diverse molecular species such as metabolites, lipids, peptides, and proteins in a sample section with spatial resolutions of 5-100 μm scales (Bjarnholt et al. 2014; Boughton et al. 2016; Lee et al. 2012; Römpf and Spengler 2013; Spengler 2014). MSI is well suited for targeted localization approaches, e.g. drug imaging (Prideaux and Stoeckli 2012) as well as for untargeted profiling of tissue sections.

In plant research, use of MS imaging is relatively new, however, knowledge of changes during plant development or by environmental variation within tissue level can be obtained with high resolution images without prior knowledge of the analytes (Grassl et al. 2011). Generally, small molecules have been the main targeted substances in plant MSI using a range of plant species like arabidopsis, medicago, wheat, soy bean, rice, and tobacco and tissues such as leaves, stems, roots, flowers or fruits (Bjarnholt et al. 2014; Boughton et al. 2016; Matros and Mock 2013). The identification of plant metabolites often focused on specific classes such as phosphatidylcholines (Zaima et al. 2010; Zaima et al. 2014) cell wall constituents (Veličković et al. 2014), anthocyanins (Yoshimura et al. 2012) or other secondary metabolites as summarized in a comprehensive review (Bjarnholt et al. 2014; Boughton et al. 2016; Matros and Mock 2013). Because sucrose is a direct precursor for the production of fructosyl oligosaccharides, characteristic fructan distribution patterns have not been established in mutant grains.

In this study, imaging mass spectrometry was used to reveal the sugar metabolite profiling at the tissue level in well-watered and water deficit conditions of *1-FEH w3* mutant grain in comparison with its parent Chara to directly relate the *1-FEH w3* gene function with sugar deposition in the grain. This comparison will help us to answer whether the absence of *1-FEH w3* affects sugar metabolism in the developing grain. This will give us an advanced level of understanding regarding the role of *1-FEH w3* in seed development under water deficit.

6.2 Materials and methods

6.2.1 Plant materials

One *1-FEH w3* gene mutation line (Mutation line Id: 18b 426) and its parental cultivar Chara were selected for study to confirm the gene function.

6.2.2 Sample collection and storage

Samples were collected from the 2014 glasshouse trial. For collecting appropriate samples, all the developing ears were tagged at anthesis (when the anthers appeared visible). Developing ears were harvested at 17 and 22 DAA (days after anthesis) from both well-watered and water-deficit plants. All the sampled heads were loosely wrapped with aluminium foil immediately after cutting and frozen in liquid nitrogen gently for 30 to 60 sec. After that, frozen samples were stored at -80°C until further use.

6.2.3 Seed slide preparation

A Leica CM 1850 cryotome machine was used for cryosectioning the frozen samples for MSI analysis. The knife temperature and machine compartment temperature were -20°C . Frozen seeds were embedded in egg white and sections $25\ \mu\text{m}$ thick prepared (Fig 6.1). The section was thaw mounted on the indium tin oxide (ITO)-coated conductive glass slides which were also kept in -20°C . Then the slides were kept in -80°C before further use.

6.2.4 Mass Spectrometer Imaging (MSI)

MALDI matrix application

An acidified hydroxyl matrix, 2, 5-dihydroxybenzoic acid (DHB) was uniformly deposited over the surface of the tissue sections. This matrix has previously been shown to be suitable for the detection of oligosaccharides (Ropartz et al. 2011). The DHB matrix was prepared at a concentration of $5\ \text{mg/mL}$ in ACN/H₂O (4:1) containing 0.1% TFA. Potassium acetate (KOAc) were also prepared and added into the matrix solution at a final concentration of $10\ \text{mM}$ to promote the potassium adduct formation of the sugar species detected ($[\text{M}+\text{K}]^{+}$).

The application of DHB was performed using the spotting approach. Glass slides containing the tissue sections were placed on dry ice and $5\ \mu\text{L}$ of matrix was spotted on each section. This was to allow even distribution of matrix across the tissue sections. The glass slides were then placed in a freeze drier to allow for the matrix to interact with sample metabolites forming crystals, which were then submitted to very short laser pulses within the ionisation source of the MS.

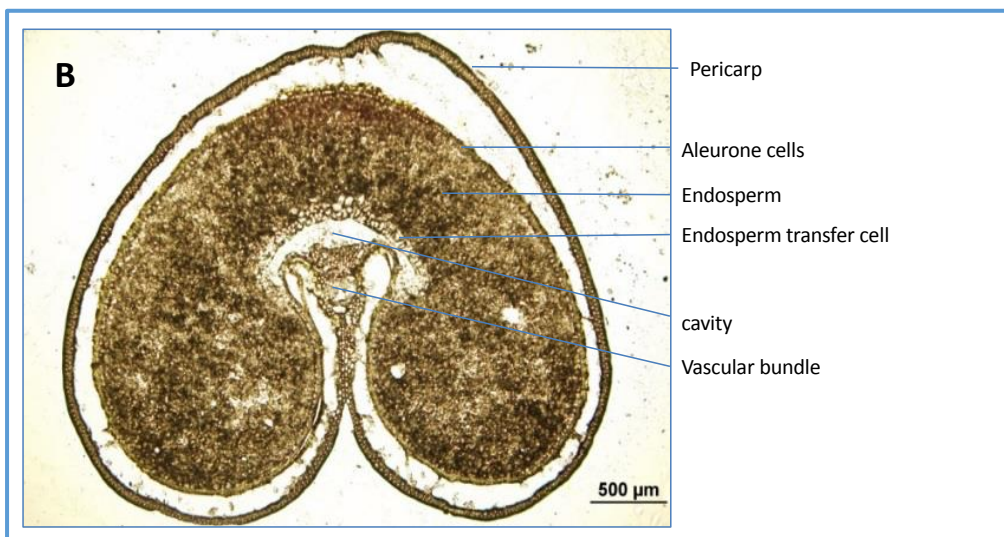
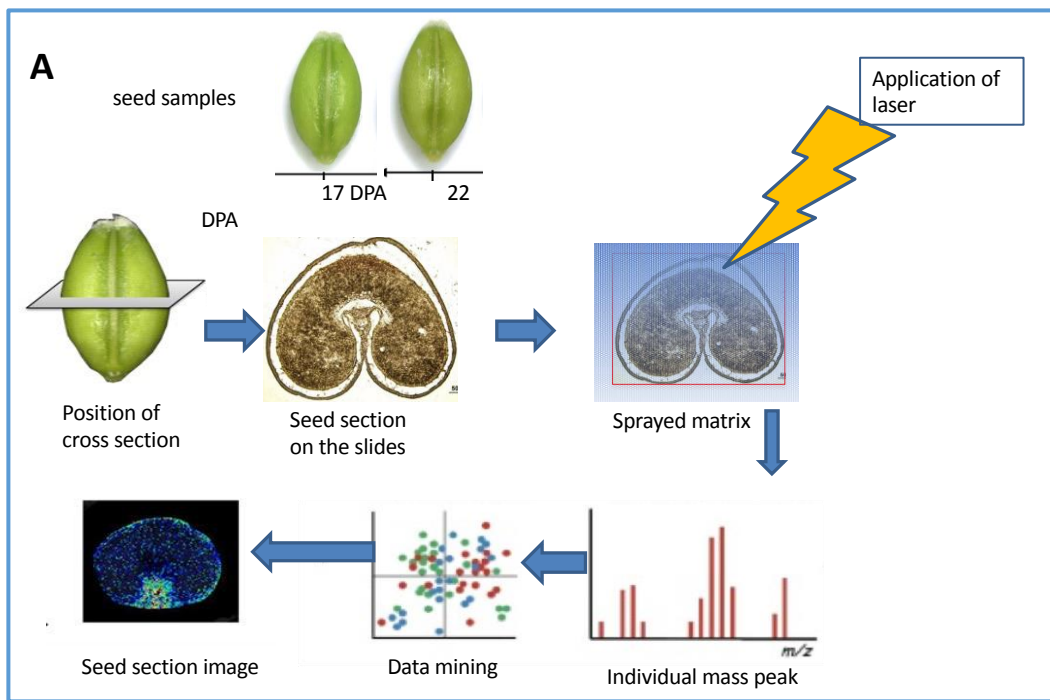


Fig. 6.1: (A) Work flow of the experimentation using Mass Spectrometry Imaging to characterise sugar deposition in developing wheat grain; (B) Showing the types of tissues on the prepared cross section slide of the seed.

MALDI-MSI acquisition

All MALDI-MSI analyses were performed using the Waters Synapt G2 mass spectrometer equipped with an orthogonal MALDI ion source and an Nd:YAG laser (Waters Corporation, Manchester, U.K.). Prior to the analytical acquisition, digital scans of the tissue sections were obtained using an Epson WorkForce Pro WP-4540 scanner (Epson America, Inc.) and then

imported into the MALDI Imaging Pattern Creator software. This allowed for the identification of regions of interest to be analyzed. Two standard sugar samples (sucrose and 1-kestose purchase from VWR International Pty Ltd.) were analyzed with the samples for the validation of the identification of sugar molecules.

Data were acquired in the positive mode operating with a 1000 Hz firing rate and 350J laser energy. All data were acquired over the mass range from 50 to 1200 Da. From each irradiated spot, a full mass spectrum consisting of signals from protonated molecular species desorbed from that tissue region was observed. The obtained spectra were then processed in MassLynx (Waters Corporation, Manchester, UK) to plot the signal intensities of the corresponding ions. The MSI images were acquired at a spatial resolution set at 600 laser shots per position and ion images were generated with Biomap 3.7.5.5 software which was used to develop a heat map of the relative amount of those ions over the entire imaged surface.

6.3 Results

6.3.1 Establishment of the seed sectioning procedure and sample preparation

An important issue of this study was to prepare slides of developing wheat seeds by cryosectioning 25 μm sections that were compatible with MS equipment. The only previous study of mass spectrometric imaging of wheat seeds (Veličković et. al. 2014) was able to use 60 μm thick slides for MSI since they followed an enzymatic digestion of the polysaccharides. This current study aimed to analyse the oligosaccharides without any digestion by MSI, and thus required thinner sections of 25 μm . An optimal cutting temperature compound (OCT compound) is normally used as embedding material for cryosectioning to produce slides of similar thickness. However, the OCT compound which is comprised of 10.24% polyvinyl alcohol, 4.26% polyethylene glycol and 85.5% non-reactive ingredients, is considered unfavourable for MSI. Thus, the cryosectioning procedure needed to be optimised in this study using a range of different embedding materials including water and egg white. Water was not suitable for cryosectioning of developing wheat seeds as it was hard to thaw the slide intact when mounting on the indium tin oxide (ITO)-coated conductive glass slides. The inability to produce any intact sections might be due to the softness of the developing seed tissues. Eventually, the cryosectioning of wheat developing seeds was successfully optimised using egg white as embedding material (Fig. 6.1). Egg white has only one protein that made it suitable to exclude the signal from mass spec analysis as well. Thus, this is the first report of its kind

that used egg white with 25 μm sections for developing wheat seeds to analyse oligosaccharides using MSI.

6.3.2 Mass spectrometry imaging successfully detected oligosaccharides and their localisation in the seeds

The matrix-assisted laser desorption/ionization (MALDI) mass spectrometry imaging (MSI) technique allowed the visualization of oligosaccharides in grain tissues with a lateral resolution of 30 μm . The MSI of the transverse sections of developing wheat seeds was able to distinguish hexose and its polymers, up to seven polymerizations, namely di-, tri-, tetra-, penta-, hexa- and hepta-saccharides (Table 6.1). Thus, MSI was able to demonstrate the pattern of oligosaccharides accumulation in the seed section. A full list of the molecular ions detected in this study is provided in Table 6.2. Intense signal was observed within a mass range between m/z 300 and 10000 (Fig. 6.3). The most abundant m/z spectra observed across all sections are 381.055, 525.135/543.135 and 687.175 which are correspondent to di-, tri- and tetra-saccharides respectively. One spectra was identified at an m/z value of 917 which we consider to be the hexa-saccharides. No strong signal has been observed in the corresponding m/z values of hexose, penta- and hepta-saccharides. The number of meaningfully detected oligosaccharides were consistent across the whole range of the samples tested. However, signal intensities of the detected oligosaccharides between the samples varied as presented in detail in the following result sections.

The image of standards samples confirmed the visual identification of oligosaccharides as presented in Fig. 6.2. The MS peaks were generally identified as $[\text{M}+\text{H}]^+$, $[\text{M}+\text{Na}]^+$, and $[\text{M}+\text{K}]^+$ ions of sugar molecules according to the standards [50] (Table 6.1). A major detection of the sugar oxidised sodium adducts $[\text{M}+\text{Na}]^+$ was revealed, followed by the detection of the potassium adducts $[\text{M}+\text{K}]^+$. The protonated $[\text{M}+\text{H}]^+$ ion was not detected. Mass spectrometric peaks were able to identify all of the target oligosaccharides. Oligosaccharides were identified according to their typical fragmentation pattern (Table 6.1). Signals derived from the cryosectioning material (egg white) were excluded from further analyses.

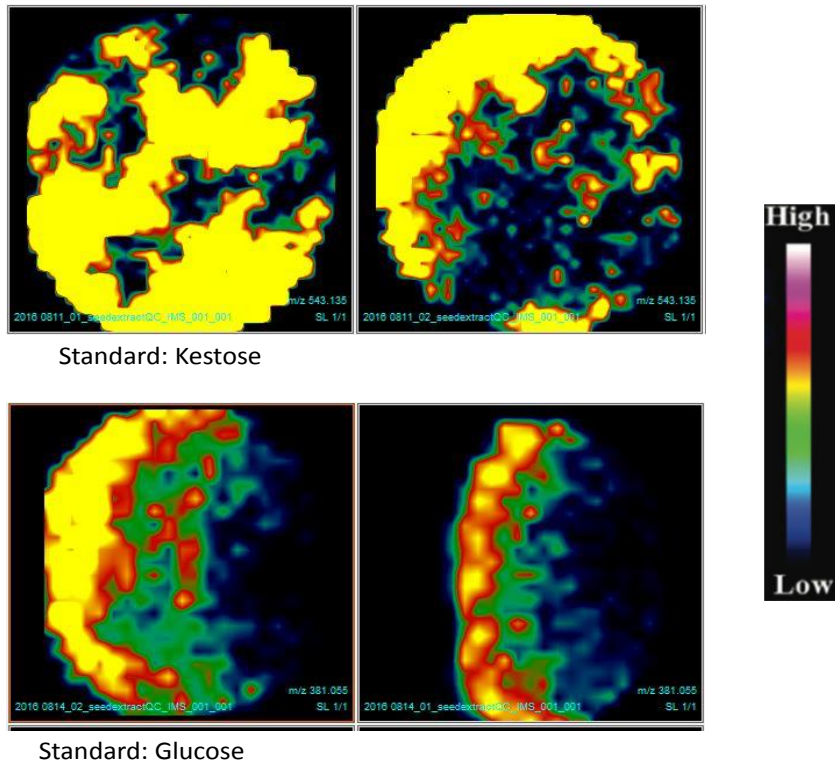


Fig. 6.2: Mass spectrometric images of the kestose and glucose standards used in the study.

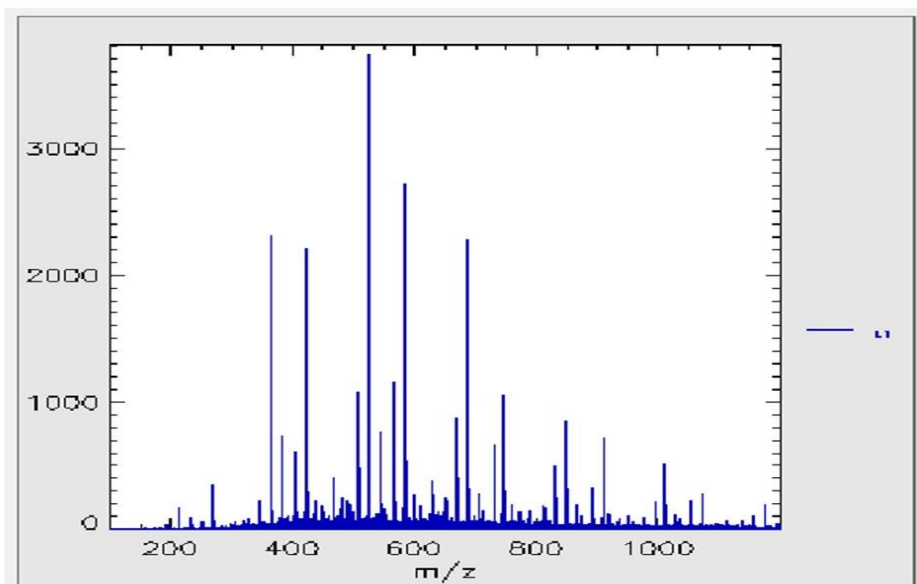


Fig. 6.3: General intense signal observed in the MSI.

Table 6.1: Sugar molecules usually detected in MALDI MSI.

		Molecular ions generated in MALDI TOF MS (m/z value)		
Sugar molecule	Chemical formula	[M+H] ⁺	[M+Na] ⁺	[M+K] ⁺
Hexose	C ₆ H ₁₂ O ₆	181.1	203.1	219
Disaccharide	C ₁₂ H ₂₂ O ₁₁	343.1	365.1	381.1
Trisaccharide	C ₁₈ H ₃₂ O ₁₆	505.2	527.2	543.1
Tetrasaccharide	C ₂₄ H ₄₂ O ₂₁	667.2	689.2	705.2
Pentasaccharide	C ₃₀ H ₅₂ O ₂₆	829.3	851.3	867.2
Hexasaccharide	C ₃₆ H ₆₂ O ₃₁	991.3	1013.3	1029.3
Heptasaccharide	C ₄₂ H ₇₂ O ₃₆	1153.4	1175.4	1191.3

(Peukert et al. 2014)

Table 6.2: Sugar molecules detected in this experiment.

Sugar Molecule	[M+Na] ⁺ (m/z value)	[M-2H+Na] ⁺ (m/z value)
Hexose	203.1	201.1 (n.d)
Disaccharide	365.1	363.1
Trisaccharide	527.2	525.2
Tetrasaccharide	689.2	687.2
Pentasaccharide	851.3	849.3 (n.d)
Hexasaccharide	1013.3	1011.2 (n.d)
Heptasaccharide	1175.4	1172.4 (n.d)

By using DHB as matrix, a major detection of the sugar oxidised sodium adducts [M+Na]⁺ was revealed followed by the detection of sugar potassium adducts [M+K]⁺. The protonated [M+H]⁺ ions were not detected.

6.3.3 Relative abundances and localisation pattern of polysaccharides in wheat grain

Considering the function of *1-FEH* genes, this study focused on the two developing stages of the sugar storage phase (Peukert et al. 2014) using three biological replications. However, due to limitation in the number of samples that could be analysed in MS we included one-time point (17 DAA) in the well-watered treatment and two time points in the drought treatment (17 DAA and 22 DAA) for the *1-FEH w3* mutation line and its parental cultivar Chara. Overall, tri- and

tetra-saccharides showed higher abundance out of seven oligosaccharides. The next abundant oligosaccharide was the di-saccharides. Notably, localisation patterns of oligosaccharides differed between seed development stages, and between water-deficit and well-watered plants. Overall, tri and tetra-saccharides followed a similar localisation pattern which was distinctly different from that of the disaccharides (Fig. 6.4). The details of the results in relation to abundance and localisation patterns are described below.

I. Differentiation in relative abundance and localisation pattern of oligosaccharides between seed from droughted and well-watered plants

Relative abundance of the oligosaccharides was influenced by drought (Fig. 6.4). At 17 DAA the tri- and tetra-saccharides were more intense in droughted compared to well-watered plants. This indicates that the oligosaccharide storage phase started earlier due to the imposition of drought. However, the differences in relative abundance of disaccharides between drought and well-watered plant was not remarkable.

In Chara at 17 DAA under the well-watered condition, the tri- and tetra-saccharides were distributed throughout the sectioned area of the grain. However, they were more condensed around the endosperm cavity. By contrast, under the drought condition, tri- and tetra-saccharides were localised more at the inner side of the seeds and appeared to be absent around the seed cavity and seed periphery (Fig. 6.4). In the case of the di-saccharides, in seed from well-watered plants, they were mostly localised around the endosperm cavity covering a wide area. However, in the drought condition, di-saccharides were detected in two localised areas in the peripheral region leaving the endosperm cavity blank.

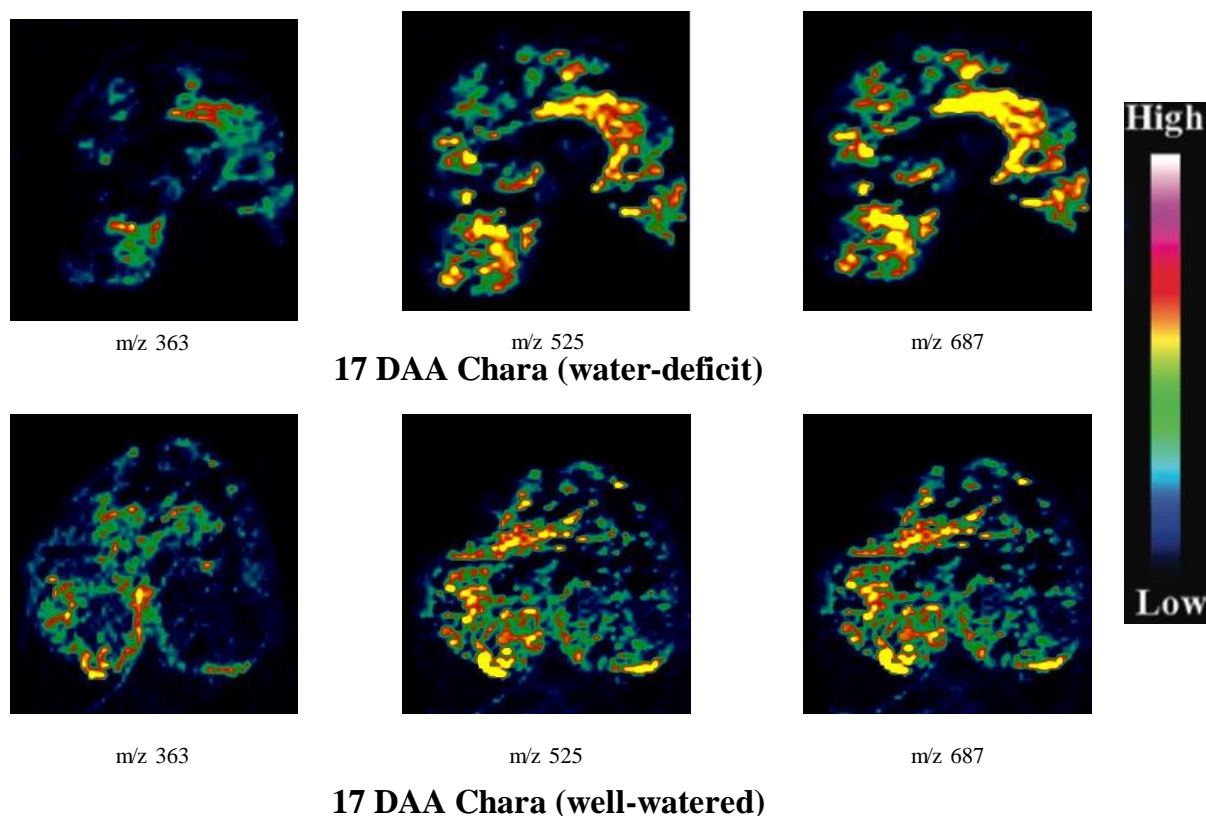


Fig. 6.4: Relative abundance and accumulation pattern of oligosaccharides at 17 DAA under drought and control conditions in the cultivar Chara.

II. Differentiation in oligosaccharide relative abundance and localisation pattern between growth stages under drought

The MSI analysis demonstrated that the relative abundances of all of the di-, tri- and tetra-saccharides have increased at 22 DAA compared to at 17 DAA under the drought condition (Fig. 6.5). At the same time, the localisation patterns of those oligosaccharides had changed between 17 and 22 DAA. In common, at 22 DAA, the oligosaccharides were more condensed compared to 17 DAA where signals were spread over a larger area of the seed. Noticeably, the localisation of the oligosaccharides in both stages were mostly in the middle region of the seeds leaving the adjacent areas of endosperm cavity and seed surface blank.

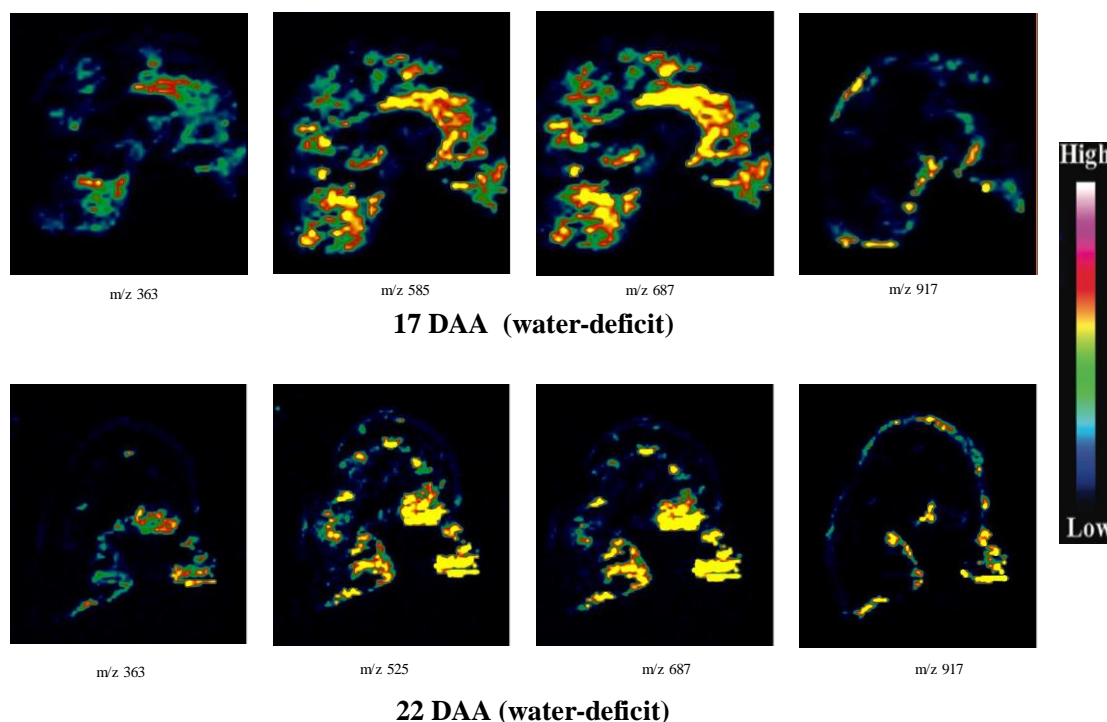


Fig. 6.5: Relative abundance and accumulation pattern of oligosaccharides at 17 DAA and 22 DAA under water-deficit in the cultivar Chara.

6.3.4 Influence of *1-FEH w3* mutation on oligosaccharide accumulation

The MSI analysis confirmed the role of the *1-FEH w3* gene in oligosaccharide accumulation in the developing seeds under the drought condition as claimed in the previous chapters. The *1-FEH w3* mutation line showed distinct differences in abundance and localisation pattern of identified three oligosaccharides under water-deficit compared to its parental cultivar Chara.

1. In water-deficit plants 1-FEH w3 mutation reduced the accumulation of oligosaccharide

At 17 DAA the *1-FEH w3* mutation line showed much less abundance of the identified three oligosaccharides compared to its parental cultivar Chara (Fig. 6.6). Similarly, at 22 DAA the *1-FEH w3* mutation line showed less abundance of the identified oligosaccharides compared to Chara (Fig. 6.7) although the differences were reduced, particularly in the case of tri and tetra saccharides. In the case of disaccharides, they were much less evident at 17 DAA and could not be detected at 22 DAA. It is unknown whether strong signals from other oligosaccharides might have masked weak signals from the disaccharides. The MSI also demonstrated that the large reduction in abundance of the oligosaccharides resulted in changes in their localisation in the seed tissues.

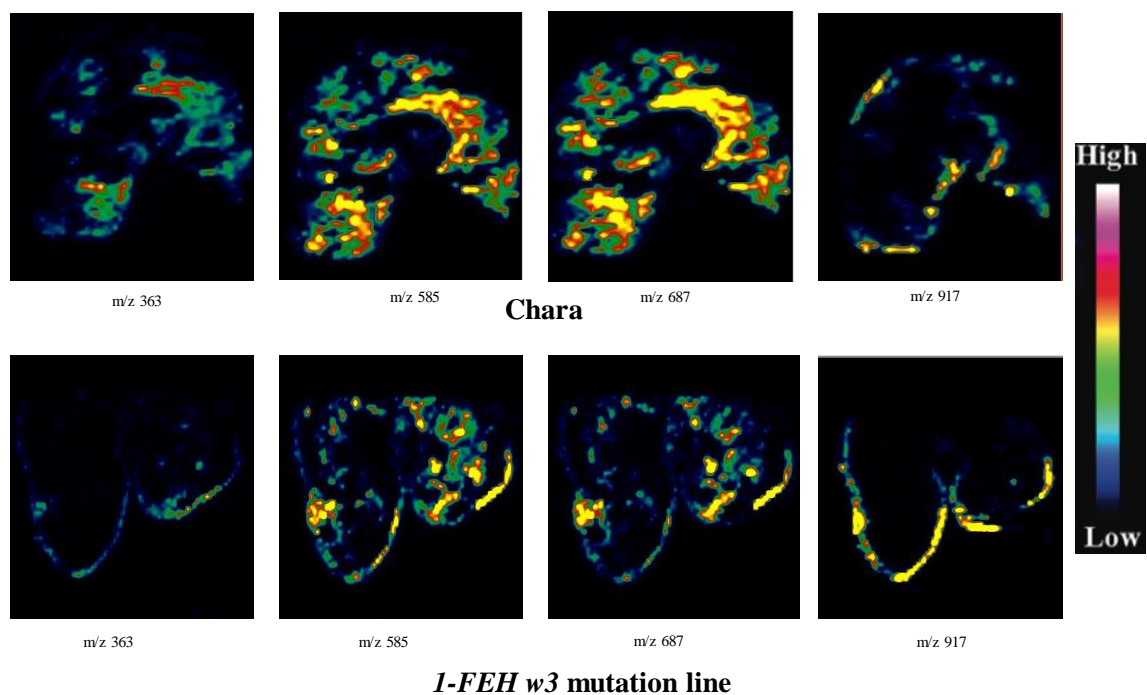


Fig. 6.6: Relative abundance and localisation pattern of oligosaccharides of *1-FEH w3* mutation line and its parental cultivar Chara under water-deficit at 17 DAA.

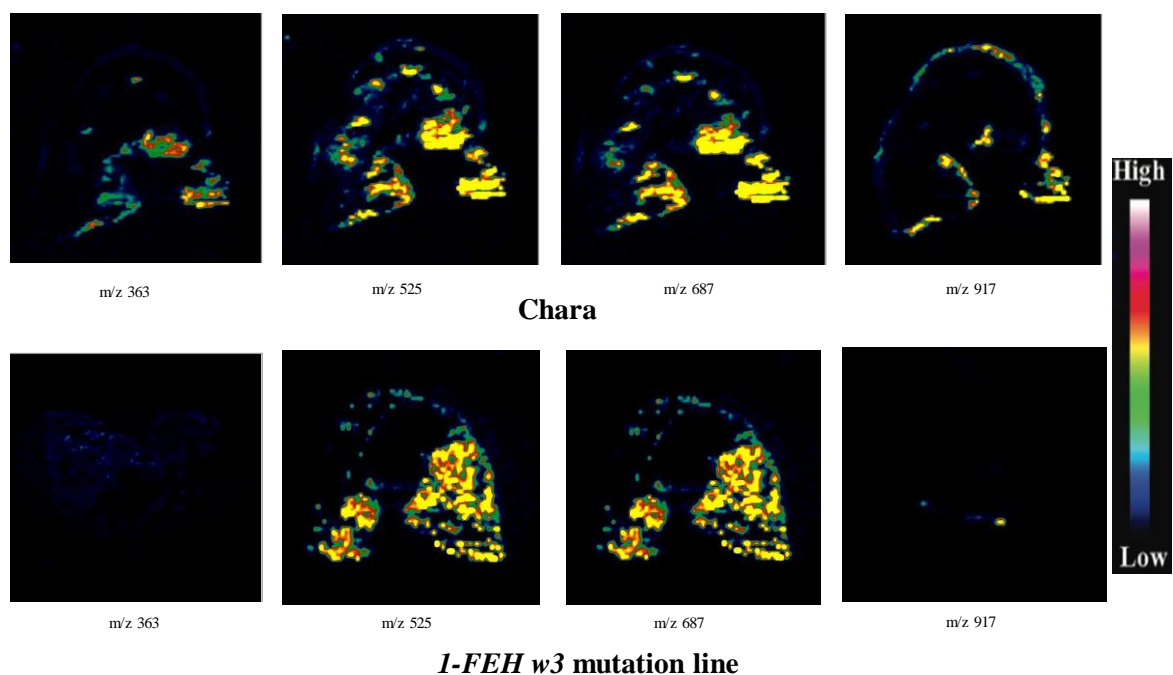


Fig. 6.7: Relative abundance and localisation pattern of oligosaccharides of *1-FEH w3* mutation line and its parental cultivar Chara under water-deficit at 22 DAA.

II. In well-watered condition *1-FEH w3* mutation delayed storage

At 17 DAA the tri- and tetra-saccharide signals were very low in the *1-FEH w3* mutation line compared to Chara (Fig. 6.8). Based on the results of the previous chapter, there was no significant differences in grain weight and yield between Chara and the *1-FEH w3* mutation line under the well-watered condition. Thus, the observed differences in sugar accumulation between those lines under the well-watered condition demonstrated that the storage phase in the developing grain was slowed down in the *1-FEH w3* mutation line compared to Chara. Generally, the storage phase started at 10 DAA and peaked at 17 DAA.

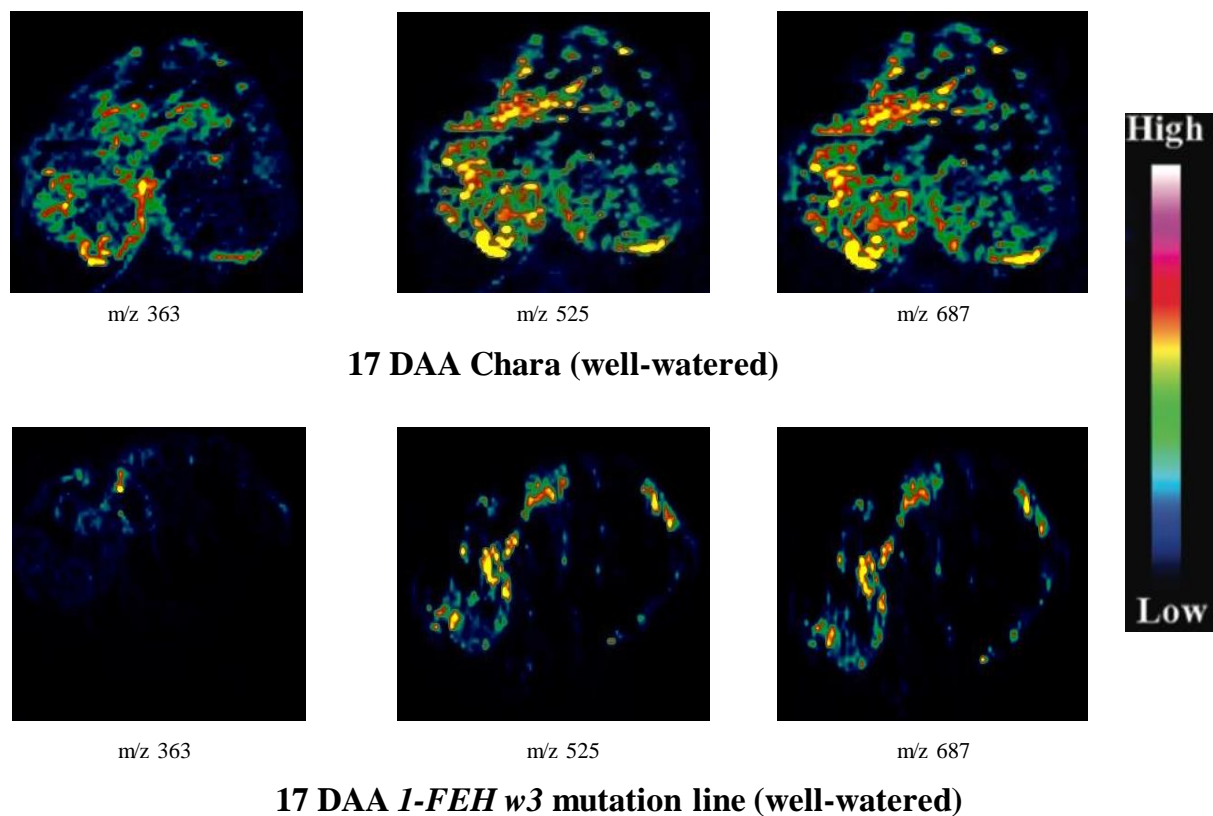


Fig. 6.8: Comparison of sugar accumulation between the *w3* mutation line and parental cultivar Chara under the well-watered condition.

6.4 Discussion

6.4.1 *Characterising sugar accumulation pattern in developing grain is important to deal with drought*

Quantitative study of sugar compounds within the seed and identifying their distribution is crucial to understand the complex molecular mechanisms involved in the process of sugar deposition in the grain. In particular, tissue specific localization information of the molecular compounds links the metabolites to potential functionality. The mechanisms involved in sugar deposition in the developing grain involves a complex network and is influenced by many factors. For example, the usual system of transferring sugar in the grain directly from regular photosynthetic assimilate is disrupted under stress conditions such as terminal drought. Accordingly, under stress, the larger portion of this sugar supply comes from stem reserves that is mainly composed of fructan (Chapter 2). As has been demonstrated in previous chapters, the *1-FEH* gene is largely involved in regulating this sugar remobilisation system. Correlation of *1-FEH*, particularly its isoforms with sugar remobilisation, is generally characterised using analytical approaches. However, the analytical methods are based on the total extraction of particular products where information of product localization is missing. Several researchers have tried to overcome this limitation by following different approaches that includes dissection of seeds into their main compartments or using *in vitro* cultivation of cells and tissues [e.g. aleurone layer (Finnie et al. 2011)]. However, those approaches to detect the localisation of compounds can be inefficient and complex. Details of metabolic activity in the developing grain are now achievable because methodology has been developed to the cellular level. Recent developments in separation sciences and mass spectrometry have enabled the localization of compounds by MALDI MSI with more accuracy and efficiency. Thus, this study characterised the abundance and distribution patterns of different oligosaccharides in developing grain using MSI. The information generated in this chapter has provided tissue level visualisation of the role of the *1-FEH w3* isoform in sugar transportation under terminal drought in wheat for the first time. Although there were limitations in the number of samples that could be processed, the findings revealed obvious differences in signal strength and distribution across sections of grain with different genetics and produced under distinct growing conditions.

6.4.2 *MSI technology has the potential to be used for characterising sugar accumulation in developing grain*

Until now MSI is the only technology with the ability of identifying and quantifying different metabolites, lipids, peptides, and proteins in a specific part or tissue sample, keeping the sample

structure intact (Bodzon-Kulakowska and Suder 2015). It provides reliable information regarding the localization and distribution pattern of molecules within an organ. However, use of MSI in plant research is relatively new and mostly has focused on small molecules. Moreover, plant MSI studies have largely been undertaken on species other than wheat and mostly on vegetative tissues. Use of MSI in cereal grain *in situ* analysis is much more limited. In particular, until now only one study has been reported using MSI on wheat seeds that investigated enzymatic hydrolysis of polysaccharides (Veličković et al. 2016). This is the first study to demonstrate the successful application of the MSI approach in direct (without enzymatic digestion) visualisation of sugar deposition and distribution pattern in wheat grain. Since there was no adequate available methodology, this study experienced challenges in regards to preparing cryosections as thin of 25 μm to enable ionisation of the sugar sitting within the seed tissue by the laser so that they can be detected by MALDI-TOF. Due to the incompatibility of the commonly used embedding material OCT with MALDI-TOF, cryosectioning of the seeds was developed using egg-white. This material has only one type of protein in which the mass peak was successfully differentiated from the mass peaks of oligosaccharides of the seed tissue. This was an important contribution to the methodology in regards to the MSI experimentation of wheat seeds.

In this study, MSI successfully visualised different oligosaccharides and demonstrated differences in their accumulation pattern as influenced by development stage and genotype. Di-, tri- and tetra-saccharides were visualised clearly due to the abundant m/z spectra observed across all sections. However, corresponding m/z signal values of hexose, penta- and hepta-saccharides did not show much strength. This might be either due to their less abundant accumulation in the developing seeds or technical difficulties in differentiating the ions generated by the laser. This need further investigation. However, this was common across the whole range of the samples tested irrespective of development stage and growth environment. In contrast, signal intensities of the detected oligosaccharides varied between samples. However, the reliability of the mass identification of different oligosaccharides was confirmed by the consistent mass peak observed from the two standard sugar samples analyzed with the seed samples. There are three different systems for detecting generated ions which are $[\text{M}+\text{H}]^+$, $[\text{M}+\text{Na}]^+$, and $[\text{M}+\text{K}]^+$. In this study the sugar potassium adducts $[\text{M}+\text{Na}]^+$ were the major detection, followed by the sodium adducts $[\text{M}+\text{K}]^+$. In contrast the protonated $[\text{M}+\text{H}]^+$ ion were not detected.

6.4.3 Sugar accumulation abundance and pattern are influenced by seed developing stage and drought

Relative abundance of the identified oligosaccharides was influenced by the developmental stages of wheat seeds which was correlated to the interaction of water availability. Under drought, all of the di-, tri- and tetra-saccharides showed increased abundance with the progress of seed development. However, under the well-watered condition, the accumulation pattern of the oligosaccharides across the seed sections was influenced by the stage of development.

Relative abundance of oligosaccharide accumulation was influenced by water-deficit. In particular, the tri- and tetra-saccharides had stronger signals in droughted plants compared to well-watered plants but there was little difference in the case of disaccharides. Similarly, the sugar accumulation pattern was also influenced by the drought. For example, tri- and tetra-saccharides were more condensed around the endosperm cavity due to the imposed drought compared to being scattered under the well-watered condition. Tri- and tetra-saccharides showed similar pattern of localisation. However, the di-saccharide showed a different localisation pattern.

Low abundance of higher oligosaccharides particularly above the tetra-saccharides in this experiment was due the selection of the storage phase to investigate. In barley seeds, Peukert et al. (2014) reported that during the prestorage phase, a generally higher abundance of DP 4-7 oligosaccharides was observed in the pericarp and at the storage phase distinctive patterns of oligosaccharide accumulation began when tri- and tetrasaccharides accumulated around the nascent endosperm cavity.

6.4.4 Mutation of *1-FEH w3* decreased sugar accumulation under water-deficit

The results of this chapter confirmed that the isoform *1-FEH w3* plays an important role in sugar transportation under water-deficit which was demonstrated by the different abundance and localisation patterns of the oligosaccharides in the *1-FEH w3* mutation line compared to its parental cultivar Chara. According to the results of the previous chapters, it was speculated that the mutation of *1-FEH w3* will reduce sugar transportation to the grain thus, sugar abundance will be reduced in the mutation line. MSI of the developing seeds clearly demonstrated (Fig. 6.6) that at both stages, the *1-FEH w3* mutation line had less abundance of the identified oligosaccharides compared to Chara. Also, the oligosaccharide localisation within the seed tissues was changed in the *1-FEH w3* mutation line due to the massive reduction in the abundance of tri- and tetra-sachharide.

6.4.5 Under well-watered condition deletion of *1-FEH w3* delayed sugar remobilisation to the grain

MSI analysis also confirmed that under the well-watered condition the isoform *1-FEH w3* does not play any different role. This was demonstrated by no obvious differences in Chara and the *1-FEH w3* mutation line in sugar abundance or pattern. However, the low abundance of tri- and tetra-saccharide in the *1-FEH w3* mutation line compared to the parental cultivar Chara at 17 DAA indicated that sugar accumulation started later in the mutation line but recovered over time.

6.5 Conclusion

Whilst the number of samples was low, this study for the first time successfully used the MSI technology to characterise the oligosaccharide accumulation within developing wheat seed without any enzymatic digestion. The cryosectioning has been developed using egg white to prepare the seed section as thin as 25 µm sections required for producing ions by burning oligosaccharides sitting within the tissues with a mass spectrometric laser. The MSI was able to identify the hexose and its polymers separately and directly from the seed section which enabled to provide the localisation information of the sugar deposition within the developing seed tissues. Furthermore, the MSI clearly demonstrated that the oligosaccharide, particularly di-, tri- and tetra-saccharides, abundance and localisation pattern is influenced by the seed developmental stages and availability of water. Ultimately this study confirmed the individual role of *1-FEH w3* in sugar transpiration under post anthesis water-deficit.

Chapter 7: General Discussion

This thesis was designed to characterise the functional and expressional behaviour of the three isoforms of the *1-FEH* gene under post anthesis water-deficit with the aim of confirming the role of individual isoforms in sugar transportation by using a set of gene mutation lines. This chapter discusses the outcomes of the four experiments in relation to the research objectives of the thesis mentioned in Chapter 1. Recommendations for further research into the mechanisms underpinning sugar remobilisation under post anthesis water-deficit are then proposed.

7.1 Major outcomes of the thesis

7.1.1 *1-FEH w3* is the most important isoform of *1-FEH* for WSC remobilisation and grain filling under post anthesis water-deficit

One of the objectives of this thesis was to identify the most important isoform of *1-FEH* for WSC remobilization under post anthesis water-deficit (Chapter 3). The null hypothesis “there is no variation in the roles of the three isoforms (*1-FEH w1*, *w2* and *w3*) of *1-FEH* on remobilisation of WSC under post anthesis water-deficit” was rejected by the experimental results. Under water-deficit during the critical period of WSC remobilization between 12 and 22 DAA, the *1-FEH w3* mutation line demonstrated slower WSC remobilisation compared to the other two isoforms (*1-FEH w1* and *w2*) mutation lines and the parent Chara (Chapter 3, Fig. 3.6). The *1-FEH w1* and *w2* mutation lines maintained statistically the same level of remobilization as the parent Chara, whereas the *1-FEH w3* mutation line had 39.8% slower remobilisation than that of Chara. The reduction in WSC remobilization resulted in reduced grain filling in the *1-FEH w3* mutation line which ultimately impaired the developing grain wt/main spike and thousand grain weight (TGW) (Chapter 3, Fig. 3.3). These two phenotypes are crucial determinants of yield. Thus, it became evident that the mutation of isoform *1-FEH w3* directly affected the process of seed development and eventually decreased the yield significantly under post anthesis water-deficit compared Chara. In contrast, mutation of other two isoforms, *1-FEH w1* and *1-FEH w2*, did not significantly affect WSC remobilisation and these plants were able to maintain similar yield as the parent Chara under water-deficit condition. Chara has been reported as a moderate drought tolerant wheat cultivar which is able to minimise the yield loss under post anthesis water-deficit condition. This thesis has confirmed that the potential of the cultivar to minimise yield loss under post anthesis water-deficit is contributed by the isoform *1-FEH w3*.

7.1.2 Gene expressional difference of *1-FEH* isoforms elucidates the degradation of WSC components in the mutation lines under water-deficit

This thesis observed differences in remobilisation of WSC components between the isoform mutation lines that can be explained by the expressional differences of the three isoforms of *1-FEH* gene across the lines. Higher expression of other genes with similar functionality of the knocked-out gene can occur in mutation lines which ultimately helps the plant to minimise the phenotypic alteration. As the result of Chapter 3 showed, and has been discussed in the earlier section, the *1-FEH w2* and *1-FEH w1* mutation lines did not show any significant phenotypic differences from the parent Chara (Chapter 3, Fig. 3.6). This might be due the increased functionality of other isoforms of *1-FEH* that ultimately made up the functional loss of the *1-FEH w2* and *w1* isoforms. To confirm this, expression of the individual isoforms at transcript level was investigated which showed that in the *1-FEH w2* and *w1* mutation lines the isoform *1-FEH w3* was highly expressed compared to Chara. However, in the *1-FEH w3* mutation line the expression of the other two isoforms had the same level of expression as Chara. This clearly indicated that functional loss of the isoforms *1-FEH w2* and *w1* was compensated by the over expression of the isoform *1-FEH w3*. In contrast, the functional loss of *1-FEH w3* was not made up by the other two isoforms.

It is worth mentioning that these gene expression patterns across different seed developmental stages was strongly correlated with WSC remobilisation under post anthesis water-deficit. Based on the WSC remobilization (Chapter 3; Fig. 3.5) and fructan degradation results (Chapter 4; Fig. 4.4), the period between 12 and 22 DAA appears to be the most vital stage for sugar remobilization into the developing grain in order to maintain grain weight when plants are under water-deficit. The isoform *1-FEH w3* was over expressed in the *1-FEH w2* and *w1* mutation lines under water-deficit at 17 and 22 DAA compared to the parental cultivar Chara, although the magnitude of the difference decreased at the later stage of grain fill (Fig. 4.11). It is worth mentioning that expression of the *1-FEH w2* and *w1* isoforms in the *1-FEH w2* and *1-FEH w1* mutation lines, respectively, was higher after 22 DAA (Figs, 4.12 and 4.13), which was outside the critical stage for sugar remobilization under water-deficit defined earlier. Thus, it appears that rapid remobilization of sugar in the *1-FEH w2* and *w1* mutation lines was largely contributed by the over expression of the *1-FEH w3* gene that helped to maintain the grain yield close to the parental cultivar under water-deficit. In contrast, there was no over expression of other two isoforms of the *1-FEH w3* mutation lines during the critical stage for sugar remobilization. Expression of the isoforms *1-FEH w2* and *w1* in the *1-FEH w3* mutation line

were significantly lower than that in the parental cultivar Chara up to 17 DAA (Figs, 4.12 and 4.13). Although at 22 DAA the expression of those two isoforms increased, it was still lower than the parental cultivar Chara (Figs, 4.10 and 4.11). That is why sugar remobilization (Chapter 3, Fig. 3.5) and grain weight (Chapter 3, Fig. 3.6) were significantly reduced in the *1-FEH w3* mutation line.

The expressional differences of the isoforms of the *1-FEH* gene across different mutation lines significantly influenced the degradation of WSC and its components under post anthesis water-deficit. The most important component of WSC post anthesis consists of fructans that comprise approximately 70% of WSC. Degradation of fructan by FEHS produces fructose and eventually its concentration in the developing grains starts to increase. Thus, fructans are considered as the key supplier of carbon structure to the developing wheat grain (Wardlaw and Willenbrink 2000; Zhang et al. 2014b). In particular, this supply of sugar from WSC degradation is crucial for grain filling under post anthesis water-deficit when reduced photosynthetic activity limits the regular sugar supply to the grain (Dreccer et al. 2009; Goggin and Setter 2004; Wardlaw and Willenbrink 1994; Zhang et al. 2015b). From the results in this thesis it is evident that the expressional variation of the three isoforms of *1-FEH* influenced fructan degradation under post anthesis water-deficit. The results described in Chapter 4 demonstrated that mutation of *1-FEH w3* slowed down fructan degradation under post anthesis water-deficit relative to the parental cultivar Chara. By contrast, the mutation of *1-FEH w2* and *1-FEH w1* did not show any significant difference in fructan degradation from Chara. Moreover, the *1-FEH w3* mutation line commenced fructan degradation 5 days later than the other two isoforms, *1-FEH w2* and *1-FEH w1* mutation lines, and Chara (Fig. 4.3). High levels of fructan and stem WSC remobilization due to the high expression of the *1-FEH w3* gene have also been reported by Zhang et al. (2015). Bifurcose is a branched fructan which also started to degrade at the same time (12 DAA) as fructan in all the mutation lines and Chara (Fig. 4.6). The fast degradation of bifurcose and rapid rise in fructose concentration in the stem is an indication of the faster remobilization of fructan (Zhang et al. 2015b). However, bifurcose degradation was very slow in the *1-FEH w3* mutation line for the first 5 days (Figs, 4.5 and 4.6) compared to the other two mutation lines and the parental cultivar.

Generally, delayed degradation of WSC and its components under post anthesis water-deficit make plants unable to transport the degraded compounds to the grain. This is because when plants reach permanent wilting point most of the normal metabolism ceases and plants lose the physiological capability to transport sugars to the grain. In this case, the delayed start to fructan degradation in the *1-FEH w3* mutation line (at 17 DAA) resulted in stem fructose

concentrations peaking at 22 DAA (Fig. 4.9). However, by that time (22 DAA) plants reached permanent wilting point meaning there was not enough time to transfer the fructose to the grain leading to a negative effect on final grain weight.

7.1.3 Sugar metabolism was influenced by *1-FEH* mutation

Generally, fructan is synthesized from sucrose and at the later stage of plant development the reverse mechanism takes place where fructan is broken down to provide additional sucrose to the plant. This is particularly crucial under post anthesis water-deficit when the regular sucrose supply from photosynthesis is significantly reduced (Yang et al. 2004). It has been clearly demonstrated that sucrose is the major transport compound in wheat plants to maintain the final grain yield (Joudi et al. 2012; Ruan 2014). Thus, to understand the flow of necessary sugar components to the grain under water-deficit condition, it is important to observe sucrose and fructan metabolism simultaneously which determines the plant's ability to manage the water-deficit, particularly after flowering. In water-deficit susceptible genotypes, sucrose and fructan concentrations in the stem peaked simultaneously and in water-deficit tolerant genotypes the fructan peak was earlier than the sucrose peak under water-deficit condition (Yáñez et al. 2017; Yang et al. 2004). It is worth mentioning that the highest levels of sucrose and fructan are indications of their subsequent degradation or conversion.

Out of the experimental results of this thesis, two distinct patterns were observed across the lines in terms of time to reach the highest levels of sucrose and fructan. The most common pattern in the stem was where the highest level of sucrose occurred 5 days after the highest level of fructan. This pattern was observed in the mutation lines *1-FEH w2* and *1-FEH w1* and Chara (Figs, 4.3 and 4.8). In the other pattern, the highest levels of sucrose and fructan occurred at the same time (12 DAA) and present only in the *1-FEH w3* mutation line (Figs, 4.8 and 4.3). Accordingly, these two patterns could be associated with their ability to tolerate post anthesis water-deficit. This indicated that mutation of the *1-FEH w3* isoforms made the line susceptible to post anthesis water-deficit as expressed in the yield phenotypes discussed earlier.

Furthermore, higher concentration of glucose also had been reported as an indicator of water-deficit tolerant genotypes compared to susceptible genotypes (Joudi et al. 2012; Yáñez et al. 2017). However, there were no significant differences in glucose concentration among the lines both in well-watered and water-deficit conditions (Fig. 4.10). Thus, it can be stated that the expression of the *1-FEH w3* isoform played a key role in tolerance against post anthesis water-deficit, but there are some other unknown factors influencing the mechanism as well. As this thesis focused on the remobilization of stored WSC, *1-FEH* gene expression was investigated

in the stem. Parallel research was undertaken by another PhD student and unveiled that there was no fructan in wheat leaves of the cultivars used. It is thus unlikely that *1-FEH* will be expressed in leaves, but it is worth while to explore if *1FEH w1* and *w2* have higher expression in other plant tissues.

Generally, it is considered that wheat fructan is a mixture of β (2,1) and β (2,6). 6-kestose contains β (2,6) which is normally broken down by *6-FEH*. Thus, the activities of both *1-FEH* and *6-FEH* genes are required to break down the fructan. The experimental results demonstrated that the concentration, accumulation and degradation pattern of 6-kestose were influenced neither by the mutation of the *1-FEH* isoforms nor by the water-deficit condition. Thus, it is clearly evident that mutation of the *1-FEH* isoforms did not restrict the activity of *6-FEH* which means that the variation in fructan degradation reported in the study resulted only from the mutation of the *1-FEH* isoforms and not by other *FEHs*.

7.1.4 Characterization of 1-FEH mutation lines using 90K SNP array

This study used gene mutation lines for the functional study of three isoforms of the *1-FEH* gene which is a powerful approach and commonly used in studies of this kind (Knoll et al. 2011; Lloyd and Meinke 2012). Targeted gene functional loss has been reflected in the gene expression and phenotypic analyses as discussed in the previous sections. However, mutational gene function studies in hexaploid bread wheat is complicated due to its three distinct genome 'A', 'B' and 'D' (Timothy et al. 2014) and, furthermore, wheat appears to be extremely tolerant of mutation. In addition, its extremely large size genome (17 Gb; 40 times the size of the rice genome) contains a high percentage of repetitive segments (80 – 90%) (Safar et al. 2010; Wanjugi et al. 2009). Commonly, most of the wheat genes have six homoeologous copies and two alleles from each of the sub-genomes, which potentially leads to a high functional redundancy causing complications in gene knockout strategies (Fitzgerald et al. 2012; Lai et al. 2012; Wang et al. 2012). Furthermore, heavy ion bombardment had been followed to produce the mutant line that could damage DNA in a random manner and cause base substitutions, deletions and chromosomal alteration (Morita et al. 2009). To explain the functional loss of the isoforms of the *1-FEH* genes, the physical modification of mutated segments on the chromosomes were investigated using a high-density SNP genotyping array and a bioinformatics approach. It is worth mentioning that a backcrossing step was followed for the analysis of mutants. Deletion mutations typically do not revert, so failure to revert is a hint that a mutation may be a deletion. Determining the position of the mutated region in the

chromosome and characterising the nature of the mutation were possible through access to the advanced wheat genome sequence databases.

In all of the mutation lines, the deleted regions were larger than the targeted gene sizes meaning some other genes were deleted located adjacent to the target gene. Eight non-target genes were identified across the mutation region of *1-FEH w1* on chromosome 6A, and 7 non-target genes were identified in the *1-FEH w3* mutation region on chromosome 6B. On the other hand, annotation of the *1-FEH w2* mutated region on chromosome 6D appeared to be more complicated. Finding out the position of the deletion region on chromosome 6D could not be done since the latest database (IWGSC WGA v0.4) assemblies of that chromosome was not fully complete (R Appels personal communication) at that time. Thus, an alternative analysis of the 6D deletion region was carried out using unmapped CDs sequence. *1-FEH w2* appeared with 3 extra copies in that region of chromosome 6D of which two copies were identified as active based on the publicly available transcriptomic data. The other copy of the gene contained a 15,831 bp insertion in the coding region and is most likely an inactive gene. Presence of multiple copies of the same gene is not an unusual case for wheat. In particular, the possible presence of additional gene copies for *1-FEH* indicated earlier (Zhang 2008) has now been confirmed by this study.

Identifying functional roles of inactivated non-target genes is crucial to validate that the phenotypic change in the mutated plant is due to the deletion of the target genes (*1-FEH w1/w2/w3*). Most of the non-target genes were identified as encoding uncharacterized protein which made it difficult to confirm functional roles. An alternative approach, prediction of protein function was carried out following computational biology. Multiple tools and databases were used to strengthen the prediction detailed in Chapter 5. In addition, 3D structure models of the proteins were generated using *Phyre²* to further confirm the function. The non-target genes were categorised into two major functional groups, namely hydrolase and ligase. Hydrolase catalyses the hydrolysis of chemical bonds. All of the target genes (*1-FEH w1, w2* and *w3*) including extra copies were identified with glycoside hydrolase activity meaning they are able to break down the sugar bond. Noticeably, a non-target gene (encoding Beta-fructofuranosidase, insoluble isoenzyme 4) in chromosome 6B has been identified with glycoside hydrolase activity. However, only a very small part of that gene was present in the mutation region and that overlapped with *1-FEH w3*. So, it is very unlikely that this small part has any influence on the sugar transport system (Fig. 5.9). The other hydrolase non-target genes of 6A and 6B (Table 5.10) deletion regions were identified as peptidase which indicate that they hydrolyse peptide bonds and do not have any relation with sugar hydrolysis. The second

largest number of non-target genes were identified as encoding ligase, an enzyme that helps in binding substrates. Since ligase does not affect sugar metabolism these annotated genes might not influence the activity of the *1-FEH* gene. Overall, none of the non-target genes had functions similar to *1-FEH w1*, *w2* and *w3* which indicates that the phenotypic differences observed in the mutation lines is due to the deletion of the particular isoform of *1-FEH*.

7.1.5 Characterising sugar accumulation pattern in developing grain

As discussed in the earlier sections, the correlation of the *1-FEH-w3* gene with sugar remobilisation was characterised using analytical approaches. Information regarding its relation with the localisation and tissue specific distribution of sugar molecules in developing grain was missing. This information is useful to understand the complex mechanism of sugar remobilisation under post anthesis water-deficit. Thus, the abundance and distribution pattern of oligosaccharides in developing grain were investigated using Mass Spectrometric Imaging (MSI) to investigate how the relative abundance and distribution of carbohydrate are influenced by the *1-FEH-w3* gene particularly under post anthesis water-deficit.

This is the very first approach to visualise the role of the *1-FEH-w3* gene in sugar transportation at the tissue level of developing grain produced under water-deficit. Use of MSI in plant research is relatively new and has mostly focused on small molecules and model plant species (Bodzon-Kulakowska and Suder 2015). Until now only one study has been reported on MSI investigation on wheat seeds using enzymatic hydrolysis unlike this study. Thus, the major challenge of this study was to proof the suitability of this technology for studying sugars in wheat seed. Optimising the procedure of preparing seed cryo-sections as thin as 25 μm to enable detecting sugars without enzymatic hydrolysis is one of the novel contributions of this thesis. Different oligosaccharides have been visualised successfully which allow identifying their distribution pattern across the seed section. Abundant m/z spectra enabled clear visualisation of di-, tri- and tetra-saccharides across all sections. In contrast, m/z values of hexose, penta- and hepta-saccharides was comparatively low and this might be due to their less abundant accumulation in seed sections. It also might be due to the technical difficulties in differentiating the ions generated by the laser which require further confirmation. Noticeably, considerable variation in signal intensities were detected between the samples which is very common in any approach that involves mass spectrometry. However, the consistent mass peak observed from the two standard sugar samples analysed provided the reliability of the mass identification of oligosaccharides. Out of three different systems of detecting generated ions, this study identified the sugar potassium adducts $[\text{M}+\text{K}]^+$ as the major detection, followed by the sodium adducts $[\text{M}+\text{Na}]^+$. In contrast the protonated $[\text{M}+\text{H}]^+$ ion were not detected.

MSI analysis demonstrated that sugar accumulation abundance and patterns in the developing grains were influenced by the grain development stage as well as by the water-deficit condition. As was expected, oligo saccharides gradually increased in abundance and became less localised in the seed with the development of seeds under normal watering. This validates the visualisation of oligosaccharide patterns in the developing grain. However, the effect of development stage on sugar localisation was influenced by the availability of water. On the other hand, water-deficit increased the concentrations of tri- and tetra-saccharides compared to normal watering although no obvious differences were observed in the case of disaccharides. Water-deficit also influenced the pattern of sugar accumulation in the developing grain which was attributed to the localisation of tri- and tetra-saccharides around the endosperm cavity under water-deficit compared to scattered distribution over the whole seed section under the well-watered condition. In general, the abundance of higher oligosaccharides (particularly above the tetra-saccharides) showed less abundance. This was most likely due to the developing phase investigated in this study being too early for detecting the higher oligosaccharides. Similar observations have been reported in young barley seed (Peukert et al. 2014).

Most strikingly, the MSI visualisation revealed that mutation of *1-FEH w3* resulted in decreased sugar accumulation under the water-deficit condition at 17 and 22 DAA. All the identified oligosaccharides, particularly the di-, tri- and tetra-saccharides, showed less abundance in the *1-FEH w3* mutation line compared to the parental cultivar Chara (Fig. 6.6). Due to the massive reduction in abundance, the localisation pattern of the oligosaccharides within the seed tissues also been changed in the *1-FEH w3* mutation line. Thus, the MSI visualisation of sugar accumulation in the developing seeds confirmed that the isoform *1-FEH w3* is playing an important role in sugar transportation under water-deficit condition in accordance with the outcome of phenotyping and transcriptomic investigations discussed in the previous sections. Lastly, although the findings are clear it must be noted that the number of replications was very limited and more needs to be done to confirm the preliminary discoveries.

7.1.6 1-FEH showed functionality only under water-deficit not under well-watered condition

The experimental results confirmed that the *1-FEH* gene, particularly the isoform *1-FEH-w3*, is playing a crucial role under post anthesis water-deficit which was ultimately reflected in yield phenotypes, particularly grain weight. The results also showed that the WSC concentration level, remobilisation rate and grain weights were not changed by the mutation of the isoforms of *1-FEH* gene under the well-watered condition. Even the transcriptional

investigation confirmed that in well-watered plants there were no significant differences in the expression level of these isoforms (Figs, 4.11, 4.12 and 4.13). Thus, the functional difference of the three isoforms of the *1-FEH* gene is visible only when the plant undergoes water-deficit. Whether other stressors can induce similar responses is unknown. It is worth noting that MSI analysis revealed low abundance of tri- and tetra-saccharides in the *1-FEH w3* mutation line compared to the parental cultivar Chara at 17 DAA in well-watered plants. This indicated that mutation of *1-FEH w3* caused a delayed start in sugar accumulation in well-watered plants, which was recovered over time; hence, there was no difference in the phenotypes at the end.

7.1.7 Post anthesis water-deficit resulted in early remobilisation of WSC

A common alteration to wheat plant physiological processes is the acceleration of grain maturity in response to environmental stress. Not surprisingly, under post anthesis water-deficit WSC remobilisation began 2 weeks earlier than in well-watered plants. The stage of the highest concentration of WSC is considered as the starting of remobilization since the process leads to a decline in the total WSC concentration (Cruz-Aguado et al. 2000). In well-watered condition, WSC peaked at 27 DAA compared to 12 DAA under water-deficit. Generally, starch and protein accumulation begin 2 weeks after anthesis since during the first two weeks of seed development only cell division takes place in the endosperm (Simmons et al. 1985). Rapid accumulation after cell division leads to a steep increase in seed weight. Thus, the very early start of sugar remobilisation might provide resources that are not effectively utilised by the developing grain.

7.2 Limitations of the thesis and future work

7.2.1 Using precise gene mutation technology like CRISPR-Cas9 for functional confirmation

This thesis studied *1-FEH* gene function using gene mutation lines. Use of plants with inactivated or deleted genes encoding particular traits of interest is a common process in research for crop improvement (Knoll et al. 2011). However, gene inactivation or deletion by mutation in wheat is complicated as has been described in the previous sections. Based on the commonly used gene mutation technologies it is hard to achieve a precise deletion of the target gene since deletion of non-target areas commonly occur. This was identified in the 90K SNP array of the mutated lines used in this study. CRISPR-Cas9 is a recently developed technology with the potential of providing a precise inactivation of the target gene (Heo et al. 2014; Kolli et al. 2017). Thus, further confirmation of the findings of this thesis using the CRISPR-Cas9 approach might add value.

7.2.2 Using recently published IWGSC data for characterising gene mutation

One of the major challenges this thesis has faced is the lack of updated wheat gene sequence database. During the time of experimentation, we did not have the complete wheat genome sequence data since it was published later in September 2018. Thus, due to the lack of gene assembly, annotation of the mutated region was challenging particularly for the *1-FEH w2* mutation region on chromosome 6D. Furthermore, the assembly for 6A and 6B has also been updated in the recently published whole genome sequence. This latest version of IWGSC can also be used to analyse SNPs in mutated lines using multiple sequence alignment in CLC and locating the SNPs in exons of the targeted genes. Accordingly, it can be identified whether each SNP polymorphism has changed the amino acid composition, which ultimately relates the SNPs to the gene function change. Thus, use of the latest wheat whole genome sequence database will be useful particularly to understand the function of the non-target mutated genes. Any future work on this area will add value to the findings of this thesis.

7.2.3 Further studying sugar accumulation patterns using mass spectrometry imaging

This thesis investigated the sugar accumulation abundance and pattern in the developing wheat grain which faces a number of challenges. MSI is well suited for targeted localization approaches as well as for untargeted profiling of tissue sections. However, use of MS imaging is relatively new in plants, particularly in wheat. There was no published methodology for studying developing wheat grain. Thus, this study only used a set of selected samples as the proof of concept. Although the target of this thesis has been achieved successfully it leaves the potential of using this approach over a complete set of samples. Thus, a complete investigation of the sugar accumulation pattern in the developing wheat grain as influenced by the mutation of *1-FEH* isoforms will enrich the knowledge base of sugar transportation mechanism.

The technology for distinguishing different types of fructans was not available for use during the PhD. Being the pioneer study, this work was focused on validating the platform for analysing the developing grain in wheat. Following the procedures of this study future experiments will be able to use this technology to identify fructan and its derivatives.

7.2.4 Future breeding research

This thesis has clearly demonstrated the potential function of the *1-FEH w3* to minimise the grain weight loss under water-deficit condition. However, due to the time constrain this thesis was not able to conduct further research to provide material which can be readily used in the

breeding program. Also, it was not possible to carry out the trial in the field which is crucial to bring the target gene into the breeding program. Thus, further work along this line might be useful to breed wheat with improved potential of water-deficit tolerance.

7.3 Conclusion

This is the first study that confirmed the functional role of *1-FEH* isoforms using gene mutation lines. The 90K SNP array confirmed the deletion of targeted *1-FEH* isoforms. Although some non-target genes were deleted, none of them has direct influence on *1-FEH* gene function which confirmed the phenotypic difference was due to the functional loss of *1-FEH* isoforms. This thesis defines the individual functional potential of three isoforms of *1-FEH* in remobilizing WSC under post anthesis water-deficit with a clear demonstration that *1-FEH w3* plays the most crucial role. Functional loss of *1-FEH w3* slowed down fructan degradation under water-deficit and resulted in lower TGW and yield. On the other hand, functional loss of *1-FEH w1* or *1-FEH w2* was compensated by the increase expression of *1-FEH w3*. Mass spectrometric imaging confirmed the potential role of *1-FEH w3* in sugar accumulation abundance and localisation pattern in the developing grain under post anthesis water-deficit. The functional difference of the isoforms of *1-FEH* gene can be visible only when the plant undergoes post anthesis water-deficit not under well-watered growing conditions. Thus, *1-FEH w3* could be a potential target for high WSC remobilization and high TGW for terminal drought tolerant wheat breeding. The outcomes can be used directly or as an integrated approach for drought tolerant breeding.

APPENDIX 1

A.1. Aim of this experiment

In the year 2013, a preliminary experiment had been carried out with the aim to identify the most drought responsive stage for WSC remobilisation and find out most suitable mutation lines for main experiment.

A.2. Materials and methods

A drought experiment was carried out in the glasshouse at Murdoch University in 2013.

Glasshouse temperature ranged from 15°C (night) -35°C (day). The humidity was 60-85%.

A.2.1. Plant material:

The plant materials included:

- one mutation line of *1-FEH w1*
 - two mutation line of *1-FEH w2*
 - two mutation line of *1-FEH w3* and
 - Parent line Chara
- (See detail description in Chapter 3)

A.2.2. Drought Experiment

A.2.2.1 Experimental design:

RCBD design was followed with 3 replications were used for each genotype for a 3 factors experiment with 288 pots (see detail description in experimental design in Chapter 3). Pots were watered three times a day, using mats underneath the pots, until anthesis. When 50% of plants were at the flowering stage, water was withheld from the pots designed for the drought treatment while the controls were kept well-watered (following the same regime as before anthesis) until maturity. All together, 8 samples were collected (Table A.1),

Table A.1.1: Growth stages for sample collection.

No. of sample	Time of sample collection
1	At anthesis
2	7 days after anthesis
3	12 days after anthesis
4	17 days after anthesis
5	22 days after anthesis
6	27 days after anthesis
7	32 days after anthesis
8	Maturity

A.2.2.2 Seed germination and soil preparation

Seeds were pre-germinated by soaking for two weeks at 4°C. Six pre-germinated seeds were planted in each 4L free-draining pot. The potting mix consisted of two parts composted pine bark, one part coconut fibre peat and one part river sand. Basal fertilizers (mg kg⁻¹: 1220 N, 368 P, 819 K plus a standard micronutrient mix) were incorporated with the potting mix.

A.2.2.3 Plant sampling for stem WSC measurements

To measure the WSC, the first sample was collected just before the onset of the drought treatment. The following samplings were carried out six times at 4 day intervals. Plants were harvested between 11.00 am to 17.00 pm to ensure stable carbohydrate reserve accumulation. The last sample was collected at grain maturity (8 weeks after anthesis). Three parts of the shoot were harvested from the main tiller (the stem, leaf sheath and blade). All samples were immediately put onto dry ice then stored at -20°C. Frozen plant samples were chopped into less than 5 mm pieces and divided into two parts. One part was stored at -80°C for molecular (RNA) analysis and the other part stored at -20°C for WSC analysis.

Harvest data were collected from each treatment combination. The number of kernel/spike, total number of seed/plant, and thousand seed weight were collected accordingly. Grains were oven dried before thousand grains weight was taken.

A.2.2.4 Carbohydrate analysis

The samples for WSC analysis were later freeze-dried and then oven-dried at 75°C (Zhang et al. 2008). The stem WSC of all lines was measured by colorimetry using the anthrone reagent (Zhang et al. 2008).

A.2.2.5 Statistical analysis

Analysis of variance on water soluble carbohydrate concentration, Kernel no/spike of main spike, kernel wt/ spike of main spike was performed using IBM SPSS Statistics V21.0 Post-hoc comparisons were conducted using Duncan Multiple Range tests at $P < 0.05$.

A.3 Results

Stem WSC concentration was measured in both well-watered and water deficit condition at 8 developmental stages of the plants grown in preliminary experiment. There was no significant variation in stem WSC remobilisation between parent Chara and the mutation lines w3, w2 and w1 under well-watered condition. However, a variation in WSC remobilisation has been recorded under water deficit condition. This difference in remobilisation rate is correlated with the grain development, which is discussed below.

A.3.1. Stem WSC Concentration in different growth stage in relation to developing grain weight:

In the preliminary experiment conducted in 2013, under water deficit condition, the WSC peaked at 12 DAA and it was 17 DAA in well-watered plants. It is worth noting that there was an unexpected light stress at the early stage of plant development that led to early senescence even in the well-watered plants. There were no significant differences ($p < 0.05$) in the level of stem WSC between the mutation lines and parent line Chara in both the well-watered and water deficit plants (Fig: A.1). However, the level of WSC was higher in the well-watered condition compared to the water deficit condition. In well-watered condition, the highest level of WSC in Chara was 13.18% followed by 12.4%, 11.09%, 11.07%, 10.39% and 11.86% in 18b-426 w3, 22-571 w3, 21-433 w2, 18b-646 w2 and 22-22 w1 mutation lines respectively. In contrast, under water deficit, the highest WSC concentrations were 10.26%, 10.80%, 9.62%, 10.07%, 11.48% and 10.25% for chara, 18b-426 w3, 22-571 w3, 21-433 w2, 18b-646 w2 and 22-22

w1mutation lines respectively (Fig. A. 1.1). In the year 2013, there was no significant difference between the lines in WSC remobilization (Fig. A. 1.2).

At different developmental stages between 12 and 32 days after anthesis, there were no significant differences in main spike seed wt (gm/ear) among the different mutation line and Chara.

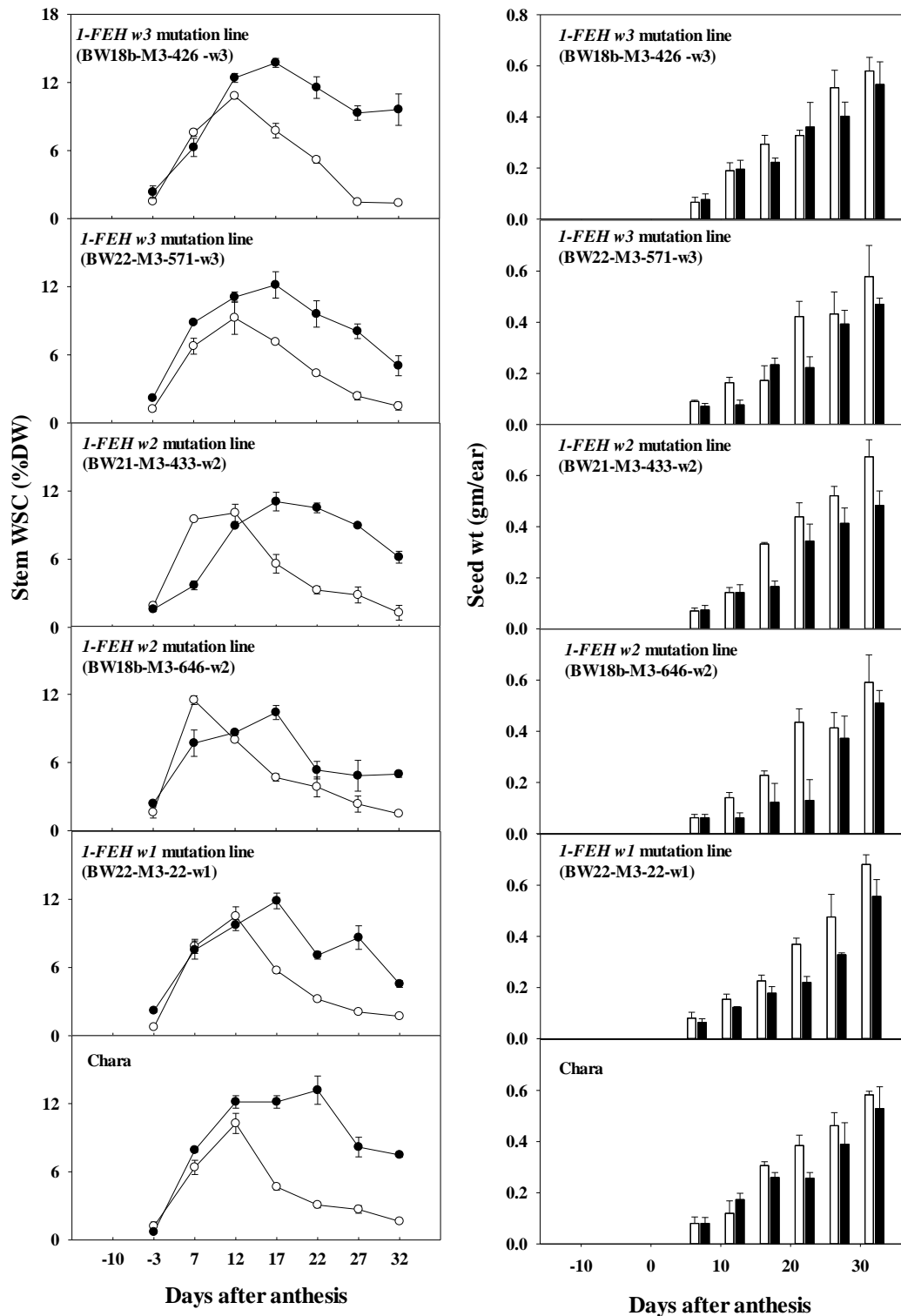


Fig. A.1.1: Stem water-soluble carbohydrate (WSC) concentration (left hand side) and grain dry weight per ear (in right hand side) in 2013 of mutation lines. Closed symbols=well-watered and open symbols=water-deficit; vertical bars represent \pm SE of the mean of three replicates).

A.3.2 Stem WSC Remobilization between 12 DAP to 22 DAP

Under water deficit from 12 days after anthesis (peak value for WSC) to 22 days after anthesis (permanent wilting point of plant), there was no significant difference between the lines in WSC remobilization (Fig. A.2). Nevertheless, remobilization rate was relatively slower in w3 mutation lines(0.57% and 0.56%) compare to parent line Chara (0.75%) and other two mutation lines of w2 (0.71% and 0.72%) and w1 (0.69%).

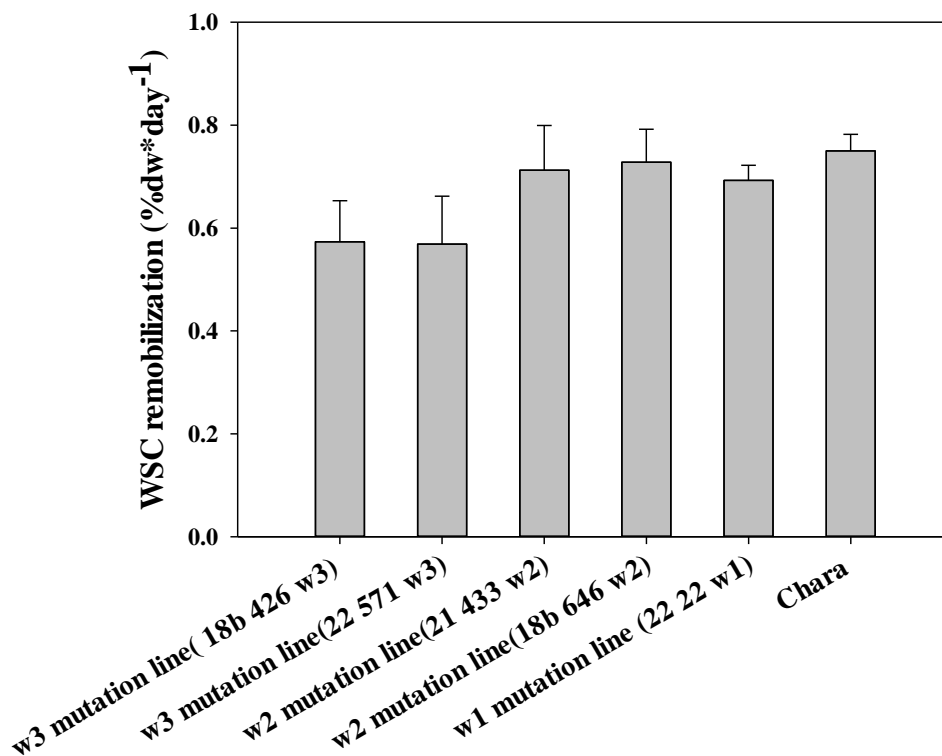


Fig. A.1.2: Decline in stem WSC (%DW) in three mutation lines and Chara in the 2013 drought experiment from 12 days after anthesis to 22 days after anthesis.

A.3.2. Matured grain weight was influenced by 1-FEH isoforms under drought

In the well-watered condition, there was no difference among the mutation lines and Chara. In the year 2013 (Table A.2), under drought condition the main stem grain wt was significantly ($p < 0.05$) lower in the w3 mutation lines (in 18b 426 w3 was 0.53 g ear⁻¹ and in 22 571 w3 was 0.50 g ear⁻¹) relative to Chara (0.88 g ear⁻¹). TGW was also significantly lower ($p < 0.05$) in w3 than Chara and other three mutation lines.

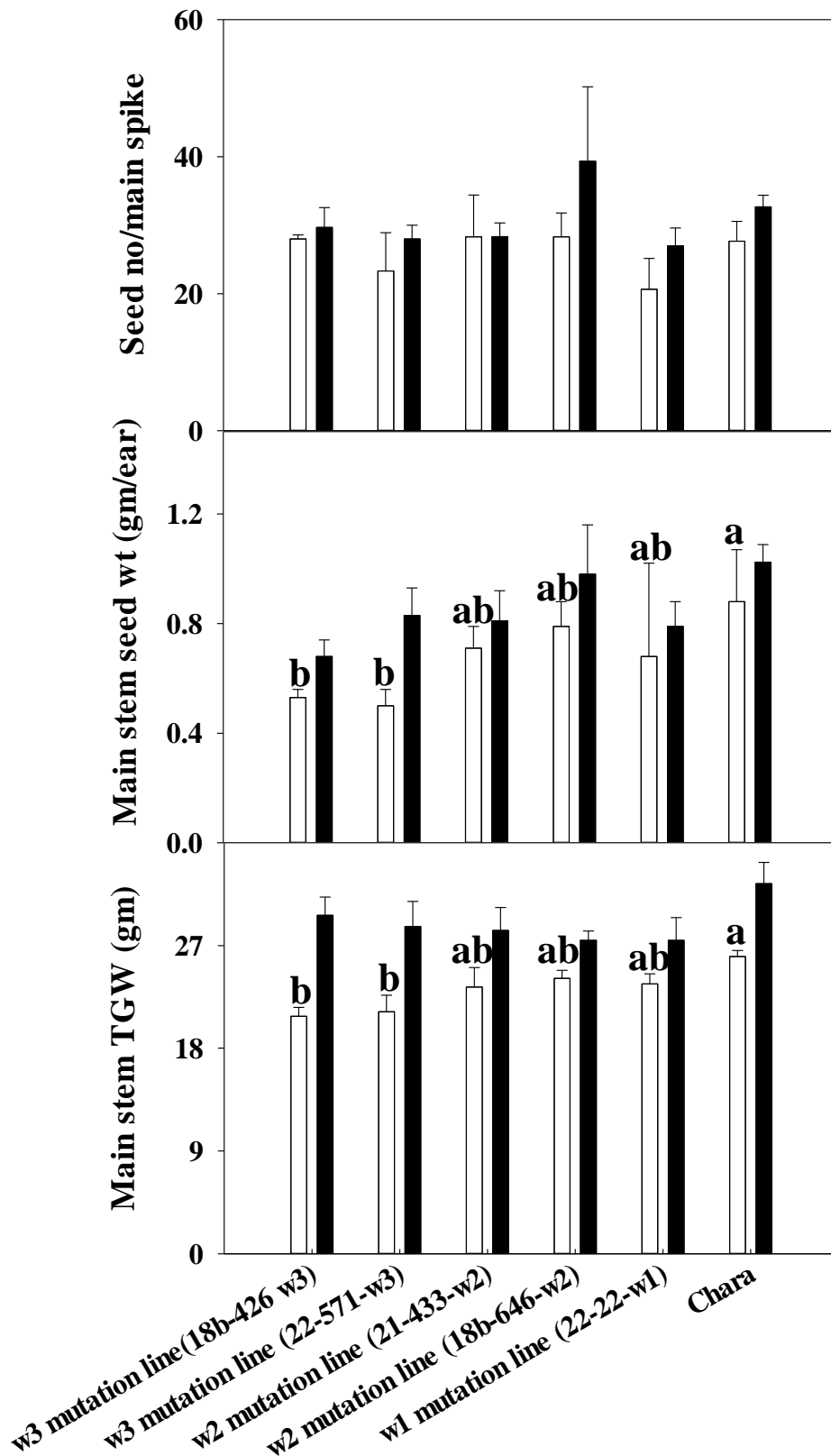


Fig. A.1.3: Main stem seed no/spike, seed wt (gm) and TGW (gm) at maturity in well-watered and water-deficit plants in all mutation lines and parent line Chara for 2013 glasshouse experiment. Closed symbols = well-watered and open symbols = water-deficit; vertical bars represent \pm SE of the mean of three replicate.

A.4 Discussion

Of the two *w3* mutation lines, BW 22-571 *w3* had lower WSC concentration (9.6%) than BW 18b 426 *w3* (10.8%) (Fig. A.1.1) in 2013. However, in 2014 values were higher being 24.2% in BW 22-571 *w3* (Fig. A.2.1) and 26.2% in BW 18b 426 *w3* (Fig. 3.4). Under terminal drought, higher WSC concentration resulted in higher seed weight. As BW 18b 426 *w3* had comparatively higher WSC concentrations in both years, data for this line was used in the main body of the thesis and called the *w3* mutation line. As *w2* mutation lines BW 18b 646 *w2* was a late flowering line, BW 21 433 *w2* was used as the *w2* mutation line.

The level of maximum WSC in mutation lines and parent Chara remained significantly lower in both well-watered and drought condition than previous GH experiments (Zhang et al. 2009) probably due to the PAR (Photosynthetically Active Radiation) being lower than optimal during initial developmental stage. However, seed wt/main stem and TGW were significantly lower in the *1-FEH w3* mutation lines than Chara and other three mutation lines, which indicate that the absence of *1-FEH w3* disrupts the sugar transportation into the developing grain in the drought condition that resulting in lower seed weight. To confirm this finding and to find out the role of each isoforms, a new experiment was set up in 2014.

APPENDIX 2

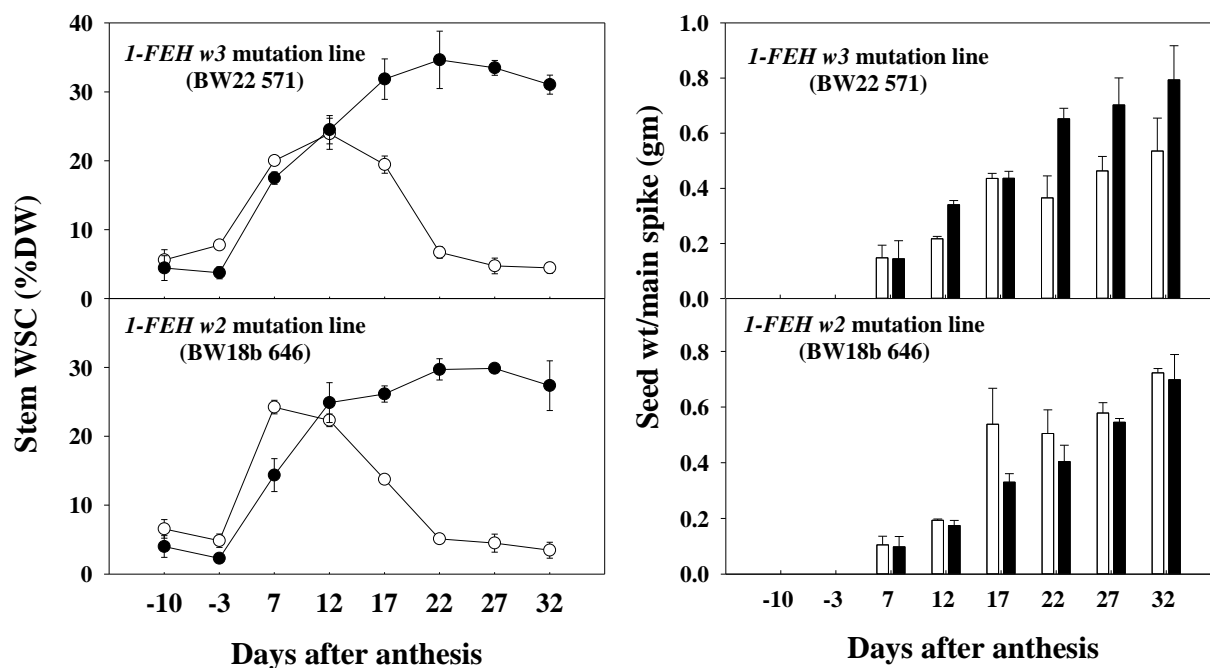


Fig A.2.1: Change in stem water soluble carbohydrate (WSC) concentration (a) and related grain dry weight per ear with time after anthesis (b) for 2014 glasshouse experiment. Closed symbols and bars = well-watered and open symbols and bars = water-deficit; from 10 days before anthesis to 32 days after anthesis, error bars indicate the \pm SE of the mean of three replicates.

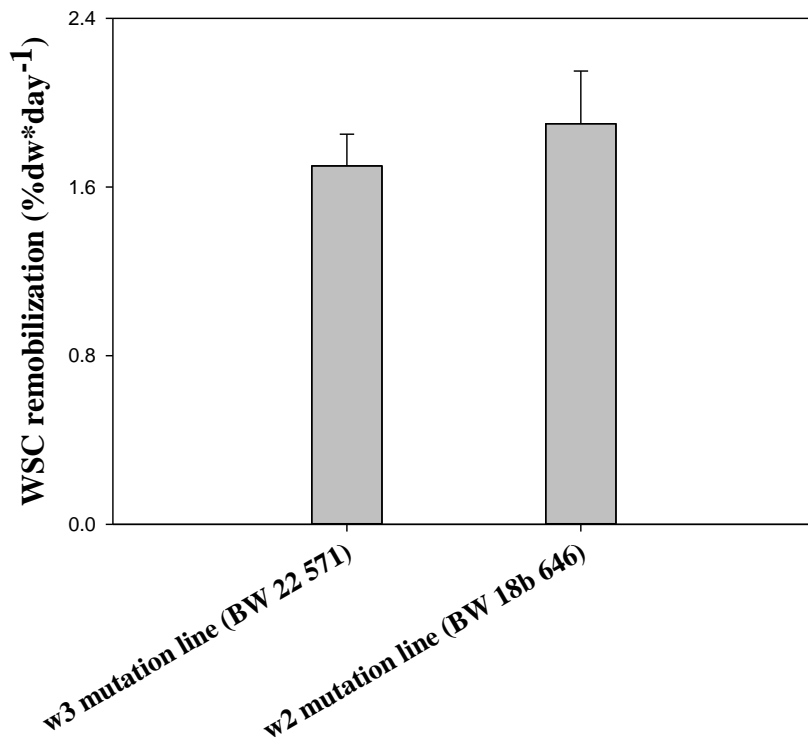


Fig. A.2.2: Decline in stem WSC (%DW) in three mutation lines and Chara in the 2014 drought experiment from 12 days after anthesis to 22 days after anthesis.

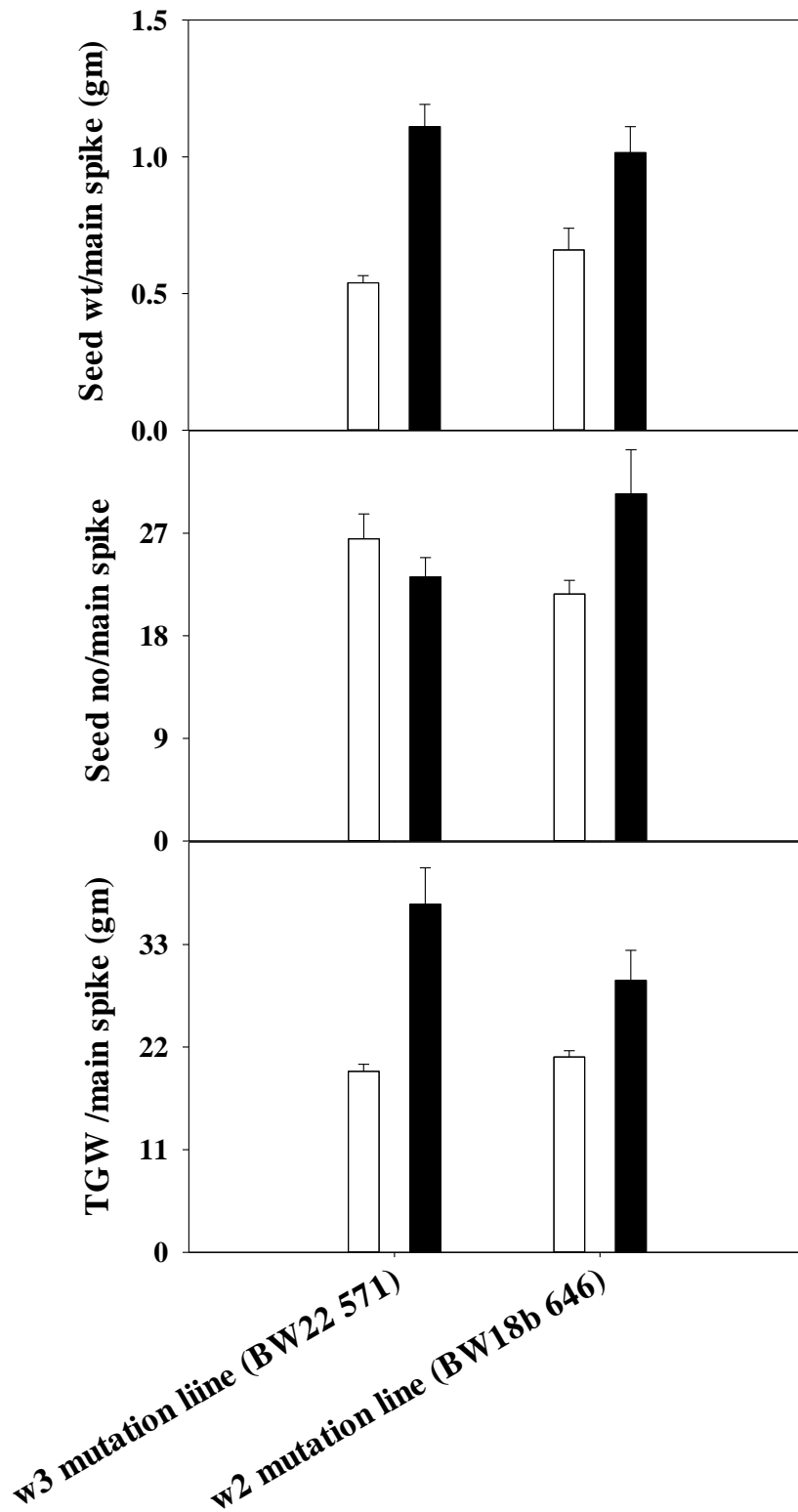


Fig. A.2.3: Main stem seed wt(g), seed no/spike and TGW at maturity in well-watered and water-deficit plants in all mutation lines and parent line Chara for 2014 glasshouse experiment. Closed symbols = well-watered and open symbols = water-deficit; vertical bars represent \pm SE of the mean of three replicates.

References

- Akbari M, Wenzl P, Caig V, Carling J, Xia L, Yang S, Uszynski G, Mohler V, Lehmensiek A, Kuchel H (2006) Diversity arrays technology (DArT) for high-throughput profiling of the hexaploid wheat genome. *Theoretical and Applied Genetics* 113:1409-1420
- Akhunov E, Nicolet C, Dvorak J (2009) Single nucleotide polymorphism genotyping in polyploid wheat with the Illumina GoldenGate assay. *Theoretical and Applied Genetics* 119:507-517
- Akond M, Liu S, Schoener L, Anderson JA, Kantartzi SK, Meksem K, Song Q, Wang D, Wen Z, Lightfoot DA (2013) SNP-based genetic linkage map of soybean using the SoySNP6K Illumina Infinium BeadChip genotyping array. *Journal of Plant Genome Sciences* 1:80–89
- Albrecht G, Mustroph A (2003) Localization of sucrose synthase in wheat roots: increased in situ activity of sucrose synthase correlates with cell wall thickening by cellulose deposition under hypoxia. *Planta* 217:252-260
- Alexandrov T, Bartels A (2013) Testing for presence of known and unknown molecules in imaging mass spectrometry. *Bioinformatics* 29:2335-2342
- Allen AM, Barker GL, Berry ST, Coghill JA, Gwilliam R, Kirby S, Robinson P, Brenchley RC, D'Amore R, McKenzie N (2011) Transcript-specific, single-nucleotide polymorphism discovery and linkage analysis in hexaploid bread wheat (*Triticum aestivum* L.). *Plant Biotechnology Journal* 9:1086-1099
- Altenbach S, DuPont F, Kothari K, Chan R, Johnson E, Lieu D (2003) Temperature, water and fertilizer influence the timing of key events during grain development in a US spring wheat. *Journal of Cereal Science* 37:9-20
- Amstalden van Hove ER, Smith DF, Heeren RMA (2010) A concise review of mass spectrometry imaging. *Journal of Chromatography A* 1217:3946-3954
- Anjum SA, Xie X-y, Wang L-c, Saleem MF, Man C, Lei W (2011) Morphological, physiological and biochemical responses of plants to drought stress. *African Journal of Agricultural Research* 6:2026-2032
- Aoki N, Hirose T, Scofield GN, Whitfield PR, Furbank RT (2003) The Sucrose Transporter Gene Family in Rice. *Plant and Cell Physiology* 44:223-232
- Appels R, Eversole K, Feuillet C, Keller B, Rogers J, Stein N, Pozniak CJ, Choulet F, Distelfeld A, Poland J (2018) Shifting the limits in wheat research and breeding using a fully annotated reference genome. *Science* 361:eaar7191
- Aprile A, Mastrangelo A, De Leonardis A, Galiba G, Roncaglia E, Ferrari F, De Bellis L, Turchi L, Giuliano G, Cattivelli L (2009) Transcriptional profiling in response to terminal drought stress reveals differential responses along the wheat genome. *BMC Genomics* 10:279
- Araus J, Slafer G, Reynolds M, Royo C (2002) Plant breeding and drought in C3 cereals: what should we breed for? *Annals of Botany* 89:925-940
- Artlip TS, Madison JT, Setter TL (1995) Water deficit in developing endosperm of maize: cell division and nuclear DNA endoreduplication. *Plant, Cell & Environment* 18:1034-1040
- Asano T, Kunieda N, Omura Y, Ibe H, Kawasaki T, Takano M, Sato M, Furuhashi H, Mujin T, Takaiwa F, Wu C-y, Tada Y, Satozawa T, Sakamoto M, Shimada H (2002) Rice SPK, a Calmodulin-Like Domain Protein Kinase, Is Required for Storage Product Accumulation during Seed Development: Phosphorylation of Sucrose Synthase Is a Possible Factor. *The Plant Cell Online* 14:619-628
- Asseng S, Foster I, Turner NC (2011) The impact of temperature variability on wheat yields. *Global Change Biology* 17:997-1012

- Barnabás B, Jáger K, Fehér A (2008) The effect of drought and heat stress on reproductive processes in cereals. *Plant, Cell & Environment* 31:11-38
- Barratt DHP, Derbyshire P, Findlay K, Pike M, Wellner N, Lunn J, Feil R, Simpson C, Maule AJ, Smith AM (2009) Normal growth of *Arabidopsis* requires cytosolic invertase but not sucrose synthase. *Proceedings of the National Academy of Sciences* 106:13124-13129
- Bechtel DB, Abecassis J, Shewry PR, Evers AD (2009) CHAPTER 3: Development, Structure, and Mechanical Properties of the Wheat Grain. *WHEAT: Chemistry and Technology*. AACC International, Inc., pp 51-95
- Bialeski RL (1993) Fructan Hydrolysis Drives Petal Expansion in the Ephemeral Daylily Flower. *Plant Physiology* 103:213-219
- Bihmidine S, Hunter III CT, Johns CE, Koch KE, Braun DM (2013) Regulation of assimilate import into sink organs: update on molecular drivers of sink strength. *Frontiers in Plant Science* 4:177
- Bingham J (1966) Varietal response in wheat to water supply in the field, and male sterility caused by a period of drought in a glasshouse experiment. *Annals of Applied Biology* 57:365-377
- Bjarnholt N, Li B, D'Alvise J, Janfelt C (2014) Mass spectrometry imaging of plant metabolites—principles and possibilities. *Natural product reports* 31:818-837
- Blum A (1998) Improving wheat grain filling under stress by stem reserve mobilization. *Euphytica* 100:77–83
- Blum A, Ramaiah S, Kanemasu ET, Paulsen GM (1990) Wheat recovery from drought stress at the tillering stage of development. *Field Crops Research* 24:67-85
- Bodzon-Kulakowska A, Suder P (2015) Imaging mass spectrometry: Instrumentation, applications, and combination with other visualization techniques. *Mass Spectrometry Reviews* 35:147-169
- Bonnett G, Sims I, Simpson R, Cairns A (1997) Structural diversity of fructan in relation to the taxonomy of the Poaceae. *New Phytologist* 136:11-17
- Borlaug NE, Dowswell CR (2005) Feeding a world of ten billion people: a 21st century challenge. In *Proceedings of “In the Wake of the Double Helix: From the Green Revolution to the Gene Revolution”*, 27-31 May 2003, Bologna, Italy, pp. 3–24.
- Boughton BA, Thinakaran D, Sarabia D, Bacic A, Roessner U (2016) Mass spectrometry imaging for plant biology: a review. *Phytochemistry Reviews* 15:445-488
- Boyer JS (1982) Plant Productivity and Environment. *Science* 218:443-448
- Briggs D (1983) Analysis of polymer surfaces by SIMS, 3—preliminary results from molecular imaging and microanalysis experiments. *Surface and Interface Analysis* 5:113-118
- Briggs KG, Kiplagat OK, Johnson-Flanagan AM (1999) Effects of pre-anthesis moisture stress on floret sterility in some semi-dwarf and conventional height spring wheat cultivars. *Canadian Journal of Plant Science* 79:515-520
- Brisson N, Gate P, Gouache D, Charmet G, Oury F-X, Huard F (2010) Why are wheat yields stagnating in Europe? A comprehensive data analysis for France. *Field Crops Research* 119:201-212
- Campbell D, Ferreira C, Eberlin L, Cooks RG (2012) Improved spatial resolution in the imaging of biological tissue using desorption electrospray ionization. *Analytical and Bioanalytical Chemistry* 404:389-398
- Caprioli RM, Farmer TB, Gile J (1997) Molecular imaging of biological samples: localization of peptides and proteins using MALDI-TOF MS. *Analytical chemistry* 69:4751-4760

- Carpita NC, Kanabus J, Housley TL (1989) Linkage structure of fructans and fructan oligomers from *Triticum aestivum* and *Festuca arundinacea* leaves. *Journal of Plant Physiology* 134:162-168
- Casson SA, Hetherington AM (2010) Environmental regulation of stomatal development. *Current Opinion in Plant Biology* 13:90-95
- Cattivelli L, Rizza F, Badeck F-W, Mazzucotelli E, Mastrangelo AM, Francia E, Mare C, Tondelli A, Stanca AM (2008) Drought tolerance improvement in crop plants: an integrated view from breeding to genomics. *Field Crops Research* 105:1-14
- Cavanagh CR, Chao S, Wang S, Huang BE, Stephen S, Kiani S, Forrest K, Saintenac C, Brown-Guedira GL, Akhunova A, See D, Bai G, Pumphrey M, Tomar L, Wong D, Kong S, Reynolds M, da Silva ML, Bockelman H, Talbert L, Anderson JA, Dreisigacker S, Baenziger S, Carter A, Korzun V, Morrell PL, Dubcovsky J, Morell MK, Sorrells ME, Hayden MJ, Akhunov E (2013) Genome-wide comparative diversity uncovers multiple targets of selection for improvement in hexaploid wheat landraces and cultivars. *Proceedings of the National Academy of Sciences* 110:8057-8062
- Cecchini E, Mulligan BJ, Covey SN, Milner JJ (1998) Characterization of gamma irradiation-induced deletion mutations at a selectable locus in *Arabidopsis*. *Mutation Research/Fundamental and Molecular Mechanisms of Mutagenesis* 401:199-206
- Chalfie M, Tu Y, Euskirchen G, Ward W, Prasher D (1994) Green fluorescent protein as a marker for gene expression. *Science* 263:802-805
- Chandra A, Jain R, Solomon S (2012) Complexities of invertases controlling sucrose accumulation and retention in sugarcane. *Current Science*:857-866
- Chaurand P (2012) Imaging mass spectrometry of thin tissue sections: A decade of collective efforts. *Journal of Proteomics* 75:4883-4892
- Chen J, Black C (1992) Biochemical and immunological properties of alkaline invertase isolated from sprouting soybean hypocotyls. *Archives of Biochemistry and Biophysics* 295:61-69
- Chen YC, Chourey PS (1989) Spatial and temporal expression of the two sucrose synthase genes in maize: immunohistological evidence. *Theoretical and Applied Genetics* 78:553-559
- Chourey P, Nelson O (1976) The enzymatic deficiency conditioned by the shrunken-1 mutations in maize. *Biochemical Genetics* 14:1041-1055
- Chourey PS, Taliercio EW, Carlson SJ, Ruan YL (1998) Genetic evidence that the two isozymes of sucrose synthase present in developing maize endosperm are critical, one for cell wall integrity and the other for starch biosynthesis. *Molecular and General Genetics MGG* 259:88-96
- Chughtai K, Heeren RM (2010) Mass spectrometric imaging for biomedical tissue analysis. *Chemical Reviews* 110:3237-3277
- Cima RD, Antuono MF, Anderson WK (2004) The effects of soil type and seasonal rainfall on the optimum seed rate for wheat in Western Australia. *Australian Journal of Experimental Agriculture* 44:585-594
- Claussen W, Loveys BR, Hawker JS (1985) Comparative investigations on the distribution of sucrose synthase activity and invertase activity within growing, mature and old leaves of some C3 and C4 plant species. *Physiologia Plantarum* 65:275-280
- Clauw P, Coppens F, De Beuf K, Dhondt S, Van Daele T, Maleux K, Storme V, Clement L, Gonzalez N, Inzé D (2015) Leaf responses to mild drought stress in natural variants of *Arabidopsis thaliana*. *Plant Physiology* 167: 800-816

- Coleman HD, Ellis DD, Gilbert M, Mansfield SD (2006) Up-regulation of sucrose synthase and UDP-glucose pyrophosphorylase impacts plant growth and metabolism. *Plant Biotechnology Journal* 4:87-101
- Coleman HD, Yan J, Mansfield SD (2009) Sucrose synthase affects carbon partitioning to increase cellulose production and altered cell wall ultrastructure. *Proceedings of the National Academy of Sciences* 106:13118-13123
- Cook JP, McMullen MD, Holland JB, Tian F, Bradbury P, Ross-Ibarra J, Buckler ES, Flint-Garcia SA (2012) Genetic architecture of maize kernel composition in the nested association mapping and inbred association panels. *Plant physiology* 158:824-834
- Cornett DS, Reyzer ML, Chaurand P, Caprioli RM (2007) MALDI imaging mass spectrometry: molecular snapshots of biochemical systems. *Nature Method* 4:828-833
- Cruz-Aguado JA, Rodés R, Pérez IP, Dorado Mn (2000) Morphological characteristics and yield components associated with accumulation and loss of dry mass in the internodes of wheat. *Field Crops Research* 66:129-139
- CSIRO, BoM (2016) State of the Climate 2016. CSIRO, Melbourne, Australia
- DAFWA (2014) Department of Agriculture and Food Western Australia. <https://www.agricwagovau/>
- Dale EM, Housley TL (1986) Sucrose Synthase Activity in Developing Wheat Endosperms Differing in Maximum Weight. *Plant Physiology* 82:7-10
- Daszkowska-Golec A, Szarejko I (2013) Open or Close the Gate – Stomata Action Under the Control of Phytohormones in Drought Stress Conditions. *Frontiers in Plant Science* 4
- Davidson DJ, Chevalier PM (1992) Storage and Remobilization of Water-Soluble Carbohydrates in Stems of Spring Wheat. *Crop Science* 32:186-190
- Day WA, R.K. (Editors), (1985) *Wheat growth and modeling*. Plenum Press., New York
- De Coninck B, Le Roy K, Francis I, Clerens S, Vergauwen R, Halliday AM, Smith SM, Van Laere A, Van Den Ende WIM (2005) Arabidopsis AtcwINV3 and 6 are not invertases but are fructan exohydrolases (FEHs) with different substrate specificities. *Plant, Cell & Environment* 28:432-443
- De Gara L, De Pinto MC, Moliterni VM, D'egidio MG (2003) Redox regulation and storage processes during maturation in kernels of *Triticum durum*. *Journal of Experimental Botany* 54:249-258
- De Oliveira ED, Bramley H, Siddique KH, Henty S, Berger J, Palta JA (2013) Can elevated CO₂ combined with high temperature ameliorate the effect of terminal drought in wheat? *Functional Plant Biology* 40:160-171
- Doblin MS, Kurek I, Jacob-Wilk D, Delmer DP (2002) Cellulose Biosynthesis in Plants: from Genes to Rosettes. *Plant and Cell Physiology* 43:1407-1420
- Dolferus R, Ji X, Richards RA (2011) Abiotic stress and control of grain number in cereals. *Plant Science* 181:331-341
- Donaghy DJ, Turner LR, Adamczewski KA (2008) Effect of Defoliation Management on Water-Soluble Carbohydrate Energy Reserves, Dry Matter Yields, and Herbage Quality of Tall Fescue. *Agronomy Journal* 100:122-127
- Dorion S, Lalonde S, Saini HS (1996) Induction of male sterility in wheat by meiotic-stage water deficit is preceded by a decline in invertase activity and changes in carbohydrate metabolism in anthers. *Plant Physiology* 111:137-145
- Doyle A, Fischer R (1979) Dry matter accumulation and water use relationships in wheat crops. *Crop and Pasture Science* 30:815-829
- Dreccer MF, van Herwaarden AF, Chapman SC (2009) Grain number and grain weight in wheat lines contrasting for stem water soluble carbohydrate concentration. *Field Crops Research* 112:43-54

- Ende W, Laere A (1995) Purification and properties of a neutral invertase from the roots of *Cichorium intybus*. *Physiologia plantarum* 93:241-248
- Fales FW (1951) THE ASSIMILATION AND DEGRADATION OF CARBOHYDRATES BY YEAST CELLS. *Journal of Biological Chemistry* 193:113-124
- FAO (2009) How to feed the world in 2050. Available at <http://www.fao.org>: [22 May 2012]
- FAO WFP IFAD (2012) Economic growth is necessary but not sufficient to accelerate reduction of hunger and malnutrition. *The State of Food Insecurity in the World 2012*:Rome, FAO
- Faostat (2009) Statistical databases. Food and Agriculture Organization of the United Nations
- FAOSTAT (2011) The agricultural production domain.
- Faostat (2018) Statistical Database. Food and Agriculture Organization of the United Nations Available from <http://www.fao.org/faostat/en/#data/QC>
- Farooq M, Wahid A, Kobayashi N, Fujita D, Basra SMA (2009) Plant Drought Stress: Effects, Mechanisms and Management. In: Lichtfouse E, Navarrete M, Debaeke P, Véronique S, Alberola C (eds) *Sustainable Agriculture* 29:185-212
- Finkelstein RR, Gibson SI (2002) ABA and sugar interactions regulating development: cross-talk or voices in a crowd? *Current Opinion in Plant Biology* 5:26-32
- Finnie C, Andersen B, Shahpiri A, Svensson B (2011) Proteomes of the barley aleurone layer: A model system for plant signalling and protein secretion. *Proteomics* 11:1595-1605
- Fischer R, Stockman Y (1980) Kernel number per spike in wheat (*Triticum aestivum* L.): responses to preanthesis shading. *Functional Plant Biology* 7:169-180
- Fischer RA, Edmeades GO (2010) Breeding and Cereal Yield Progress *Crop Science* 50:S-85-S-98
- Fisher DB, Gifford RM (1986) Accumulation and conversion of sugars by developing wheat grains: VI. Gradients along the transport pathway from the peduncle to the endosperm cavity during grain filling. *Plant Physiology* 82:1024-1030
- Fitzgerald TL, Kazan K, Li Z, Morell MK, Manners JM (2010) A high-throughput method for the detection of homoeologous gene deletions in hexaploid wheat. *BMC Plant Biology* 10:1-15
- Fitzgerald TL, Kazan K, Manners JM (2012) The application of reverse genetics to polyploid plant species. *Critical Reviews in Plant Sciences* 31:181-200
- Fleury D, Jefferies S, Kuchel H, Langridge P (2010) Genetic and genomic tools to improve drought tolerance in wheat. *Journal of Experimental Botany* 61:3211-3222
- Gallagher JA, Cairns AJ, Thomas D, Charlton A, Williams P, Turner LB (2015) Fructan synthesis, accumulation, and polymer traits. I. *Festulolium* chromosome substitution lines. *Frontiers in Plant Science* 6
- Ganal MW, Durstewitz G, Polley A, Bérard A, Buckler ES, Charcosset A, Clarke JD, Graner E-M, Hansen M, Joets J (2011) A large maize (*Zea mays* L.) SNP genotyping array: development and germplasm genotyping, and genetic mapping to compare with the B73 reference genome. *PloS One* 6:e28334
- Gazzarrini S, McCourt P (2001) Genetic interactions between ABA, ethylene and sugar signaling pathways. *Current Opinion in Plant Biology* 4:387-391
- Gebbing T, Schnyder H (1999) Pre-Anthesis Reserve Utilization for Protein and Carbohydrate Synthesis in Grains of Wheat. *Plant Physiology* 121:871-878
- Goetz M, Godt DE, Guivarc'h A, Kahmann U, Chriqui D, Roitsch T (2001) Induction of male sterility in plants by metabolic engineering of the carbohydrate supply. *Proceedings of the National Academy of Sciences* 98:6522-6527

- Goggin DE, Setter TL (2004) Fructosyltransferase activity and fructan accumulation during development in wheat exposed to terminal drought. *Functional Plant Biology* 31:11-21
- Gordon K, McKeon D, Whiteley C, Southan M, Price Ca, MacAulay G (2016) State of the Australian Grains Industry. In: Nicholls C (ed) *Gain Growers*
- Grassl J, Taylor NL, Millar AH (2011) Matrix-assisted laser desorption/ionisation mass spectrometry imaging and its development for plant protein imaging. *Plant methods* 7:21-21
- Gul A, Allan RE (1976) Stand Establishment of Wheat Lines under Different Levels of Water Potential. *Crop Science* 16:611-615
- Gupta NK, Gupta S, Kumar A (2001) Effect of Water Stress on Physiological Attributes and their Relationship with Growth and Yield of Wheat Cultivars at Different Stages. *Journal of Agronomy and Crop Science* 186:55-62
- Haouazine-Takvorian N, Tymowska-Lalanne Z, Takvorian A, Tregear J, Lejeune B, Lecharny A, Kreis M (1997) Characterization of two members of the *Arabidopsis thaliana* gene family, At β fruct3 and At β fruct4, coding for vacuolar invertases. *Gene* 197:239-251
- Haritatos E, Ayre BG, Turgeon R (2000) Identification of phloem involved in assimilate loading in leaves by the activity of the galactinol synthase promoter. *Plant Physiology* 123:929-938
- Harris D, Tripathi R.S., A. J (2002) On-farm seed priming to improve crop establishment and yield in dry direct-seeded rice, . In: Pandey S. MM, Wade L., Tuong T.P., Lopes K., Hardy B (ed). *Direct seeding: Research Strategies and Opportunities*, International Research Institute, Manila, Philippines, pp 231–240.
- Heinlein M, Starlinger P (1989) Tissue- and cell-specific expression of the two sucrose synthase isoenzymes in developing maize kernels. *Molecular and General Genetics* MGG 215:441-446
- Henchion M, Hayes M, Mullen A, Fenelon M, Tiwari B (2017) Future Protein Supply and Demand: Strategies and Factors Influencing a Sustainable Equilibrium. *Foods* 6:53
- Hendrix DL (1990) Carbohydrates and carbohydrate enzymes in developing cotton ovules. *Physiologia Plantarum* 78:85-92
- Hendry GAF (1993) Evolutionary origins and natural functions of fructans – a climatological, biogeographic and mechanistic appraisal. *New Phytologist* 123:3-14
- Heo YT, Quan X, Xu YN, Baek S, Choi H, Kim N-H, Kim J (2014) CRISPR/Cas9 nuclease-mediated gene knock-in in bovine-induced pluripotent cells. *Stem cells and development* 24:393-402
- Hincha DK, Hellwege EM, Heyer AG, Crowe JH (2000) Plant fructans stabilize phosphatidylcholine liposomes during freeze-drying. *European Journal of Biochemistry* 267:535-540
- Hubert B, Rosegrant M, van Boekel MAJS, Ortiz R (2010) *The Future of Food: Scenarios for 2050* All rights reserved. *Crop Science* 50:S-33-S-50
- Hufford MB, Xu X, Van Heerwaarden J, Pyhäjärvi T, Chia J-M, Cartwright RA, Elshire RJ, Glaubitz JC, Guill KE, Kaeppeler SM (2012) Comparative population genomics of maize domestication and improvement. *Nature Genetics* 44:808-811
- Imai T, Tanabe K, Kato T, Fukushima K (2005) Localization of ferruginol, a diterpene phenol, in *Cryptomeria japonica* heartwood by time-of-flight secondary ion mass spectrometry. *Planta* 221:549-556
- IOCI IOCI (2002) *Climate variability and change in southwest Western Australia.*
- Jamieson P, Martin R, Francis G (1995) Drought influences on grain yield of barley, wheat, and maize. *New Zealand Journal of Crop and Horticultural Science* 23:55-66

- Jeong B-R, Housley TL (1990) Fructan metabolism in wheat in alternating warm and cold temperatures. *Plant physiology* 93:902-906
- Ji X, Ende W, Laere A, Cheng S, Bennett J (2005) Structure, Evolution, and Expression of the Two Invertase Gene Families of Rice. *Journal of Molecular Evolution* 60:615-634
- Ji X, Shiran B, Wan J, Lewis DC, Jenkins CLD, Condon AG, Richards RA, Dolferus R (2010) Importance of pre-anthesis anther sink strength for maintenance of grain number during reproductive stage water stress in wheat. *Plant, Cell & Environment* 33:926-942
- Joudi M, Ahmadi A, Mohamadi V, Abbasi A, Vergauwen R, Mohammadi H, Van den Ende W (2012) Comparison of fructan dynamics in two wheat cultivars with different capacities of accumulation and remobilization under drought stress. *Physiologia Plantarum* 144:1-12
- Jungmann JH, Heeren RMA (2012) Emerging technologies in mass spectrometry imaging. *Journal of Proteomics* 75:5077-5092
- Kaspar S, Peukert M, Svatos A, Matros A, Mock H-P (2011) MALDI-imaging mass spectrometry – An emerging technique in plant biology. *PROTEOMICS* 11:1840-1850
- Kawakami A, Yoshida M (2005) Fructan: fructan 1-fructosyltransferase, a key enzyme for biosynthesis of graminan oligomers in hardened wheat. *Planta* 223:90-104
- Kawakami A, Yoshida M, Van den Ende W (2005) Molecular cloning and functional analysis of a novel 6⟩1-FEH from wheat (*Triticum aestivum* L.) preferentially degrading small graminans like bifurcose. *Gene* 358:93-101
- Kaya MD, Okçu G, Atak M, Çıkılı Y, Kolsarıcı Ö (2006) Seed treatments to overcome salt and drought stress during germination in sunflower (*Helianthus annuus* L.). *European Journal of Agronomy* 24:291-295
- Kelley LA, Mezulis S, Yates CM, Wass MN, Sternberg MJ (2015) The Phyre2 web portal for protein modeling, prediction and analysis. *Nature protocols* 10:845
- Keunen E, Peshev D, Vangronsveld J, Van Den Ende W, Cuypers A (2013) Plant sugars are crucial players in the oxidative challenge during abiotic stress: extending the traditional concept. *Plant, cell & environment* 36:1242-1255
- Khoshro H, Taleei A, Bihamta M, Shahbazi M, Abbasi A, Ramezani-pour S (2014) Expression analysis of the genes involved in accumulation and remobilization of assimilates in wheat stem under terminal drought stress. *Plant Growth Regul* 74:165-176
- Klann EM, Hall B, Bennett AB (1996) Antisense acid invertase (TIV1) gene alters soluble sugar composition and size in transgenic tomato fruit. *Plant Physiology* 112:1321-1330
- Knoll JE, Ramos ML, Zeng Y, Holbrook CC, Chow M, Chen S, Maleki S, Bhattacharya A, Ozias-Akins P (2011) TILLING for allergen reduction and improvement of quality traits in peanut (*Arachis hypogaea* L.). *BMC Plant Biology* 11:81
- Kobata T, Palta JA, Turner NC (1992) Rate of Development of Postanthesis Water Deficits and Grain Filling of Spring Wheat. *Crop Science* 32:1238-1242
- Koch K (2004) Sucrose metabolism: regulatory mechanisms and pivotal roles in sugar sensing and plant development. *Current Opinion in Plant Biology* 7:235-246
- Koch KE, Wu Y, Xu J (1996) Sugar and metabolic regulation of genes for sucrose metabolism: potential influence of maize sucrose synthase and soluble invertase responses on carbon partitioning and sugar sensing. *Journal of Experimental Botany* 47:1179-1185
- Kolli N, Lu M, Maiti P, Rossignol J, Dunbar GL (2017) CRISPR-Cas9 mediated gene-silencing of the mutant Huntingtin gene in an in vitro model of Huntington's disease. *International Journal of Molecular Sciences* 18:754

- Koonjul PK, Minhas JS, Nunes C, Sheoran IS, Saini HS (2005) Selective transcriptional down-regulation of anther invertases precedes the failure of pollen development in water-stressed wheat. *Journal of Experimental Botany* 56:179-190
- Kueger S, Steinhäuser D, Willmitzer L, Giavalisco P (2012) High-resolution plant metabolomics: from mass spectral features to metabolites and from whole-cell analysis to subcellular metabolite distributions. *The Plant Journal* 70:39-50
- Kühn C (2003) A Comparison of the Sucrose Transporter Systems of Different Plant Species. *Plant Biology* 5:215-232
- Kühn C, Grof CPL (2010) Sucrose transporters of higher plants. *Current Opinion in Plant Biology* 13:287-297
- Lai K, Duran C, Berkman PJ, Lorenc MT, Stiller J, Manoli S, Hayden MJ, Forrest KL, Fleury D, Baumann U (2012) Single nucleotide polymorphism discovery from wheat next-generation sequence data. *Plant Biotechnology Journal* 10:743-749
- Lalonde S, Beebe DU, Saini H (1997) Early signs of disruption of wheat anther development associated with the induction of male sterility by meiotic-stage water deficit. *Sexual Plant Reproduction* 10:40-48
- Le Roy K, Lammens W, Verhaest M, De Coninck B, Rabijns A, Van Laere A, Van den Ende W (2007) Unraveling the Difference between Invertases and Fructan Exohydrolases: A Single Amino Acid (Asp-239) Substitution Transforms Arabidopsis Cell Wall Invertase1 into a Fructan 1-Exohydrolase. *Plant Physiology* 145:616-625
- Lee YJ, Perdian DC, Song Z, Yeung ES, Nikolau BJ (2012) Use of mass spectrometry for imaging metabolites in plants. *The Plant Journal* 70:81-95
- Lemoine R, La Camera S, Atanassova R, Dédaldéchamp F, Allario T, Pourtau N, Bonnemain J-L, Laloi M, Coutos-Thévenot P, Maurousset L (2013) Source-to-sink transport of sugar and regulation by environmental factors. *Frontiers in Plant Science* 4
- Lev-Yadun S, Gopher A, Abbo S (2000) The Cradle of Agriculture. *Science* 288:1602-1603
- Lewis D (1993) Nomenclature and diagrammatic representation of oligomeric fructans—a paper for discussion. *New Phytologist* 124:583-594
- Lim JD, Cho J-I, Park Y-I, Hahn T-R, Choi S-B, Jeon J-S (2006) Sucrose transport from source to sink seeds in rice. *Physiologia Plantarum* 126:572-584
- Livingston D, III, Hinch D, Heyer A (2009) Fructan and its relationship to abiotic stress tolerance in plants. *Cellular and Molecular Life Sciences* 66:2007-2023
- Livingston DP, Chatterton NJ, Harrison PA (1993) Structure and quantity of fructan oligomers in oat (*Avena* spp.). *New Phytologist* 123:725-734
- Lloyd J, Meinke D (2012) A comprehensive dataset of genes with a loss-of-function mutant phenotype in Arabidopsis. *Plant physiology* 158:1115-1129
- Lohaus G, Winter H, Riens B, Heldt H (1995) Further Studies of the Phloem Loading Process in Leaves of Barley and Spinach. The Comparison of Metabolite Concentrations in the Apoplastic Compartment with those in the Cytosolic Compartment and in the Sieve Tubes1. *Botanica Acta* 108:270-275
- Lukowitz W, Gillmor CS, Scheible W-R (2000) Positional Cloning in Arabidopsis. Why It Feels Good to Have a Genome Initiative Working for You. *Plant Physiology* 123:795-806
- Ma D, Yan J, He Z, Wu L, Xia X (2012) Characterization of a cell wall invertase gene TaCwi-A1 on common wheat chromosome 2A and development of functional markers. *Mol Breeding* 29:43-52
- Maas C., S Schaal, Werr W (1990) A feedback control element near the transcription start site of the maize Shrunken gene determines promoter activity. *The EMBO Journal* 9:3447-3452

- Maqsood M, Shehzad MA, Ahmad S, Mushtaq S (2012) Performance of Wheat (*Triticum aestivum* L.) Genotypes Associated with Agronomical Traits under Water Stress Conditions. *Asian Journal of Pharmaceutical & Biological Research* 2:45-50
- Matros A, Mock H-P (2013) Mass spectrometry based imaging techniques for spatially resolved analysis of molecules. *Frontiers in Plant Science* 4
- McDonnell LA, Heeren RMA (2007) Imaging mass spectrometry. *Mass Spectrometry Reviews* 26:606-643
- Moore B, Zhou L, Rolland F, Hall Q, Cheng W-H, Liu Y-X, Hwang I, Jones T, Sheen J (2003) Role of the Arabidopsis Glucose Sensor HXK1 in Nutrient, Light, and Hormonal Signaling. *Science* 300:332-336
- Morita R, Kusaba M, Iida S, Yamaguchi H, Nishio T, Nishimura M (2009) Molecular characterization of mutations induced by gamma irradiation in rice. *Genes & Genetic Systems* 84:361-370
- Muhammad Waseem AA, M.Tahir, M. A. Nadeem, M. Ayub, Asif Tanveer, R. Ahmad and M.Hussain (2011) MECHANISM OF DROUGHT TOLERANCE IN PLANT AND ITS MANAGEMENT THROUGH DIFFERENT METHODS. *Continental Journal of Agricultural Science*, 5:10-25
- Nagaraj VJ, Altenbach D, Galati V, Lüscher M, Meyer AD, Boller T, Wiemken A (2004) Distinct regulation of sucrose: sucrose-1-fructosyltransferase (1-SST) and sucrose: fructan-6-fructosyltransferase (6-SFT), the key enzymes of fructan synthesis in barley leaves: 1-SST as the pacemaker. *New Phytologist* 161:735-748
- Nemes P, Barton AA, Vertes A (2009) Three-Dimensional Imaging of Metabolites in Tissues under Ambient Conditions by Laser Ablation Electrospray Ionization Mass Spectrometry. *Analytical Chemistry* 81:6668-6675
- Nemes P, Vertes A (2007) Laser Ablation Electrospray Ionization for Atmospheric Pressure, in Vivo, and Imaging Mass Spectrometry. *Analytical Chemistry* 79:8098-8106
- Nemeskéri E, Molnár K, Vígh R, Nagy J, Dobos A (2015) Relationships between stomatal behaviour, spectral traits and water use and productivity of green peas (*Pisum sativum* L.) in dry seasons. *Acta Physiologiae Plantarum* 37:34
- Nicolas ME, Gleadow RM, Dalling MJ (1985) Effect of Post-anthesis Drought on Cell Division and Starch Accumulation in Developing Wheat Grains. *Annals of Botany* 55:433-444
- Nonami H (1998) Plant water relations and control of cell elongation at low water potentials. *Journal of Plant Research* 111:373-382
- Nordström KJ, Albani MC, James GV, Gutjahr C, Hartwig B, Turck F, Paszkowski U, Coupland G, Schneeberger K (2013) Mutation identification by direct comparison of whole-genome sequencing data from mutant and wild-type individuals using k-mers. *Nature Biotechnology* 31:325-330
- O'Toole JC, Moya TB (1981) Water deficits and yield in upland rice. *Field Crops Research* 4:247-259
- Ohshima A, Ito H, Sato T, Nishimura S, Imai T, Hirai M (1995) Suppression of acid invertase activity by antisense RNA modifies the sugar composition of tomato fruit. *Plant and cell physiology* 36:369-376
- Olsen O-A (2001) Endosperm development: cellularization and cell fate specification. *Annual Review of Plant Biology* 52:233-267
- Parish RW, Phan HA, Iacuone S, Li SF (2012) Tapetal development and abiotic stress: a centre of vulnerability. *Functional Plant Biology* 39:553-559
- Passioura J (1983) Roots and drought resistance. *Agricultural Water Management* 7:265-280

- Peshev D, Vergauwen R, Moglia A, Hideg É, Van den Ende W (2013) Towards understanding vacuolar antioxidant mechanisms: a role for fructans? *Journal of Experimental Botany* 64:1025-1038
- Peukert M, Thiel J, Peshev D, Weschke W, Van den Ende W, Mock H-P, Matros A (2014) Spatio-Temporal Dynamics of Fructan Metabolism in Developing Barley Grains. *The Plant Cell Online*
- Pheloung P, Siddique K (1991) Contribution of Stem Dry Matter to Grain Yield in Wheat Cultivars. *Functional Plant Biology* 18:53-64
- Pittock AB (2003) Climate change: an Australian guide to the science and potential impacts. Australian Government (Australian Greenhouse Office), Canberra, Australia
- Plaut Z, Butow BJ, Blumenthal CS, Wrigley CW (2004) Transport of dry matter into developing wheat kernels and its contribution to grain yield under post-anthesis water deficit and elevated temperature. *Field Crops Research* 86:185-198
- Pollock CJ, Cairns AJ, Gallagher J, Harrison J (1999) The integration of sucrose and fructan metabolism in temperate grasses and cereals. *Regulation of Primary Metabolic Pathways in Plants*. Springer, pp 195-226
- Powell N, Ji X, Ravash R, Edlington J, Dolferus R (2012) Yield stability for cereals in a changing climate. *Functional Plant Biology* 39:539-552
- Pradhan GP, Prasad PVV, Fritz AK, Kirkham MB., Gill BS. (2012) Effects of drought and high temperature stress on synthetic hexaploid wheat. *Functional Plant Biology* 39: 190-198
- Prasher DC (1995) Using GFP to see the light. *Trends in Genetics* 11:320-323
- Prideaux B, Stoeckli M (2012) Mass spectrometry imaging for drug distribution studies. *Journal of Proteomics* 75:4999-5013
- Rampino P, Pataleo S, Gerardi C, Mita G, Perrotta C (2006) Drought stress response in wheat: physiological and molecular analysis of resistant and sensitive genotypes. *Plant, Cell & Environment* 29:2143-2152
- Rauf M, Munir M, ul Hassan M, Ahmad M, Afzal M (2007) Performance of wheat genotypes under osmotic stress at germination and early seedling growth stage. *African Journal of Biotechnology* 6
- Ray DK, Mueller ND, West PC, Foley JA (2013) Yield Trends Are Insufficient to Double Global Crop Production by 2050. *PLoS ONE* 8:e66428
- Rickert K, Sedgley R, Stern W (1987) Environmental response of spring wheat in the southwestern Australian cereal belt. *Crop and Pasture Science* 38:655-670
- Roessner-Tunali U, Hegemann B, Lytovchenko A, Carrari F, Bruedigam C, Granot D, Fernie AR (2003) Metabolic profiling of transgenic tomato plants overexpressing hexokinase reveals that the influence of hexose phosphorylation diminishes during fruit development. *Plant Physiology* 133:84-99
- Roitsch T (1999) Source-sink regulation by sugar and stress. *Current Opinion in Plant Biology* 2:198-206
- Roitsch T, González M-C (2004) Function and regulation of plant invertases: sweet sensations. *Trends in Plant Science* 9:606-613
- Römpp A, Spengler B (2013) Mass spectrometry imaging with high resolution in mass and space. *Histochemistry and Cell Biology* 139:759-783
- Ropartz D, Bodet PE, Przybylski C, Gonnet F, Daniel R, Fer M, Helbert W, Bertrand D, Rogniaux H (2011) Performance evaluation on a wide set of matrix-assisted laser desorption ionization matrices for the detection of oligosaccharides in a high-throughput mass spectrometric screening of carbohydrate depolymerizing enzymes. *Rapid Communications in Mass Spectrometry* 25:2059-2070

- Rosegrant MW, Cline SA (2003) Global Food Security: Challenges and Policies. *Science* 302:1917-1919
- Roy S, Gallagher J (1985) Production and survival of wheat tillers in relation to plant growth and development. *Wheat Growth and Modelling*. Springer, pp 59-67
- Ruan Y-L (2014) Sucrose metabolism: gateway to diverse carbon use and sugar signaling. *Annual Review of Plant Biology* 65:33-67
- Ruan Y-L, Jin Y, Huang J (2009) Capping invertase activity by its inhibitor: roles and implications in sugar signaling, carbon allocation, senescence and evolution. *Plant Signaling & Behavior* 4:983-985
- Ruan Y-L, Jin Y, Yang Y-J, Li G-J, Boyer JS (2010) Sugar Input, Metabolism, and Signaling Mediated by Invertase: Roles in Development, Yield Potential, and Response to Drought and Heat. *Molecular Plant* 3:942-955
- Ruan Y-L, Llewellyn DJ, Furbank RT (2003) Suppression of sucrose synthase gene expression represses cotton fiber cell initiation, elongation, and seed development. *The Plant Cell Online* 15:952-964
- Ruan YL, Chourey P (2006) Carbon partitioning in developing seed, New York: The Haworth Press
- Ruuska SA, Rebetzke GJ, van Herwaarden AF, Richards RA, Fettell NA, Tabe L, Jenkins CLD (2006) Genotypic variation in water-soluble carbohydrate accumulation in wheat. *Functional Plant Biology* 33:799-809
- Šafař J, Šimková H, Kubaláková M, Číhalíková J, Suchánková P, Bartoš J, Doležel (2010) Development of chromosome-specific BAC resources for genomics of bread wheat. *Cytogenetic and Genome Research* 129:211-223
- Saini H, Aspinall D (1981) Effect of water deficit on sporogenesis in wheat (*Triticum aestivum* L.). *Annals of Botany* 48:623-633
- Saini H, Sedgley M, Aspinall D (1984) Development Anatomy in Wheat of Male Sterility Induced by Heat Stress, Water Deficit or Abscisic Acid. *Functional Plant Biology* 11:243-253
- Saini HS (1997) Effects of water stress on male gametophyte development in plants. *Sexual Plant Reproduction* 10:67-73
- Saini HS, Westgate ME (1999) Reproductive Development in Grain Crops during Drought. In: Donald LS (ed) *Advances in Agronomy*. Academic Press, pp 59-96
- Salnikov VV, Grimson MJ, Seagull RW, Haigler CH (2003) Localization of sucrose synthase and callose in freeze-substituted secondary-wall-stage cotton fibers. *Protoplasma* 221:175-184
- Salter PJ, Goode JE (1967) *Crop Responses to Water at Different Stages of Growth*. Commonwealth Agricultural Bureaux, Bucks, England
- Sarin S, Prabhu S, O'Meara MM, Pe'er I, Hobert O (2008) *Caenorhabditis elegans* mutant allele identification by whole-genome sequencing. *Nature Methods* 5:865
- Sarsby J, Towers MW, Stain C, Cramer R, Koroleva OA (2012) Mass spectrometry imaging of glucosinolates in *Arabidopsis* flowers and siliques. *Phytochemistry* 77:110-118
- Schnyder H (1993) The role of carbohydrate storage and redistribution in the source-sink relations of wheat and barley during grain filling — a review. *New Phytologist* 123:233-245
- Schnyder H, Gillenberg C, Hinz J (1993) Fructan contents and dry matter deposition in different tissues of the wheat grain during development. *Plant, Cell & Environment* 16:179-187
- Schwamborn K (2012) Imaging mass spectrometry in biomarker discovery and validation. *Journal of Proteomics* 75:4990-4998

- Setou M, Shrivastava K, Sroyraya M, Yang H, Sugiura Y, Moribe J, Kondo A, Tsutsumi K, Kimura Y, Kurabe N, Hayasaka T, Goto-Inoue N, Zaima N, Ikegami K, Sobhon P, Konishi Y (2010) Developments and applications of mass microscopy. *Medical Molecular Morphology* 43:1-5
- Shariatgorji M, Svenningsson P, Andren PE (2014) Mass spectrometry imaging, an emerging technology in neuropsychopharmacology. *Neuropsychopharmacology* 39:34
- Sheen J, Zhou L, Jang J-C (1999) Sugars as signaling molecules. *Current Opinion in Plant Biology* 2:410-418
- Sheoran I, Saini H (1996) Drought-induced male sterility in rice: Changes in carbohydrate levels and enzyme activities associated with the inhibition of starch accumulation in pollen. *Sexual Plant Reproduction* 9:161-169
- Sherson SM, Alford HL, Forbes SM, Wallace G, Smith SM (2003) Roles of cell-wall invertases and monosaccharide transporters in the growth and development of *Arabidopsis*. *Journal of Experimental Botany* 54:525-531
- Shewry PR, Mitchell RA, Tosi P, Wan Y, Underwood C, Lovegrove A, Freeman J, Toole GA, Mills EC, Ward JL (2012) An integrated study of grain development of wheat (cv. Hereward). *Journal of Cereal Science* 56:21-30
- Shiomi N (1989) Properties of fructosyltransferases involved in the synthesis of fructan in liliaceous plants. *Journal of Plant Physiology* 134:151-155
- Siddique MRB., Hamid A, Islam M.S (2001) Drought stress effects on water relations of wheat. *Botanical Bulletin of Academia Sinica* 41:35 -39
- Siegel TP, Hamm G, Bunch J, Cappell J, Fletcher JS, Schwamborn K (2018) Mass Spectrometry Imaging and Integration with Other Imaging Modalities for Greater Molecular Understanding of Biological Tissues. *Molecular Imaging and Biology*:1-14
- Sim S-C, Durstewitz G, Plieske J, Wieseke R, Ganai MW, Van Deynze A, Hamilton JP, Buell CR, Causse M, Wijeratne S (2012) Development of a large SNP genotyping array and generation of high-density genetic maps in tomato. *PLoS ONE* 7:e40563
- Simmons S, Oelke E, Anderson P (1985) Growth and development guide for spring wheat
- Smith IN, McIntosh P, Ansell TJ, Reason CJC, McInnes K (2000) Southwest Western Australian winter rainfall and its association with Indian Ocean climate variability. *International Journal of Climatology* 20:1913-1930
- Spengler B (2014) Mass spectrometry imaging of biomolecular information. *Analytical chemistry* 87:64-82
- Spiegel M, Noordam MY, Fels-Klerx HJ (2013) Safety of Novel Protein Sources (Insects, Microalgae, Seaweed, Duckweed, and Rapeseed) and Legislative Aspects for Their Application in Food and Feed Production. *Comprehensive Reviews in Food Science and Food Safety* 12:662-678
- Sreenivasulu N, Schnurbusch T (2012) A genetic playground for enhancing grain number in cereals. *Trends in plant science* 17:91-101
- Stepanova A, Alonso J (2009) Ethylene signaling and response: where different regulatory modules meet. *Current Opinion in Plant Biology* 12:548 - 555
- Sturm A (1996) Molecular characterization and functional analysis of sucrose-cleaving enzymes in carrot (*Daucus carota* L.). *Journal of Experimental Botany* 47:1187-1192
- Sturm A (1999) Invertases. Primary Structures, Functions, and Roles in Plant Development and Sucrose Partitioning. *Plant Physiology* 121:1-8
- Sturm A, Tang G-Q (1999) The sucrose-cleaving enzymes of plants are crucial for development, growth and carbon partitioning. *Trends in Plant Science* 4:401-407
- Subbaiah CC, Sachs MM (2001) Altered Patterns of Sucrose Synthase Phosphorylation and Localization Precede Callose Induction and Root Tip Death in Anoxic Maize Seedlings. *Plant Physiology* 125:585-594

- Takáts Z, Wiseman JM, Gologan B, Cooks RG (2004) Mass Spectrometry Sampling Under Ambient Conditions with Desorption Electrospray Ionization. *Science* 306:471-473
- Tilman D, Cassman KG, Matson PA, Naylor R, Polasky S (2002) Agricultural sustainability and intensive production practices. *Nature* 418:671-677
- Torres-Ruiz JM, Díaz-Espejo A, Morales-Sillero A, Martín-Palomo M, Mayr S, Beikircher B, Fernández J (2013) Shoot hydraulic characteristics, plant water status and stomatal response in olive trees under different soil water conditions. *Plant and Soil* 373:77-87
- Trebbi D, Maccaferri M, de Heer P, Sørensen A, Giuliani S, Salvi S, Sanguineti MC, Massi A, van der Vossen EAG, Tuberosa R (2011) High-throughput SNP discovery and genotyping in durum wheat (*Triticum durum* Desf.). *Theoretical and Applied Genetics* 123:555-569
- Truernit E (2001) Plant physiology: the importance of sucrose transporters. *Current Biology* 11:R169-R171
- Tsien RY (1998) The green fluorescent protein. *Annual Review of Biochemistry* 67:509-544
- Tuberosa R, Salvi S (2006) Genomics-based approaches to improve drought tolerance of crops. *Trends in Plant Science* 11:405-412
- Tymowska-Lalanne Z, Kreis M (1998) The Plant Invertases: Physiology, Biochemistry and Molecular Biology. In: Callow JA (ed) *Advances in Botanical Research*. Academic Press, pp 71-117
- Ugalde T, Jenner C (1990) Substrate gradients and regional patterns of dry matter deposition within developing wheat endosperm. I. Carbohydrates. *Functional Plant Biology* 17:377-394
- Valluru R, Van den Ende W (2008) Plant fructans in stress environments: emerging concepts and future prospects. *Journal of Experimental Botany* 59:2905-2916
- Van den Ende W (2013) Multifunctional fructans and raffinose family oligosaccharides. *Frontiers in Plant Science* 4:247
- Van den Ende W, Clerens S, Vergauwen R, Van Riet L, Van Laere A, Yoshida M, Kawakami A (2003) Fructan 1-Exohydrolases. β -(2,1)-Trimmers during Graminan Biosynthesis in Stems of Wheat? Purification, Characterization, Mass Mapping, and Cloning of Two Fructan 1-Exohydrolase Isoforms. *Plant Physiology* 131:621-631
- Van den Ende W, De Coninck B, Van Laere A (2004) Plant fructan exohydrolases: a role in signaling and defense? *Trends in Plant Science* 9:523-528
- Van den Ende W, Michiels A, De Roover J, Van Laere A (2002) Fructan biosynthetic and breakdown enzymes in dicots evolved from different invertases. Expression of fructan genes throughout chicory development. *The Scientific World Journal* 2:1281-1295
- Van den Ende W, Michiels A, Van Wontergem D, Clerens SP, De Roover J, Van Laere AJ (2001) Defoliation Induces Fructan 1-Exohydrolase II in Witloof Chicory Roots. Cloning and Purification of Two Isoforms, Fructan 1-Exohydrolase IIa and Fructan 1-Exohydrolase IIb. Mass Fingerprint of the Fructan 1-Exohydrolase II Enzymes. *Plant Physiology* 126:1186-1195
- Van den Ende W, Valluru R (2008) Sucrose, sucrosyl oligosaccharides, and oxidative stress: scavenging and salvaging? *Journal of Experimental Botany* 60:9-18
- Van Laere A, Van Den Ende W (2002) Inulin metabolism in dicots: chicory as a model system. *Plant, Cell & Environment* 25:803-813
- Van Riet L, Altenbach D, Vergauwen R, Clerens S, Kawakami A, Yoshida M, Van den Ende W, Wiemken A, Van Laere A (2008) Purification, cloning and functional differences of a third fructan 1-exohydrolase (1-FEHw3) from wheat (*Triticum aestivum*). *Physiologia Plantarum* 133:242-253

- Van Riet L, Nagaraj V, Van den Ende W, Clerens S, Wiemken A, Van Laere A (2006) Purification, cloning and functional characterization of a fructan 6-exohydrolase from wheat (*Triticum aestivum* L.). *Journal of Experimental Botany* 57:213-223
- Veličković D, Ropartz D, Guillon F, Saulnier L, Rogniaux H (2014) New insights into the structural and spatial variability of cell-wall polysaccharides during wheat grain development, as revealed through MALDI mass spectrometry imaging. *Journal of Experimental Botany* 65:2079-2091
- Veličković D, Saulnier L, Lhomme M, Damond A, Guillon F, Rogniaux H (2016) Mass Spectrometric Imaging of Wheat (*Triticum* spp.) and Barley (*Hordeum vulgare* L.) Cultivars: Distribution of Major Cell Wall Polysaccharides According to Their Main Structural Features. *Journal of Agricultural and Food Chemistry* 64:6249-6256
- Vereyken IJ, Albert van Kuik J, Evers TH, Rijken PJ, de Kruijff B (2003) Structural Requirements of the Fructan-Lipid Interaction. *Biophysical Journal* 84:3147-3154
- Vergauwen R, Van den Ende W, Van Laere A (2000) The role of fructan in flowering of *Campanula rapunculoides*. *Journal of Experimental Botany* 51:1261-1266
- Verslues PE, Agarwal M, Katiyar-Agarwal S, Zhu J, Zhu J-K (2006) Methods and concepts in quantifying resistance to drought, salt and freezing, abiotic stresses that affect plant water status. *The Plant Journal* 45:523-539
- Verspreet J, Cimini S, Vergauwen R, Dornez E, Locato V, Le Roy K, De Gara L, Van den Ende W, Delcour JA, Courtin CM (2013a) Fructan Metabolism in Developing Wheat (*Triticum aestivum* L.) Kernels. *Plant and Cell Physiology* 54:2047-2057
- Verspreet J, Hemdane S, Dornez E, Cuyvers S, Pollet A, Delcour JA, Courtin CM (2013b) Analysis of Storage and Structural Carbohydrates in Developing Wheat (*Triticum aestivum* L.) Grains Using Quantitative Analysis and Microscopy. *Journal of Agricultural and Food Chemistry* 61:9251-9259
- Wakai J, Takagi A, Nakayama M, Miya T, Miyahara T, Iwanaga T, Takenaka S, Ikeda Y, Amano M (2004) A novel method of identifying genetic mutations using an electrochemical DNA array. *Nucleic Acids Research* 32:e141-e141
- Wang TL, Uauy C, Robson F, Till B (2012) TILLING in extremis. *Plant biotechnology journal* 10:761-772
- Wanjugi H, Coleman-Derr D, Huo N, Kianian SF, Luo M-C, Wu J, Anderson O, Gu YQ (2009) Rapid development of PCR-based genome-specific repetitive DNA junction markers in wheat. *Genome* 52:576-587
- Wardlaw I, Moncur L (1995) The response of wheat to high temperature following anthesis. I. The rate and duration of kernel filling. *Functional Plant Biology* 22:391-397
- Wardlaw IF, Willenbrink J (1994) Carbohydrate storage and mobilisation by the culm of wheat between heading and grain maturity: the relation to sucrose synthase and sucrose-phosphate synthase. *Functional Plant Biology* 21:255-271
- Wardlaw IF, Willenbrink J (2000) Mobilization of fructan reserves and changes in enzyme activities in wheat stems correlate with water stress during kernel filling. *New Phytologist* 148:413-422
- Watrous JD, Alexandrov T, Dorrestein PC (2011) The evolving field of imaging mass spectrometry and its impact on future biological research. *Journal of Mass Spectrometry* 46:209-222
- Weber H, Borisjuk L, Wobus U (1997) Sugar import and metabolism during seed development. *Trends in Plant Science* 2:169-174
- Webster H, KG, Dell Bernard, Fosu-Nyarko John, Mukai Y., Moolhuijzen Paula, Bellgard Matthew, Jia Jizeng, Kong Xiuying, Feuillet Catherine, Choulet Frédéric (2012) Genome-level identification of cell wall invertase genes in wheat for the study of drought tolerance. *Functional Plant Biology* 39:569-579

- Weschke W, Panitz R, Gubatz S, Wang Q, Radchuk R, Weber H, Wobus U (2003) The role of invertases and hexose transporters in controlling sugar ratios in maternal and filial tissues of barley caryopses during early development. *The Plant Journal* 33:395-411
- Westgate M, Passioura J, Munns R (1996) Water status and ABA content of floral organs in drought-stressed wheat. *Functional Plant Biology* 23:763-772
- Wiedmann RT, Smith TP, Nonneman DJ (2008) SNP discovery in swine by reduced representation and high throughput pyrosequencing. *Bmc Genetics* 9:81
- Wiemken A, Frehner M, Keller F, Wagner W (1986) Fructan metabolism, enzymology and compartmentation. *Current topics in plant biochemistry and physiology: Proceedings of the Plant Biochemistry and Physiology Symposium held at the University of Missouri, Columbia*
- Wind J, Smeekens S, Hanson J (2010) Sucrose: metabolite and signaling molecule. *Phytochemistry* 71:1610-1614
- Winter H, Huber SC (2000) Regulation of Sucrose Metabolism in Higher Plants: Localization and regulation of Activity of Key Enzymes. *Critical Reviews in Plant Sciences* 19:31-67
- Wittich P, Vreugdenhil D (1998) Localization of sucrose synthase activity in developing maize kernels by in situ enzyme histochemistry. *Journal of Experimental Botany* 49:1163-1171
- Xue G-P, McIntyre CL, Jenkins CL, Glassop D, van Herwaarden AF, Shorter R (2008) Molecular dissection of variation in carbohydrate metabolism related to water-soluble carbohydrate accumulation in stems of wheat. *Plant physiology* 146:441-454
- Yáñez A, Tapia G, Guerra F, del Pozo A (2017) Stem carbohydrate dynamics and expression of genes involved in fructan accumulation and remobilization during grain growth in wheat (*Triticum aestivum* L.) genotypes with contrasting tolerance to water stress. *PLoS ONE* 12:e0177667
- Yang J, Zhang J (2006) Grain filling of cereals under soil drying. *New Phytologist* 169:223-236
- Yang J, Zhang J, Huang Z, Zhu Q, Wang L (2000) Remobilization of carbon reserves is improved by controlled soil-drying during grain filling of wheat. *Crop Science* 40:1645-1655
- Yang J, Zhang J, Liu L, Wang Z, Zhu Q (2002) Carbon Remobilization and Grain Filling in Japonica/Indica Hybrid Rice Subjected to Postanthesis Water Deficits. *Agron J* 94:102-109
- Yang J, Zhang J, Wang Z, Zhu Q, Liu L (2001) Water Deficit-Induced Senescence and Its Relationship to the Remobilization of Pre-Stored Carbon in Wheat during Grain Filling. *Agron J* 93:196-206
- Yang J, Zhang J, Wang Z, Zhu Q, Liu L (2004) Activities of fructan- and sucrose-metabolizing enzymes in wheat stems subjected to water stress during grain filling. *Planta* 220:331-343
- Yoshida M, Kawakami A, Ende W, Norio S, Noureddine B, Shuichi O (2007) Graminan metabolism in cereals: wheat as a model system. *Recent Advances in Fructooligosaccharides Research*:201-212
- Yoshimura Y, Zaima N, Moriyama T, Kawamura Y (2012) Different Localization Patterns of Anthocyanin Species in the Pericarp of Black Rice Revealed by Imaging Mass Spectrometry. *PLoS ONE* 7:e31285
- Yukawa T WY (1991) Studies on fructan accumulation in wheat (*Triticum aestivum* L.) I. Relationship between fructan concentration and overwintering ability from aspect on the pedigree. *Japanese Journal of Crop Science* 60:385-391

- Zahedi M, Sharma R, Jenner CF (2003) Effects of high temperature on grain growth and on the metabolites and enzymes in the starch-synthesis pathway in the grains of two wheat cultivars differing in their responses to temperature. *Functional Plant Biology* 30:291-300
- Zaima N, Goto-Inoue N, Hayasaka T, Setou M (2010) Application of imaging mass spectrometry for the analysis of *Oryza sativa* rice. *Rapid Communications in Mass Spectrometry* 24:2723-2729
- Zaima N, Yoshimura Y, Kawamura Y, Moriyama T (2014) Distribution of lysophosphatidylcholine in the endosperm of *Oryza sativa* rice. *Rapid Communications in Mass Spectrometry* 28:1515-1520
- Zhang B, Li W, Chang X, Li R, Jing R (2014a) Effects of favorable alleles for water-soluble carbohydrates at grain filling on grain weight under drought and heat stresses in wheat. *PLoS ONE* 9:e102917
- Zhang J (2008) Water deficit in bread wheat : charaterisation using genetic and physiological toole. Faculty of Sustainability, Environmental and Life Sciences. Murdoch University, p 163
- Zhang J, Chen W, Dell B, Vergauwen R, Zhang X, Mayer J, Van den Ende W (2015a) Wheat genotypic variation in dynamic fluxes of WSC components in different stem segments under drought during grain filling. *Frontiers in Plant Science* 6
- Zhang J, Dell B, Biddulph B, Khan N, Xu Y, Luo H, Appels R (2014b) Vernalization gene combination to maximize grain yield in bread wheat (*Triticum aestivum* L.) in diverse environments. *Euphytica* 198:439-454
- Zhang J, Dell B, Conocono E, Waters I, Setter T, Appels R (2009) Water deficits in wheat: fructan exohydrolase (1-FEH) mRNA expression and relationship to soluble carbohydrate concentrations in two varieties. *New Phytologist* 181:843-850
- Zhang J, Dell B, Ma W, Vergauwen R, Zhang X, Oteri T, Foreman A, Laird D, Van den Ende W (2016) Contributions of root WSC during grain filling in wheat under drought. *Frontiers in Plant Science* 7
- Zhang J, Huang S, Fosu-Nyarko J, Dell B, McNeil M, Waters I, Moolhuijzen P, Conocono E, Appels R (2008) The genome structure of the 1-FEH genes in wheat (*Triticum aestivum* L.): new markers to track stem carbohydrates and grain filling QTLs in breeding. *Molecular Breeding* 22:339-351
- Zhang J, Jia W, Yang J, Ismail AM (2006) Role of ABA in integrating plant responses to drought and salt stresses. *Field Crops Research* 97:111-119
- Zhang J, Xu Y, Chen W, Dell B, Vergauwen R, Biddulph B, Khan N, Luo H, Appels R, Van den Ende W (2015b) A wheat 1-FEH w3 variant underlies enzyme activity for stem WSC remobilization to grain under drought. *New Phytologist* 205:293-305
- Zhao K, Tung C-W, Eizenga GC, Wright MH, Ali ML, Price AH, Norton GJ, Islam MR, Reynolds A, Mezey J (2011) Genome-wide association mapping reveals a rich genetic architecture of complex traits in *Oryza sativa*. *Nature Communications* 2:467
- Zrenner R, Schüler K, Sonnwald U (1996) Soluble acid invertase determines the hexose-to-sucrose ratio in cold-stored potato tubers. *Planta* 198:246-252
- Zuryn S, Le Gras S, Jamet K, Jarriault S (2010) A strategy for direct mapping and identification of mutations by whole-genome sequencing. *Genetics* 186: 427-430